MISCELLANEOUS PAPER GL-88-10

(2)

US Army Corps of Engineers

EXPERIMENTAL RESEARCH INTO THE BEHAVIOR OF PILES AND PILE GROUPS SUBJECTED TO CYCLIC LATERAL LOADING

by

Lymon C. Reese, Dan Allen Brown, Shin-Tower Wang

11512 Tin Cup Drive, No. 19
Austin, Texas 78750

June 1988
Final Report

Prepared for Minerals Management Service
US Department of Interior, Reston, Virginia 22090

and

Department of Research, Federal Highway Administration
Washington, DC 20590

and

US Army Engineer Division, Lower Mississippi Valley
PO Box 80, Vicksburg, Mississippi 39180-0080

Monitored by Geotechnical Laboratory
US Army Engineer Waterways Experiment Station
PO Box 631, Vicksburg, Mississippi 39180-0631

Under Contract No DACW39-88-M-0867

Unclassified
SECURITY CLASSIFICATION OF THIS PAGE

REPORT DOCUMENTATION PAGE

Form Approved
OMB No 0704-0188
Exp Date Jun 30 1986

1a REPORT SECURITY CLASSIFICATION Unclassified	1b RESTRICTIVE MARKINGS
2a SECURITY CLASSIFICATION AUTHORITY	3 DISTRIBUTION / AVAILABILITY OF REPORT Approved for public release; distribution unlimited
2b DECLASSIFICATION / DOWNGRADING SCHEDULE	
4 PERFORMING ORGANIZATION REPORT NUMBER(S)	5 MONITORING ORGANIZATION REPORT NUMBER(S) Miscellaneous Paper GL-88-10
6a NAME OF PERFORMING ORGANIZATION / 6b OFFICE SYMBOL (If applicable)	7a NAME OF MONITORING ORGANIZATION USAEWES Geotechnical Laboratory
6c ADDRESS (City, State, and ZIP Code) 11512 Tin Cup Drive, No. 19 Austin, TX 78750	7b ADDRESS (City, State, and ZIP Code) PO Box 631 Vicksburg, MS 39180-0631
8a NAME OF FUNDING / SPONSORING ORGANIZATION See reverse / 8b OFFICE SYMBOL (If applicable)	9 PROCUREMENT INSTRUMENT IDENTIFICATION NUMBER Contract No. DACW39-87-M-0867
8c ADDRESS (City, State, and ZIP Code) See reverse	10 SOURCE OF FUNDING NUMBERS PROGRAM ELEMENT NO / PROJECT NO / TASK NO / WORK UNIT ACCESSION NO

11 TITLE (Include Security Classification)
Experimental Research Into the Behavior of Piles and Pile Groups Subjected to Cyclic Lateral Loading

12 PERSONAL AUTHOR(S)
Reese, Lymon C.; Brown, Dan Allen; Wang, Shin-Tower

13a TYPE OF REPORT	13b TIME COVERED	14 DATE OF REPORT (Year, Month, Day)	15 PAGE COUNT
Final report	FROM _____ TO _____	June 1988	228

16 SUPPLEMENTARY NOTATION
Available from National Technical Information Service, 5825 Port Royal Road, Springfield, VA 22161.

17 COSATI CODES			18 SUBJECT TERMS (Continue on reverse if necessary and identify by block number)
FIELD	GROUP	SUB-GROUP	Cyclic lateral loading, Piles, Scour, Interaction factors, Pile groups, Pile structures

19 ABSTRACT (Continue on reverse if necessary and identify by block number)

A research program to study the behavior of piles and pile groups subjected to cyclic lateral loading was conducted at a Houston, Texas site. A single pile and a nine-pile group situated in the natural clay were tested and then the upper several feet of clay were removed and replaced with sand and the tests were repeated.

Following these tests, another study was undertaken to measure experimentally pile-head flexibility reduction (interaction) factors for the pile group in sand. Tests were made cyclically at varying magnitudes of applied groundline shear on single piles and two-pile and three-pile subgroups, and the response of unloaded piles in the group was measured.

Concurrent with these studies, pressuremeter (PMT) and cone penetrometer (CPT) tests were performed in both the clay and the sand from which capacity predictions were made.

Each of these studies generated a report with voluminous data. This report summarizes the major findings into one volume.

20 DISTRIBUTION / AVAILABILITY OF ABSTRACT	21 ABSTRACT SECURITY CLASSIFICATION
☒ UNCLASSIFIED/UNLIMITED ☐ SAME AS RPT ☐ DTIC USERS	Unclassified
22a NAME OF RESPONSIBLE INDIVIDUAL	22b TELEPHONE (Include Area Code) / 22c OFFICE SYMBOL

DD FORM 1473, 84 MAR — 83 APR edition may be used until exhausted. All other editions are obsolete.

SECURITY CLASSIFICATION OF THIS PAGE
Unclassified

8a. & 8c. NAME AND ADDRESS OF FUNDING/SPONSORING ORGANIZATION

Minerals Management Service
US Department of Interior
Reston, VA 22090

Department of Research
Federal Highway Administration
Washington, DC 20590

US Army Engineer Division, Lower Mississippi Valley
PO Box 80
Vicksburg, MS 39180-0080

PREFACE

This is a summary report of several studies performed by the University of Texas at Austin, the University of Houston, and Texas A&M University under contract to the US Army Engineer Waterways Experiment Station (WES), Vicksburg, Mississippi, for the Minerals Management Service, US Department of Interior; the Department of Research, Federal Highway Administration; and the US Army Engineer Division, Lower Mississippi Valley. The report was prepared under Contract No. DACW39-87-M-0867.

This report was prepared by Drs. Lymon C. Reese, Dan Allen Brown, and Shin-Tower Wang, consulting engineers, and was reviewed by Mr. G. Britt Mitchell, Chief, Engineering Group, Soil Mechanics Division (SMD), Geotechnical Laboratory (GL), WES. General supervision was provided by Mr. Clifford L. McAnear, Chief, SMD, and Dr. William F. Marcuson III, Chief, GL.

COL Dwayne G. Lee, CE, is Commander and Director of WES. Dr. Robert W. Whalin is Technical Director.

Table of Contents

LISTING OF NOTATIONS

b	pile diameter
CPMT	cone pressuremeter test
CPT	quasi-static cone penetration test
c	cohesion of the soil
c_u	undrained shear strength
DCPMT	driven cone pressuremeter test
E	modulus of pile material
F	unit skin-friction component in pressuremeter method
FVT	field vane-shear test
I	moment of inertia
J	empirical constant, = 0.25
K_o	coefficient for at-rest earth pressure
k	soil modulus
G_s	the secant modulus to the pressuremeter curve
N	number of cycles
P_j	averaged lateral load on each pile in a group
P_L	limit pressure
P_r	pressure related to the injected volume V_r
P_u	force per unit of length
p	lateral soil reaction per unit length
PCPMT	pushed cone pressuremeter test
Q	unit frontal resistance in pressuremeter method
q_c	cone tip resistance
$R_{(pile)}$	pile radius

$R_{(pmt)}$	initial radius on the soil cavity in the pressuremeter test
r_o	radius of pressuremeter probe
S(Q), S(F)	shape factor
$S_{p5\%}$	a load on the single pile that causes a displacement at the pile head corresponding to 5% of the pile diameter
V_r	injected volume in pressuremeter
x	depth
$y_{(pile)}$	lateral deflection of the pile
$y_{(pmt)}$	increase in radius of the soil cavity in the pressuremeter test
α_{ij}	interaction factor between piles i and j
α	parameter related to the degradation model
β	parameter related to the degradation model
γ	unit weight of soil
γ'	effective unit weight
ε_{50}	axial strain of soil corresponding to one-half the maximum principal stress difference
ρ	parameter related to the degradation model
σ_{rr}	radial stress
$\tau_{r\theta}$	shear stress
ξ	departure angle

LISTING OF TABLES

LISTING OF FIGURES

CHAPTER 1

INTRODUCTION

This report provides a summary of a research program on the behavior of piles and pile groups subjected to lateral loading. The program was sponsored jointly by the Minerals Management Service (MMS), U.S. Department of Interior; The Office of Research, Federal Highway Administration (FHWA); and the U.S. Army Corps of Engineers, Waterways Experiment Station (WES). The primary focus of the research consists of field testing of a full-scale pile group at the University of Houston Pile Test Facility. The availability of an existing pile group, as well as a wealth of geotechnical data and previous pile test data provided an opportunity to conduct the experimental studies in an efficient and cost-effective manner. The nine-pile group was tested first in the natural clays at the site. Then several feet of the clay was excavated and replaced with sand and the group was retested.

A number of reports and voluminous data have been generated as a result of these studies, and this report summarizes the major findings into one volume of convenient size. References to the complete reports are provided to allow the interested reader to investigate a particular topic in detail. This report will include only data necessary to

illustrate observed trends or to support relevant conclusions.

Chapter 2 of this report describes the site conditions, both for the clay and the sand, and also describes the arrangement for the testing. The test setup is described for the single pile and for the pile group.

Chapter 3 deals with the performance of piles and pile groups in the natural stiff clays, and Chapter 4 deals with the behavior of piles and groups of piles under similar loading conditions in sand. Care was taken to not load the piles to structural yield during the tests in clay, thus allowing the same testing arrangement to be used for the tests in sand.

The chapters on pile behavior in stiff clay and sand are subdivided into sections discussing the research on single piles, and sections on the group response. The research on single piles was originally intended to provide the basis for the evaluation of group effects, but the study was expanded to include research into prediction of behavior under lateral loading by use of the pressuremeter.

The sections on group performance include both a discussion of major findings related to the behavior of

groups of piles compared with that of isolated single piles and a comparison of results with available analytical procedures. Some additional work to experimentally determine the "interaction factors" used with some of these available design procedures was also performed.

Chapter 5 presents information on the use of results from the pressuremeter in the analysis of piles under lateral loading. Because the installation and procedure used in conducting pressuremeter tests are so critical to the interpretation of the data and use of the pressuremeter design method, such relevant information is included in Chapter 5.

Presented in Table 1 is a chronological history of the pile installation and testing relevant to this research. The original installation of the piles in the natural stiff clay was part of an FHWA sponsored study of pile group action during axial loading. Considerable data on the pile and soil response during and after driving was generated during that study, along with geotechnical data. The lateral test of the single pile in clay was performed as a part of an industry-sponsored research project into the effects of pile diameter and loading rate; this testing is relevant to the current research in that the results are utilized for the response of the single pile in clay. The reports generated by the

current research and which are of direct importance to this research are listed below.

Test of the single pile in clay:

> O'Neill, M.W. and Dunnavant, T.W., "A Study of the Effects of Scale, Velocity, and Cyclic Degradability on Laterally Loaded Single Piles in Overconsolidated Clay," Report No. CE 84-7, Dept. of Civil Engineering, University of Houston University Park, Oct., 1984.

Test of the group in clay and summary of the single pile in clay:

> Brown, D. and Reese, L.C., "Behavior of a Large-Scale Pile Group Subjected to Cyclic Lateral Loading," Geotechnical Engineering Report GR85-12, Geotechnical Engineering Center, The University of Texas at Austin, Austin, Texas, May, 1985.

Tests of the single pile and pile group in sand:

> Morrison, C. and Reese, L.C., "A Lateral Load Test of a Full-Scale Pile Group in Sand," Geotechnical Engineering Report GR86-1, Geotechnical Engineering Center, The University of Texas at Austin, Austin, Texas, August, 1986.

Experimental determination of group interaction factors in sand:

Ochoa, M. and O'Neill, M.W., "Lateral Pile-Group Interaction Factors for Free-Headed Pile Groups in Sand from Full-Scale Experiments," Report No. UHCE 86-12, Department of Civil Engineering, University of Houston University Park, Houston, Texas, Oct., 1986.

Pressuremeter testing in clay:

Makarim, C.A. and Briaud, J.L., "Pressuremeter Method for Single Piles Subjected to Cyclic Lateral Loads in Overconsolidated Clay," Research Report, Department of Civil Engineering, Texas A&M University, Dec., 1986.

Pressuremeter testing in sand:

Little, R.L. and Briaud, J.L., "A Pressuremeter Method for Single Piles Subjected to Cyclic Lateral Loads in Sand," Research Report No. 5357, Department of Civil Engineering, Texas A&M University, April, 1987.

While not directly used in the current research program, several references in the bibliography are relevant to the specific piles and soils at the site. These include the references by O'Neill, Hawkins, and Mahar (1981,1982), by O'Neill, Hawkins, and Audibert (1982), and by Mahar and O'Neill (1983).

The chapters which follow present the major findings of this research, followed by a summary of the most important conclusions affecting design, and recommendations for further research.

Note: Because this report is a summary of the several reports that are listed above, the usual rules of referencing are not followed in all instances in order to streamline this presentation. However, referencing is used where it is desired to advise the reader that more detailed information is available elsewhere.

Table 1.1 Chronology of Pile Test Program

Installation of test piles (FHWA study)	Oct., 1979
Axial load testing of group	Nov., 1979-Apr,1980
Flood test pit for single pile in clay	June, 1982
Installation of single pile in clay	Nov., 1982
Lateral test of single pile in clay	Feb., 1983
Excavate and flood test pit for group	Oct., 1983
Lateral test of group in clay	May, 1984
Excavate clay, place sand, flood site	July-Aug., 1984
Lateral test of single pile in sand	Oct., 1984
Lateral test of group in sand	Oct.-Dec., 1984

CHAPTER 2

SITE CONDITIONS AND FIELD-TEST SETUP

INTRODUCTION

A brief description of the site conditions for the pile-testing program is presented in this chapter. Also presented is a discussion of the most important features of the test setup, loading, and experimental measurements. The section on site conditions covers both the test conditions for the natural, stiff clay and the conditions of the sand fill.

SOIL CONDITIONS AT THE TEST SITE

Natural Clay

The natural, stiff clay soils of the upper 24 ft. consist of preconsolidated clays and silty clays of the Pleistocene-age Beaumont Clay formation. These materials encompass the zone of primary importance during lateral loading. Underlying the Beaumont is the Montgomery formation, a similar but older Pleistocene deposit. Both were formed as deltaic terraces, deposited during interglacial periods and preconsolidated by desiccation during periods of glaciation (when the sea level was lowered).

The stratigraphy of the test site, along with classification test results, are presented in Fig. 2.1. Observations during excavation after load testing revealed a pattern of very closely spaced joints and fissures in much of Stratum I. Stratum II had numerous slickensides, as indicated during geotechnical sampling and laboratory testing.

A variety of data on the strength of the clay was acquired in the considerable geotechnical research at the test site (Mahar and O'Neill, 1983; O'Neill and Dunnavant, 1984). Testing for shear-strength evaluation was concentrated on undrained laboratory and in-situ tests, including:

1. unconsolidated, undrained (UU) triaxial tests,
2. isotropically consolidated, undrained (CIU) triaxial compression tests,
3. quasi-static cone penetration tests (CPT),
4. field vane-shear tests (FVT),
5. pressuremeter tests (PMT),
6. Ko-consolidated (CKoU) triaxial compression tests, and
7. one-dimensional consolidation tests.

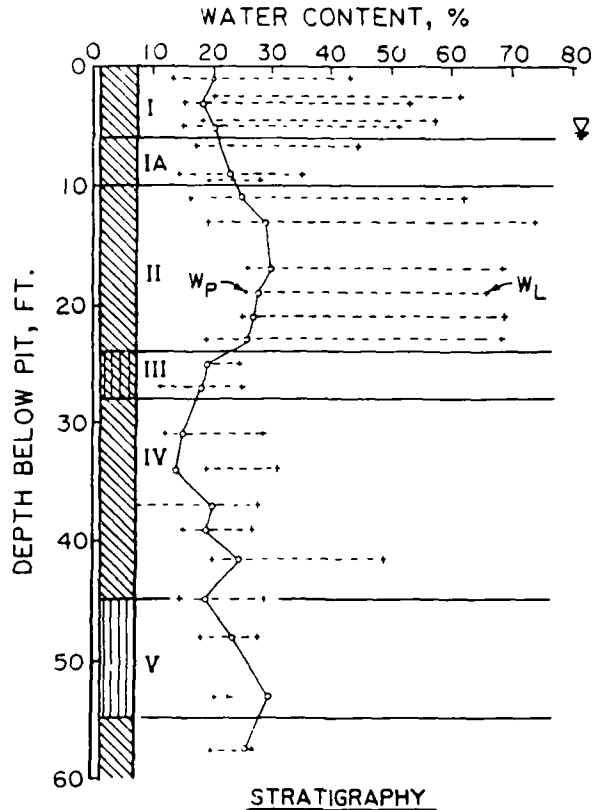

STRATIGRAPHY

I STIFF TO VERY STIFF GRAY AND TAN CLAY (CL-CH)
IA STIFF TO VERY STIFF GRAY AND TAN SANDY CLAY (CL)
II STIFF TO VERY STIFF RED AND LIGHT GRAY CLAY (CH)
III MEDIUM STIFF LIGHT GRAY VERY SILTY CLAY (CL)
IV STIFF TO HARD LIGHT GRAY AND TAN SANDY CLAY (CL)
V DENSE RED AND LIGHT GRAY SILT WITH CLAYEY SILT AND SAND LAYERS (ML)

Fig. 2.1 Stratigraphy of the test site, natural clay

Items 6 and 7 were performed prior to flooding the site and are reported by Mahar and O'Neill (1983). The pressuremeter tests are described in detail in Chapter 5.

The strength tests listed as Items 1 through 4 are presented in Fig. 2.2. These tests were performed after flooding the site for a period of at least several months. Measurements of compression-wave velocities with cross-hole seismic tests indicated that flooding was effective in achieving substantially complete saturation of the soils above the natural water table. Except for the top few inches, pore pressure changes due to flooding produced only subtle changes in shear strength. The UU triaxial tests were performed with a cell pressure of 1.5 times the total overburden pressure, and the CIU triaxial tests were consolidated to a stress equal to 1.2 times the effective vertical stress. The undrained shear strengths (s_u) from results of the CPT test were computed from the cone tip resistance (q_c) using:

$$S_u = \frac{q_c - \sigma_v}{N_c}$$

where N_C is the cone tip bearing capacity factor (=13.6, based on correlations with the results from the field vane test) and σ_v is the total vertical overburden stress.

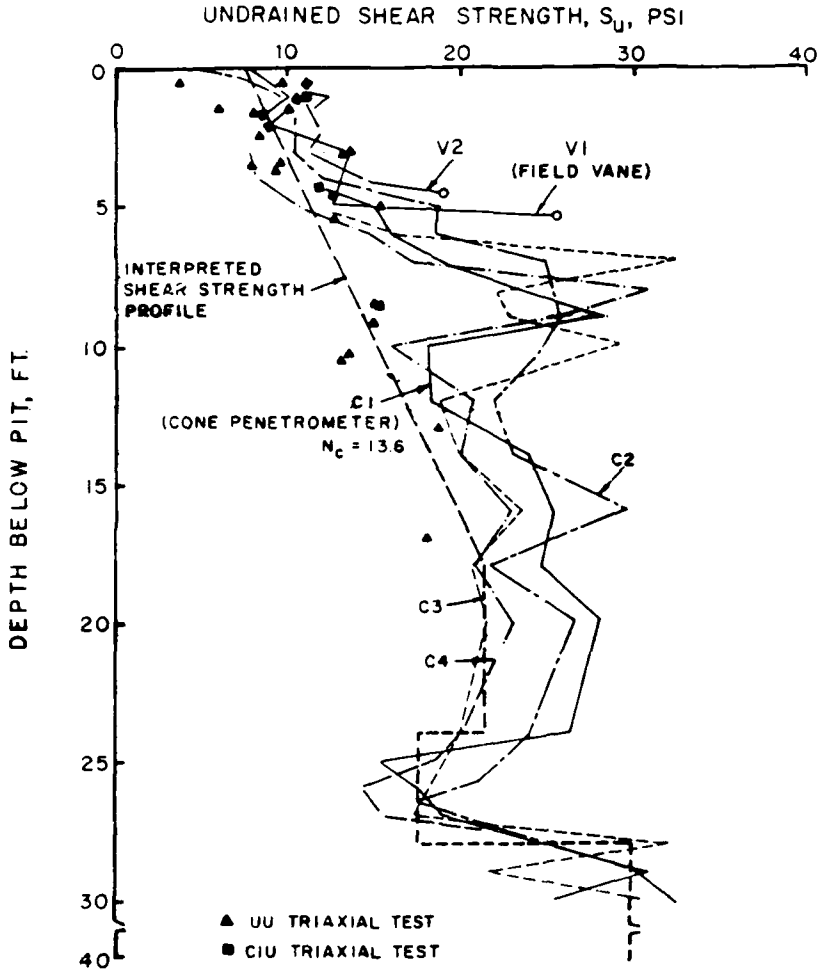

Fig. 2.2 Shear-strength data, natural clay

Results from the FVT provide an estimate of sensitivity; comparison of peak and residual shear resistance indicates a sensitivity in the upper 5.5 ft. of about 2.

The scatter in test data on undrained strength shown in Fig. 2.2 is typical of desiccated clay. Mahar and O'Neill hypothesize that the cracks produced during desiccation allow spatially-variable suction pressures in the pore spaces, which leads to pointwise and directional variability in shear strength and water content. The relatively close joint spacing in Stratum I could account for less variability in this zone than in deeper strata that are slickensided. Thin partings and pockets of sand in Stratum IA likely contributed to scatter in this zone, particularly in the CPT values.

Compacted Sand

The experiments in sand were performed after completion of the work in clay. An excavation was made to a depth of 9.5 ft. and sand was compacted around the piles. Because the sand extends to a depth of slightly more than 10 pile diameters, the response of the piles to lateral loading is dominated by the response of the sand.

The sand was placed in a relatively dry state and compacted in 6-inch lifts using a Dyna-pac EY15 vibrating-plate compactor, as shown in Fig. 2.3. The compaction achieved a medium density, with an average dry density after

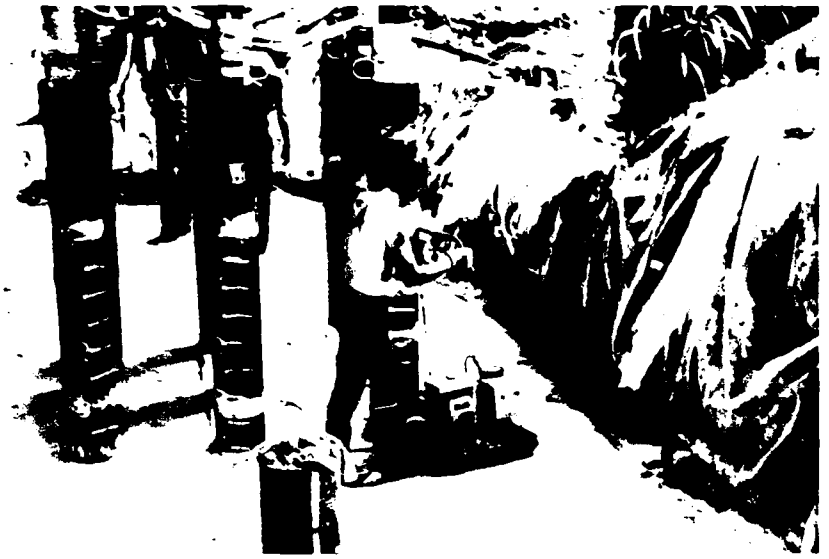

Fig. 2.3 Compaction of sand with vibratory-plate compactor

compaction of about 98 lbs/ft^3. As indicated by the range of grain-size curves from seven samples shown on Fig. 2.4, the sand is of uniform gradation and is classified SP by the Unified Soil Classification System. Results of direct shear tests indicated the compacted sand to have an angle of internal friction, ϕ, of 38.5°. Results from in-situ CPT and standard penetration tests (SPT) are shown in Fig. 2.5, along with a correlation with the angle of internal friction. In-situ PMT's were performed using a variety of installation techniques; these test results are reported in detail in Chapter 5 of this report.

The geometry of the excavation and backfill is illustrated in Fig. 2.6. As shown in that figure, perforated PVC pipes were embedded at the base of the sand fill and were used to saturate the sand by flooding from below. As the sand backfill was placed, the water level was brought to the top of each preceeding layer. Upon completion of placing all of the sand, the water level was "flexed" several times by drawing the water level all the way down and reflooding. The site was then maintained in a flooded condition.

ARRANGEMENT FOR LATERAL TESTING

The testing arrangement for the two programs of testing of the pile group was virtually identical. The arrangement

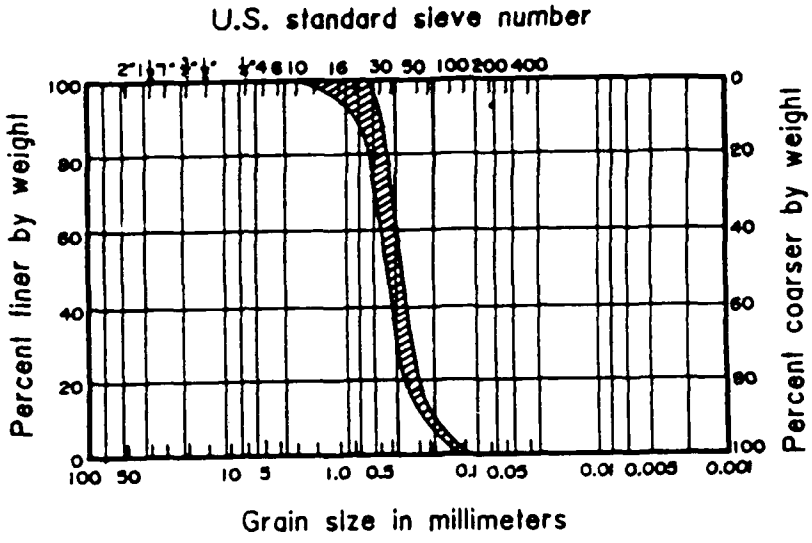

Fig. 2.4 Grain size distribution for sand

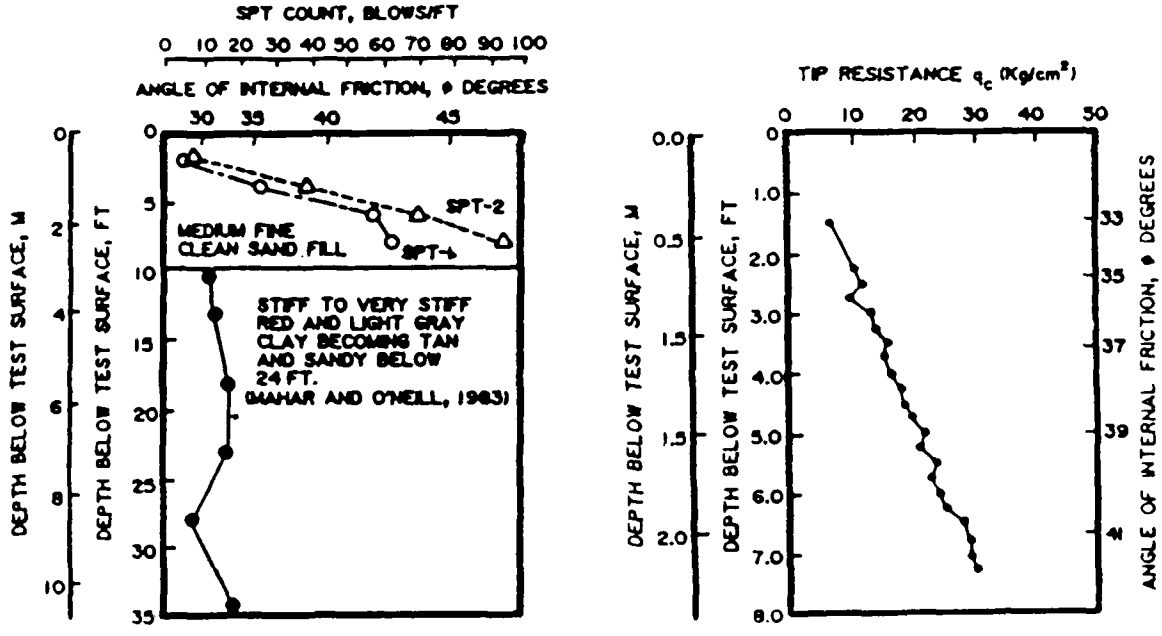

a. Results from the standard penetration test and estimated values of the angle of internal friction

b. Results from the cone penetration test and estimated values of the angle of internal friction

Fig. 2.5 Information on strength of sand at test site (from Ochoa and O'Neill, 1986)

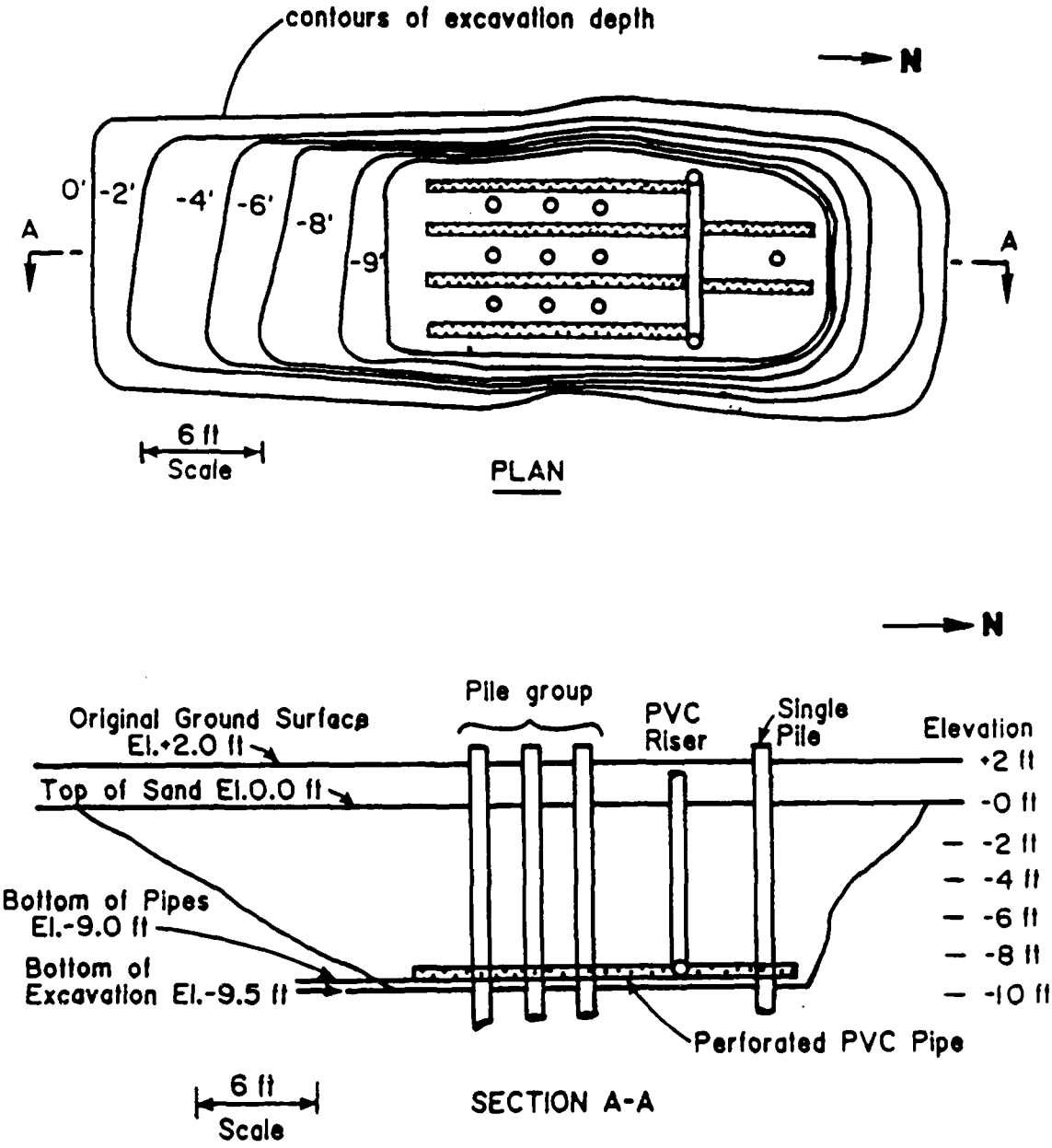

Fig. 2.6 Excavation and pipe system for saturating the sand

for testing the single piles was also virtually the same for the test in clay and in sand. The general testing arrangement for all of the pile tests is described in the following paragraphs. Any significant differences between tests will be noted. The testing arrangement used by Ochoa and O'Neill in the interaction factor study was similar to that described in this chapter, except that all of the piles in the group were not connected simultaneously to the loading frame. Specific details related to the interaction factor will be noted in Chapter 4.

Site Preparation

In order to simulate the offshore and riverine environments as closely as possible (for cyclic loading), a shallow pit was excavated around all of the piles and flooded with water. The general layout of the site is shown in Fig. 2.7. The pit was 1.5 to 2 feet deep and was continually submerged for several months prior to testing. For the tests in sand the pit was filled by flooding from the perforated pipes below the sand as described previously. Cyclic load is to be expected on pile groups in most applications. The assumption is made that submerged soil will behave less favorably under cyclic loading than will partially saturated soil or dry soil. The pore pressures that are generated in submerged soil during cyclic loading and scour due to a gap

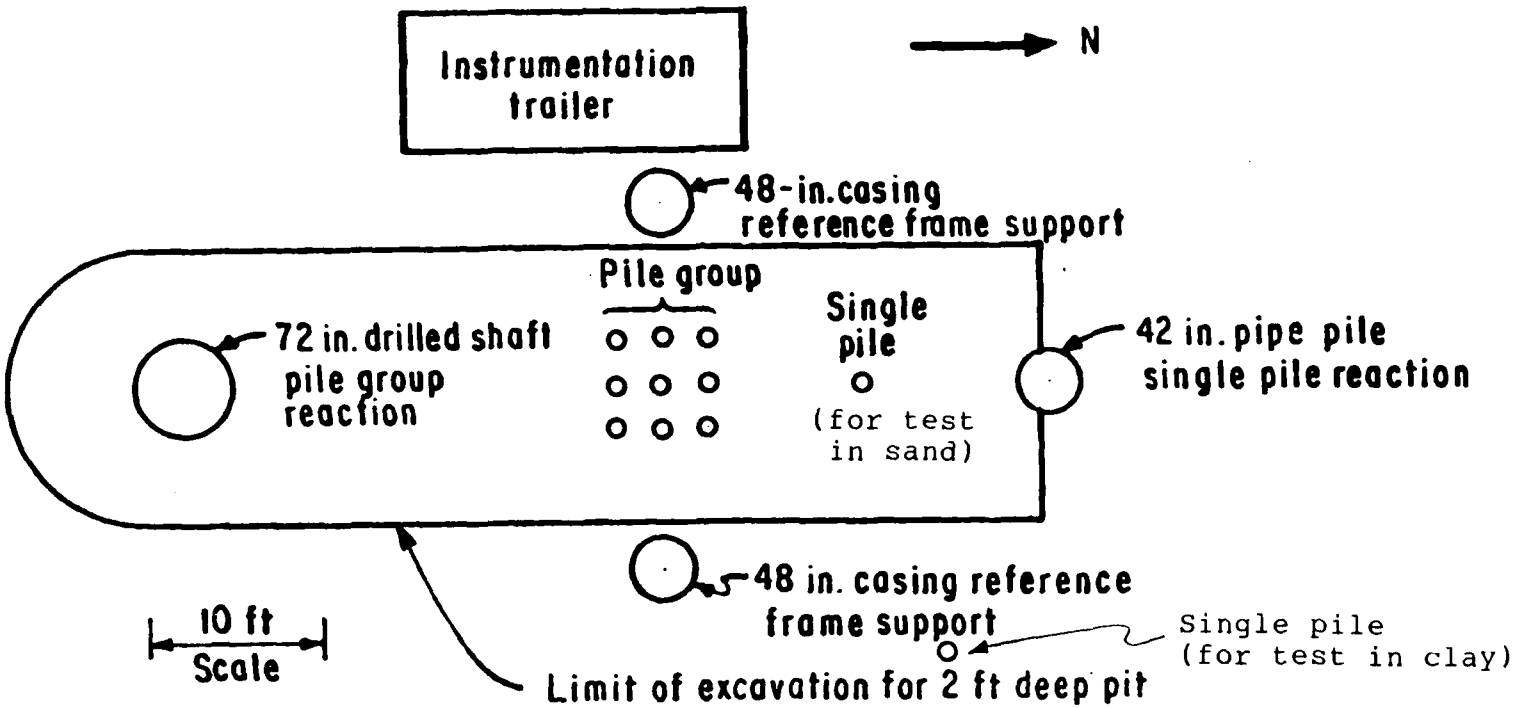

Fig. 2.7 Site layout

that can develop between the soil and a pile are important factors related to pile-soil interaction.

Measurement of Bending Moments

In order to determine the distribution of stresses along the length of the piles in the group and to derive p-y curves for the soil, bending moments were measured at various depths on all piles for all of the tests. For the single pile tests, these measurements were made using electrical resistance strain gauges on the outside of the piles. Because the piles in the group were already in place, measurements were made in these piles by first applying the strain gauge network to a smaller diameter pipe (6.625 in. O.D.) and grouting this instrumented pipe into place within each pile. A schematic diagram of the gauge locations is shown in Fig. 2.8.

For the single pile in clay (by Dunnavant and O'Neill), the bending-moment gauges on the pile were calibrated in the laboratory prior to driving. For the group piles and the single pile in sand, calibration was performed in the field after excavation of the pit for placement of the sand.

Because the gauges are not at the extreme fiber of the piles and because of the influence of the small amount of cement grout, the instrumentation for the group piles

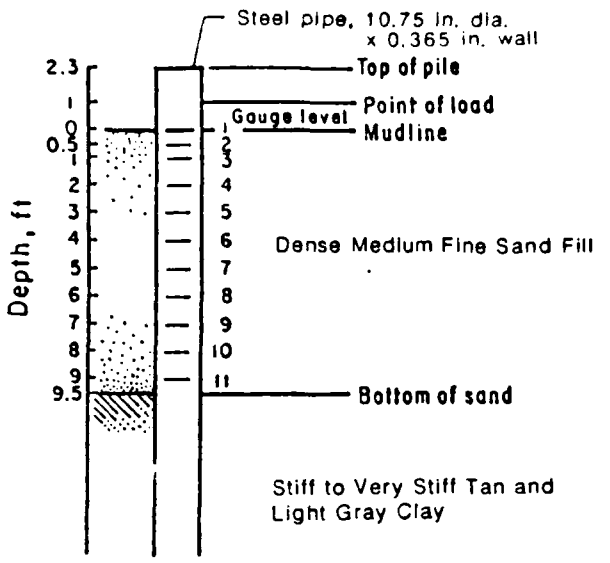

a. Single pile in sand

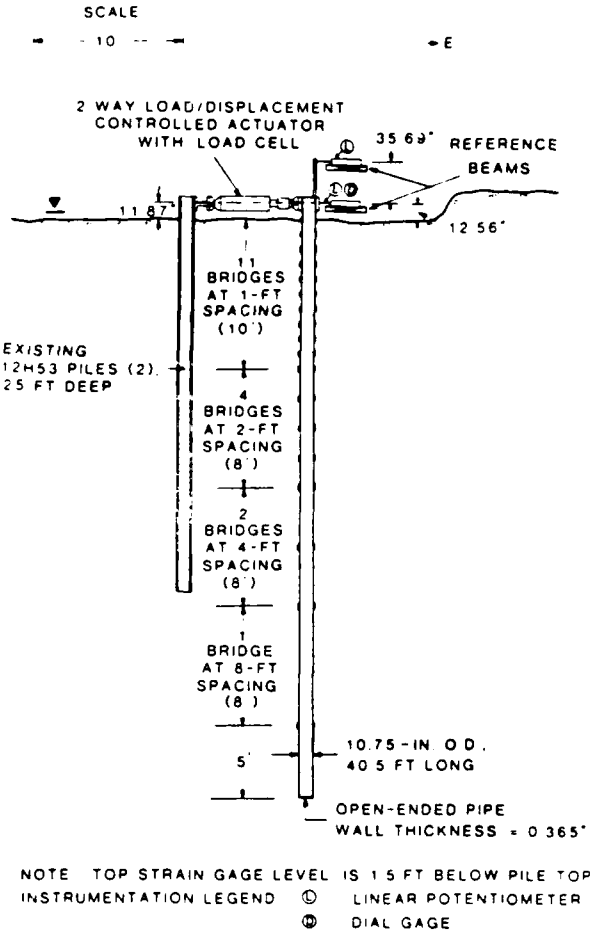

b. Single pile in clay

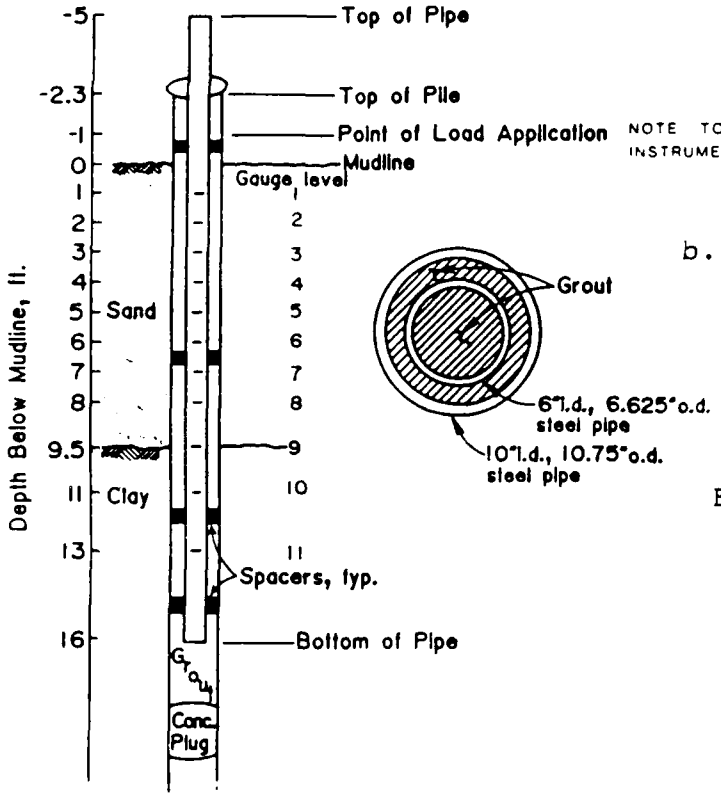

c. Group piles (sand or clay)

Fig. 2.8 Instrumentation for Measurement of bending moment

provides a less accurate indication of bending moments than does the instrumentation for the single piles. The accuracy of the bending measurements on the group piles are thought to be in the range of plus or minus 10 in.-kips.

Loading Frame and Load Measurement

In order to accurately control the restraint conditions at the pilehead and to measure the shear force distributed to each pile, the piles were loaded using a frame with moment-free connections. Each of the pinned joints used to connect the piles to the frame was instrumented to serve as a load cell for measuring the load that came to a pile. A similar connection was used for the single-pile tests. The loading of selected piles for the interaction-factor study was easily accomplished by simply disconnecting some of these joints. A diagram of the load-cell assembly and a photograph of the loading frame is provided in Fig. 2.9.

Measurement of Deflection and Slope

Although the loading frame was quite rigid with respect to the piles, measurements of deflection were made for each pile. These measurements were made from a separate frame attached to the large, embedded steel casings shown on Fig. 2.10. Deflection measurements were made near the point of loading using linear conductive-plastic potentiometers. Similar measurements were made at points four feet or more

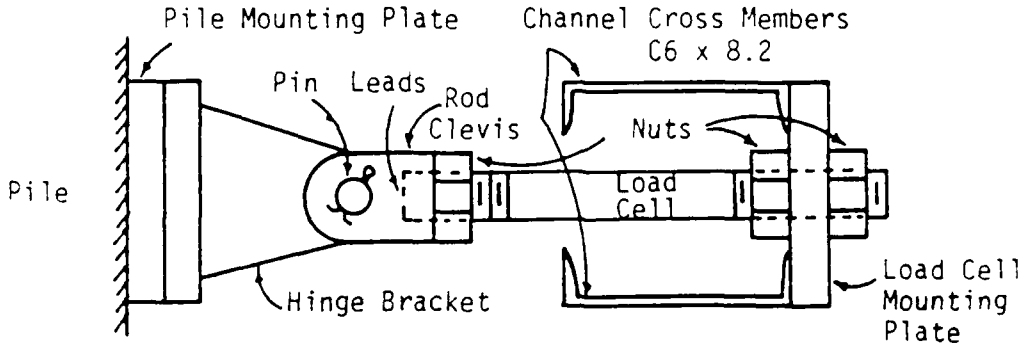

Load cell assembly

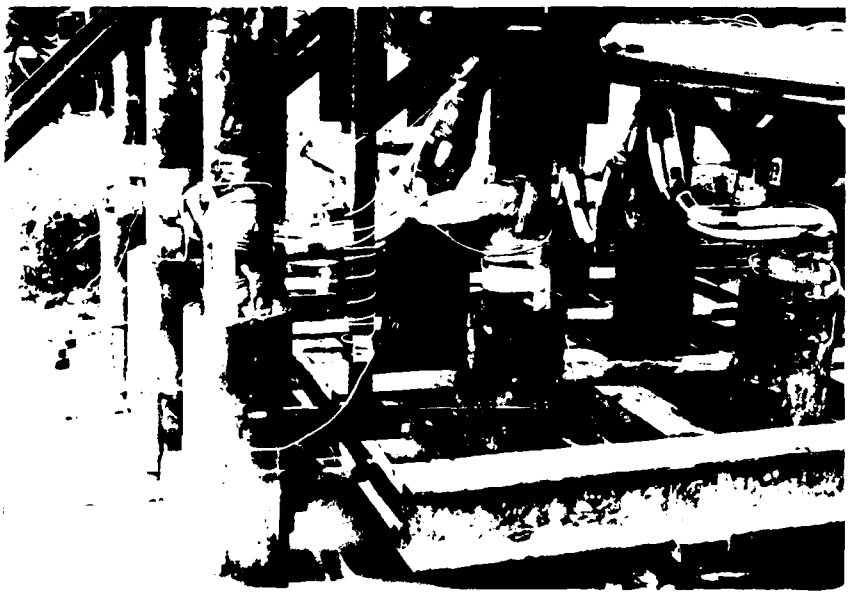

Fig. 2.9 Load-cell assembly and view of the loading frame from the northwest (from Brown & Reese report)

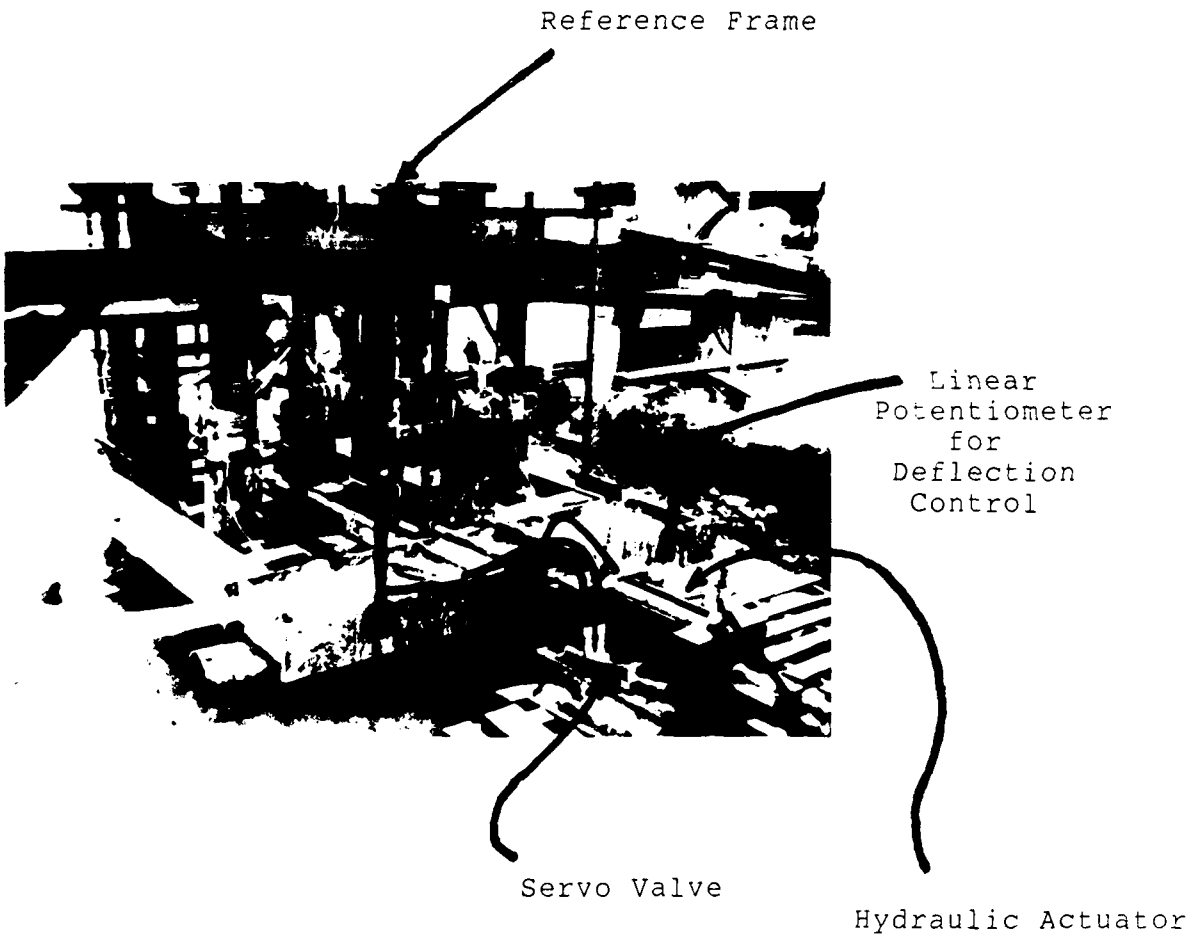

Fig. 2.10 Reference frame and loading system

above the loading point to allow determination of the slope at the top of the pile. Identical techniques were used for the single pile tests, except that wooden reference frames were constructed.

Load Application and Control

Loads during testing were in all cases provided by a double acting hydraulic cylinder with a closed-loop system of servo-control. Cyclic loading was two-way in all cases and tracked a sinusoidal curve of deflection vs time. The periods for a full cycle of loading were generally maintained between 15 and 30 seconds, although some cycling at higher frequencies was performed on the single pile in clay (pile response was found not to be very sensitive to frequency by Dunnavant and O'Neill). Overall load on the group was measured by a single large load cell mounted on the hydraulic cylinder (as well as the individual load cells). A linear potentiometer was mounted on the loading frame for deflection feedback.

The first cycle of load was applied by slowly loading the pile or group to a predetermined load, measuring the deflection at that load, and continuing to cycle at a constant deflection equal to that measured on the first cycle. The load was thus allowed to vary as loading continued at a constant value of peak deflection. The load

was stopped and maintained for the few seconds required for data acquisition at the cycles for which measurements were made. Two hundred cycles of loading were typically made at each load level.

Data-Acquisition System

The electronic instrumentation was monitored and the data recorded using the computer-controlled system shown in Fig. 2.11. The data were stored on magnetic tape and later transferred to the mainframe computer at the University of Texas for processing. As a backup, data were also printed on paper tape before leaving the test site. Display of selected data was used during the testing to evaluate the progress of the experiment and to ensure that the group piles were not yielded during the test in clay (to allow later use in the sand test).

Other Comments

The system described above generally worked well; however there was a structural failure in the loading frame during the test of the pile group in sand because of misalignment of the hydraulic cylinder. This failure occurred as the second level of load was applied to the group in October 1984. The necessary repairs were made and the test was completed in December.

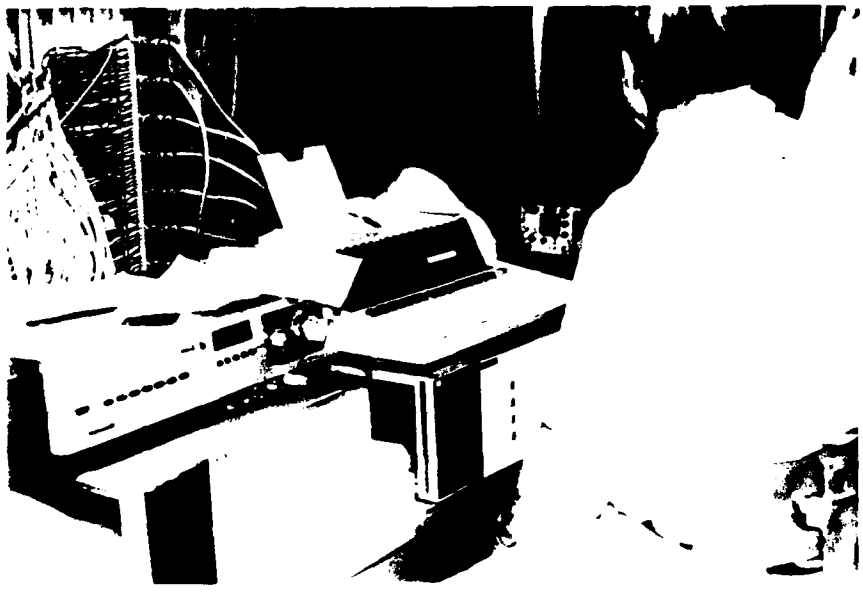

Fig. 2.11 View of data-acquisition system

CHAPTER 3
BEHAVIOR OF LATERALLY LOADED PILES AND PILE GROUPS IN CLAY

A major portion of the research was directed toward the behavior of laterally loaded piles and pile groups in the native stiff and overconsolidated Beaumont clay at the test site. Tests of an individual pile behavior were performed as a part of earlier research by O'Neill and Dunnavant (1984); the sponsors of that work graciously consented to allow the results of that research to be used as a part of this study. The tests of the individual pile provided the baseline for comparison of pile-group effects as found in the testing of the nine-pile group.

This chapter is arranged into two major sections, with the first dealing with the behavior of single piles in stiff clay and the second addressing the behavior of pile groups. The section on single piles includes a discussion of the pile behavior and p-y curves derived for both static (monotonic) and cyclic loading, and provides comparisons of the experimental data obtained with predictions made using traditional methods of analysis for single piles.

The section on pile groups provides a comparison of the group-test results with those of the single pile for both monotonic and cyclic loading. A comparison of predicted and

measured response of the pile group is also made using relevant procedures of analysis. The test results for the single pile are utilized as much as possible to "calibrate" the available design procedures and to ensure that the discrepancies between predicted and measured results which occur are related to the problem of pile-group effects.

Finally, a summary of the major research findings, relating to the behavior of piles and pile groups in stiff clays, is presented. The most important parameters influencing pile response, the major shortcomings in existing procedures, and areas in which additional research might be most fruitful are listed.

BEHAVIOR OF SINGLE PILES IN STIFF CLAY SUBJECTED TO LATERAL LOADING

Lateral-load tests for single piles were scheduled and performed at the University of Houston Pile Test Facility in order to provide information for evaluating group effects. The program on single piles includes the testing of pipe piles with diameters of 48 in. and 10.75 in. Cyclic loading with a maximum of 200 cycles was applied at the top of the pile through a pinned connection. The 10.75-in.-diameter pile used for the single-pile test had the same dimensions as the piles in the group and was tested under similar conditions. It was thoroughly instrumented for the purpose

of deriving p-y curves from the results. The measured and predicted results will be summarized in this section.

Both of the single piles were tested as a part of another program; the results from the 48-in.-diameter test were used only marginally in this report.

Measured and Computed Results for Static Loading

The behavior of two test piles in Beaumont clay was measured by O'Neill and his research team and the data presented here are excerpted from their original report. More detailed and complete information can be found in Report No. UHCE 84-7, by O'Neill and Dunnavant (1984). Because a relatively large increment in load was used between each successive load level, and because cyclic loading was performed at constant deflection rather than at constant load, the first-cycle measurements are considered to be representative of behavior under static-load conditions. Therefore, the static load or monotonic load mentioned hereafter applies to the first cycle of loading. More than one cycle of load for each constant deflection at the pile top will be called cyclic loading and will be discussed after the sections on static loading.

Response of Pile

The variation of pile-head load with deflection for the 10.75-in.-diameter pile under static loading is shown in Fig. 3.1. Points are shown for the first cycle at each load level and for measurements taken in each of two directions. Figure 3.2 illustrates the pile-head loads versus maximum bending moments that were measured by use of the strain gauges. The deflection, slope, and bending moment along the length of the pile were also computed and were used to investigate the soil response (p-y curves).

The variation of pile-head load with deflection for the 48-in.-diameter pile under static loading is shown in Fig. 3.3. The variation of pile-head load with maximum bending moment in the pile is shown in Fig. 3.4. The data on testing for the 48-in.-diameter pile provided additional data on behavior of a single pile.

Response of Soil

The soil-resistance curves were derived from the bending moments as indicated by the strain gauges at the various depths. A third-degree polynomial was generally used to fit the data from the eleven gauge stations. The soil reaction, p, was obtained by double differentiation of the data on bending moment, and the deflection, y, was obtained by double integration of the same data. The p-y curves for static

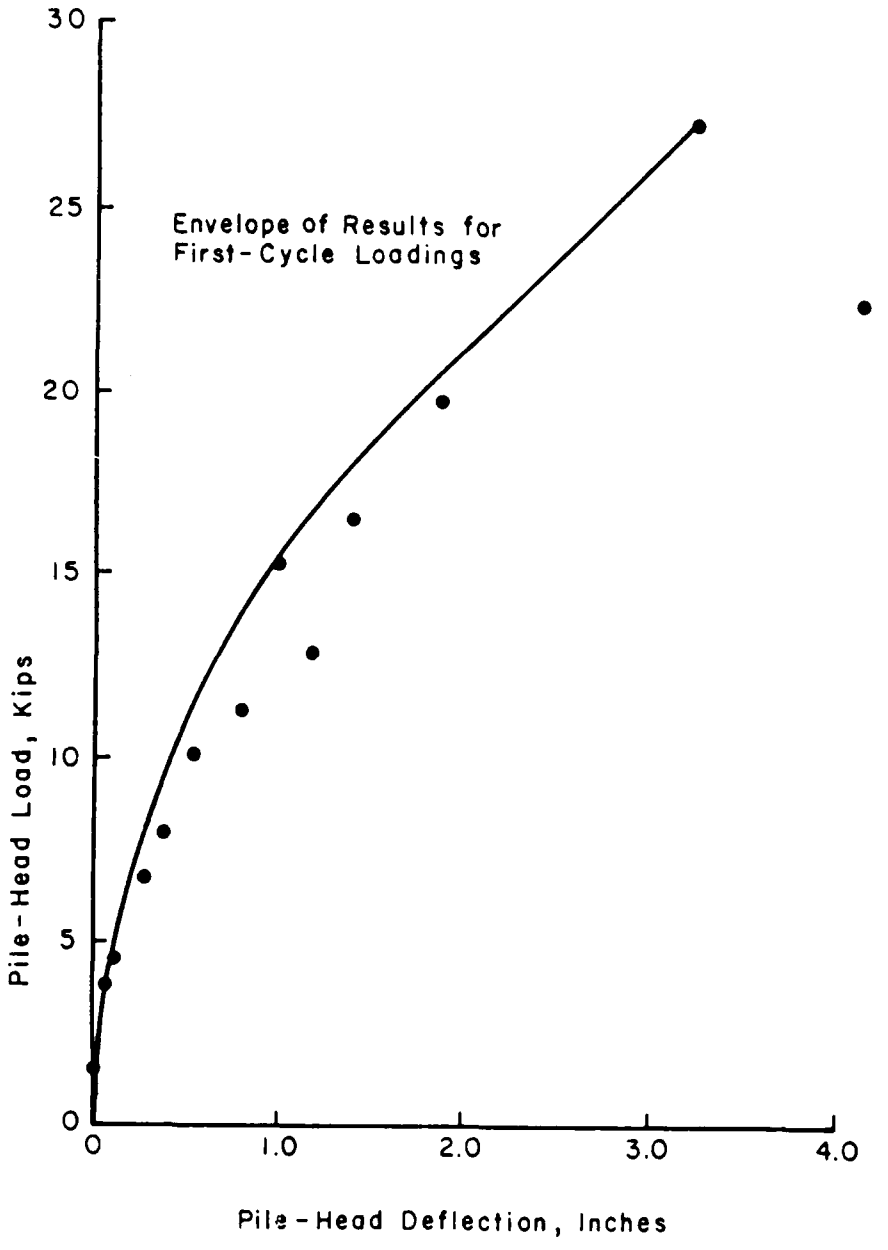

Fig. 3.1 Pile-head load vs deflection for 10.75-in. pile during loading

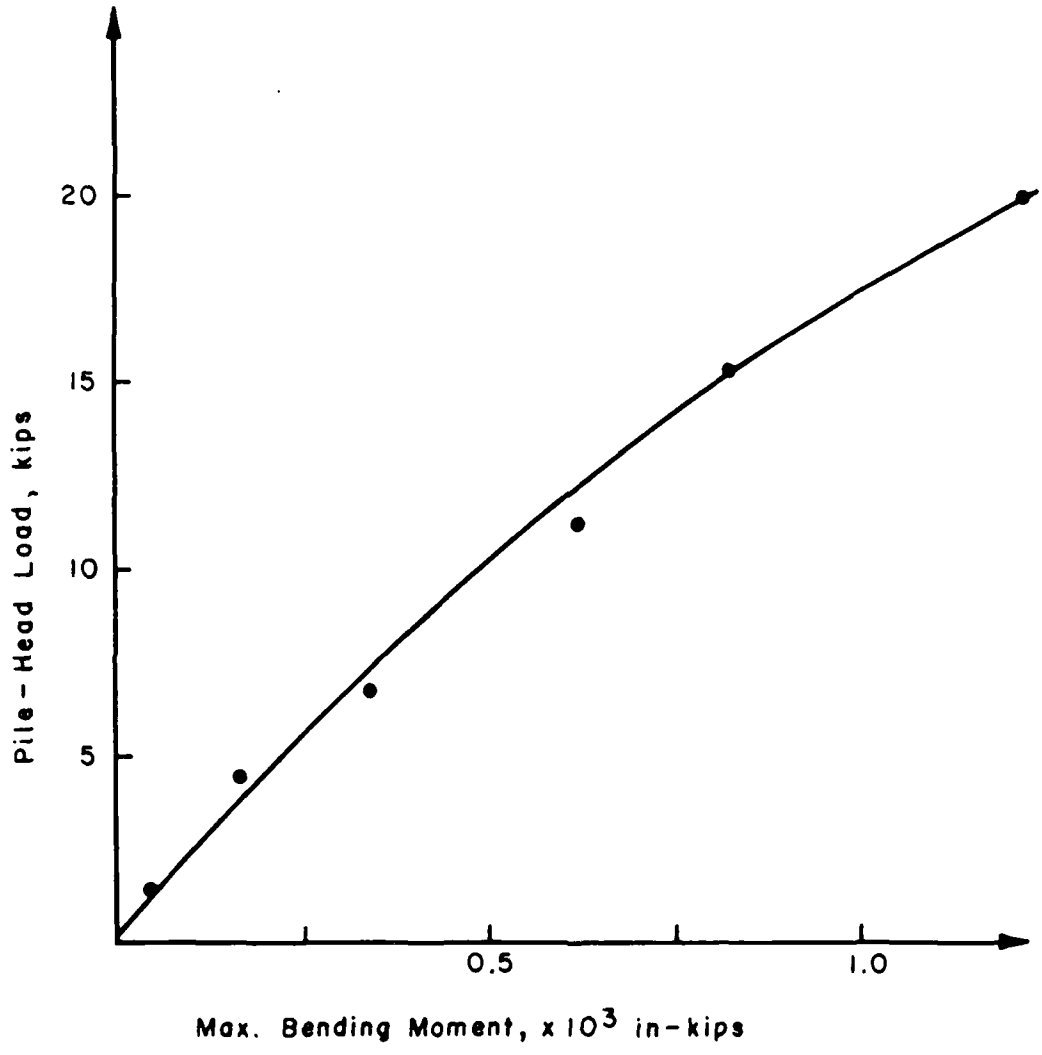

Fig. 3.2 Pile-head load vs maximum bending moment for 10.75-in. pile during static loading

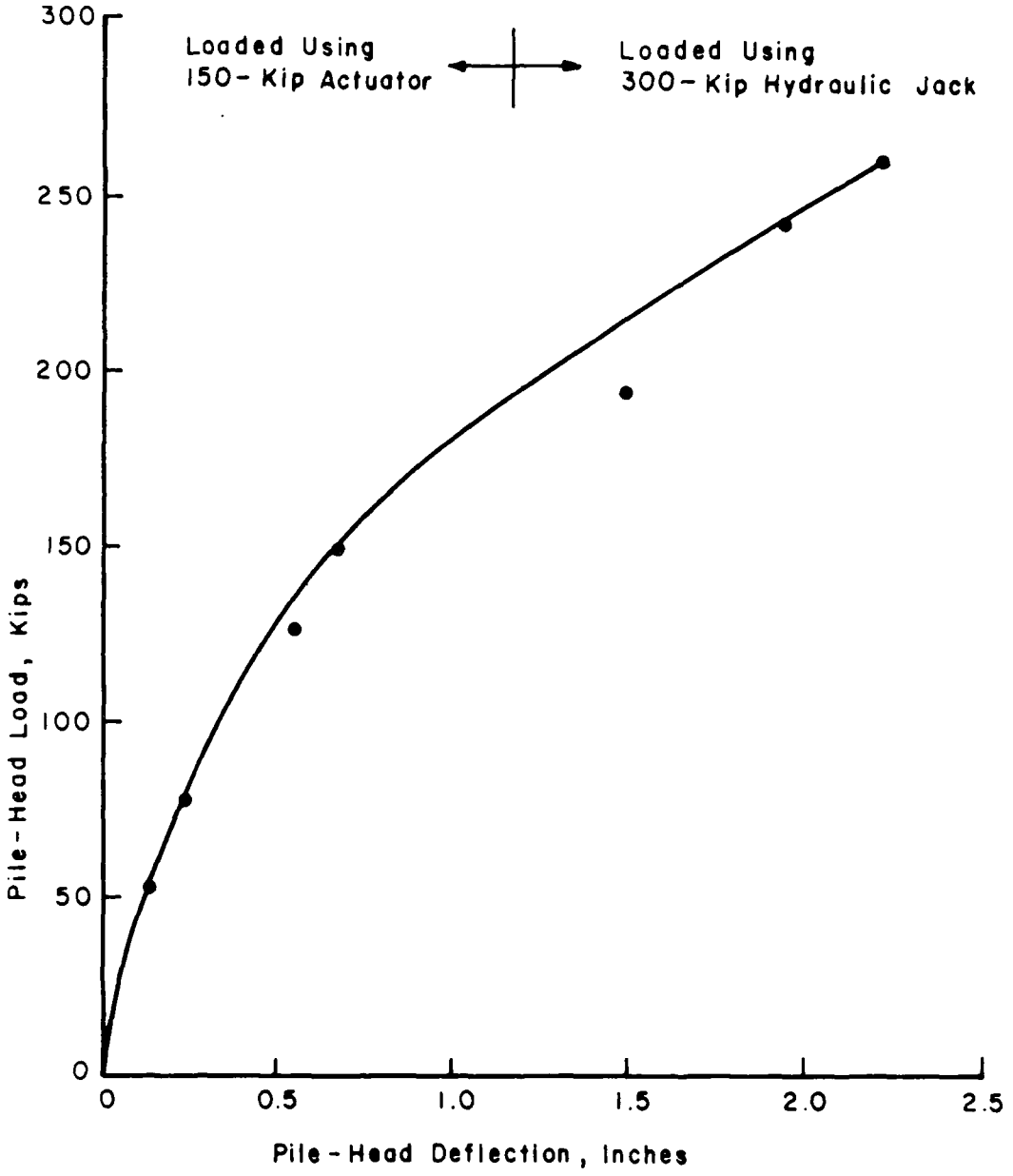

Fig. 3.3 Pile-head load vs deflection for 48-in. pile during static loading

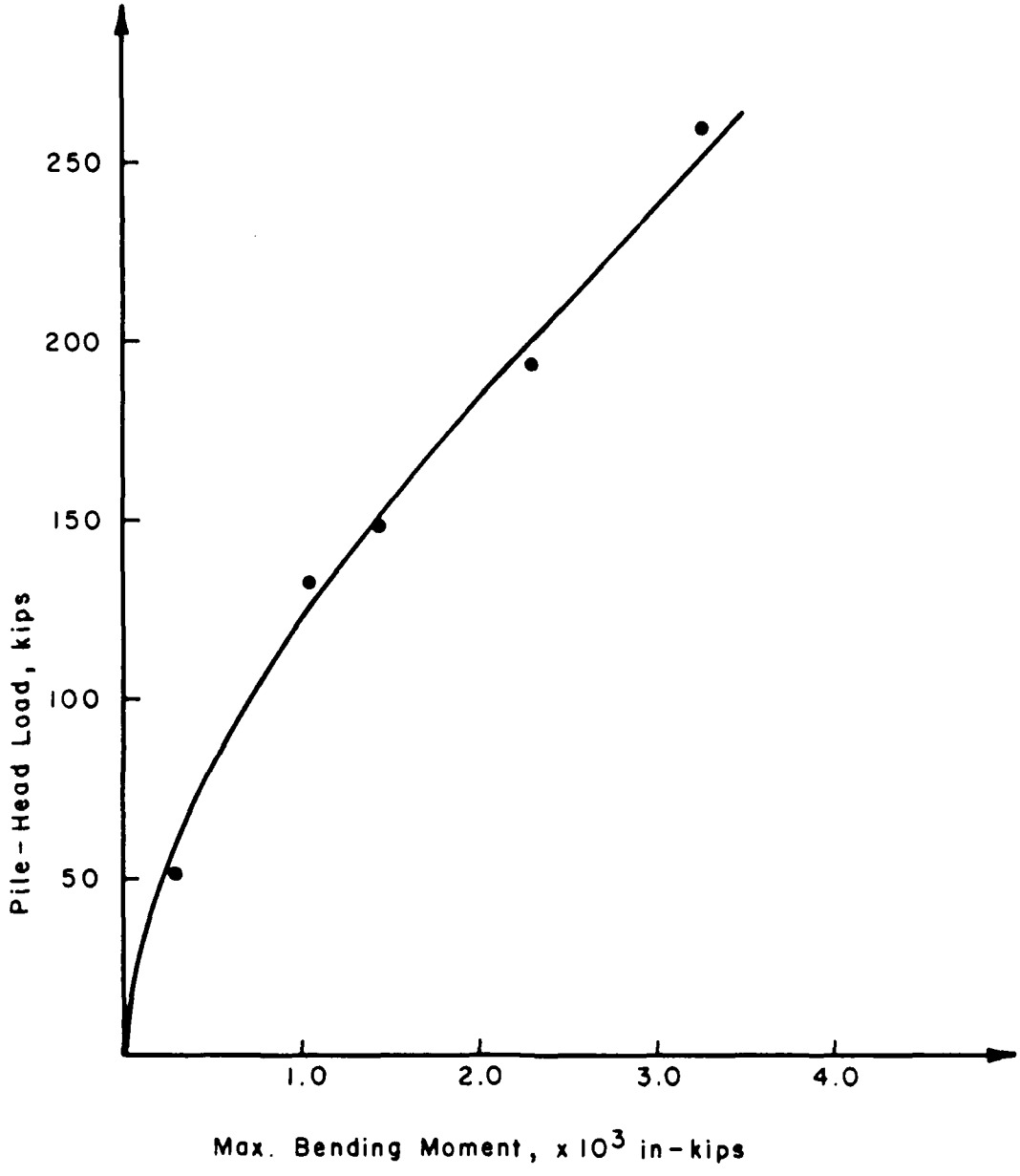

Fig. 3.4 Pile-head load vs maximum bending moment for 48-in. pile during static loading

loading (first cycle) from a depth of 12 in. to a depth of 72 in. are shown in Fig. 3.5. As was expected, the ultimate soil resistance increases with depth. Several of the curves exhibit severe dips in resistance at some deflections. It is believed that these dips were caused by soil softening due to cycling at lower deflection levels and inaccuracies in the numerical methods that were employed.

The current p-y criteria recommended by API (1980) did not adequately predict the soil resistance for the clay at this site. A modified (site-specific, SS) procedure for prediction was used for comparison with group test results. In the SS procedure, the ultimate soil resistance was calculated using

$$P_u = A\ c\ b + \gamma\ x\ b + B\ c\ x \qquad 3.1$$

where:

A = 0.8 (determined from the measured data),

B = 0.6 (determined from the measured data),

x = depth,

c = averaged undrained shear strength from the ground surface to the depth x,

γ = effective unit weight, and

b = pile diameter.

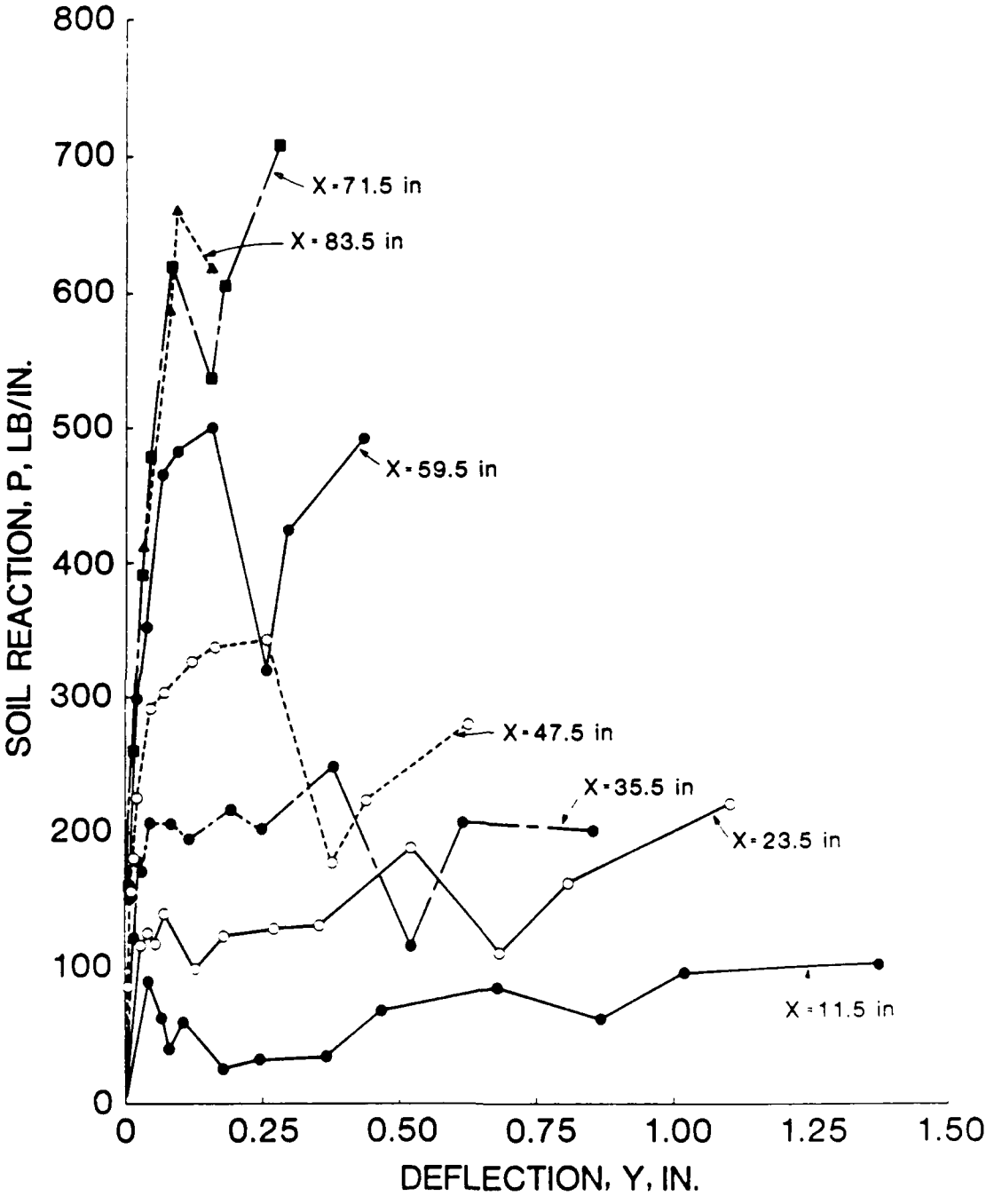

Fig. 3.5 Experimental first-cycle p-y results, 10.75-in. pile

The measured ultimate soil resistance is significantly lower than expected due to the following possible reasons.

1. There was wide scatter in the results from the UU tests at shallow depths.
2. Values of undrained shear strength of clay vary widely with test type and soil type.
3. The soil at this site had a secondary structure that could affect shear strength as well as drainage.

Measured and Computed Results for Cyclic Loading

The lateral cyclic tests for 10.75-in.-diameter piles were performed by displacement-control, two-way cycles, in which the deflection both away from and toward the actuator were equal. It should be noted that a one-way cycle was used for the 48-in.-diameter pile when the applied load was above 93 kips.

Response of Pile

For cyclic loading, a number of cycles, up to 200 for each deflection, was applied to the single pile. The experimental results indicate that the pile-head deflections for 100 cycles are significantly greater than those for static loading(cycle 1) for both 12-in. and 48-in.-diameter piles as shown in Figs. 3.6 and 3.7, respectively. In order to observe cyclic-degradation effects, measured data for cycles 1, 10, 20, 50, 100, and 200 are all presented in Fig.

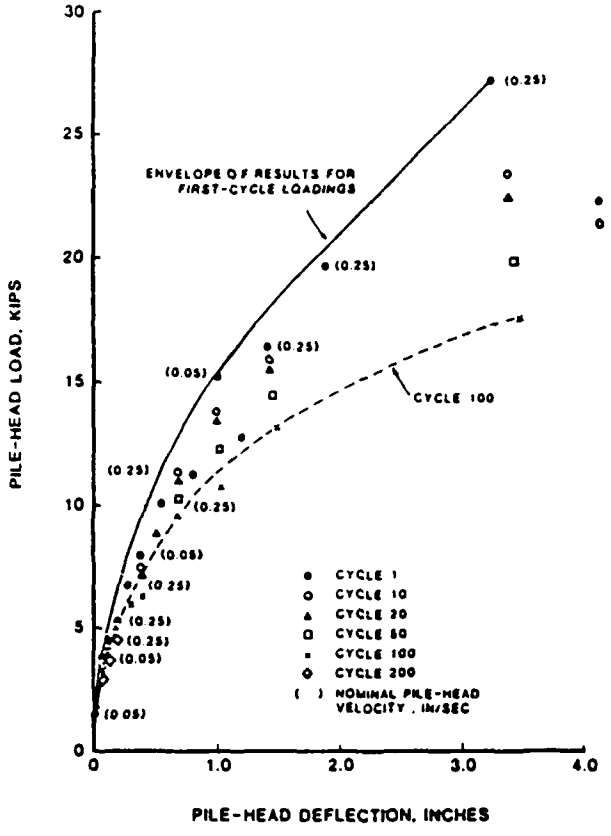

Fig. 3.6 Pile-head load vs deflection for 10.75-in. diameter pile during primary loading (after O'Neill and Dunnavant, 1984)

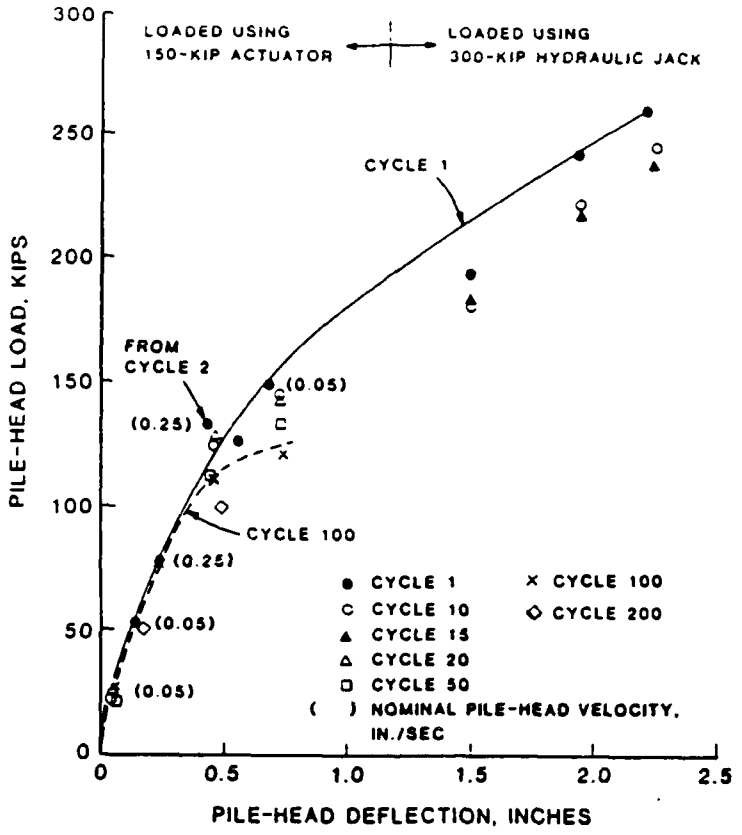

Fig. 3.7 Pile-head load versus deflection for 48.00-in. diameter pile during primary loading (after O'Neill and Dunnavant, 1984)

3.6 and 3.7. The following observations regarding the data are made:

(1) Cycle-degration effects become significant at deflections of about 0.8 percent of the pile diameter.

(2) At deflections greater than 0.8 percent of the pile diameter, the lateral stiffness of pile head, defined as pile-head shear divided by pile-head deflection, continuously degraded with increased numbers of cycles. The degradation did not stabilize after a given number of cycles.

(3) In the range of deflections where cyclic degradation was significant, loading to 100 cycles typically reduced the lateral stiffness about 25 to 30 percent with respect to the static loading (one cycle) for the 12.75-in.-diameter pile and approximately 16 percent for the 48-in.-diameter pile.

Some of the experimental moment curves for cycle 1 and cycle 100 for the same deflection are shown in Fig. 3.8. The moments are normalized by dividing by the pile-head load in order to compare curves for different loads. The experimental moments for 100 cycles, in general, are higher than those from static tests. It simply indicates that the soil resistance decreases due to the cyclic motion.

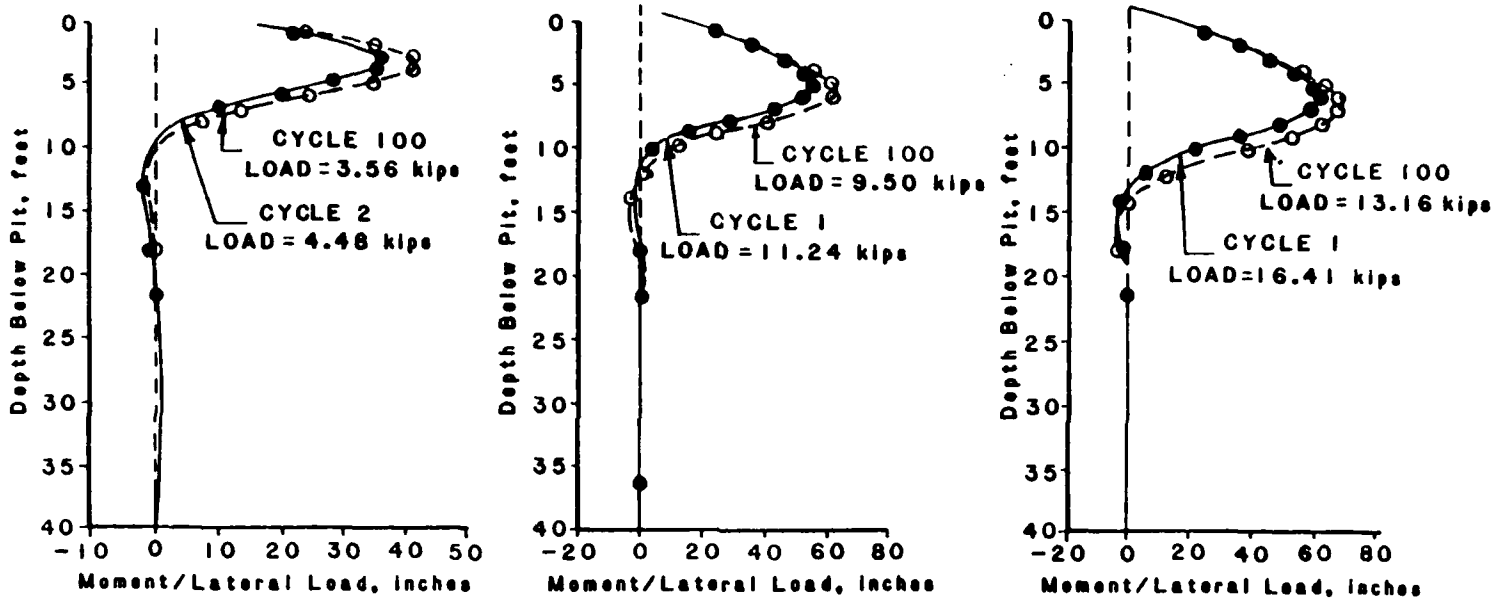

Fig. 3.8 Bending moment vs depth for single pile

Response of Soil

The soil-resistance curves for cyclic loading were derived from the bending-moment data. The p-y curves for cycle 1 and cycle 100, at depths of 48 in. and 72 in., are both shown in Fig. 3.9 for easy comparison. The data from all the cyclic p-y curves indicate that up to 100 cycles the ratio of maximum cyclic soil resistance, p_{cu}, to maximum static soil resistance, p_u, varied from 0.40 to 0.50 near the surface to a value of 0.70 to 0.75 at and below a depth of 4ft. The ratio had intermediate values between the surface and 4-ft depth. The cyclic p-y relations degraded to a residual value less than p_{cu} at each of depths shown. The degradation was essentially complete at a deflection of about $12y_{50}$. It is apparent that the soil resistance decreases with the increase in the number of cycles.

During testing, large gaps formed around each of the piles. Substantial clouds of fine-grained sediment were observed to be forced out of these gaps during cycling. Because the sediment pumped out of the gaps was gray and the soil surface predominantly brown, the effect was very noticeable. Figures 3.10 and 3.11 show the estimated gap size at the end of the primary testing for the 10.75-in.-diameter pile and the measured gap size for the 48-in.-diameter pile. Volumes of about one cubic foot and five cubic feet of sand were used to fill the gaps of the 10.75

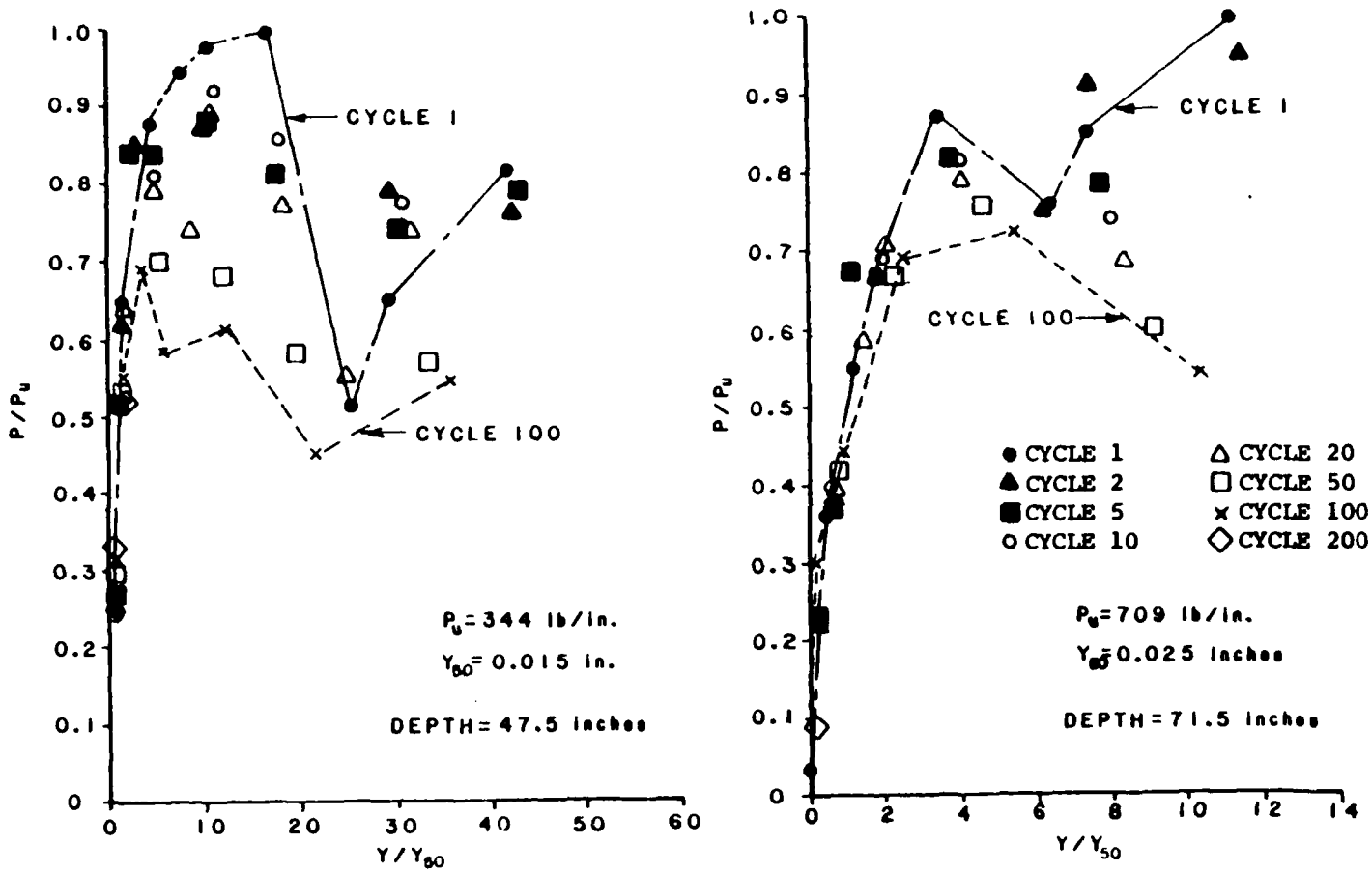

Fig. 3.9 Effect of repeated loading on normalized p-y response for single pile at selected depths

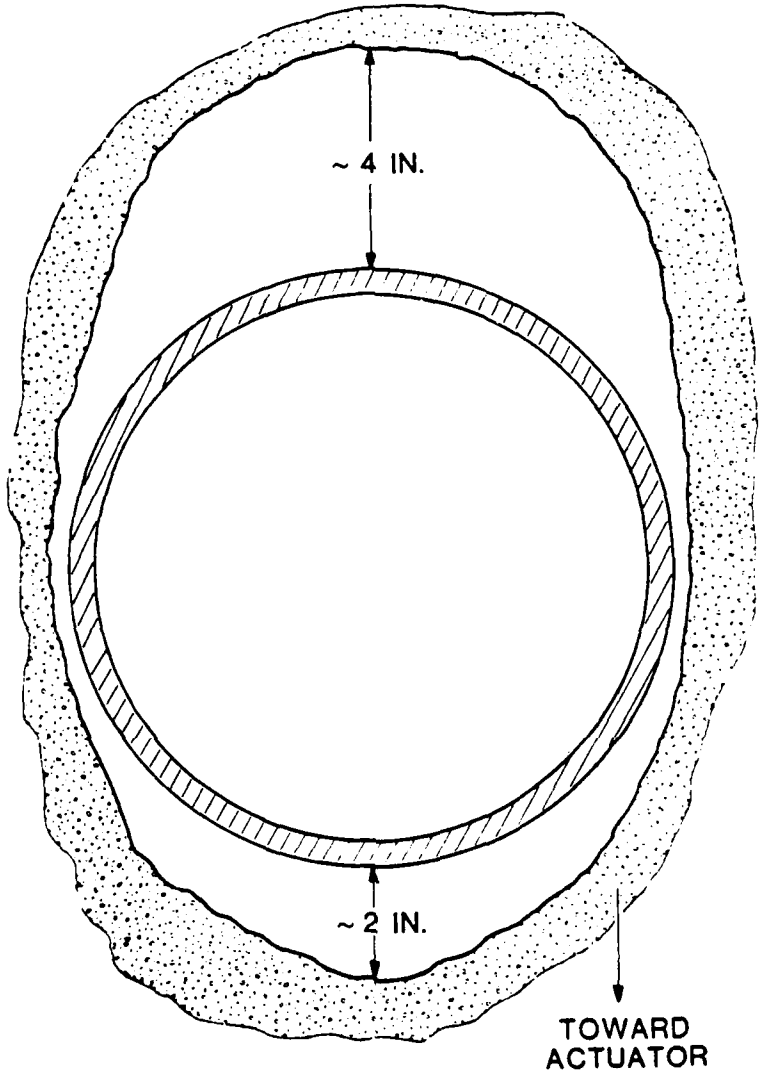

Fig. 3.10 Ground surface gap around 10.75-in. pile at end of primary testing. Gap size is estimated.

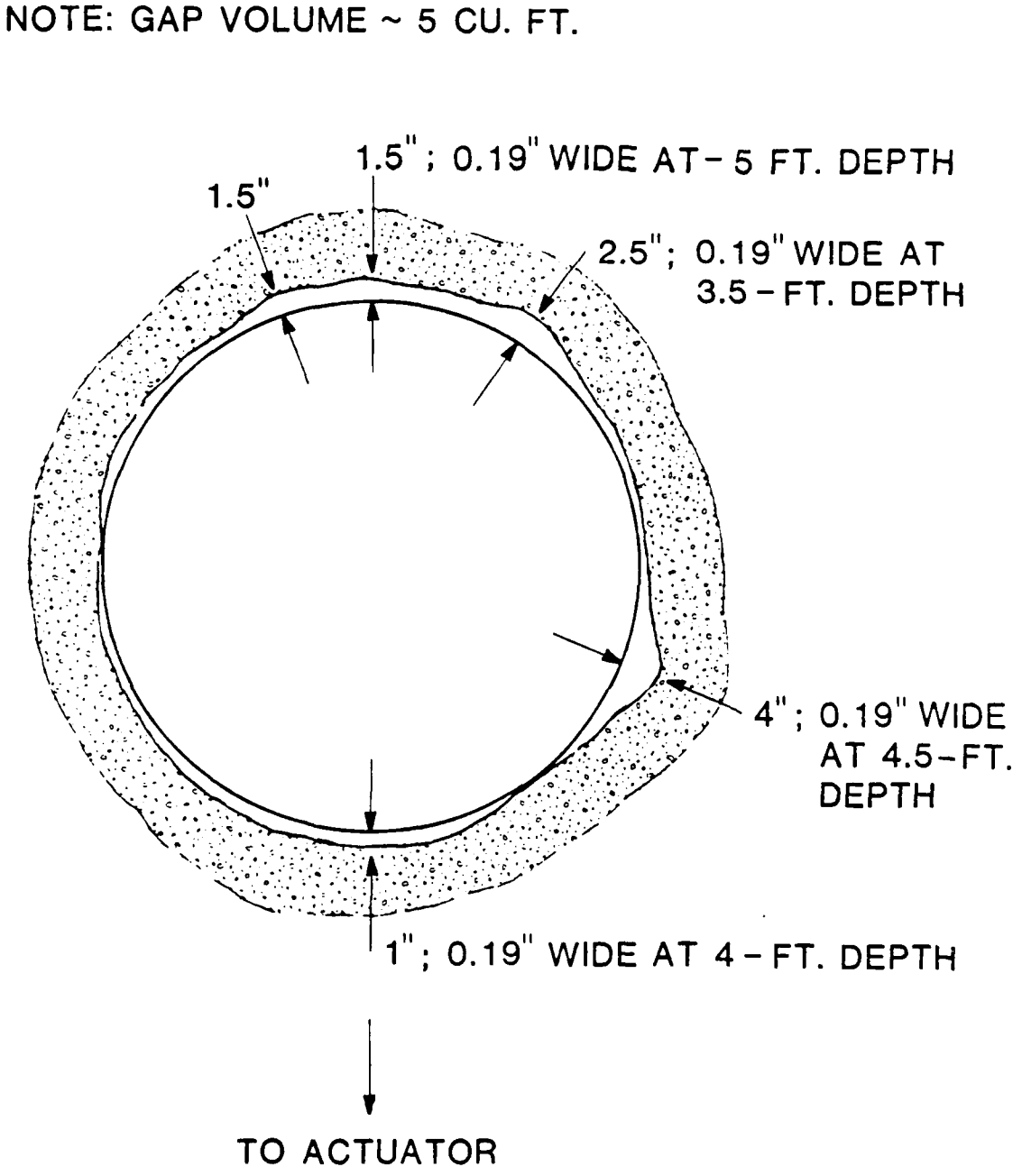

Fig. 3.11 Ground surface gap around 48-in. pile at end of primary testing

in. and 48 in. diameter piles, respectively. It is apparent that the scouring during cyclic loading will have significant influence on the soil resistance. However, there is at present no available method to quatitatively calculate the percentage of loss of soil resistance due to scouring.

Behavior during the healing and sand-filled tests are shown by the curves in Fig. 3.12. It should be mentioned that all of the tests after filling the gaps with sand were performed after the pile had been deflected 4 in. and after some plastic strains had occurred in the pile. The lateral pile-head stiffnesses for each series of tests are well below those obtained during primary loading. A comparison of the results between the primary tests and the healing tests indicates some of the original soil resistance was destroyed. The sand placed in the pile-soil gap was not effective in producing a regain in lateral capacity. The reduction of pile-head stiffness with increasing deflection during cyclic loads must be taken into account.

Concluding Comments for Single Piles in Stiff Clay

The results of lateral load tests for a single pile in clay have been summarized in this section. Based on the results presented, the following conclusions can be drawn.

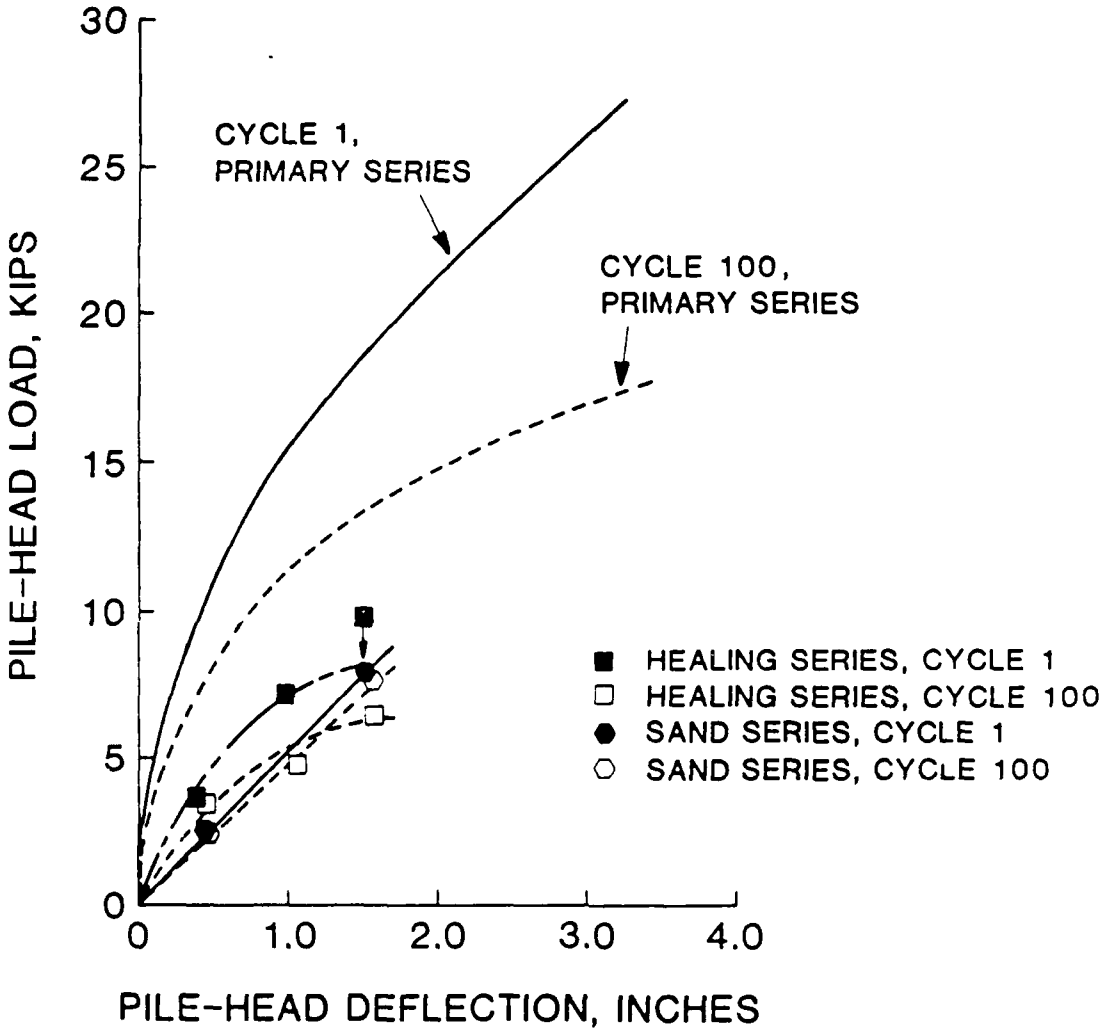

Fig. 3.12 Pile-head load vs deflection for 10.75-in. pile during healing and sand series

1. The response of single piles to static loading is stiffer than that to cyclic loading.

2. The maximum bending moment in a pile measured for cyclic loads is greater than that for static loading under the same deflection at the pile top due to a softened soil resistance.

3. The current p-y criteria recommended by API-RP2A does not accurately predict the soil resistance for soils encountered at the test site. Modified procedures for the prediction of p-y curves are recommended.

4. The scouring during cyclic loading in stiff clay has significant influence on the soil resistance.

BEHAVIOR OF GROUPS OF PILES IN STIFF CLAY SUBJECTED TO LATERAL LOADING

This section is subdivided into two parts. The first presents the major results of the experimental program and provides a comparison of the pile group behavior with that of the single pile for monotonic and cyclic lateral loading. The second section presents some predictions using available analytical procedures and comments upon the ability of these procedures to model the most important effects of pile-soil-pile interaction in pile groups.

Results of the Pile Group Experiment and Comparison of Pile Group Behavior with Single Pile Behavior

General Response

Load-Deflection Response The general load-deflection response of the pile group and the single pile are presented in Fig. 3.13 in terms of average pile-head load vs pile-head deflection. For the piles of the group, average pile-head load is defined as the lateral load on the group divided by nine, the number of piles. Curves of load vs deflection are presented for cycle 1 (monotonic loading) and cycle 100 (cyclic loading). As described in previous sections of this report, loading consisted of 2-way cyclic loading at constant peak deflection. The monotonic loading is thus not a true "static" loading, but is thought to be representative of the static loading because relatively wide separations between load levels were used. Curves for other than 1 and 100 cycles are presented in the detailed report by Brown and Reese (1985). Data points shown in Fig. 3.13 represent the load and deflection measured in each of two directions; the load-deflection response in the two directions was similar, but not identical.

The data presented in Fig. 3.13 clearly indicate that significant group effects exist; the group capacity appears to be greatly reduced relative to the single-pile capacity in

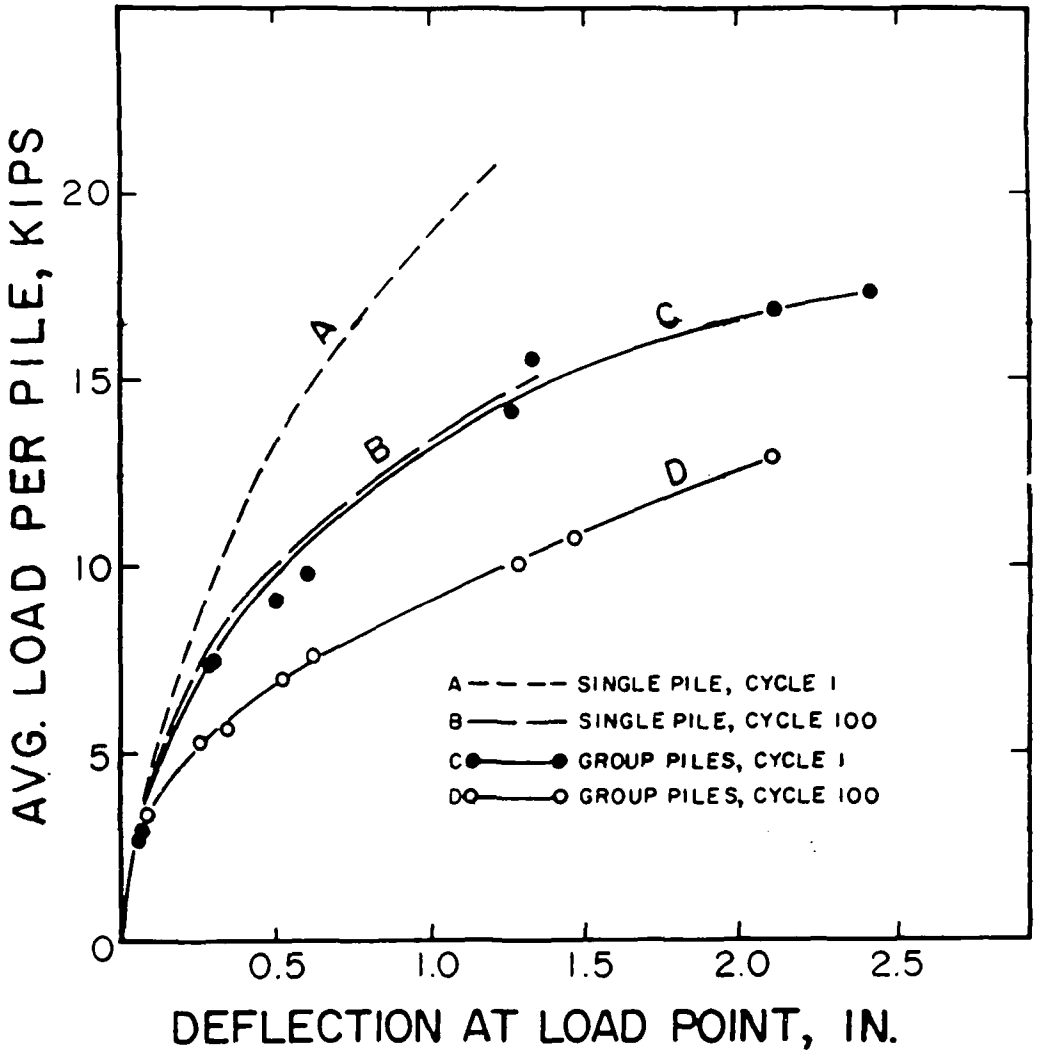

Fig. 3.13 Curves showing deflection of piles as a function of lateral load

terms of the average load per pile. The group effects are observed to be small at loads less than about 5 kips per pile, but become more significant with increasing load level.

Bending Moments The maximum bending moments for the piles in the group and for the instrumented single pile are presented as a function of lateral load in Fig. 3.14. A range is shown for the piles in a group that encompasses the variations for a given load (expressed as an average load per pile). The line marked "average pile" represents an average in the sense that the bending moments for the piles at each gauge station were averaged; because all of the piles did not attain the maximum moment at the same depth, this line represents the maximum of the average moments rather than an average of the maximum moments.

The data presented in Fig. 3.14 exhibit a similar trend to that observed for the load versus deflection of the pile head. The piles in the group behave similarly to the single pile at average pile-head loads of about 5 kips per pile or less, but the difference in behavior increases with increasing load. Maximum bending moments in the group piles were typically 25 to 30 percent higher than those in the single pile for a given pile-head load at loads approaching failure in the piles.

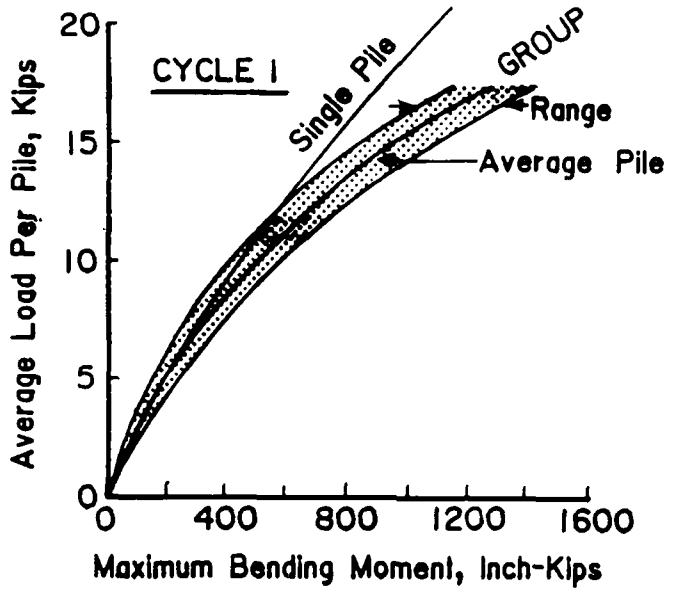

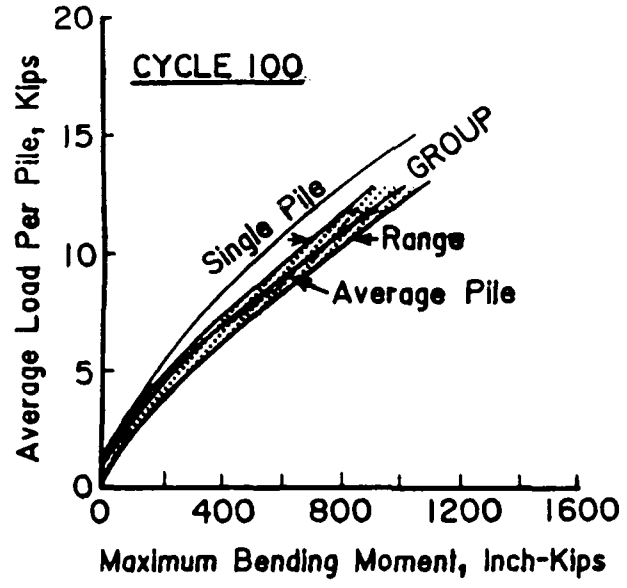

Fig. 3.14 Maximum bending moment as a function of lateral load

Cyclic Loading A comparison of the effects of cyclic loading on the piles in the group relative to that of the single pile indicates that cyclic loading has a significant effect on the piles in the group. Data plotted in Fig. 3.15 illustrate the magnitude of pile-head deflection and maximum bending moment for cyclic loading (cycle 100) relative to monotonic loading (cycle 1) for both the single pile and piles in the group. The terms "Deflection Ratio" and "Moment Ratio" as used in Fig. 3.15 are defined as follows:

$$\text{Deflection Ratio} = \frac{\text{Pilehead Deflection at 100 Cycles}}{\text{Pilehead Deflection at 1 Cycle}}$$

$$\text{Moment Ratio} = \frac{\text{Maximum Moment at 100 Cycles}}{\text{Maximum Moment at 1 Cycle}}$$

The relative increase in deflections and moments due to cyclic loading is seen to be proportionally greater for the group piles than for the single pile. The data plotted in

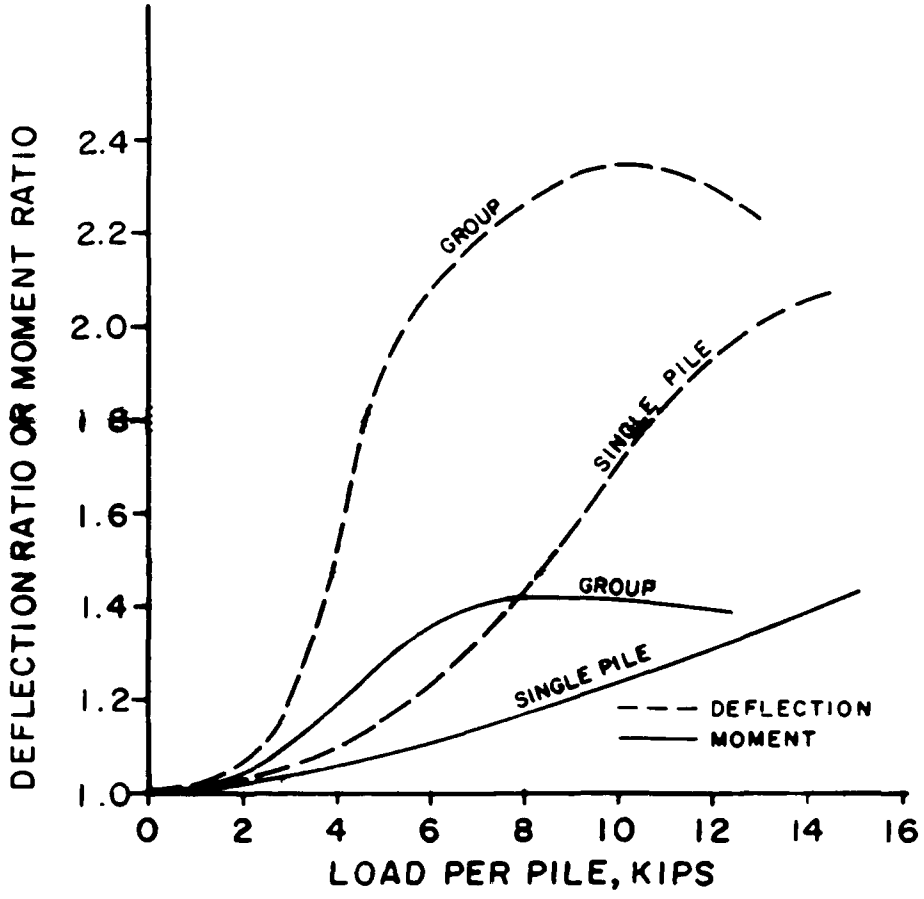

Fig. 3.15 Cyclic response normalized to static response

Fig. 3.15 also reveals that the effect of cyclic loading is increased with increased load levels.

The relatively more significant effect of cyclic loading on the piles in the group described above is quite surprising in that the major effects of cyclic loading in stiff clays has generally been thought to be more of an individual-pile phenomenon (McClelland (1974), Focht and Koch (1973)). The justification for this belief has been that effects of cyclic loading were thought to be dominated by gapping and scour in the immediate vicinity of each pile. As shown by the photographs in Fig. 3.16, the gapping around each pile in the group was significant; no evidence was observed of any connecting gaps or cracks between the piles. The scour due to rapid expulsion of water from the gap around each pile left a gray sediment covering the pit to a depth of several inches.

Distribution of Load to the Piles

Because a knowledge of the distribution of load to the piles in the group is important to understanding group effects and for proper design of piles in the group, this experiment was designed to allow independent measurement of the load transferred to each pile.

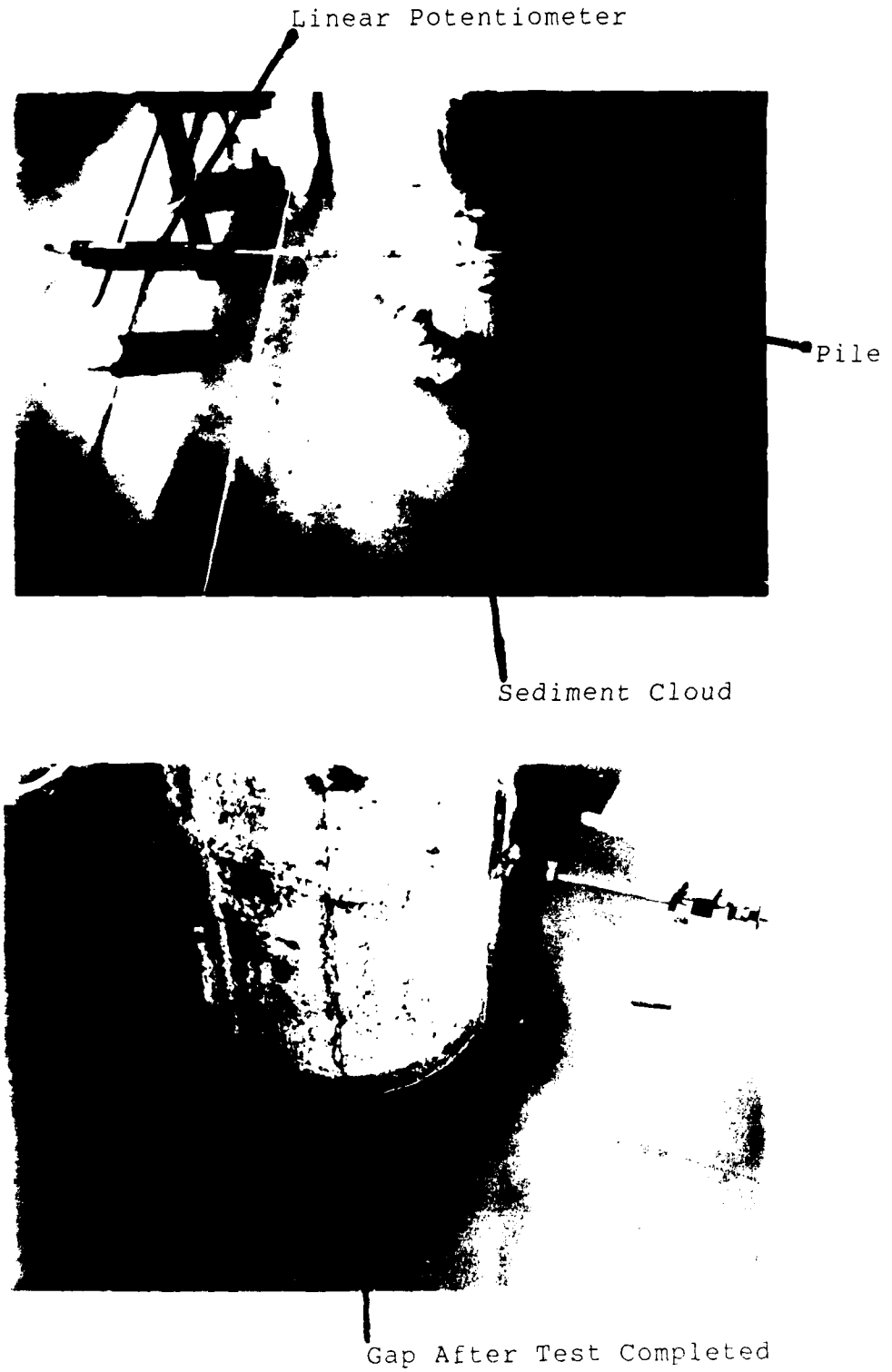

Fig. 3.16 Scour and gapping around piles

The results of the load measurements on individual piles indicate that the distribution of load was predominantly a function of row position within the group. No consistent trend was apparent regarding the effect of position within a given row (perpendicular to the direction of loading). Plotted in Fig. 3.17 is the general load-deflection response by row for both the monotonic and cyclic cases. Because measurements were made in each of two directions, the back row for the compression direction acted as the front row for the tension direction and vice versa. The data presented for a given row, therefore, represent an average of six piles for each row.

The distribution of load observed in this experiment follows a pattern quite different from that anticipated by elasticity-based procedures. The distribution can be thought of best as related to "shadowing" in which the trailing row piles are cast into the shadow of leading piles and are able to mobilize less soil resistance. Such patterns are likely related to areas of shearing deformation in the soil ahead of each pile as opposed to a simple superposition of elastic strains.

As is evident from the data presented in Fig. 3.17, the major effect of row position was at loads approaching failure. The maximum load applied to the trailing rows was

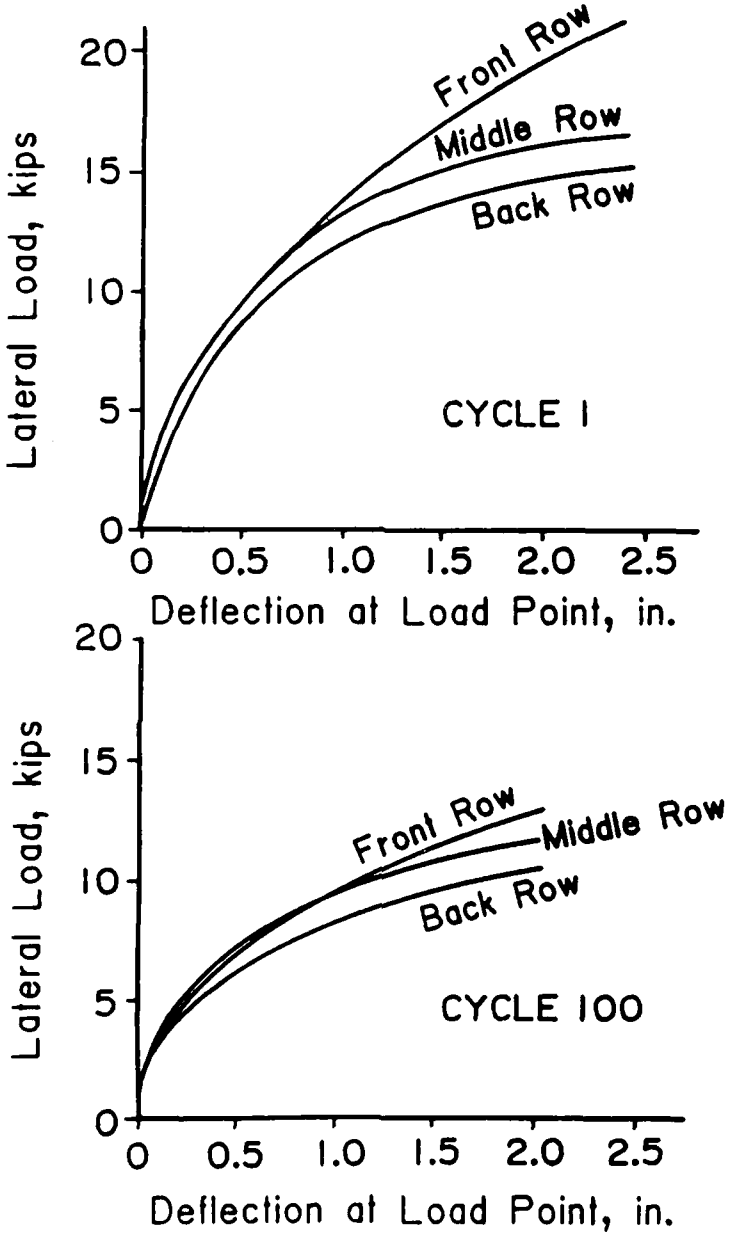

Fig. 3.17 Distribution of load by row

significantly less than the maximum applied to the front row. At loads approaching pile failure for monotonic loading, the front-row piles are seen to continue to carry load with increasing deflection while the trailing rows deflect without supporting additional load. There was little difference in behavior between rows up to about one-half the maximum load.

The relative difference between rows was less significant after 100 cycles of load, although a similar pattern is evident. The more heavily loaded piles apparently shed load with increasing number of cycles to less heavily loaded piles in the group, producing a more uniform distribution of load.

Row position also influenced the distribution of bending stresses, as illustrated by the data in Fig. 3.18. The figure presents plots of bending moment as a function of depth for selected loads that are typical of the observed patterns. The front-row piles have the largest moments in the upper 5 to 6 ft., reflecting the greater load on these piles. The middle-row piles have lesser moments in the upper 5 to 6 ft., but attain a higher maximum moment below that depth. The front-row piles are obviously transferring more load to near-surface soil than are the middle-row piles, thus accounting for the shallower depth to the peak moments in the front-row piles. The back-row piles have peak moments even

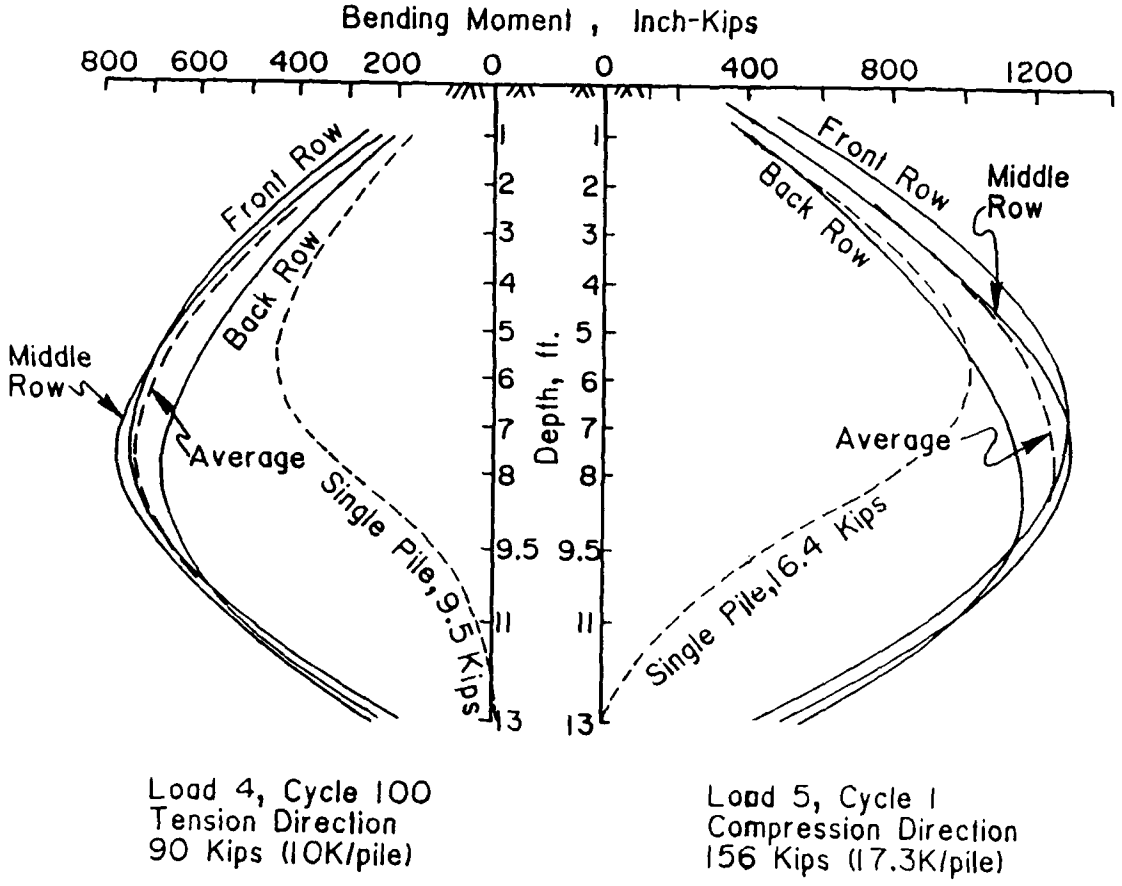

Fig. 3.18 Bending moment vs depth

deeper than the middle-row piles, but because less load was supported by these piles the absolute maximum moments in the group occurred in the middle-row piles.

In all rows the maximum moments were larger and occurred at a greater depth than for the single pile at a load similar to the average load per pile in the group.

As was the case for load-deflection response, cyclic loading tended to spread the loads and stresses in the group toward a more uniform distribution. The trends are similar, however. The data in Fig. 3.18 show that the maximum moments in the group after 100 cycles of load are larger and occur at a greater depth.

Load-Transfer (p-y) Curves

Using a Winkler-type soil model, polynomial curves were fitted to the bending moment data in a manner similar to that described by Matlock and Ripperger (1956) and described earlier in this report. This technique allows derivation of the load-transfer relationships (p-y curves) relating p, soil resistance per unit length of pile at a given point on the pile to y, horizontal deflection of the pile at that point.

Shown in Fig. 3.19 are the derived p-y curves for the piles at a depth of 4 ft. These curves are selected to be

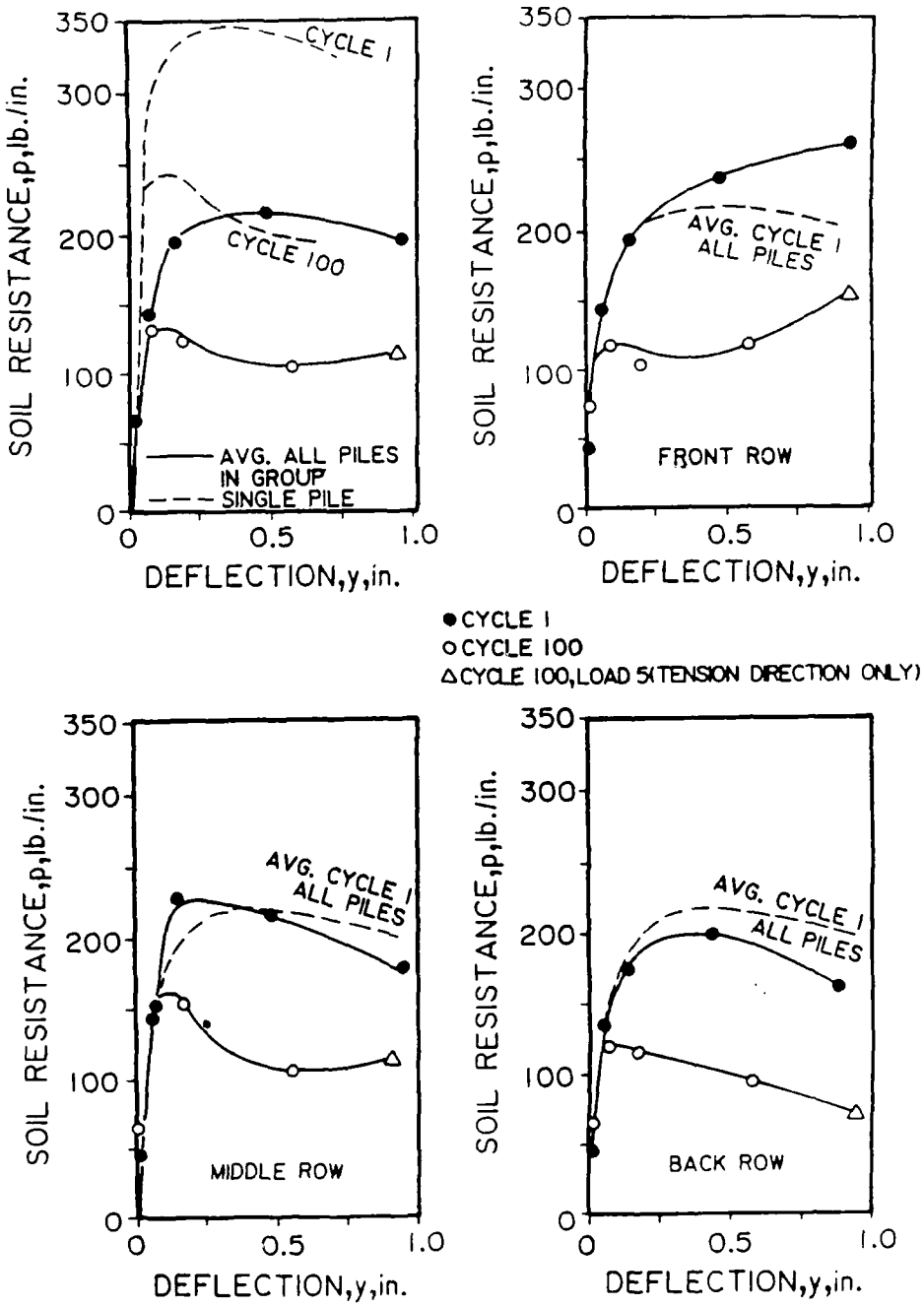

Fig. 3.19 Measured p-y curves, depth of 4 ft

representative of the trends exhibited at other depths (presented in detail in Brown and Reese, (1985)). The curves shown are averages for all piles and for piles in a given row for load cycles 1 and 100. A p-y curve from the single pile test at the same depth is also shown for comparison.

The major feature of the load-transfer relationships revealed by these data is the reduction in the maximum load transfer for the piles in the group relative to the single pile. Deflections at small loads are not significantly greater for the piles in the group than for the single pile.

The relative differences between rows in the group are less dramatic than between the group and the single pile, but the load-transfer curves vary with row position consistent with the trends revealed by the pile-head load-deflection response and the bending moment data. Deflections at small values of soil resistance are similar for all rows, but the maximum soil resistance diminished from front to back row. The shape of the curves suggests strain-hardening behavior for the front row p-y curves and strain-softening behavior for the trailing rows.

The p-y curves for cyclic loading exhibited similar trends for the group as for the single pile, with loss of soil resistance occurring during cyclic loading at values of

p greater than about one-half the maximum p value for monotonic loading. The maximum soil resistance after 100 cycles of load for the piles in the group is greatly reduced from that of the single pile after similar loading.

A comparison of the ultimate soil resistance mobilized by the piles in the group relative to that of the single pile is demonstrated in Fig. 3.20. Data from measured p-y curves are summarized in the form of a graph of ultimate soil resistance (taken as the last measured value) vs depth for monotonic (cycle 1) loading. Also shown is the predicted relationship using the 1980 API design rules (1979), that follow the guidelines of Matlock (1970):

$$p_u = 3 + \frac{\gamma}{b}(x) + \frac{J}{b}(x)(s_u)(b) \qquad 3.2$$

where: J = empirical constant, = 0.25 for many cases,

γ = effective unit weight of soil,

x = depth below ground surface,

b = pile diameter, and

s_u = undrained shear strength for UU triaxial tests.

The prediction using API rules was made with the undrained strength fro. 'U triaxial tests as stated in the API method.

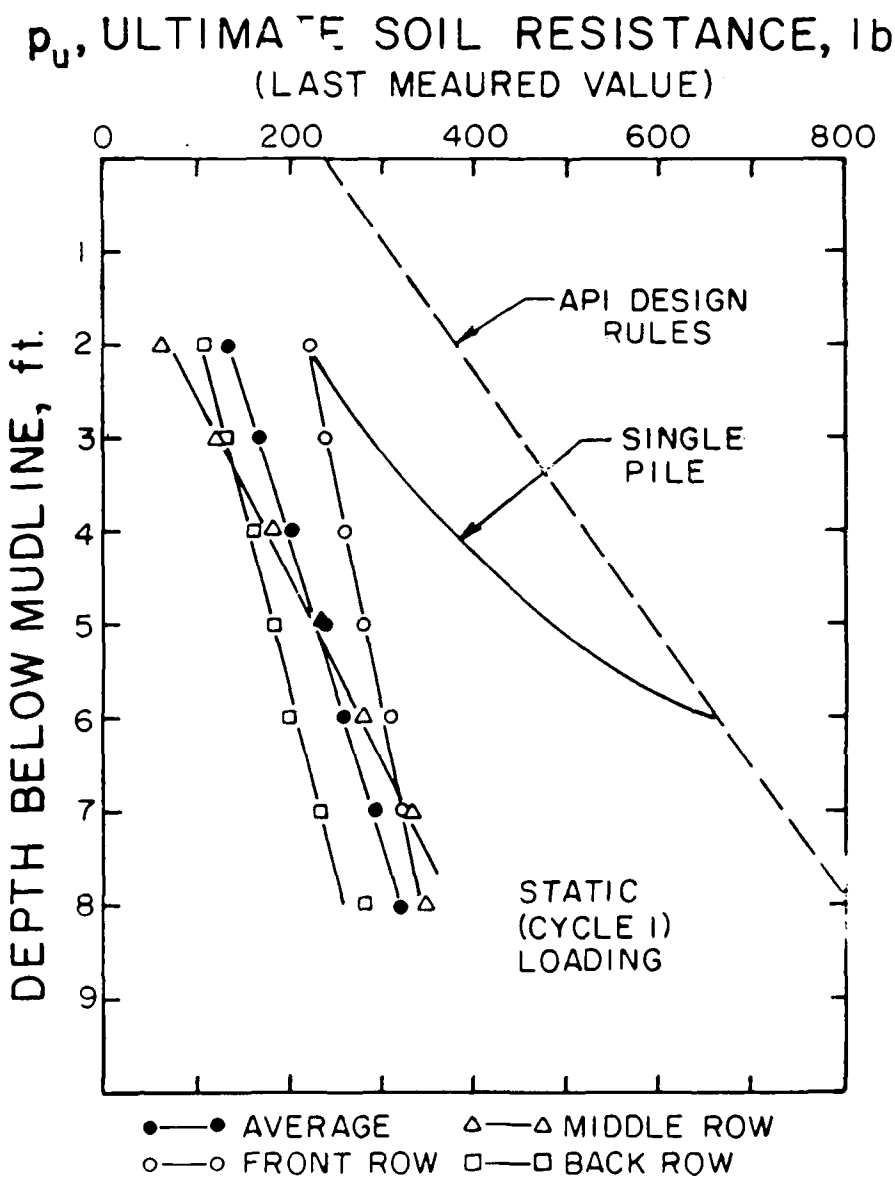

Fig. 3.20 Ultimate soil resistance vs depth

The data in Fig. 3.21 clearly illustrate the large and relatively consistent reduction in ultimate soil resistance due to group effects. The reduction in p_u is more pronounced with increasing depth and is generally greater for the trailing-row piles than for the leading row. An understanding of the mechanisms producing the loss of soil resistance is undoubtedly the key to understanding group effects for lateral loading.

The patterns of p-y responses for the piles in the group and for the rows within the group appear to be related to :

a) modification of the shear zone around the individual piles in the group by the surrounding piles, and/or
b) modification of the effective stresses around the individual piles in the group by the surrounding piles to produce a reduced shearing resistance of the soil.

It was noted previously that the maximum soil resistance mobilized after 100 cycles of load was considerably less for the piles in the group than for the single pile. This observation is in contrast with the widely used design assumption that the loss of soil resistance during cyclic loading is primarily a single-pile pheromenon, and that after many cycles of load the soil resistance in the piles of a

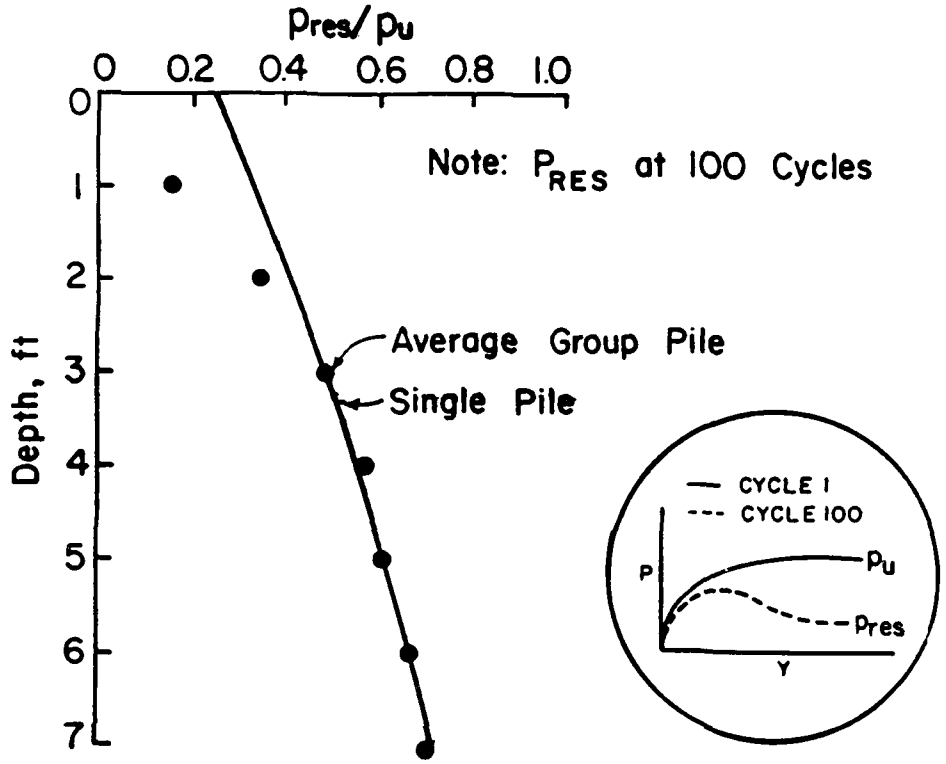

Fig. 3.21 Ratio of the values of residual soil resistance to the ultimate soil resistance

group is equal to that of an isolated single pile that is similarly loaded.

In Fig. 3.21 the ultimate soil resistance after 100 cycles of loading (labeled p_{res}) normalized by the ultimate soil resistance for monotonic loading (cycle 1) is plotted against depth for both the single and the average of the piles in the group. These data indicate that the loss of maximum soil resistance during cyclic loading is similar for the group and single piles when taken in proportion to the soil resistance for cycle 1. Based on these data, the effect of cyclic loading on piles in a group is more appropriately modelled as a proportional loss of soil resistance from some initial (cycle 1) value rather than as a loss to some absolute minimum value, independent from group effects.

Comparison of Experimental Results with Predictions Using Relevant Procedures of Analysis

Introduction

This section provides a comparison of the results of the group test in clay with the results predicted by use of analytical techniques that are available and widely used at the time of this study. A more complete description of these techniques and a detailed presentation of the predictions with these procedures is available in the report by Brown and

Reese (1985). The paragraphs which follow provide a brief discussion of the procedures and a summary of the relevant findings regarding the ability of the methods to reproduce the important aspects of the findings concerning pile-soil-pile interaction.

The analytical procedures can be categorized into two types. The first is an elasticity-based procedure in which the deformations at a given point within the group due to all of the other piles within the group, is computed using the equations of elasticity. These procedures generally use superposition of strains that are computed using Mindlin's equations, for strains due to a point load beneath the surface of an elastic half-space. These deformations produced by other nearby loads are then added in some manner to the deformations at a point that are predicted using a normal analytical procedure for an isolated pile. The procedures differ in the way in which the magnitudes of these point loads are determined, the way in which the strains are added to the single pile solution, and the type of single pile solution used. Elasticity-based procedures provide a rational method of predicting the distribution of load to the piles in the group as well as accounting for increased deflections of the group due to group interaction.

The second type of procedure (described as the "modified unit-load-transfer" model by O'Neill, (1983)) models the pile group as a large pile in which the pile group and the soil within the group area are assumed to move together. The stiffness of this large, imaginary pile is equal to the sum of the stiffnesses of the individual piles. The behavior of the group as a whole is analyzed by using p-y curves for single-pile behavior for this large imaginary pile. No means are available to predict the distribution of load to the piles with this type of procedure, but it does offer some rational way (albeit a purely empirical one) of predicting a loss in ultimate soil resistance due to group effects and cyclic loading.

Elasticity-Based Methods

Procedures of this type which were analyzed include the DEFPIG code which follows the well-known elastic method of Poulos' (1971,75), the Focht-Koch procedure (1973) developed to analyze offshore groups, and the code PIIGP2R developed by Ha and O'Neill (1981). DEFPIG is the most true to elasticity theory, although the authors make some provisions for local yield by including user-specified limits on soil resistance. DEFPIG extends Poulos' solution for flexure of a thin-strip pile within an elastic medium to pile groups in terms of two interaction factors. These are defined as the relative increase in deflection (or rotation) at the groundline of a

pile due to another pile. The computation of these interaction factors is made similarly to that for the single pile, except that the soil displacement must include the additional displacement due to the nearby pile. The DEFPIG code available to the authors did not have provisions for computing bending moments as a function of depth.

The Focht-Koch method represents an early attempt to combine the computation of pile-soil-pile interaction using Poulos' elastic solution with the widely used Winkler model for single piles which includes nonlinear p-y curves. The procedure consists basically of computing the displacement of an individual pile using the accepted beam-column procedure, and computing the increase in deflection due to pile-group action using the elasticity procedure. The p-y curves for the piles are then "stretched" by multiplying the y values on the curves by a constant until the beam-column solution yields a pile-head deflection equal to that computed for the group. The desirable features of the Focht-Koch procedure for designers are that the modification of p-y curves allows computation of bending stresses as a function of depth, the distribution of shear to the piles in the group is computed, and the use of nonlinear p-y curves allows cyclic-loading effects to be incorporated into the analysis.

PILGP2R is perhaps a logical extension of the Focht-Koch procedure in order to provide a more rigorous analytical model. This code was developed to model three-dimensional geometry of pile groups, to apply at working loads, and to yield behavior of axially-loaded groups of vertical piles for the full range of loading. The model differs from Focht-Koch in that the individual p-y curves on each pile are modified individually for the deformations produced by other piles. After solution of the group problem without pile-soil-pile interaction, Mindlin's equation is used to compute deformation at a p-y curve location due to all of the other p values at all of the other p-y curve locations within the group. The group problem is then resolved using the modified p-y curves, with additional iterations as necessary with modified p-y curves. PILGP2R is a powerful model but requires a large amount of computations.

The input parameters for all of these procedures were "fitted" to the experimental data for the single pile to minimize variability due to predictions of individual pile behavior and to concentrate on the modelling of pile-group effects. Where possible, a range in elastic moduli was used to examine the sensitivity of the predictions to relevant input parameters.

Presented in Figs. 3.22 through 3.24 are some of the predictions of load versus deflection for the pile group. It is clearly evident from these figures that the elasticity-based procedures did not predict the great increase in group deflection at large loads and tended to overpredict group deflection at small loads.

The elasticity-based predictions of load distribution to the piles in the group were significantly in error. The elastic solutions predict a symmetric distribution of load with the greatest proportion of load coming to the corner piles and the least to the center pile. No difference is predicted between the front and back rows. The actual distribution of load was predominantly associated with row position as discussed in the previous section. At small loads (which one would expect to be most realistically represented by elasticity), no distinct pattern of load distribution to the piles in the group was evident. In fact, at small loads there was no appearance of group effects at all.

As shown in Figs. 3.25 and 3.26, the Focht-Koch and PILGP2R methods at large loads underpredicted both maximum moments and depth to maximum moments at large loads. Consistent with the load-deformation predictions, the methods overpredicted moments somewhat at small loads. With

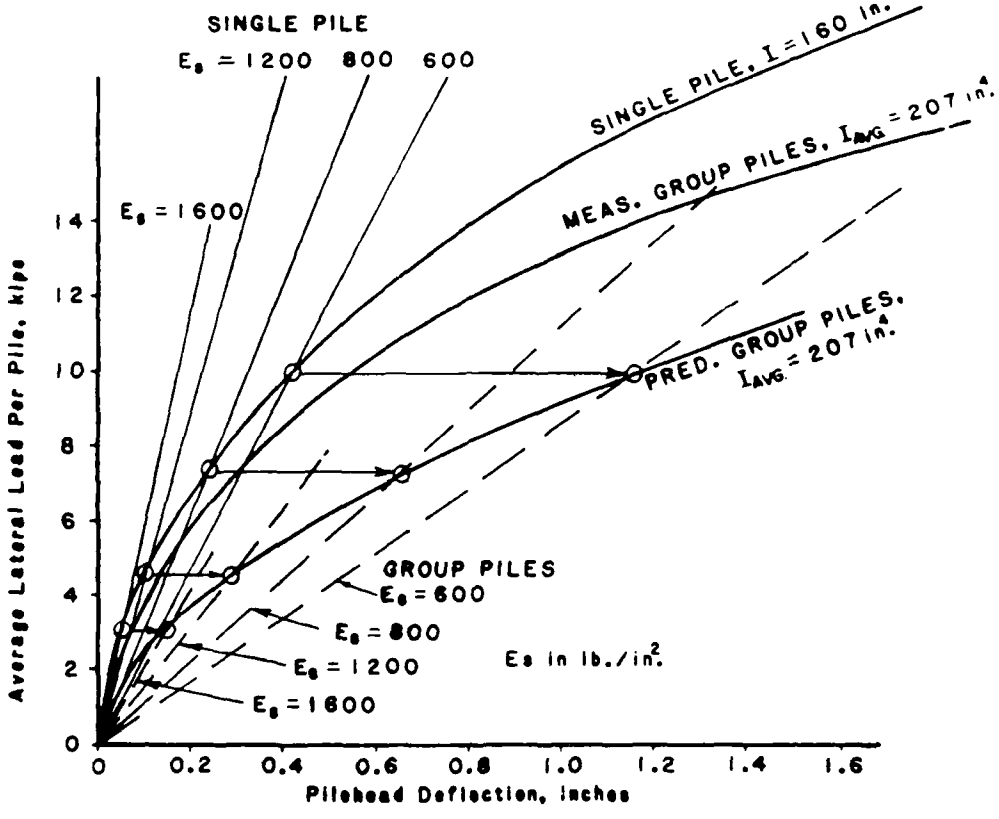

Fig. 3.22 DEFPIG of lateral load versus deflection at working loads using constant E_S by DEFPIG method, fitted to single pile data

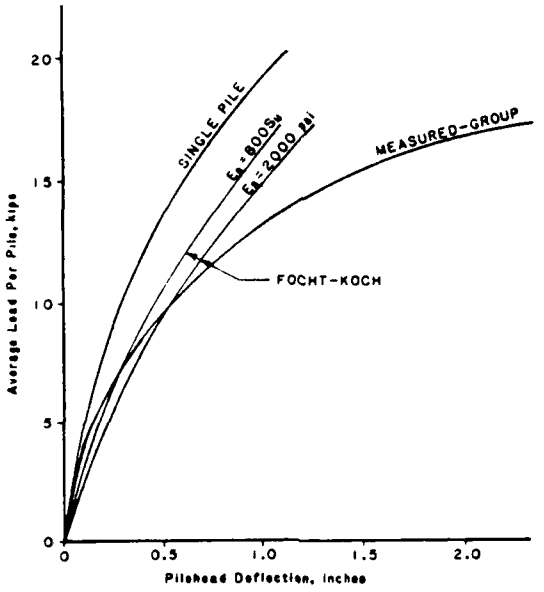

Fig.3.23a. Predictions of lateral load vs deflection by use of Focht-Koch Method, Cycle 1 (static)

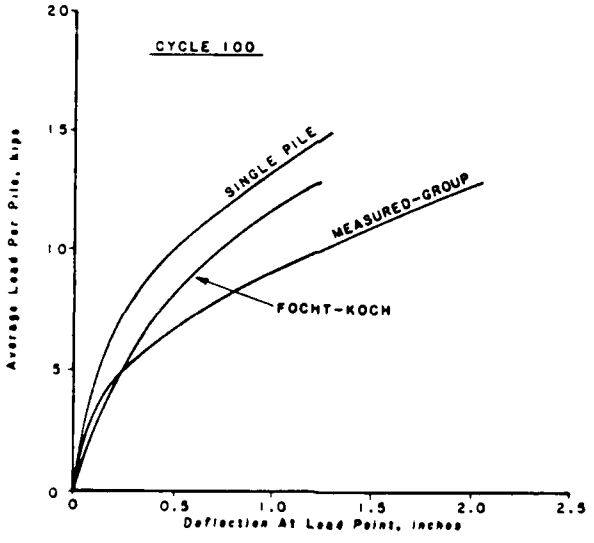

b. Predictions of lateral load vs deflection by use of Focht-Koch Method, Cycle 100

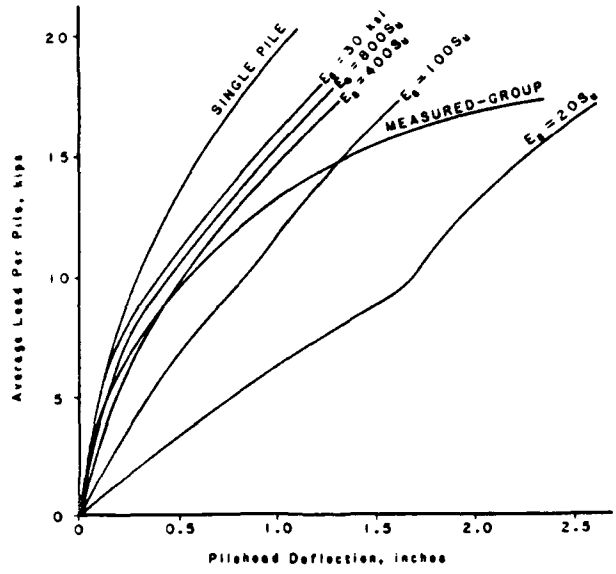

Fig. 3.24a. Predictions of lateral load vs deflection by use of PILGP2R Method, Cycle 1 (static)

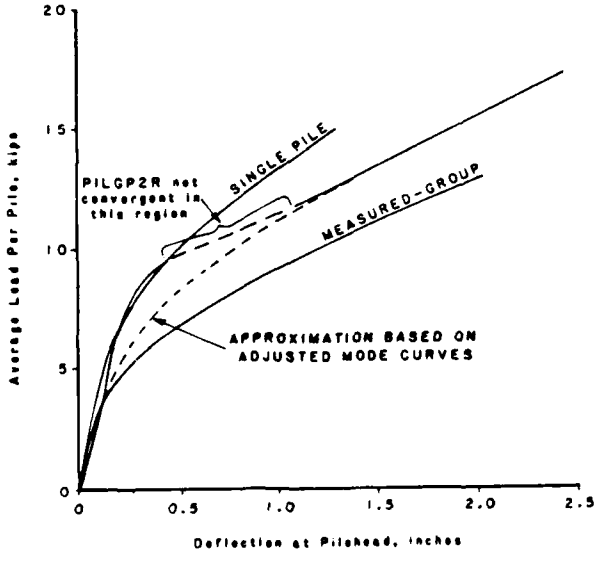

b. Predictions of lateral load vs deflection by use of PILGP2R Method, Cycle 100

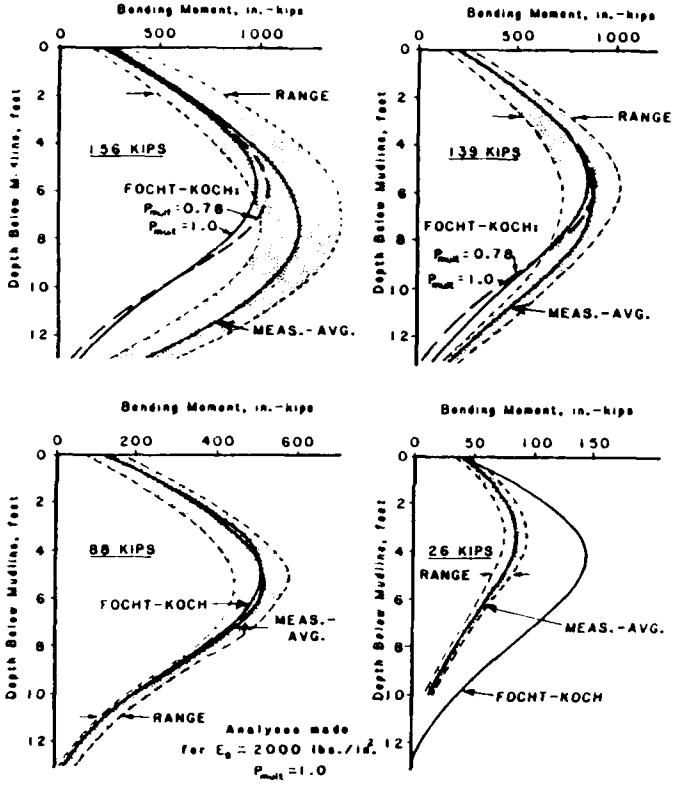

Fig. 3.25 Predictions of bending moment vs depth by Focht-Koch method, Cycle 1 (static)

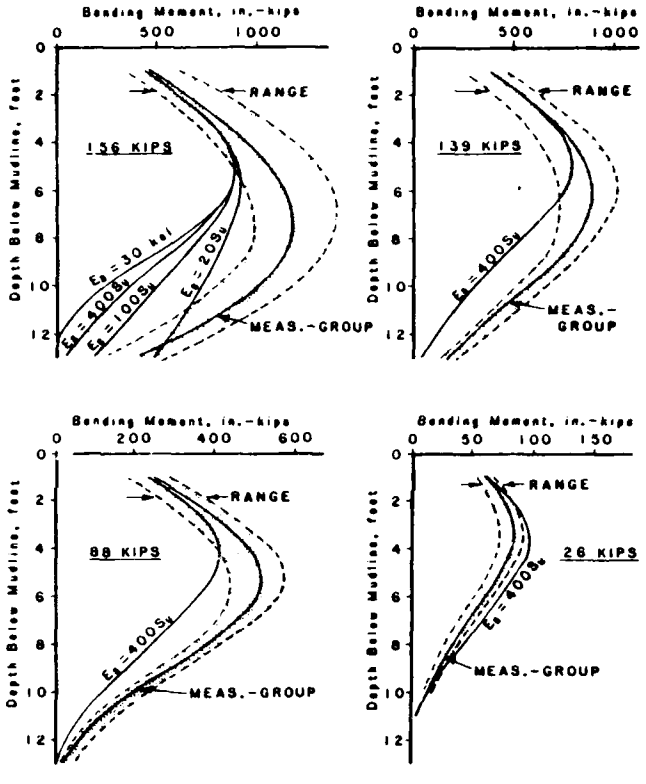

Fig. 3.26 Predictions of bending moment vs depth by PILGP2R method, Cycle 1 (static)

increasing loads, the depth to maximum moment in the experiment was observed to shift significantly deeper. These procedures do not reproduce this shift of depth to maximum moment.

In conclusion it can be stated that the superposition of elastic deformations did not model the most significant factors that influence group behavior. The group effects observed in the experiment were highly nonlinear and associated with shadowing and row position of the piles; the elasticity-based procedures did not reproduce these effects. Although one might suggest that elastic solutions could best represent group behavior at working loads, there was no evidence in this experiment that group effects at small loads were significant. Furthermore, without a knowledge of the failure loads for the group (which was unconservatively predicted by these procedures) one has no guidance as to what level of loading might appropriately be called "working" load.

Modified Unit-Load-Transfer Models

Procedures included in this category include the single-pile method and the Bogard-Matlock method. The former is not really a formal method of analysis which has been described and reviewed in the technical literature, but rather a means of providing an upper bound on the predicted response of a

pile group. All of the piles in the group, along with the soil within the group are assumed to act as one unit. This assumption should thus represent the extreme of group interaction in which the behavior of an individual pile is insignificant. The response is computed by analyzing a large, imaginary pile which has a flexural stiffness equal to the sum of the stiffnesses of the individual piles. The diameter of the imaginary pile is taken as the diameter of a circular pile having the same area in plan as that of the group. For this case, that diameter is 85 inches. Obviously, no predictions are made about the distribution of loads and stresses to the piles. Bending moments are estimated by dividing the moment computed for the large, imaginary pile by the number of piles in the group.

The Bogard-Matlock procedure (1983) is an extension of the concept of the single-pile method and provides a more formalized procedure for limiting the ultimate soil resistance. The procedure combines the single pile p-y curves with a modification of the p-y curves for a large, imaginary pile (similar to that described in the paragraph above) to produce p-y curves for the analysis of a generic pile in the group. All piles in the group are assumed to behave in the same manner. Although the authors recognize that such behavior is not necessarily the case (their procedure is not represented as a rigorously correct

solution), they propose that variations are small and can adequately be accommodated by a small overdesign. This procedure was derived from an experimental study of circular groups of 5 to 10 piles with 6-inch diameter (Matlock et al, 1980). The test site was located in Harvey, Louisiana, and consists of soft clay.

Because both of the methods described above involve the use of empirical p-y curves for a large, imaginary pile, these procedures are quite sensitive to the particular criteria used for generating the p-y curves. Of special importance is the influence of diameter on the predicted p-y response, a subject about which there is widespread disagreement for even isolated piles. The p-y criteria for soft clay (SO) recommended by Bogard and Matlock in their procedure, was used in these analyses, but the SO procedure did not reproduce accurately the response of the isolated pile. The site-specific criteria (SS), described previously, was also used. The SS curves are thought to represent the best use of the methods in principle, because the use of those curves actually will yield results that match results of the test of the single pile. However, the SS p-y curves, derived from a modification of the SO curves, are not unique in that other criteria could also be used to match the single-pile data. The use of a different form for the p-y curves would result in different predictions for the

imaginary pile and subsequently would produce different predictions for the group. Such is always the problem with a method so dependent on empirical correlations; the approach used herein represents an attempt to follow Bogard and Matlock's concepts as closely as possible and still provide feedback on the validity of the approach.

Presented in Figs. 3.27 and 3.28 are the load-deflection predictions with the two modified unit-load-transfer procedures. It is evident that these procedures significantly overpredict deflections for a given load for cycle 1. The single-pile procedure was not used to predict the 100 cycle behavior because the gapping and degradation around a large imaginary pile due to cyclic loading did not appear to be relevant to this problem (no such large gap occurred in the field experiment). The Bogard-Matlock method was used to predict cyclic response with the SS criteria and appeared to yield excellent results; this good agreement is fortuitous, however, and is due solely to the fact that the method grossly overpredicted the cycle-1 deflections. The loss in lateral resistance due to cyclic loading is very much underpredicted relative to the cycle-1 data.

The predictions of ultimate soil resistance and bending moment vs depth, shown in Figs. 3.29 and 3.30, give some indication of the effects of the Bogard-Matlock modifications

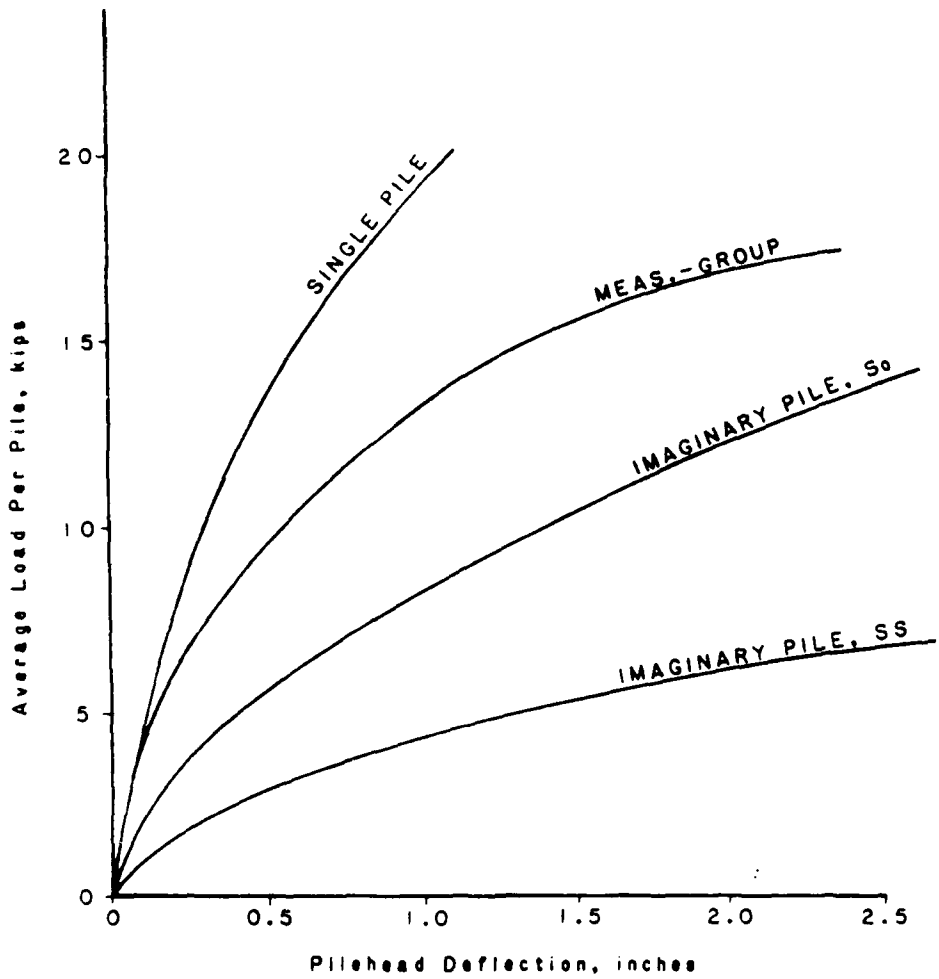

Fig. 3.27 Predictions of load vs deflection by single-pile method, Cycle 1 (static)

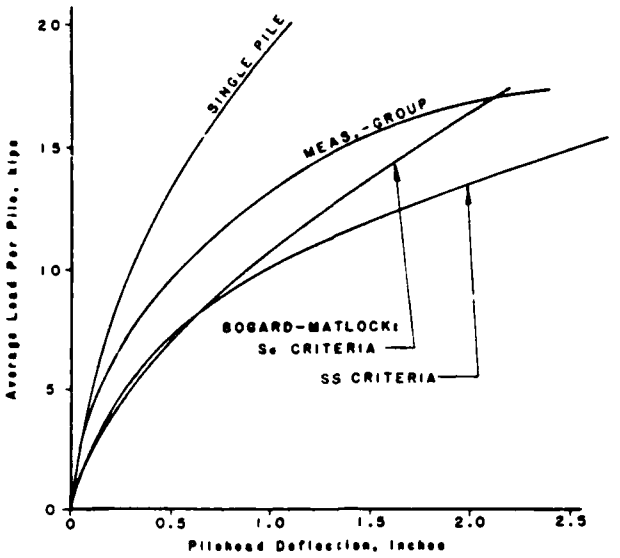

Fig. 3.28a Predictions of load vs deflection by Bogard-Matlock method, Cycle 1 (static)

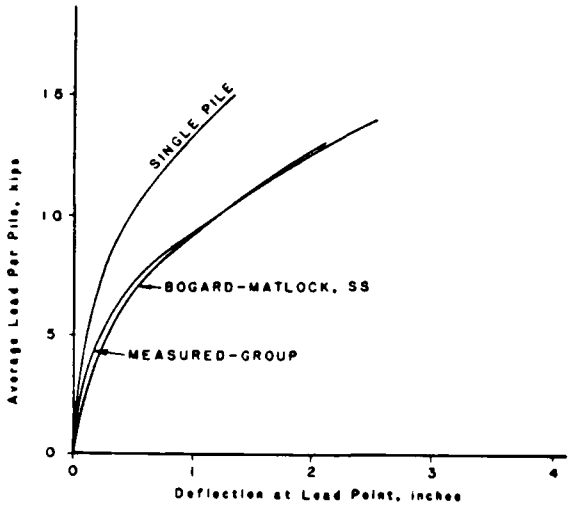

b. Predictions of load vs deflection by Bogard-Matlock Method, Cycle 100

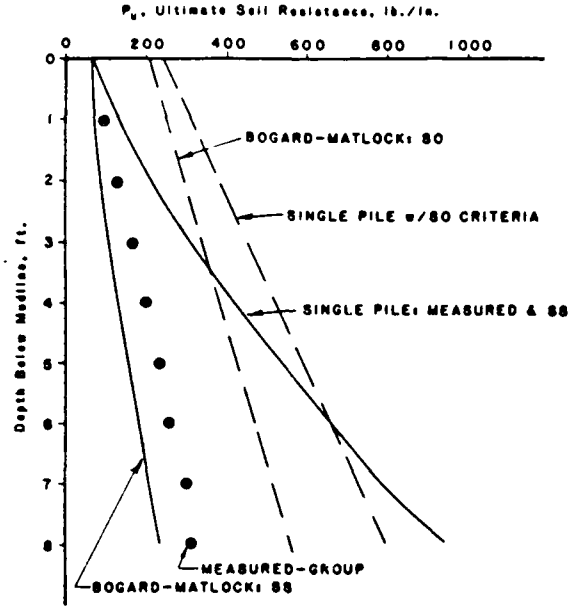

Fig. 3.29 Predictions of ultimate soil resistance vs depth by Bogard-Matlock method, Cycle 1

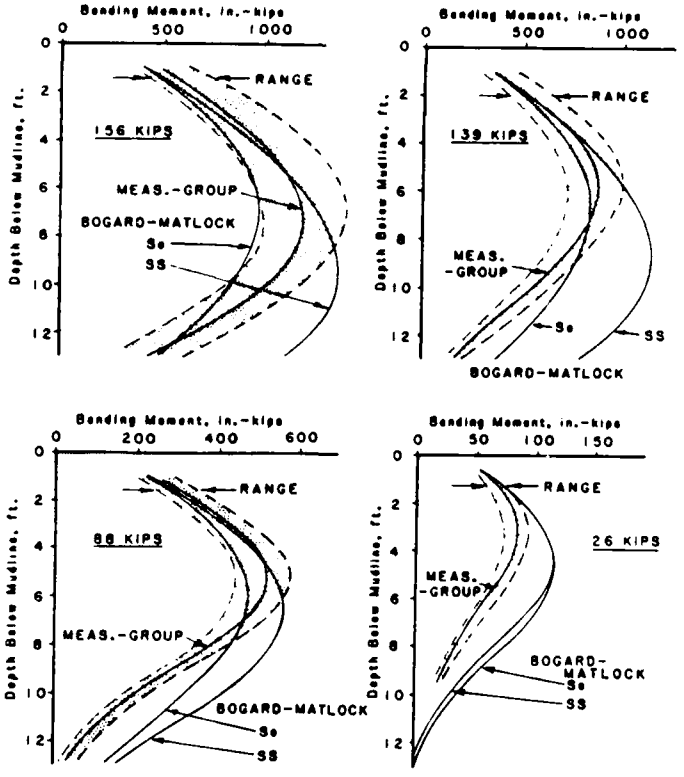

Fig. 3.30 Predictions of bending moment vs depth by Bogard-Matlock method, Cycle 1

to the p-y curves. The procedure appears to match the trend of the reduction in soil resistance with depth that was observed in the experiment; the SO criteria originally proposed by Bogard and Matlock for soft clay predicts only a small loss due to group effects while the extension of the method with the SS criteria overpredicts the loss in soil resistance somewhat. Bending-moment predictions indicate an increasing depth to maximum moment with increasing loads, and are conservative for the SS criteria.

With regards to cyclic loading, the predicted load-deflection response was observed to be quite good for the SS criteria; this agreement is attributed largely to the fact that the cycle-1 soil resistance was significantly underpredicted. As shown in Fig. 3.31, the reduction in soil resistance due to cyclic loading is greater than that predicted by the Bogard-Matlock procedure when normalized to the cycle-1 data. If the Bogard-Matlock predictions of cycle-1 behavior had been more nearly correct, the cyclic response would have been unconservatively estimated.

In summary, it can be stated that the model proposed by Bogard and Matlock is the only design procedure reviewed which predicts trends of nonlinearity in group response due to reduced ultimate soil resistance of the piles in the group. This appears to be the key to accurate prediction of

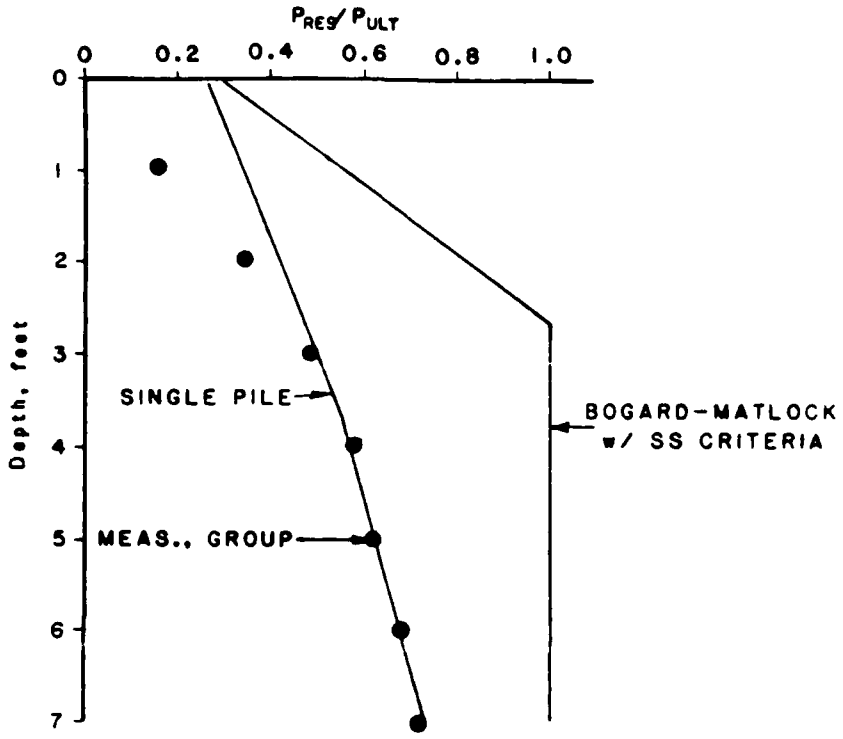

Fig. 3.31 Predicted ratio of P_{RES} to P_{ULT} vs depth using Bogard-Matlock procedure

group response. However, the method is empirical and based upon the results of a single experimental study (the test program at Harvey, Louisiana). Some elements of the procedure appeared arbitrary because of forcing a fit with the test data. Although Bogard and Matlock do not claim their method to be a rigorously correct solution, the application of such an approach to design problems is extremely sensitive to calibration to experimental data and to the p-y criteria that are used. This sensitivity does not encourage designers to use the method without caution.

CHAPTER 4
BEHAVIOR OF LATERALLY LOADED PILES AND PILE GROUPS IN SAND

In addition to the research in the native Beaumont clay, a study was made to investigate the behavior of pile groups in sands. The work in sand took maximum advantage of the existing group of instrumented piles and the testing arrangement. An excavation was made to a significant depth in the clay and sand was placed under controlled conditions. The sand was saturated by introducing water at the bottom of the excavation. The test setup is described briefly in Chapter 2, and in detail in the report by Morrison and Reese (1986). A lateral-load test of an isolated single pile was performed initially to provide baseline data for comparison with group response. The single pile was instrumented and loaded in a manner similar to that used for the group. After completion of the load test of the group, additional experiments were performed on the group piles in which selected piles were subjected to small loads and all piles were monitored; this study was aimed at an experimental determination of interaction factors for the piles in a group. Interaction factors are employed in several design procedures, primarily those which model pile-soil-pile interaction by use of the theory of elasticity.

As was done in Chapter 3, this chapter is divided into two major sections. The first deals with the behavior of single piles in sand and test results are compared with predictions made using available design criteria for both the monotonic loading (cycle 1) and cyclic loading (cycle 100).

The second major section on pile groups in sand provides a comparison of the response of the group with the response of the single pile. In addition a comparison is presented of the experimental results from the group with results from computations with available analytical methods. Experimental data from the study on interaction factors are also summarized.

Finally, a summary of the major research findings, relating to the behavior of piles and pile groups in sands, is presented. The most important parameters influencing pile response are listed, along with the major shortcomings in existing analytical procedures. Areas are indicated where additional research would be most fruitful.

BEHAVIOR OF SINGLE PILES IN SAND SUBJECTED TO LATERAL LOADING

As described at the beginning of this chapter, the 12.75-in.-diameter pile was tested in a soil condition which

consisted of a 9.5-ft thickness of back-filled sand for the first layer. Below the sand layer, the formations are the same as those for clay tests. The information presented here is excerpted from the report by Morrison and Reese (1986).

Measured and Computed Results for Static Loading

Response of Pile

The variation of pile-head load with deflection for a single pile under static loading is shown in Fig. 4.1. The largest load that was applied was 28 kips and the maximum deflection that was measured was 1.6 in. The variation of pile-head load with maximum bending moment in the pile is shown in Fig. 4.2.

Response of Soil

Soil resistance curves (p-y curves) were derived from the bending-moment data by procedures that were presented earlier. The p-y curves for depths of 12 in. to 72 in. are shown in Figs. 4.3 through 4.5. The predicted soil response is based on the current p-y criteria for sand proposed by Reese, Cox, and Koop (1975) and does not agree well with the measured p-y curves. An empirical multiplier of 1.55 for the maximum soil resistance that is computed by the Reese-Cox-Koop (RCK) method can provide a better prediction. The comparison between measured p-y curves and predicted p-y

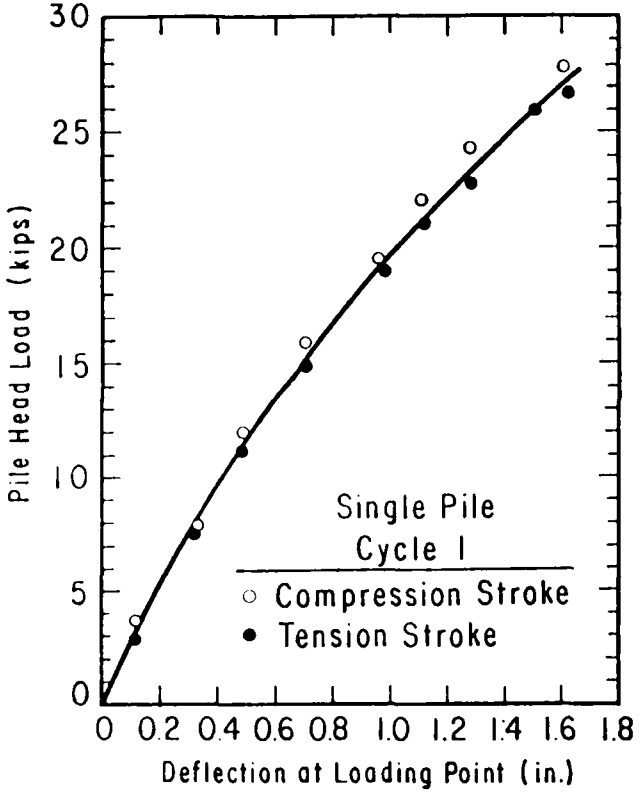

Fig. 4.1 Load-deflection curve for single pile in sand under static loading (Compression stroke - the pile is pushed by the loading ram. Tension stroke - the pile is pulled by the loading ram.)

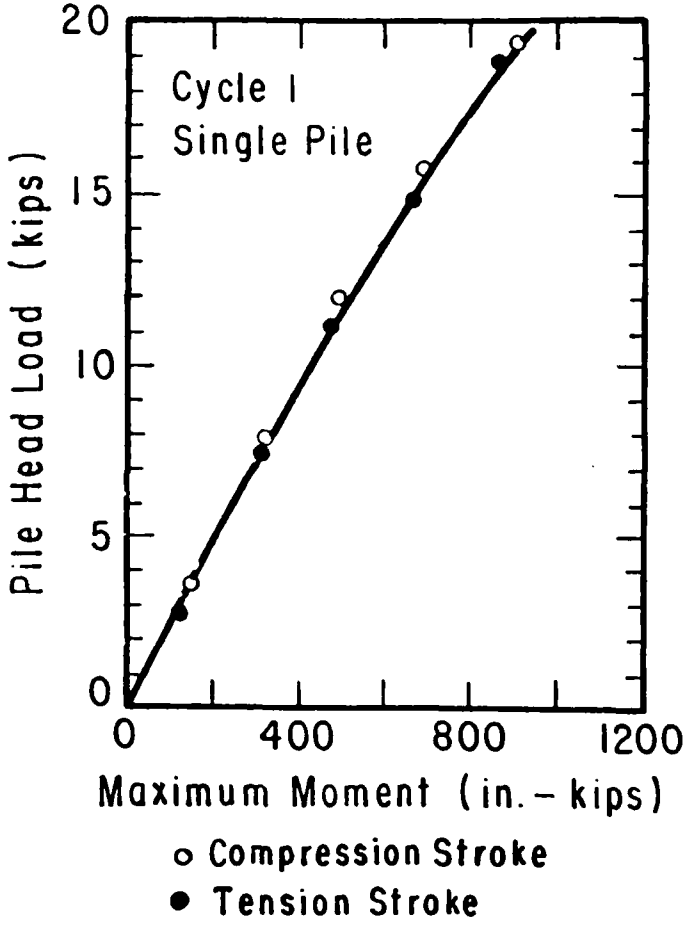

Fig. 4.2 Measured maximum bending moment for single pile under static loading

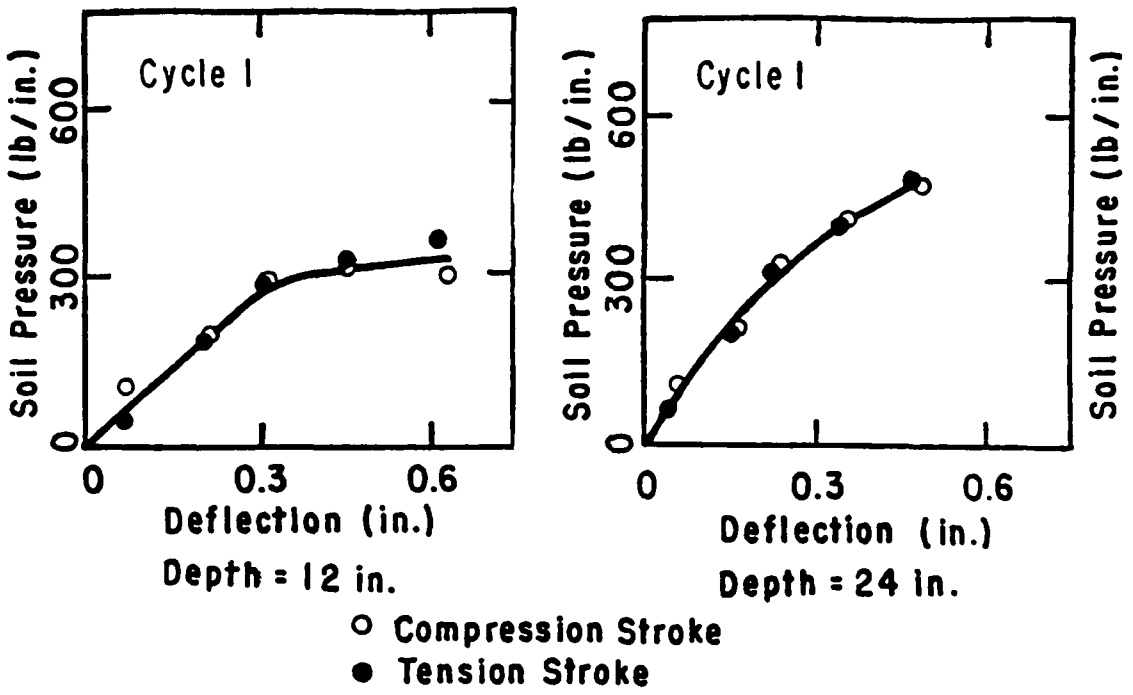

Fig. 4.3 Experimental p-y curves for depths of 12 in. and 24 in. for single pile under static loading

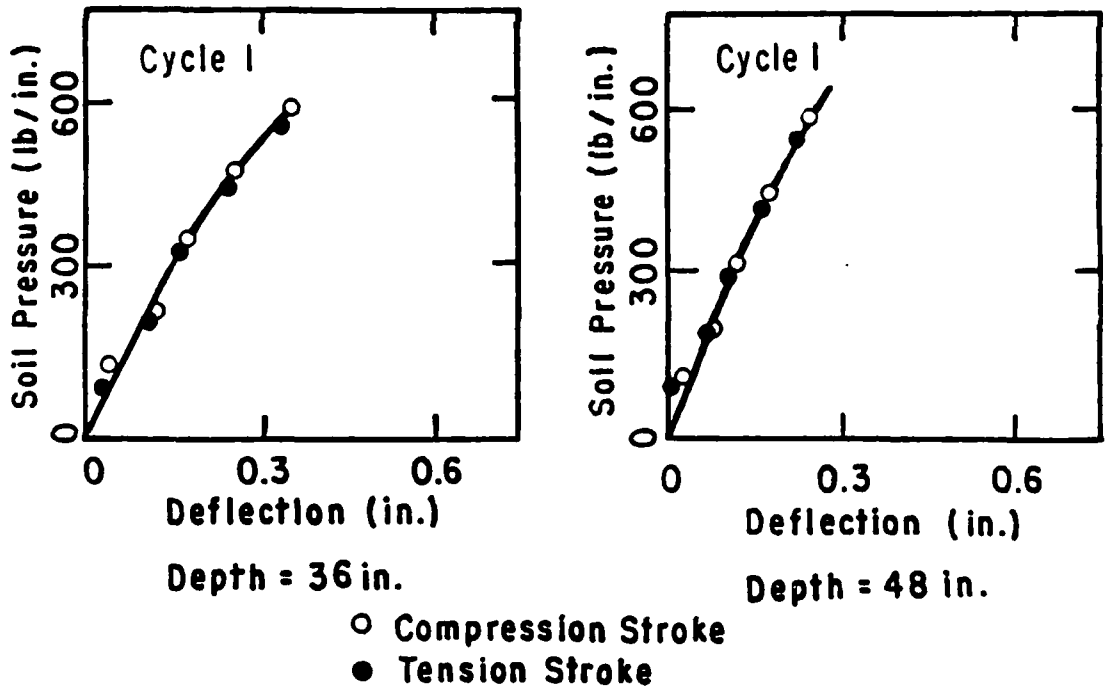

Fig. 4.4 Experimental p-y curves for depths of 36 in. and 48 in. for single pile under static loading

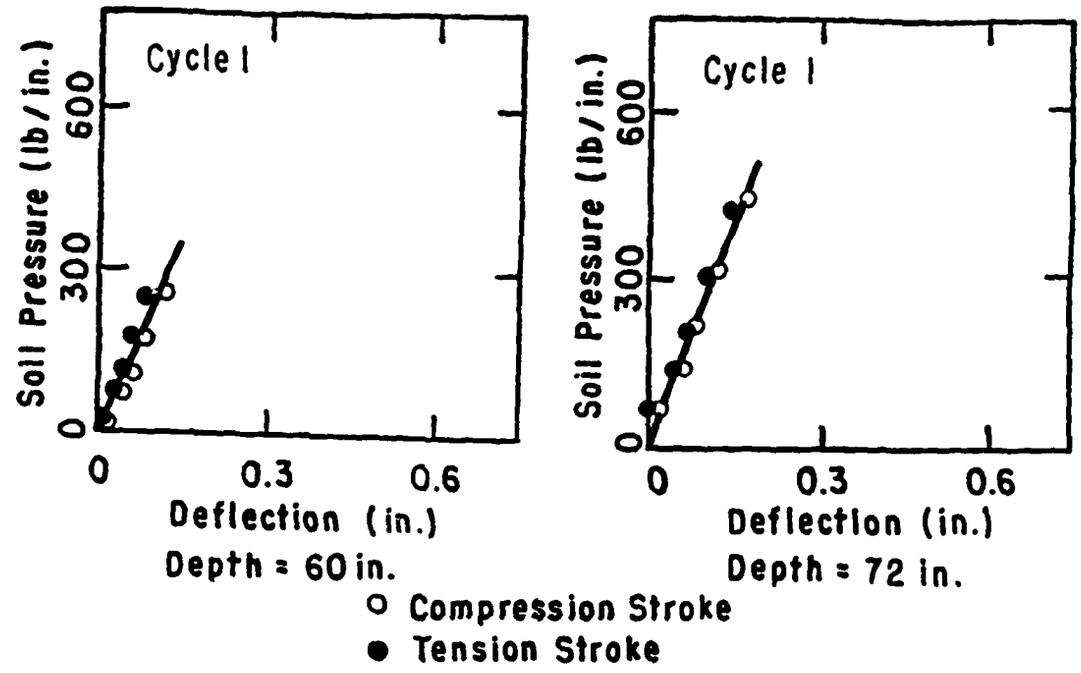

Fig. 4.5 Experimental p-y curves for depths of 60 in. and 72 in. for single pile under static loading

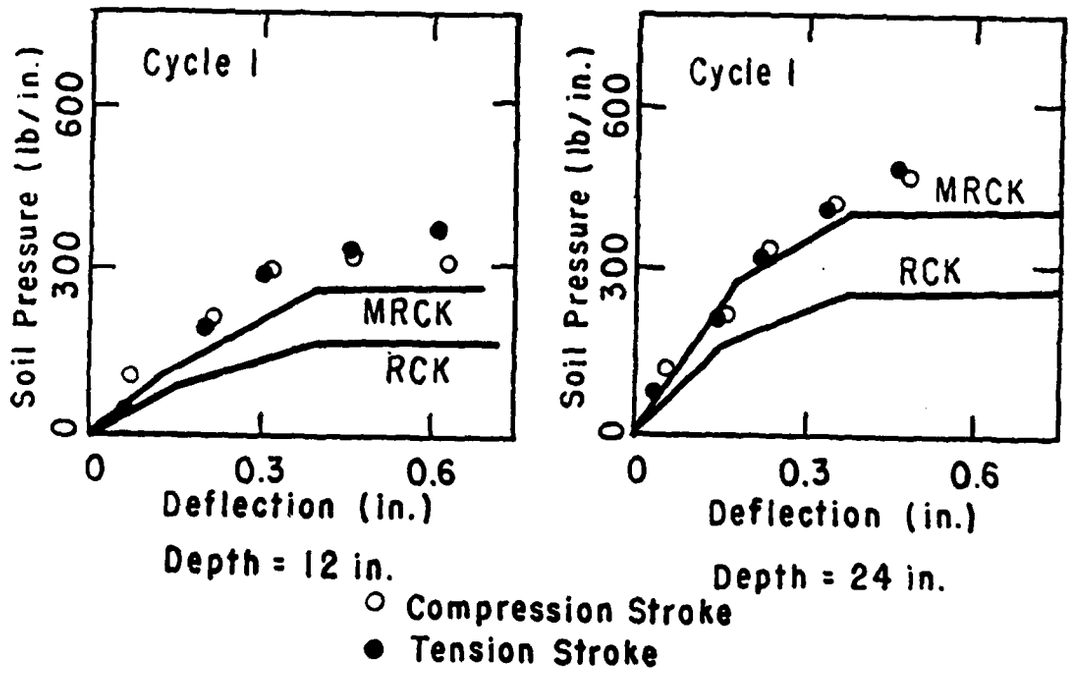

Fig. 4.6 Comparison of experimental and computed p-y curves for single pile under static loading

curves are shown in Figs. 4.6 through 4.8. One set of curves is labelled RCK and the set of curves based on the modified procedure is labelled MRCK.

The p-y curves generated by the modified procedure were then used in a computer program to compute deflection and maximum moments for a pile with the properties of the pile used in the load test. The deflections and moments computed in this manner are compared with measured values in Figs. 4.9 and 4.10. It is believed that the p-y curves generated by the modified procedure adequately predict the response of the soil in this particular sand deposit.

The modified procedure was formulated in order to have a site-specific method for the single pile that can be used for studying the effects due to the placing of piles in a group.

Measured and Computed Results for Cyclic Loading

Response of Pile

For cyclic loading, a number of cycles of a constant deflection was applied to the single pile. The deflection found for the first cycle was maintained constant in both the compression and tension directions. In general, a total of 100 to 200 cycles were applied for most preselected loading levels. A depression of the sand around a pile is generally

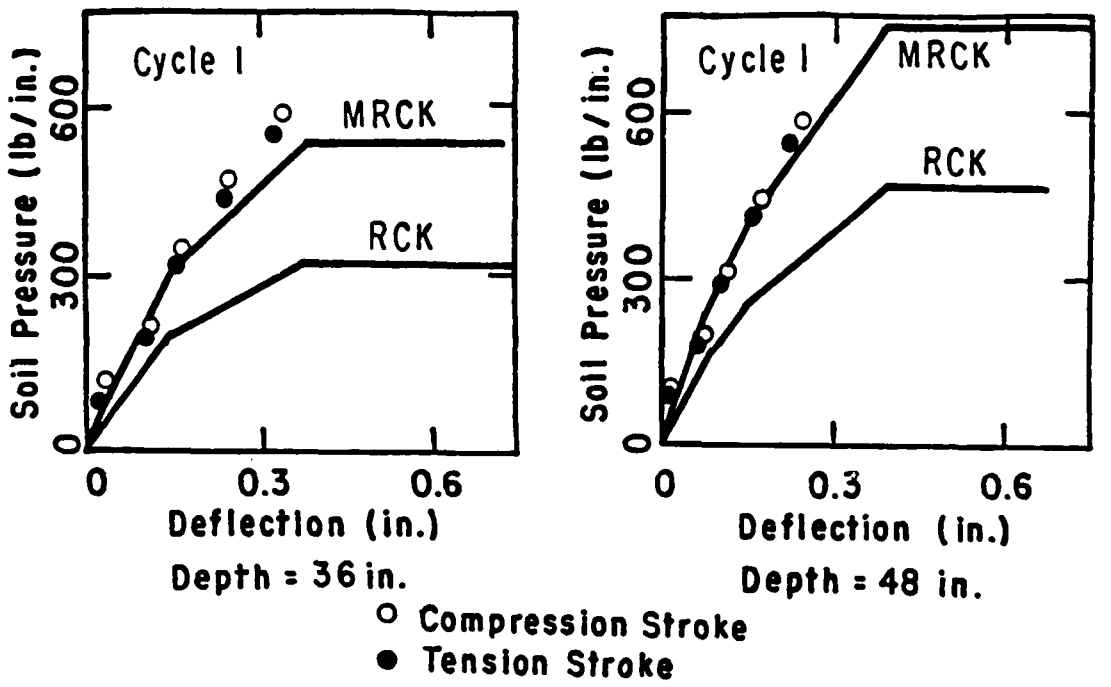

Fig. 4.7 Comparison of experimental and computed p-y curves for single pile under static loading

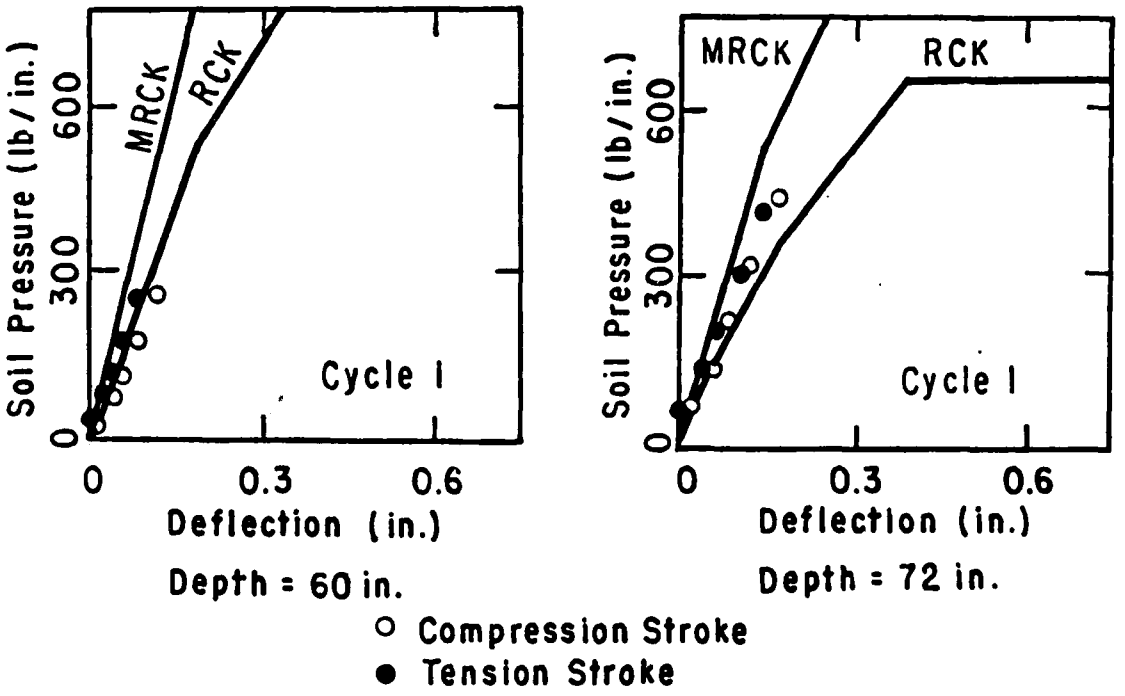

Fig. 4.8 Comparison of experimental and computed p-y curves for single pile under static loading

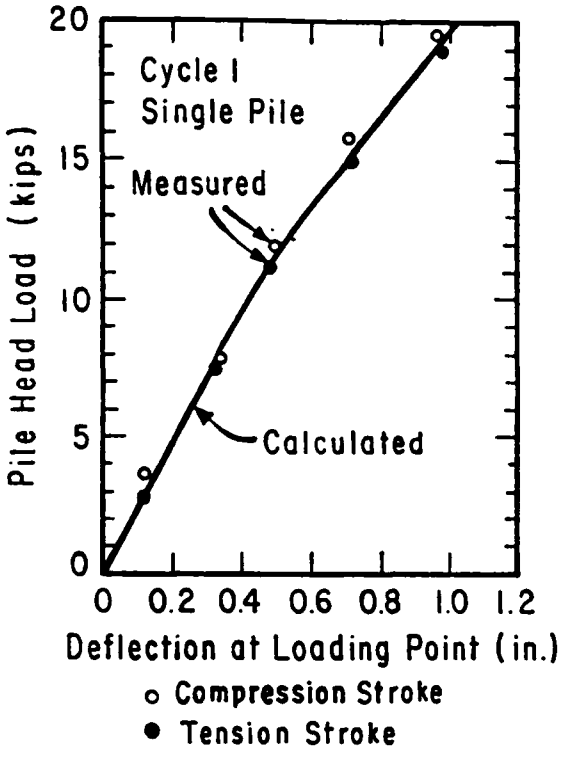

Fig. 4.9 Comparison of computed and measured deflections for the single pile under static loading

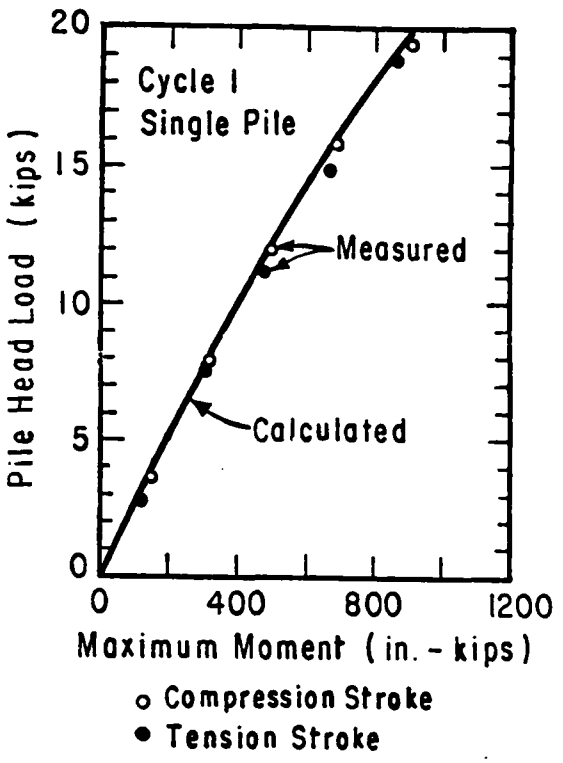

Fig. 4.10 Comparison of computed and measured maximum bending moment for the single pile under static loading

found during cyclic loading. A typical shape of the depression in sand at the end of 200 cycles for the fifth loading level is shown in Fig. 4.11.

The experimental results indicate that the pile-head deflections for 100 cycles of loading are slightly greater than those for cycle 1 (static loading) as shown in Fig. 4.12. The measured moment curves for cycle 1 and cycle 100 for various loadings are shown in Figs. 4.13 through 4.15. The moments are normalized by dividing by the pile-head load in order to compare curves for different loads. For the first loading, the maximum normalized moment is slightly smaller for cycle 100 than cycle 1. This implies that cycling at small deflections caused the sand to densify and the soil response to become stiffer. For the third and fifth loadings, the maximum normalized moment is larger for cycle 100 than for cycle 1. This implies that cycling at larger deflections causes the sand to loosen and the soil response to become softer.

The relationships between pile-head load and maximum bending moment for both cycle 1 and cycle 100 are shown in Fig. 4.16. As may be seen, for higher loads, the maximum moment for cycle 100 is slightly larger than for cycle 1.

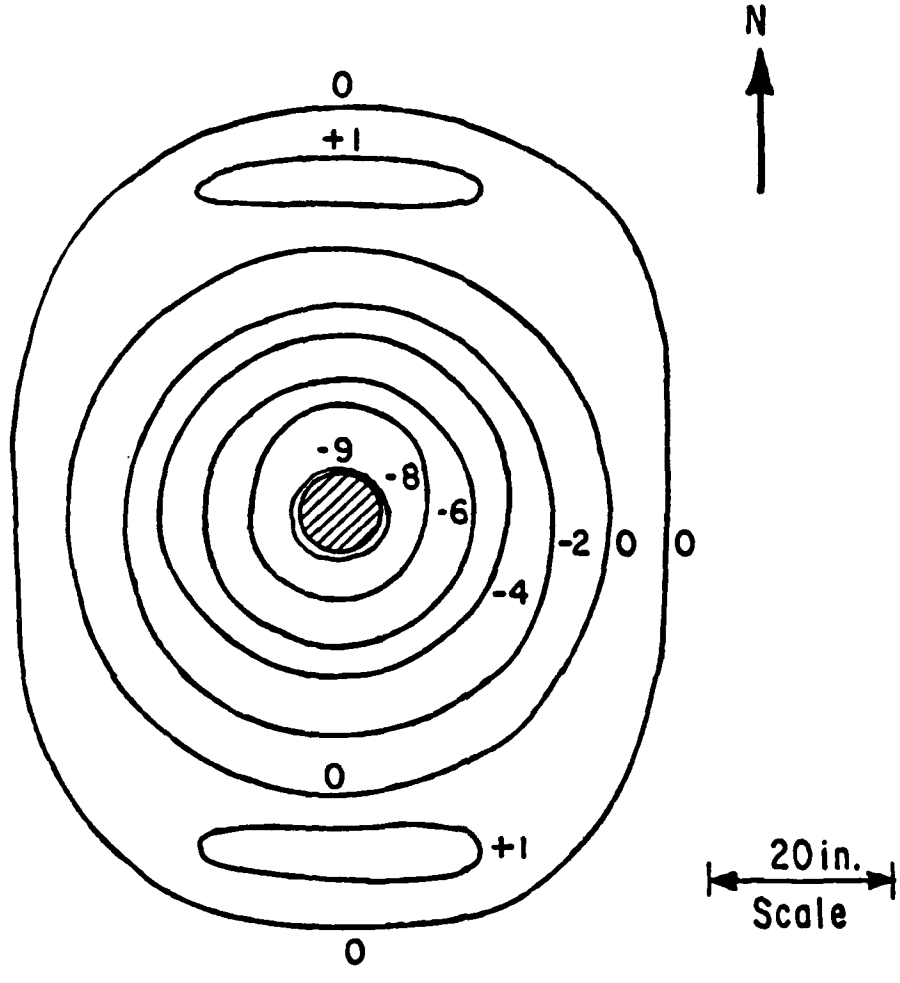

Elevations shown are relative to original sand surface in inches.

Fig. 4.11 Topography of depression around the single pile

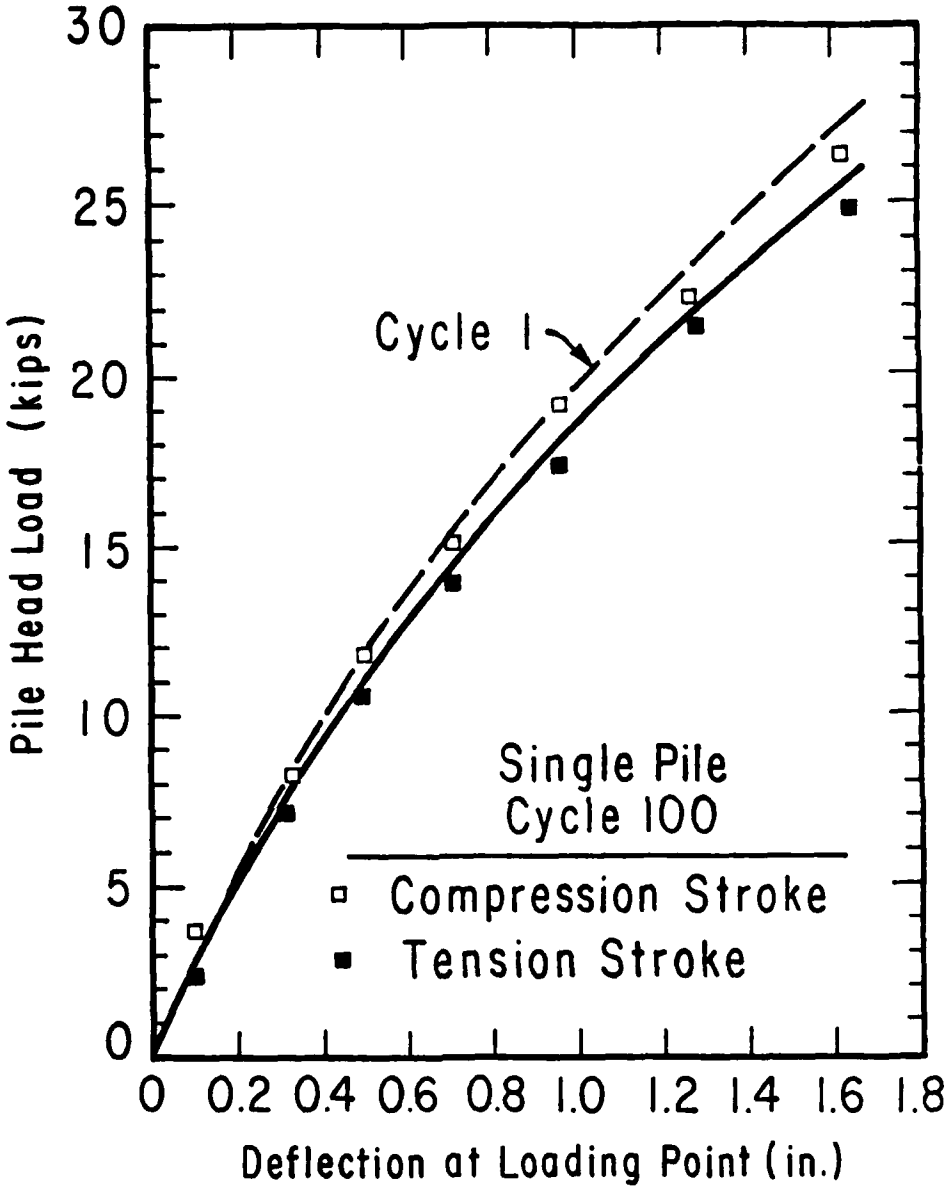

Fig. 4.12 Load-deflection curves for single pile for cycle 100

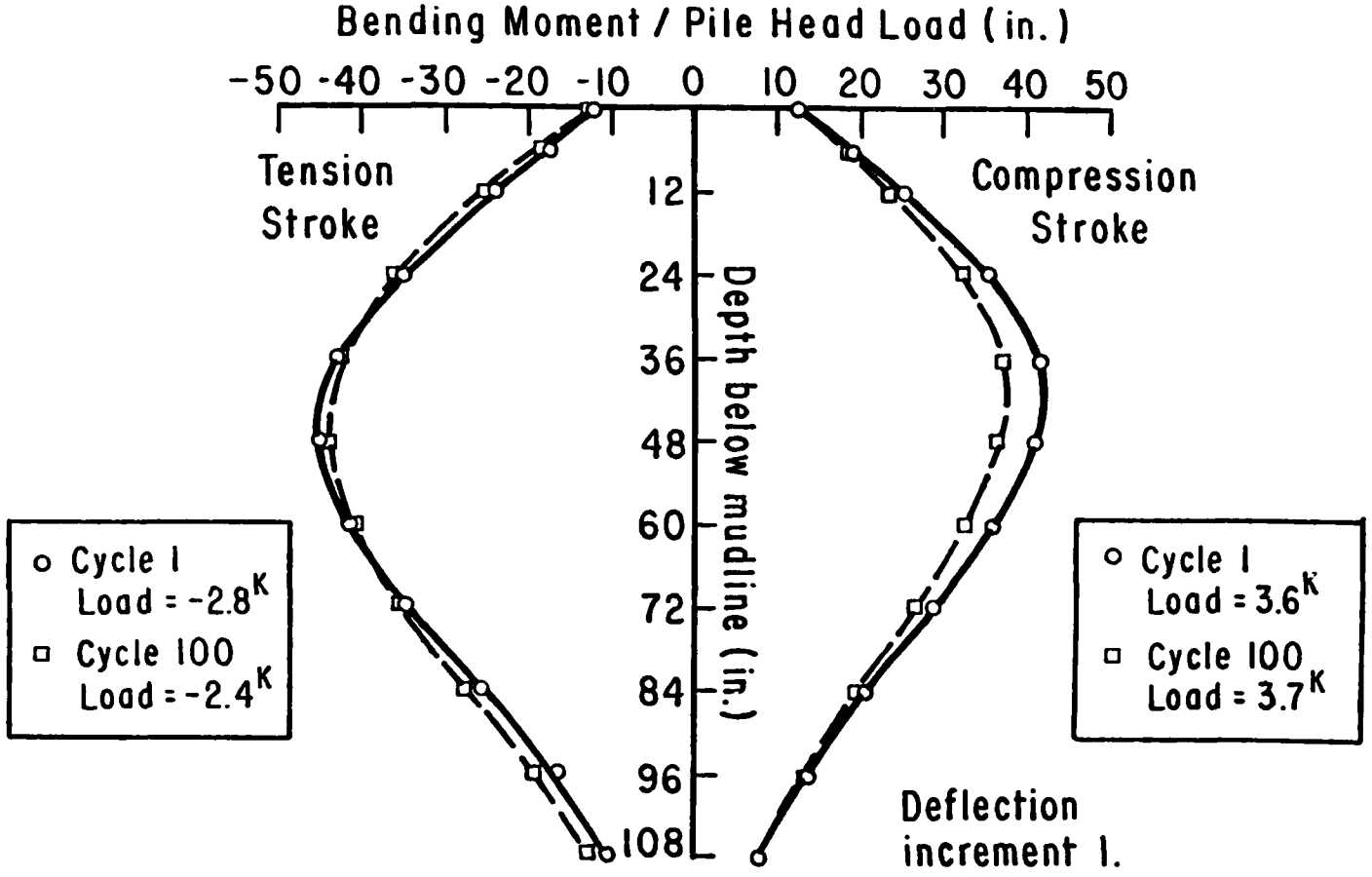

Fig. 4.13 Normalized moment curves for single pile for first deflection increment

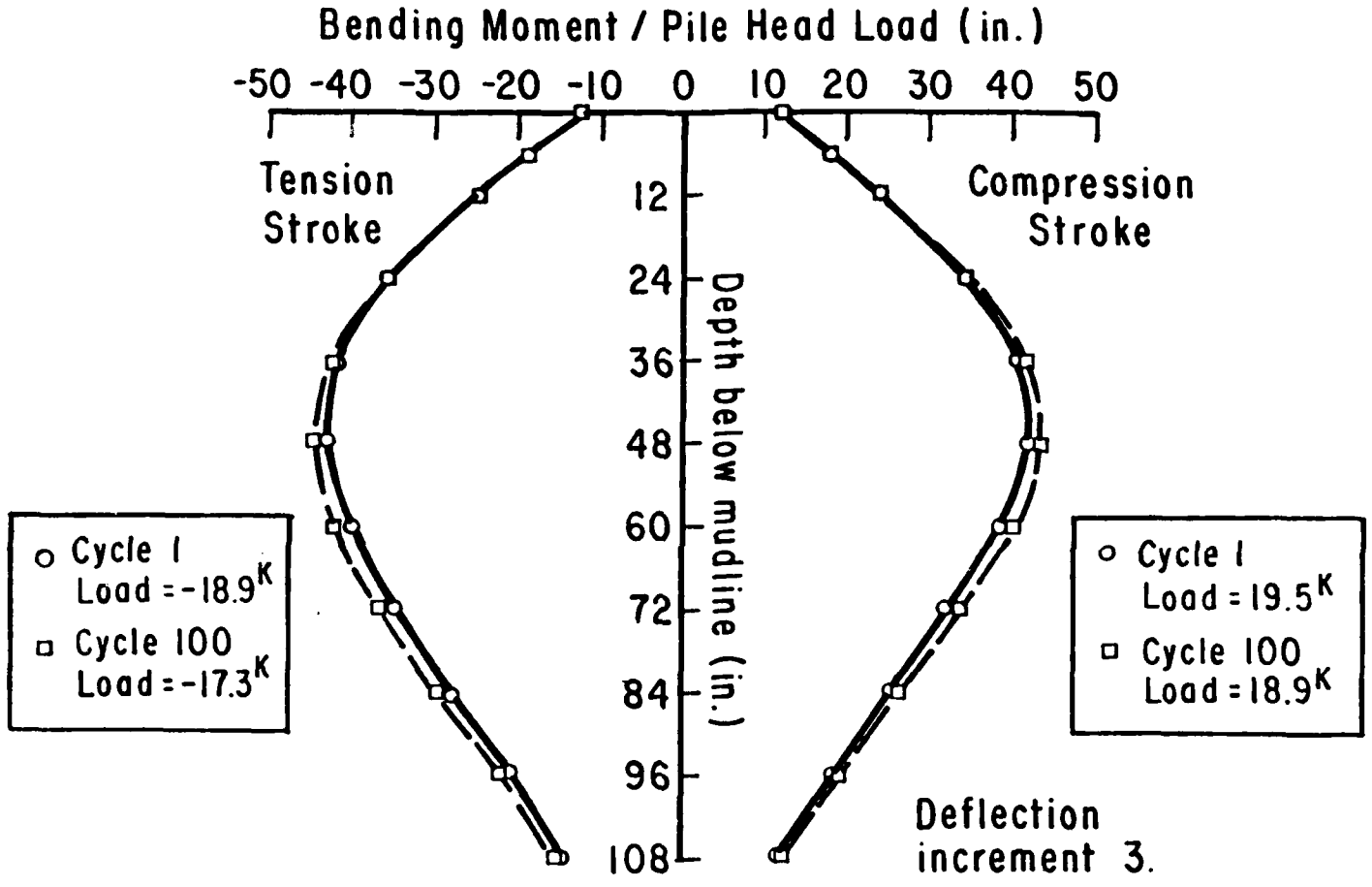

Fig. 4.14 Normalized moment curves for single pile for third deflection increment

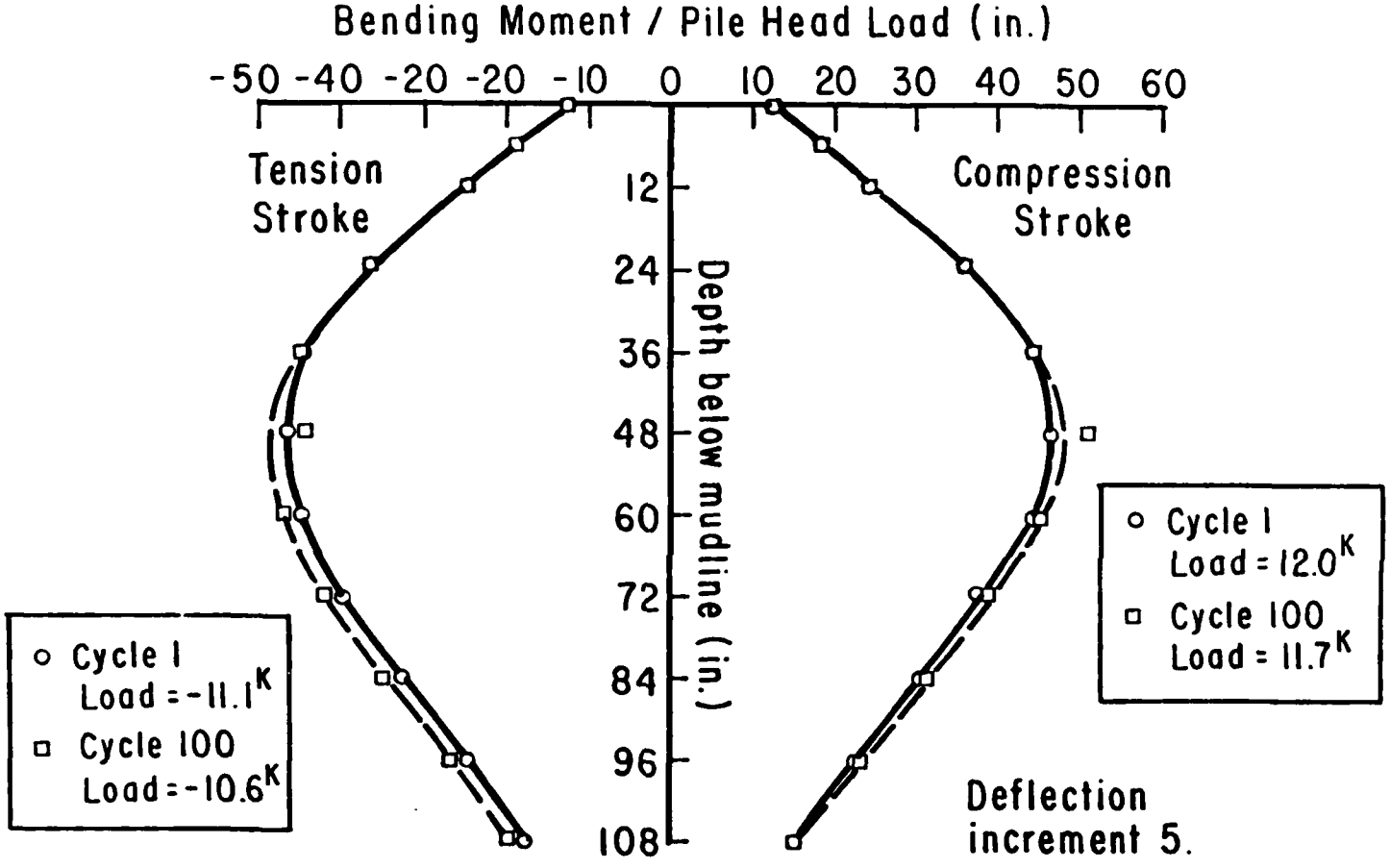

Fig. 4.15 Normalized moment curves for single pile for fifth deflection increment

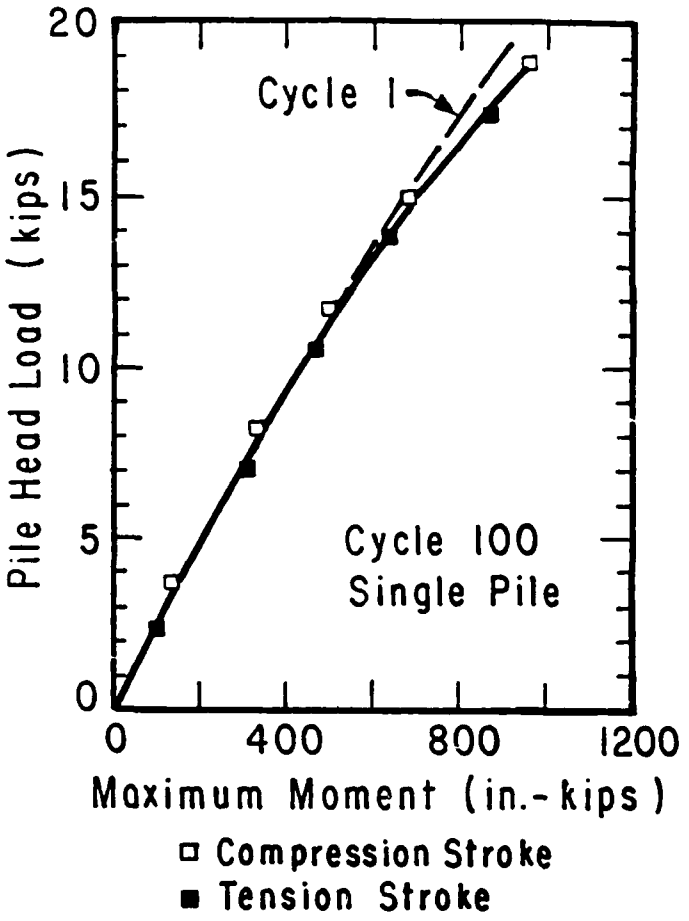

Fig. 4.16 Pile-head load vs maximum moment for single pile during cyclic loading

The measured pile-head loads and corresponding deflections of the point of loading for the two-way cyclic tests are shown in Fig. 4.17 and 4.18. As can be seen from these figures, deflections were maintained constant to within about 0.02 in. For a given deflection, the pile-head load only changed slightly as additional cycles of deflection were applied. In most cases the pile-head load decreased slightly up to cycle 10 and then increased slightly up to the last cycle. The load measured on the tension stroke was always less than that measured on the compression stroke.

Response of Soil

The p-y curves obtained for cycle 1 and cycle 100 at depths of 12 in. to 72 in. are shown in Figs. 4.19 through 4.21. The p-y curves become stiffer with increasing depth. For depths of 12 in. to 36 in. the p-y curve for cycle 100 is softer than for cycle 1. Below 36 in. cycling has negligible effect on p-y curves. The predicted p-y curves based on the procedure from Reese et al (1975) for cyclic loads underestimate the soil resistance. The modified procedure for static loads was used for cyclic loads and the predicted and experimental p-y curves for cycle 100 are shown in Figs. 4.22 through 4.24. Good agreement for pile-head deflection and maximum bending moment was found between the results for experiment and from prediction using the modified p-y criteria (Fig. 4.25).

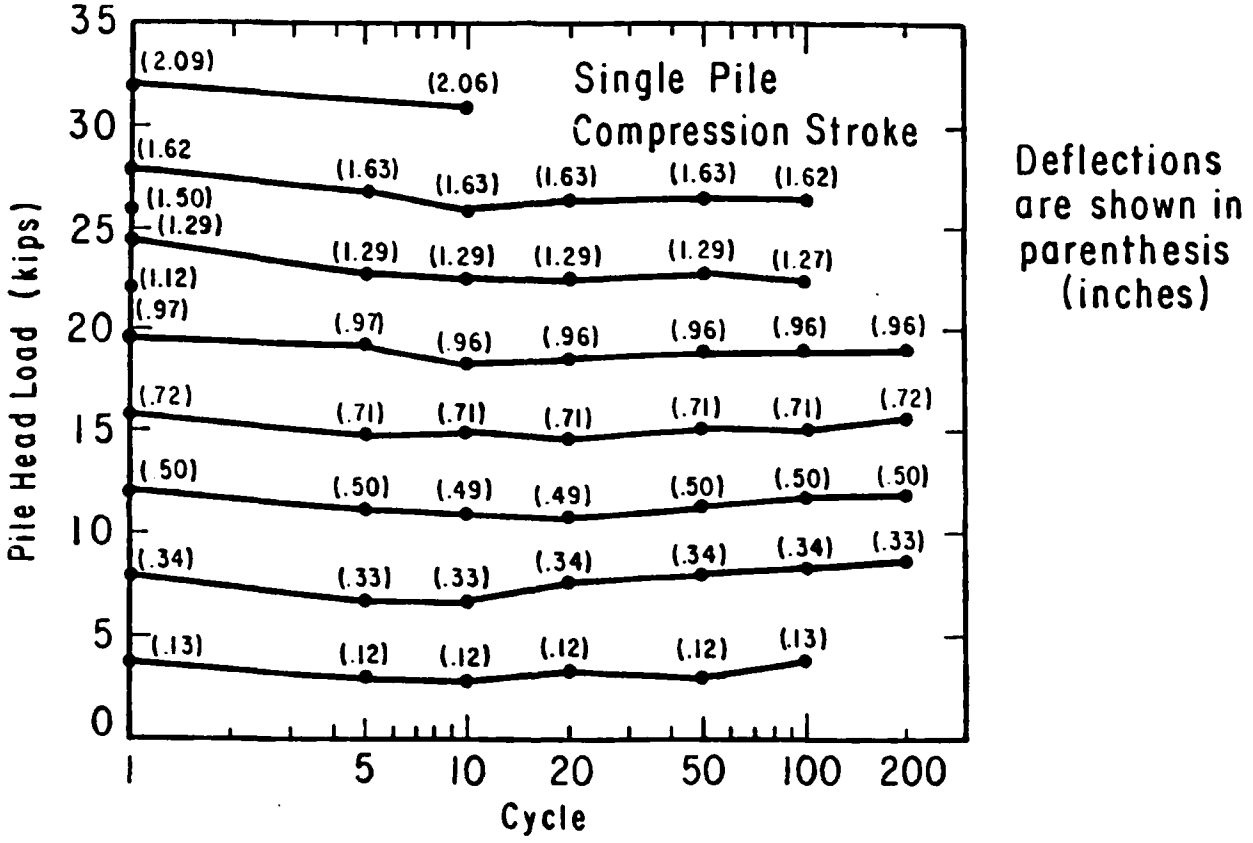

Fig. 4.17 Loads and deflections applied on compression stroke of cycle, single-pile test

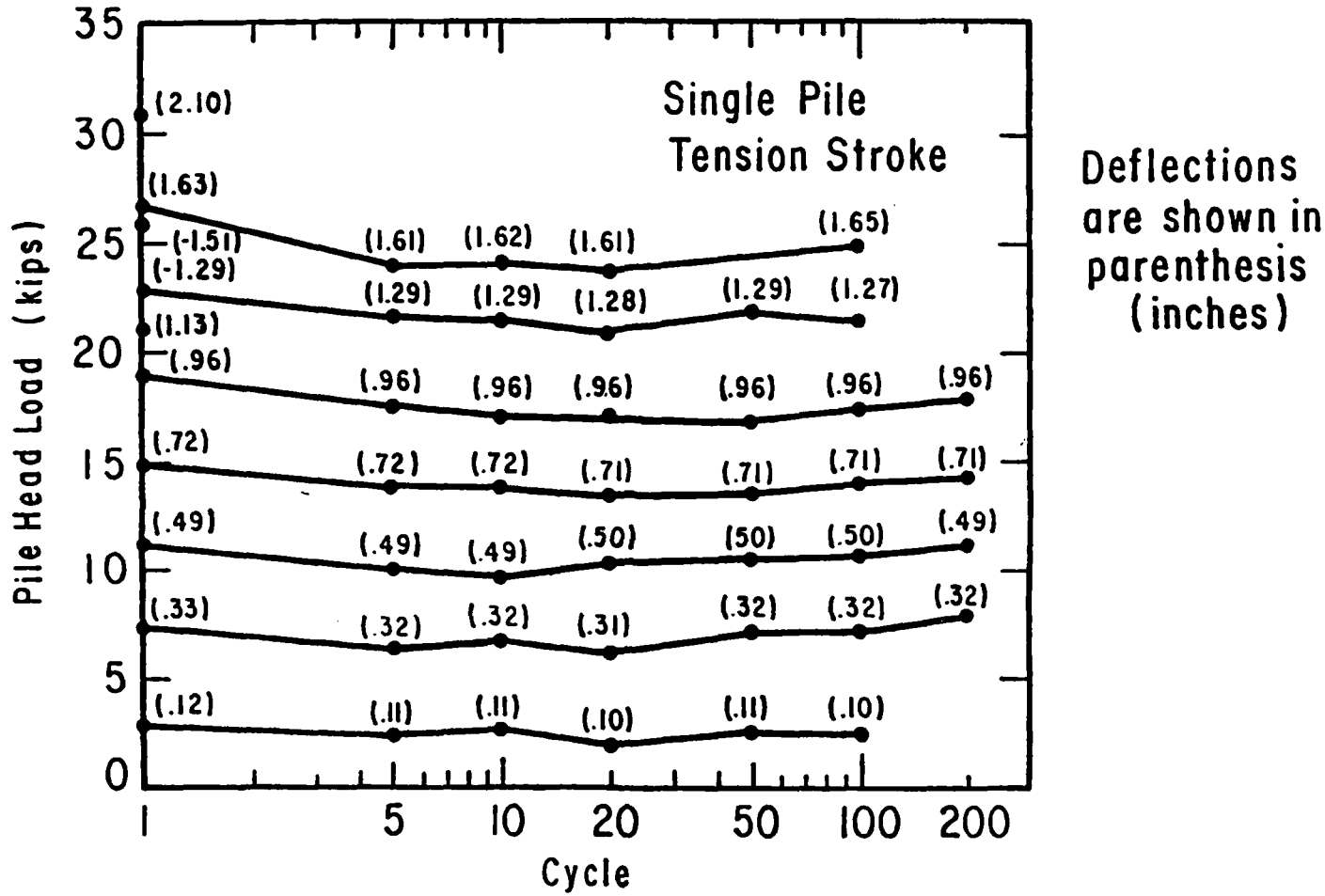

Fig. 4.18 Loads and deflections applied on tension stroke of cycle, single-pile test

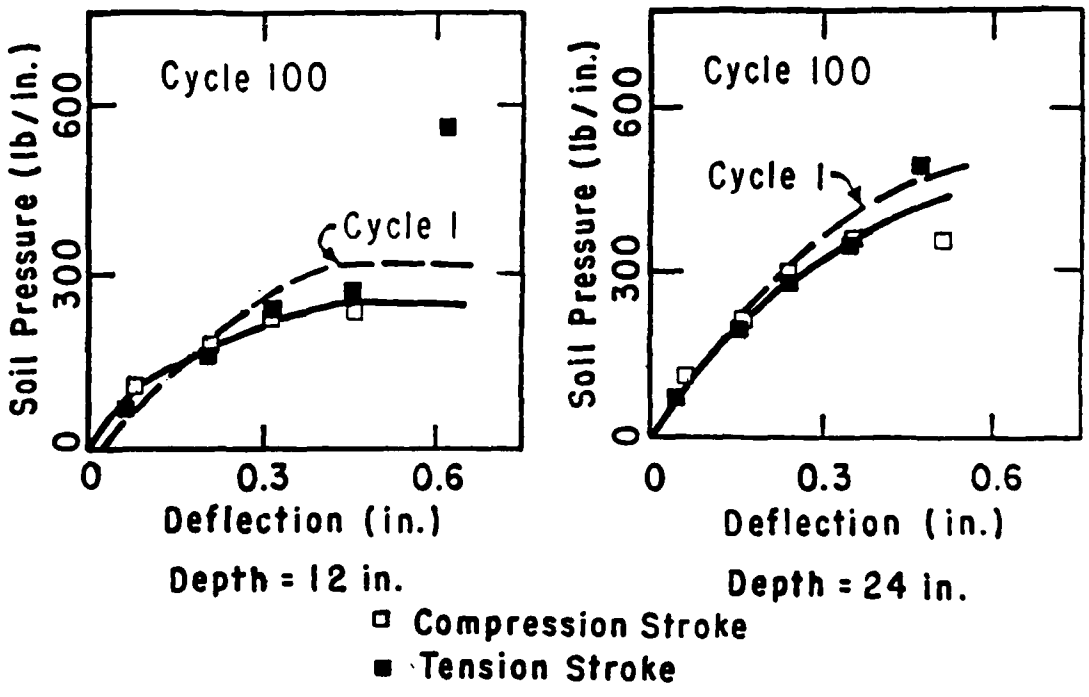

Fig. 4.19 Experimental p-y curves for depths of 12 in. and 24 in. for single pile under cyclic loading

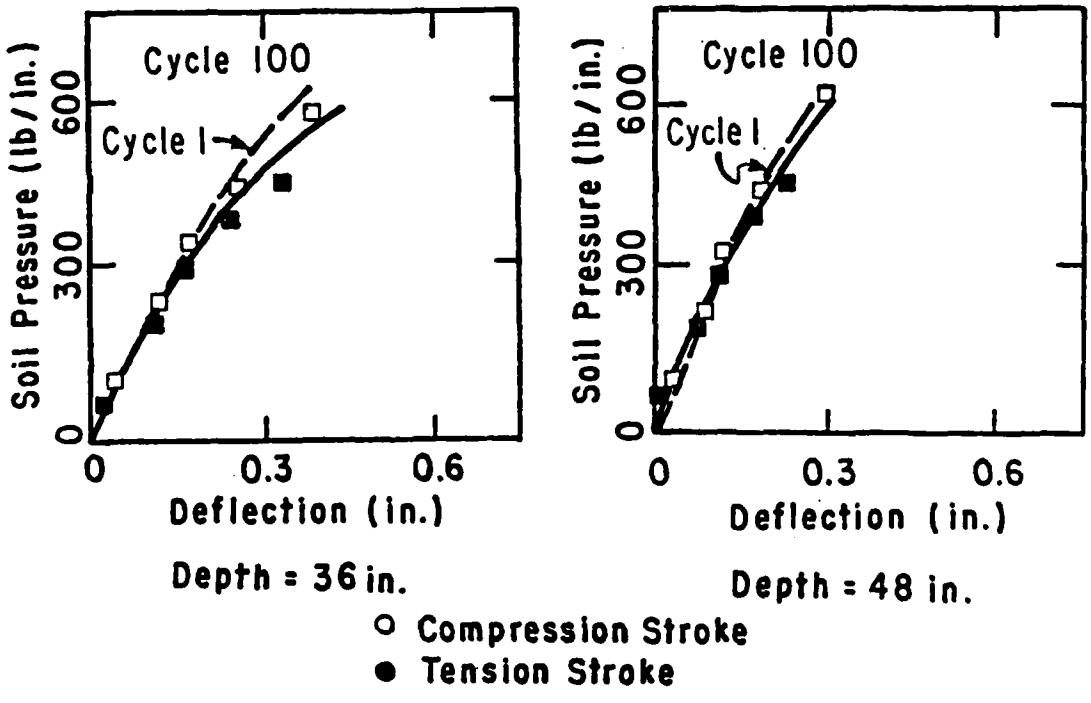

Fig. 4.20 Experimental p-y curves for depths of 36 in. and 48 in. for single pile under cyclic loading

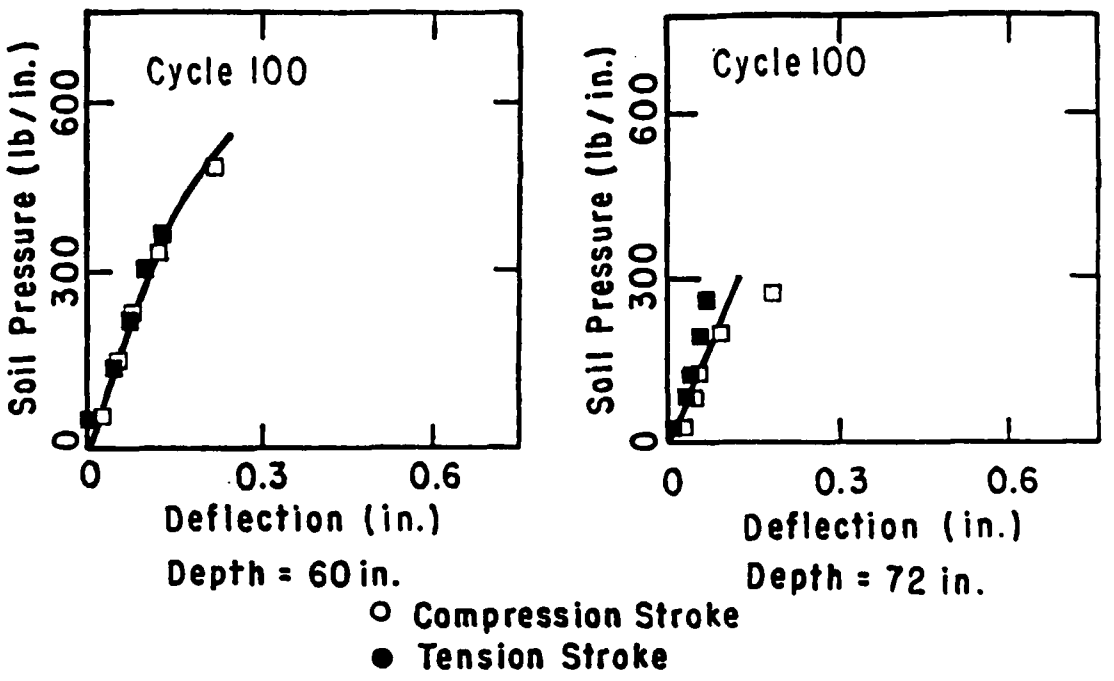

Fig. 4.21 Experimental p-y curves for depths of 60 in. and 72 in. for single pile under cyclic loading

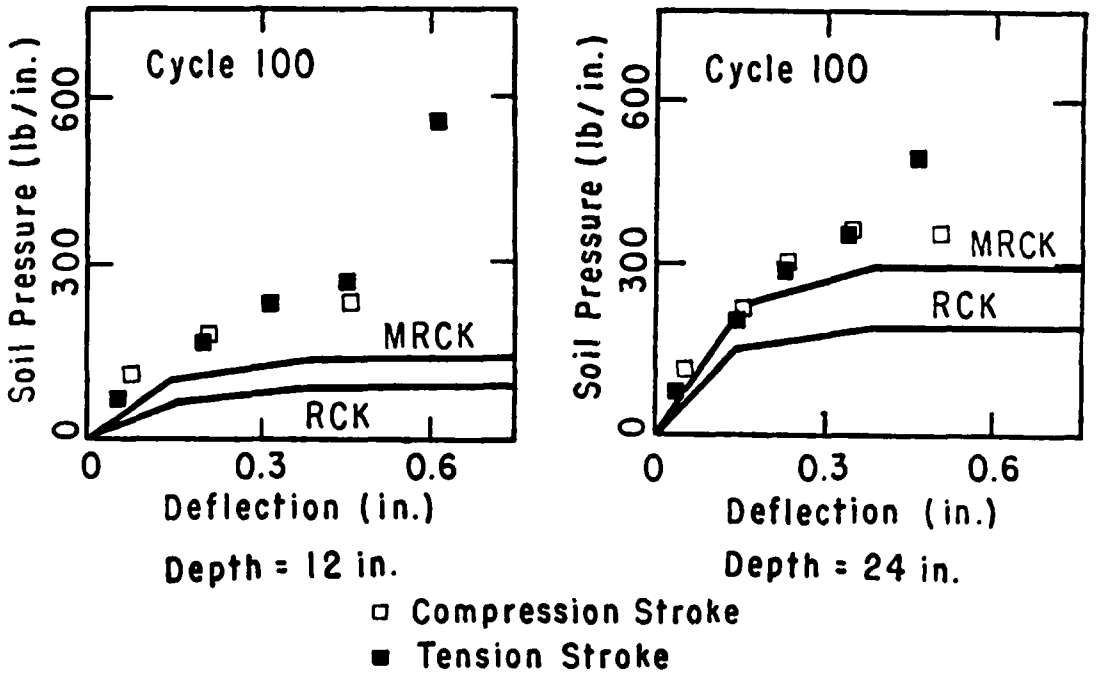

Fig. 4.22 Comparison of experimental and computed p-y curves for single pile under cyclic loading

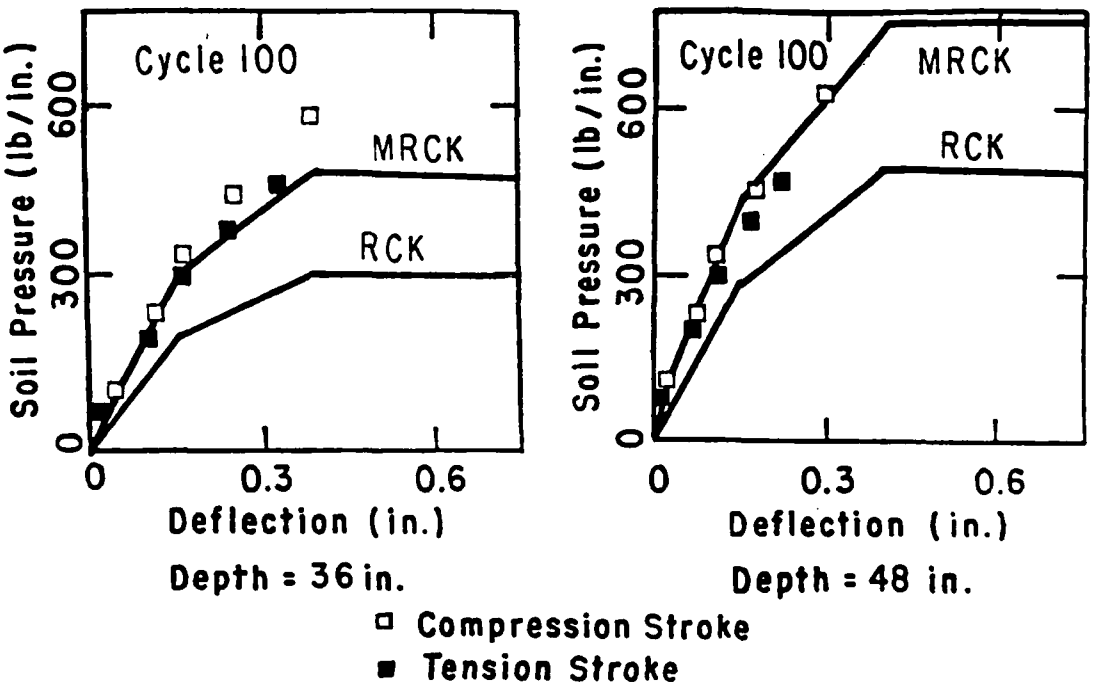

Fig. 4.23 Comparison of experimental and computed p-y curves for single pile under cyclic loading

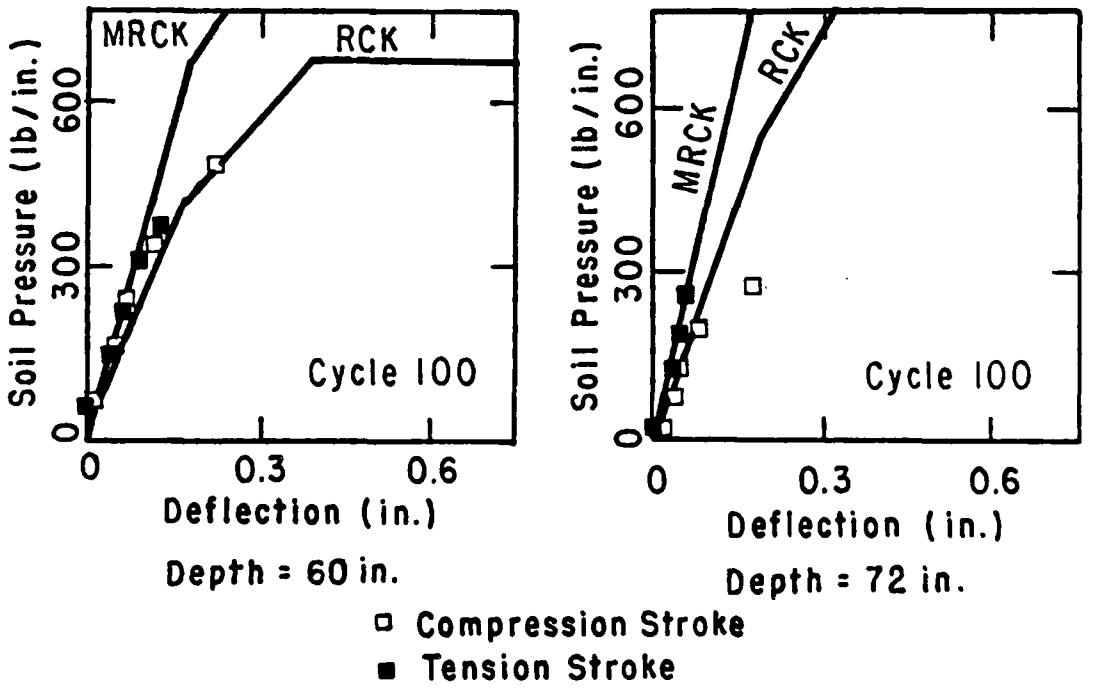

Fig. 4.24 Comparison of experimental and computed p-y curves for single pile under cyclic loading

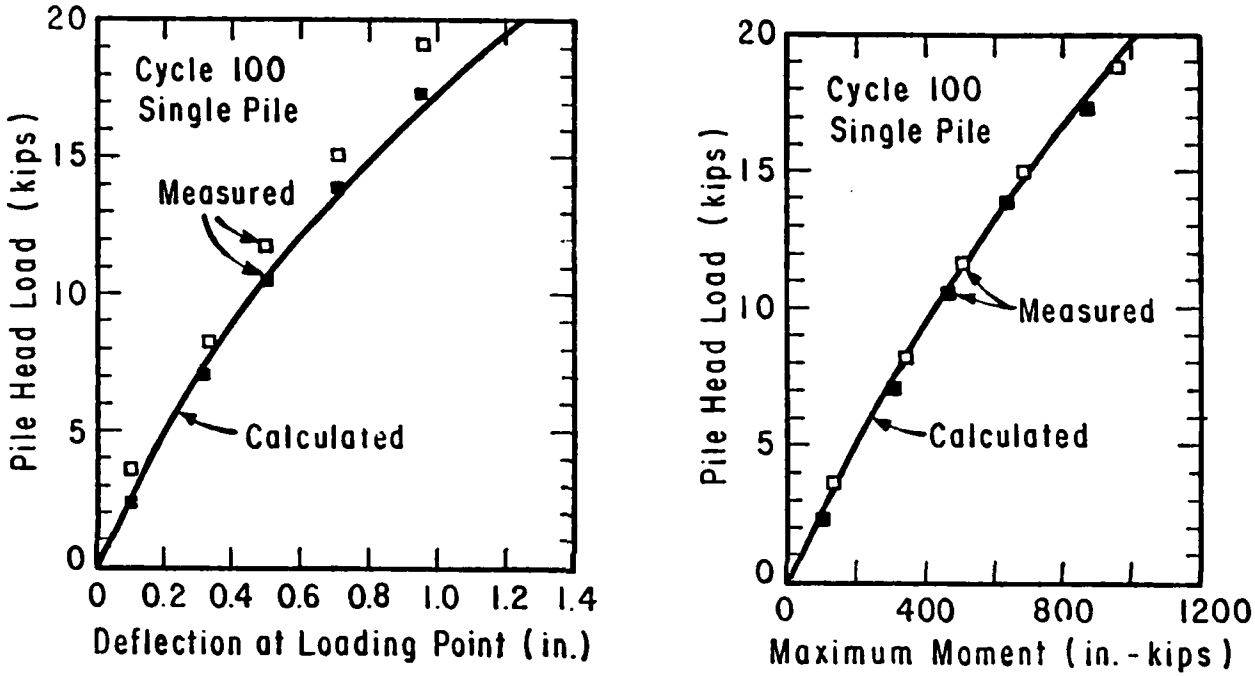

Fig. 4.25 Comparison of computed and measured deflection and maximum bending moment for the single pile under cyclic loading

Concluding Comment for Single Piles in Sand

The results of the lateral-load tests of a single pile in sand have been summarized and the following conclusions can be drawn.

1. The response of single piles to static loading is stiffer than that to cyclic loading.

2. The maximum bending moment in a pile under cyclic loading is greater than that for static loading.

3. The current p-y criteria recommended by API-RP2A fail to predict the soil resistance for soils at the test site. A modified procedure for the prediction of p-y curves was presented for the purpose of evaluating the effects due to the placing of piles in a group.

BEHAVIOR OF GROUPS OF PILES IN SAND SUBJECTED TO LATERAL LOADING

This section is subdivided into three parts. The first presents the major results of the experimental program and provides a comparison of the pile-group behavior with that of the single pile for monotonic and cyclic loading. The second presents some predictions using available procedures of analysis and comments upon the ability of these procedures to model the most important effects of pile-soil-pile interaction in pile groups. The third presents the data from

the experimental study of interaction factors for pile groups in sand and compares these results with those anticipated using relevant guidelines for analytical models using interaction factors.

Results of the Pile-Group Experiment and Comparison of Pile-Group Behavior with Single-Pile Behavior

Load-Deflection Response

As expected, the group as a whole was observed to deflect significantly more than the isolated pile when the average load per pile for the group was about the same as that for the single pile. An examination of the pattern of distribution of load to the piles indicated that the pile response was closely related to row position within the group; the piles in the front row were significantly stiffer than the piles in trailing rows. No distinct pattern emerged regarding the effect of position within a given row.

The load-deflection response for the single pile and for each row in the pile group is presented in Fig. 4.26. The data on the group are presented by row instead of as an overall average because the difference in load-deflection response between rows was much more significant in sand than was the case in stiff clay. Although the points representing actual measurements are shown for the single pile, the line

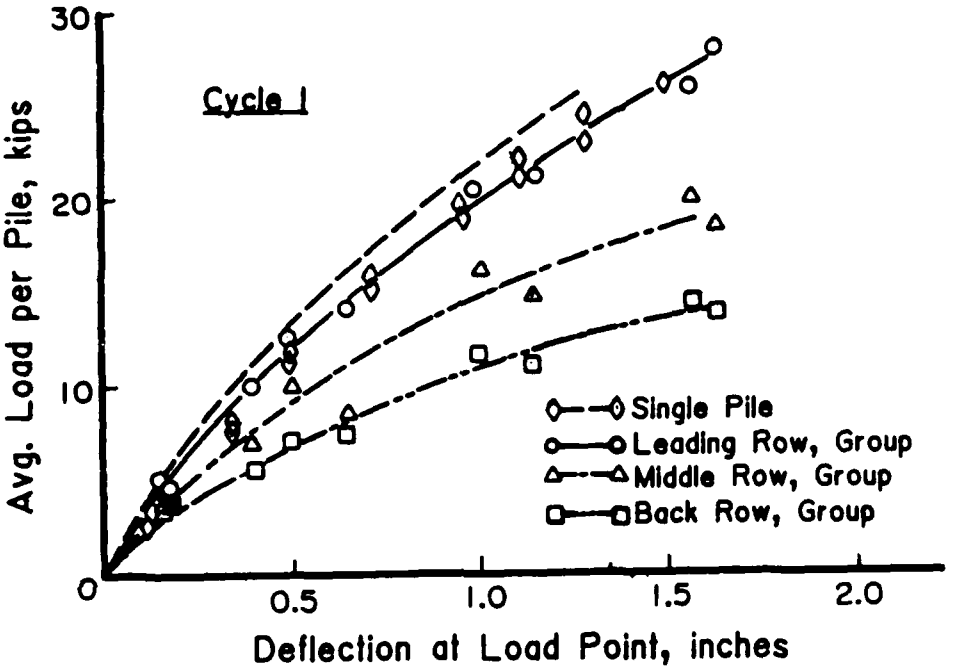

Fig. 4.26 Pile-head load vs deflection by row position, cycle 1

drawn for the single pile response represents the projected result for a pile having the slightly greater stiffness of the piles in the group (the group piles were filled with cement grout). The measured points shown for the rows of piles in the group reflect the loading in each direction; the leading row in the compression direction acted as the back row in the tension direction. Because the response in each direction was not precisely the same, the lines drawn represent the average of the two sets of data.

The data presented in Fig. 4.26 clearly indicate that the most significant group effect is associated with "shadowing", in which the soil resistance of a pile in a trailing row is reduced because of the shadowing effect of the pile ahead of it. This effect was greater for the group in sand than for the group in stiff clay, especially at small loads (less than one-half of failure).

As shown in Fig 4.27, the shadowing effect was not appreciably diminished by two-directional cyclic loading, as was the case for clays. It may be noted, however, that the response of the group as a whole was not substantially softened by cyclic loading as was the response in clay. The relatively small effect of cyclic loading in sands can be attributed in large part to densification of the sand around the piles during cycling. Ground-surface settlements in the

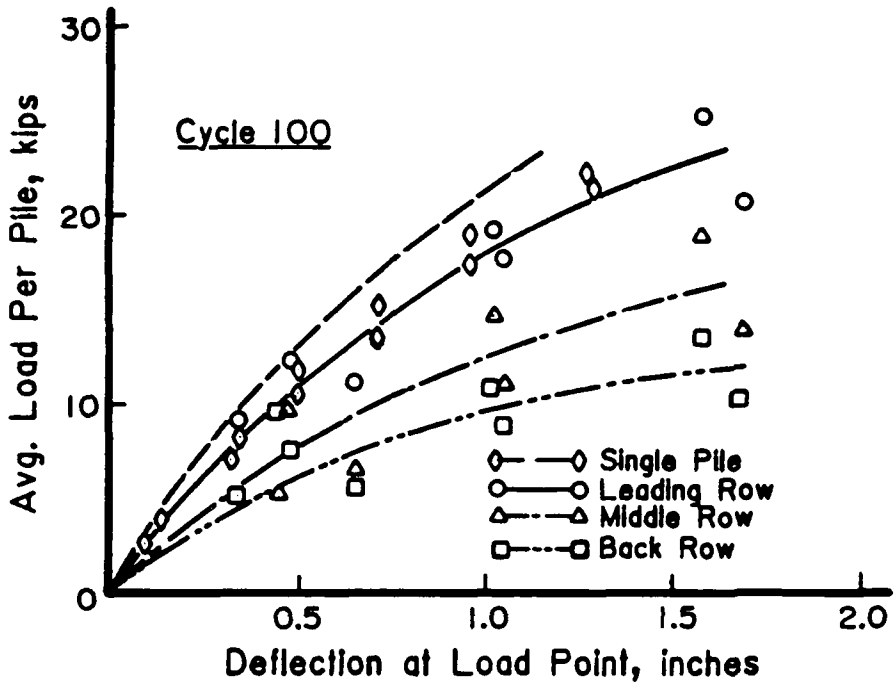

Fig. 4.27 Pile-head load vs deflection by row position, cycle 100

range of 8 to 10 inches were noted in and around the group, similar in magnitude to that measured near the single pile, as described earlier in this chapter.

Distribution of Bending Stresses

Maximum bending moments, as a function of average pile-head load, are shown in Fig. 4.28 for the single pile and by row for the piles in the group. For a given pile head load, piles in the middle and back rows sustain larger bending moments; this trend reflects the loss of soil resistance due to the shadowing effect discussed earlier. However, the load to the piles in the group is distributed in greater proportion to the piles in the leading row and, as a result, the maximum bending moments for a given load on the pile group tended to be in the leading-row piles. For the group of piles in clay, the load was distributed with less bias to the front row, and the absolute maximum bending moments were often in the trailing-row piles.

A typical plot of distribution of bending moment with depth for the single pile and by row for the piles in the group is presented in Fig. 4.29. The maximum moment for the trailing rows in the group occurs at a greater depth (due to the reduced load transfer near the ground surface) and is greater when normalized by pile head load. The data presented in Fig. 4.29 illustrate the actual distribution of

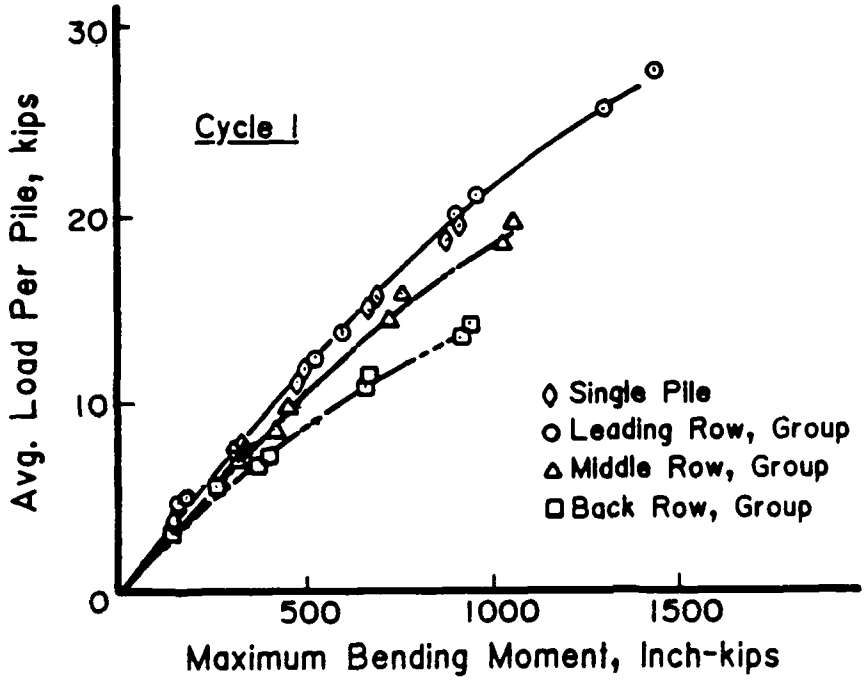

Fig. 4.28 Pile-head load vs maximum bending moment by row position

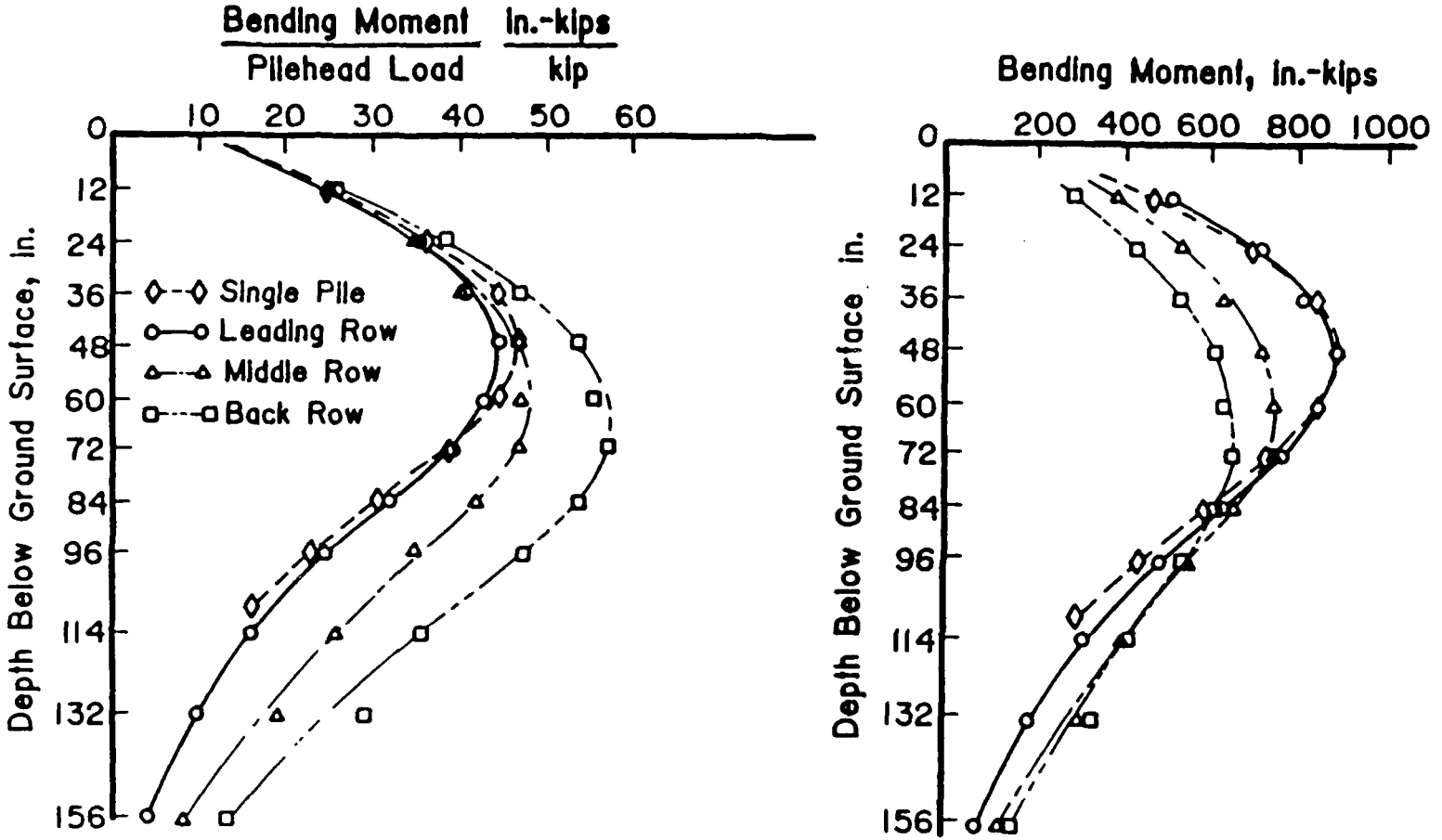

Fig. 4.29 Bending moment vs depth by row position, normalized to pile-head load

bending moments for a specific load on the group. The moments in the single pile and the front row piles are similar.

From an examination of the data it appears that a conservative approach to design might be to assume that the stresses in all of the piles may be computed by analyzing an individual pile using loads anticipated on the front-row piles. Of course, the difficulty in this approach lies in predicting the distribution of load to the front row for a given load on the group. None of the currently available procedures provide a realistic approach to this problem.

Load-Transfer (p-y) Curves

In a manner similar to that described elsewhere in this report, p-y curves were derived from the bending-moment data. Presented in Fig. 4.30 are the p-y curves for the 3 ft (36 in.) and 4 ft (48 in.) depths; these curves are representative of the trends observed at other depths. The data points that are shown are averages for the single pile in two directions and for the piles in a given row position in each of the two directions.

The p-y curves for the piles of the leading row are only slightly softer than those for the single pile, consistent with the load-deflection response. The slight softening in

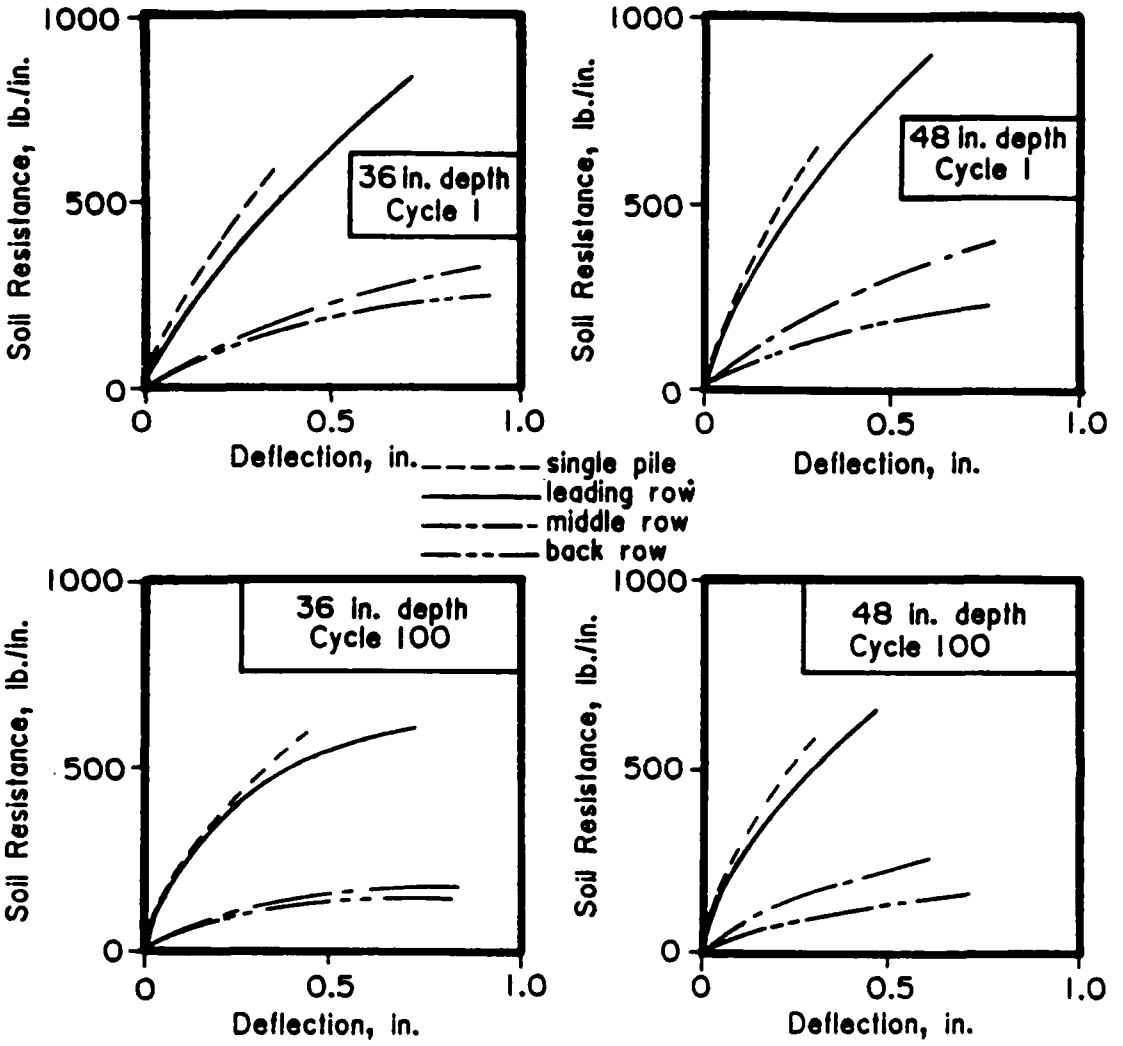

Fig. 4.30 Typical p-y curves by row position

the front row is likely due to the superposition of strains in the far-field soils ahead of the front row piles; increasing stiffness with increasing stresses apparently made the front-row piles in sand less influenced by adjacent piles than was the case for the front-row piles in clay.

The reduction in soil resistance in the trailing-row piles is quite evident in the data presented in Fig. 4.30, and correlate with observations made earlier regarding distribution of load and bending moment. In contrast to the p-y curves from the group test in clay, a significant bias in soil resistance between rows is present at even relatively small loads.

As was evident from the load-displacement relationships for the pile head, two-way cyclic loading did not produce a great loss of soil resistance. This observation is in stark contrast to the experimental results in stiff clay, in which reductions in soil resistance due to cyclic loading were even more significant for the group piles than for the single pile. As discussed previously, the soil response during cyclic loading in sands appears to be quite sensitive to load history; cycling at small loads produced substantial densification which appeared to improve the soil resistance at subsequent larger loads. The amount of densification was

surprising, because a considerable effort was expended to compact the sand during placement.

The densification during lateral loading appeared to be related to compaction of the sand which falls into the void behind the pile when the pile is loaded in the reverse direction. It is likely that cyclic lateral loading, which is primarily in one direction only (as opposed to the full two-directional load cycles used in this experiment), would not produce as much densification and would result in greater loss of soil resistance with increasing cycles of load. In this respect, the results of this experiment may not reflect the "worst case" cyclic loading in sands for many field conditions, although there are not sufficient experimental data to provide much judgement in this respect. It may also be the case that many cycles of small lateral loads prior to the occurrence of the design event may serve to improve the response of a pile group, so long as significant permanent strains have not occurred.

Summary

In summarizing the results from the analysis of data from the lateral-load test of the pile group in sand, it may be concluded that:

1. The deflection of the pile group is significantly larger than that of a single pile under a load equal to the average load per pile,

2. The reduced efficiency of the group for lateral loading is largely due to the effect of "shadowing" in which the trailing row piles can mobilize only a limited soil resistance,

3. Maximum bending moments occurred in the piles of the leading row and were similar to those in the isolated pile under the same load per pile,

4. The key element needed in predicting group effects is an understanding of the mechanisms producing the loss of soil resistance in the piles within the trailing rows,

5. Cyclic loading in two directions had a relatively small effect on pile response relative to a similar test conducted in clay

6. The relatively small loss of soil resistance due to cyclic loading may be due to the significant amount of densification which occurred during two-way cyclic loading.

Comparison of Experimental Results with Predictions Using Available Analytical Design Procedures

Introduction

This section provides a comparison of the results of the group test in sand with the results predicted with the analytical techniques which are available, and widely used, at the time of this study. A more complete description of these techniques is available in the report by Brown and Reese (1985). A detailed presentation of the predictions using these procedures is available in the report by Morrison and Reese (1986).

A brief discussion of the procedures that are used was presented in Chapter 3 and will not be repeated here. The procedures described previously were used to analyze the group in sand, with the exception of the computer code PILGP2R. The elasticity-based procedures include DEFPIG and the Focht-Koch method, while the modified unit-load-transfer models include the single-pile procedure and the Bogard-Matlock method. The paragraphs which follow provide a summary of the relevant findings regarding the ability of these models to reproduce the important aspects of the problem of pile-soil-pile interaction.

Elasticity-Based Methods

Predictions of group behavior using the DEFPIG code and the Focht-Koch procedure are presented in Figs. 4.31 through 4.33. The input parameters were "fitted" to the experimental data for the single pile to minimize variability due to predictions of individual-pile behavior and to isolate the pile-group effect.

DEFPIG

As is clear from Fig. 4.31a, no single elastic modulus, or even rate of increase of elastic modulus with depth, could be found which modelled the nonlinear behavior of the single pile. Input parameters for DEFPIG were therefore fitted for each selected value of load per pile to produce the curve shown in Fig. 4.31b. This curve is seen to overpredict deflection somewhat for the static-load case. It should be noted that the use of a variable elastic modulus as a function of depth is not incorporated rigorously in the elastic theory; the solution uses an approximate technique to include variable elastic properties. Although the code includes provisions for limiting load transfer at given depths along the pile (as for the p-y curve approach), this is also an approximate technique and no guidelines exist for estimating limiting values of load transfer outside of the empirical p-y curve values. Limiting values of load transfer were therefore not used.

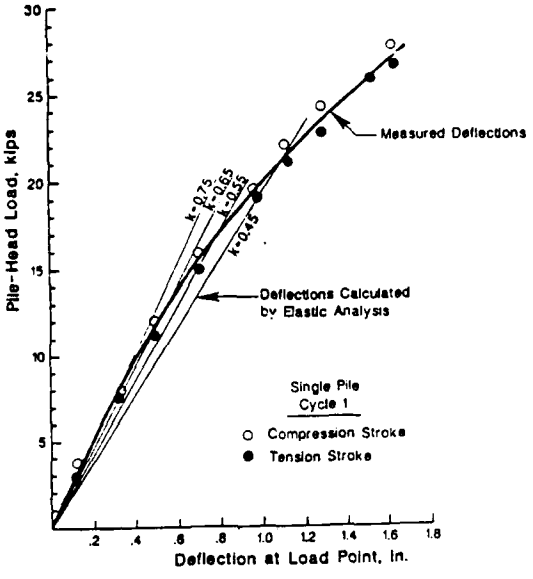

a. Comparison of measured deflections with single pile deflections computed by elastic analysis

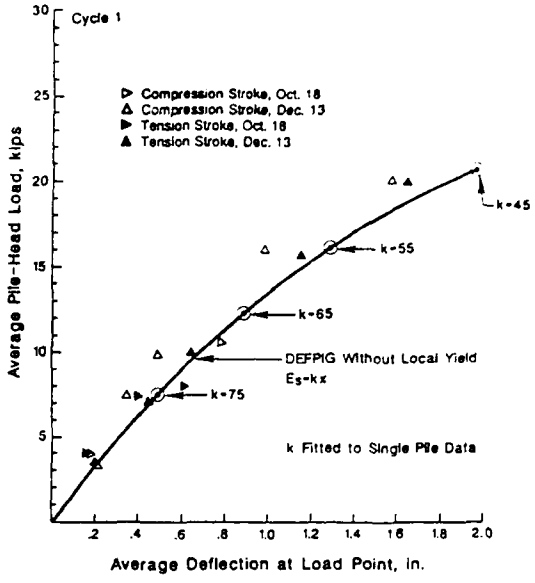

b. Comparison of measured deflections with deflections computed by DEFPIG without local yield

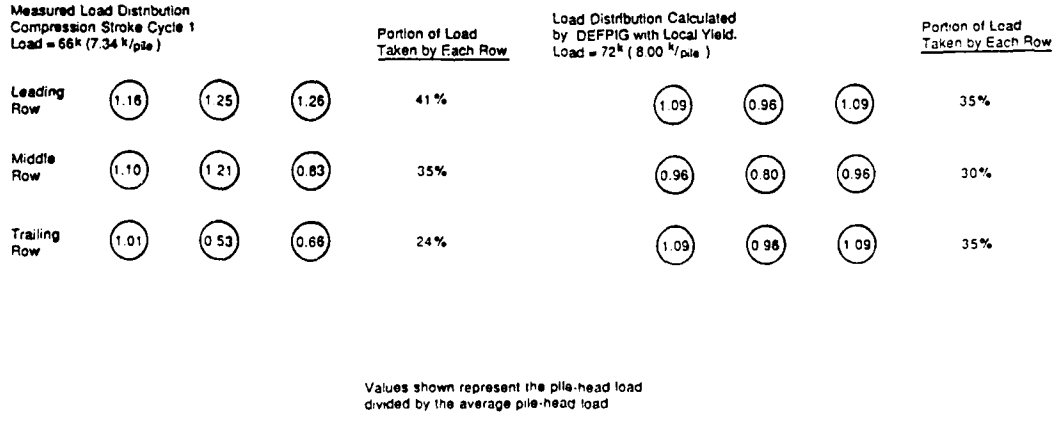

c. Comparison of measured load distribution with load distribution computed by DEFPIG with local yield

Fig. 4.31 DEFPIG predictions of group response

Although the load-deflection prediction for the group shown in Fig. 4.31b appears to be reasonably good, the predictions of distribution of load shown in Fig. 4.31c indicate that the elastic solution does not really model the group behavior; the symmetric pattern of load spread to the four corners of the group is at odds with the bias between leading and trailing rows as revealed in the experiment.

The version of DEFPIG available for this research had no provisions for estimating bending moments or for including cyclic-load effects. Cyclic loading can presently be accounted for only by empirical modifications.

Focht-Koch

The Focht-Koch procedure uses empirical p-y curves to reproduce nonlinear effects for a single pile, as is typically done for routine design of piles for lateral loading. The Focht-Koch predictions of static load vs deflection for the group, shown in Fig. 4.32a, are seen to match the gross behavior of the group in sand reasonably well. As was the case with DEFPIG, the distribution of load is incorrectly modelled. The symmetric distribution shown in Fig. 4.32c does not match the row-by-row behavior observed in the experiment.

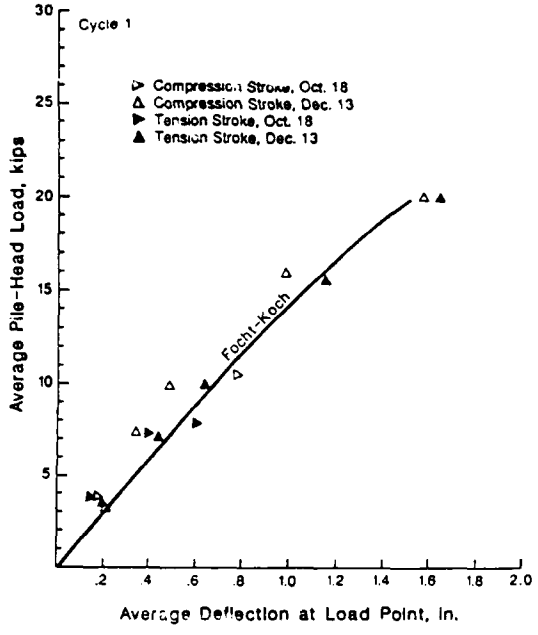

a. Comparison of measured deflections with static deflections computed by the Focht-Koch method

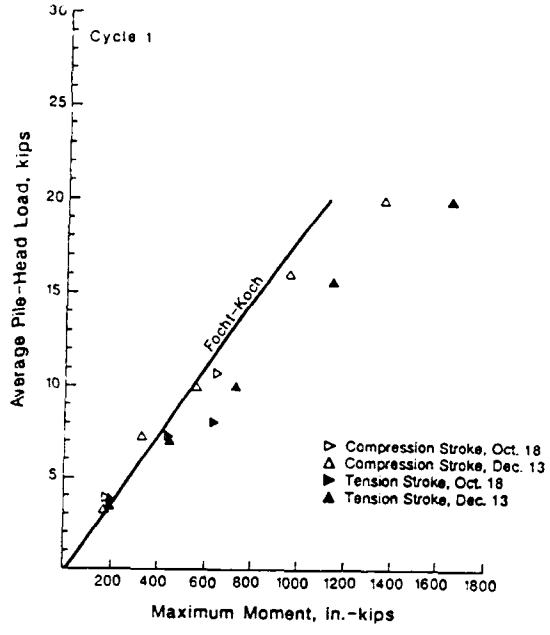

b. Comparison of measured maximum moment with static maximum moments computed by the Focht-Koch method

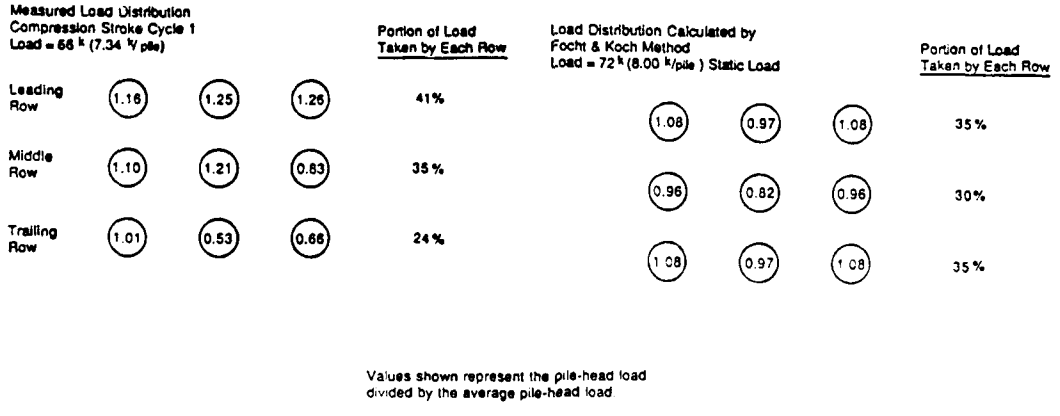

c. Comparison of measured load distribution with load distribution computed by the Focht-Koch method

Fig. 4.32 Focht-Koch predictions of group response for static loading

Maximum bending moments as a function of static load, shown in Fig. 4.32b, are seen to be unconservative at static loads above a small value. The maximum moments plotted for both the prediction and the experiment represent the maximum value on any pile in the group. The bending moments are unconservatively predicted, in spite of the reasonably good prediction of gross deflection of the group, because of the much larger proportion of load distributed to the front-row piles than predicted. The Focht-Koch procedure also underestimated the depth to maximum moment similarly to the trend described for the group in clay, but with a less severe error. The greatest factor contributing to the bending-moment error was the load distribution effect.

Similar trends were noted for the Focht-Koch predictions of cyclic-load response, shown in Fig. 4.33. Reasonable agreement was observed for the gross load-deflection behavior, although the group response appeared more nonlinear than predicted and Focht-Koch was somewhat unconservative near failure. Patterns of distribution of load were incorrect and contributed to a significant underestimation of bending stresses at virtually all levels of load.

Modified Unit-Load-Transfer Models

The procedures in this group include the single-pile method and the Bogard-Matlock method. Both use empirical p-y

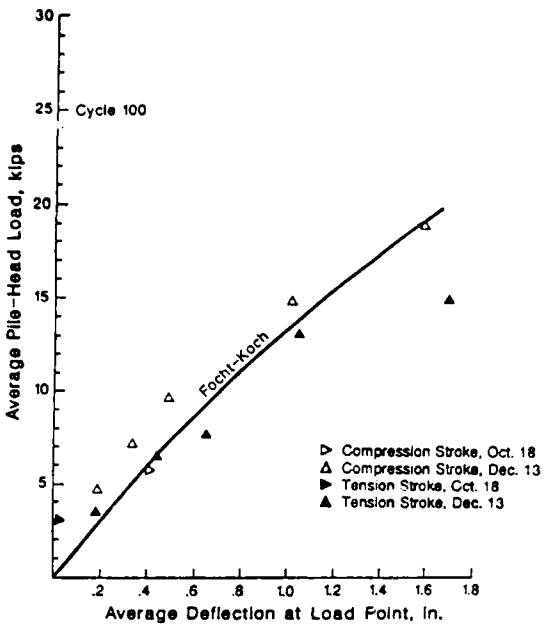

a. Comparison of measured deflections with cyclic deflections computed by the Focht-Koch method

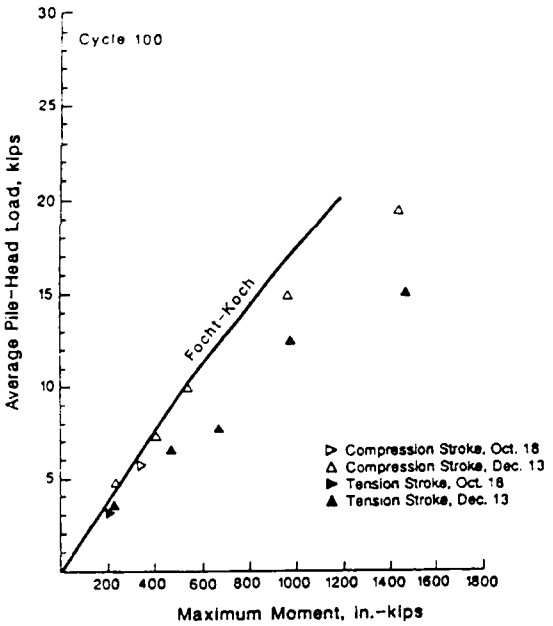

b. Comparison of measured maximum moments with cyclic maximum moments computed by the Focht-Koch method

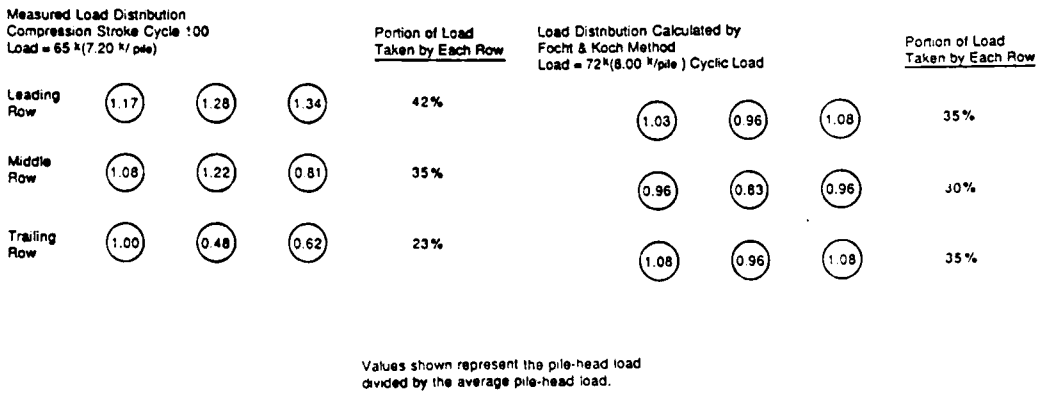

c. Comparison of measured load distribution with load distribution computed by the Focht -Koch method

Fig. 4.33 Focht-Koch prediction of group response for cyclic loading

curves and empirical modifications of these curves deriving from the concept that the piles and the soil within the group move together. Neither of these models was intended to be used with pile groups in sand, and the predictions which follow represent an "unauthorized extrapolation" of the original intent. The researchers in this study felt that it represents an interesting look at a different type of analytical procedure.

Single-Pile Method

Using the p-y criteria of Reese, Cox, and Koop, fitted to the single pile experimental data, the overall behavior of the group was predicted. Analyses were performed considering a circular pile with a circumference equal to the perimeter of the group and a stiffness in bending equal to nine times the stiffness of an individual pile. Presented in Fig. 4.34 are the predicted load-deflection relationships using this procedure in terms of the average load per pile; the load is assumed to be distributed uniformly. The deflection at a particular load is greatly overpredicted, largely because the deflection, y, used in the p-y relationship is a function of pile diameter.

For the group in clay, the loss in soil resistance due to cyclic loading was seen to be related to gapping around individual piles as well as related to group effects; for the

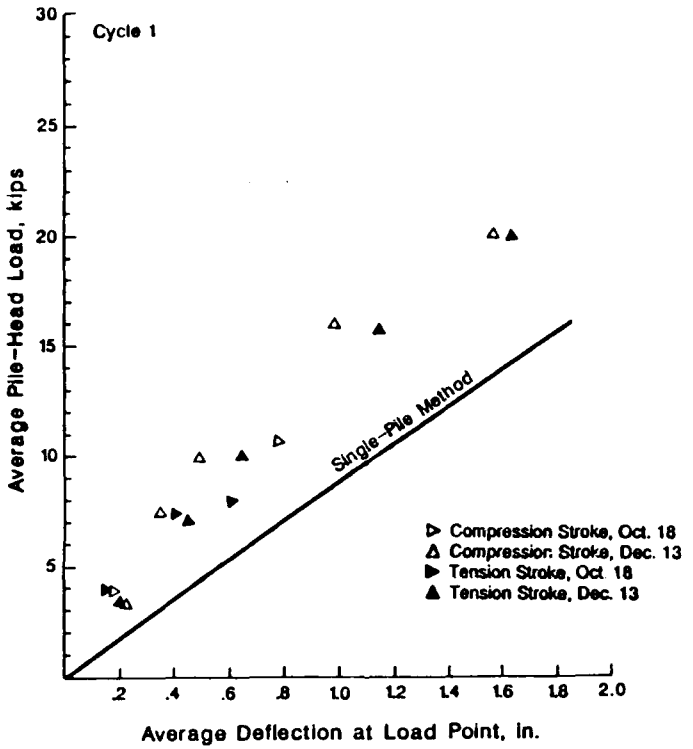

a. Comparison of measured deflections with static deflections computed by the single pile method

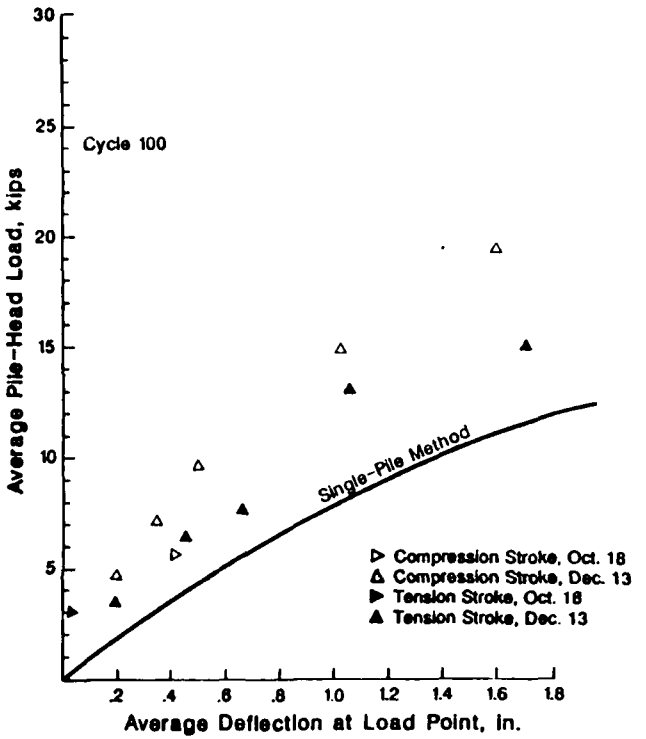

b. Comparison of measured deflections with cyclic deflections computed by the single pile method

Fig. 4.34 Predictions of group response using the single pile method

group in sand the mechanisms are less clear. The relationship between cyclic loading for a large imaginary pile and for the group may be similar, but other factors observed in the experiment such as the distribution of load and the shadowing are not considered in the single-pile method.

Bogard-Matlock Procedure

As described in Chapter 3, the Bogard-Matlock procedure combines the p-y curves for an individual pile with a modified "large-pile" p-y curve to account for group effects. Presented in Figs. 4.35 and 4.36 are the load-deflection and load-moment predictions using this procedure, for both static and cyclic loading. As for the single-pile method, the load is assumed to be distributed uniformly to the piles.

Although the load-deflection relationships are seen to be reasonably close, the method is unconservative as an indicator of maximum bending moment. As was the case for the Focht-Koch method, this error is due partly to the fact that the front-row piles support much greater loads than predicted. Because of the large differences in load between rows in the experiment, any predictions based on a uniform distribution of load cannot match both overall load deflection response in the group and the maximum stresses in the piles of the group.

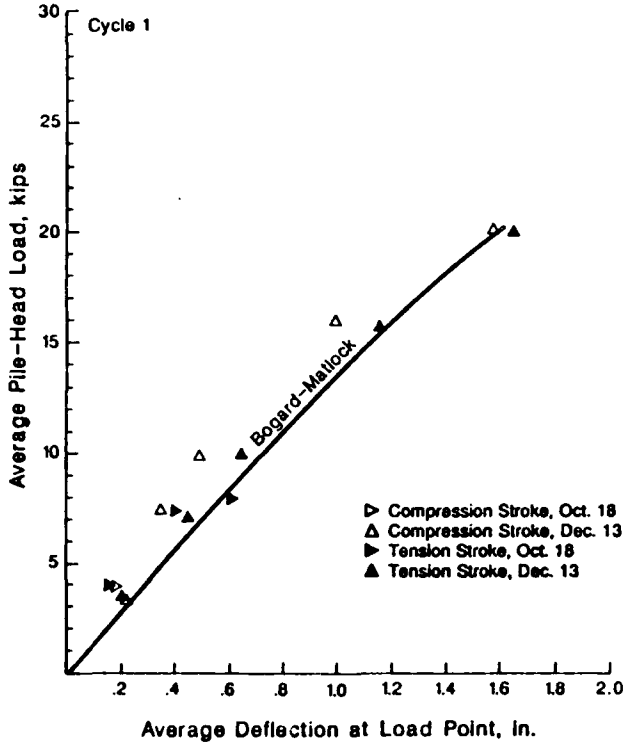

a. Comparison of measured deflections with static deflections computed by the Bogard-Matlock method

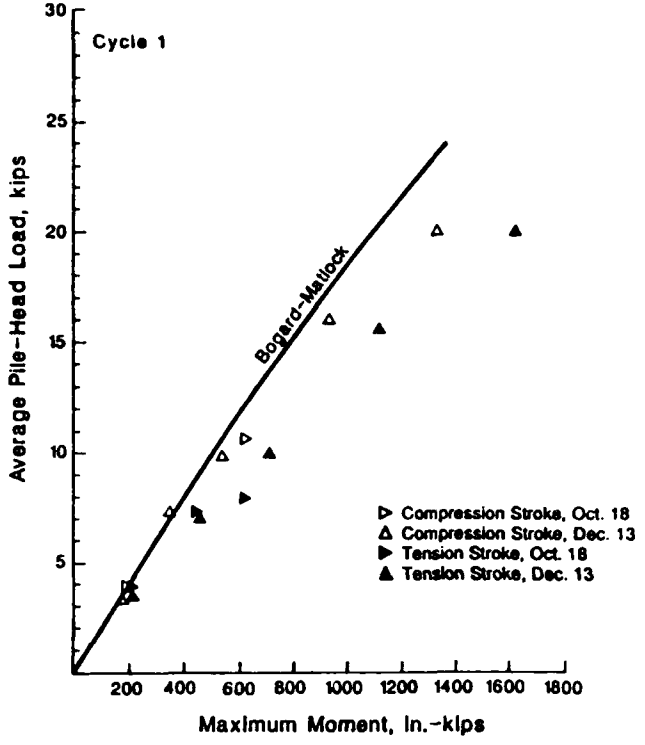

b. Comparison of measured maximum moments with static maximum moments computed by the Bogard-Matlock method

Fig. 4.35 Bogard-Matlock predictions of group response for static loading

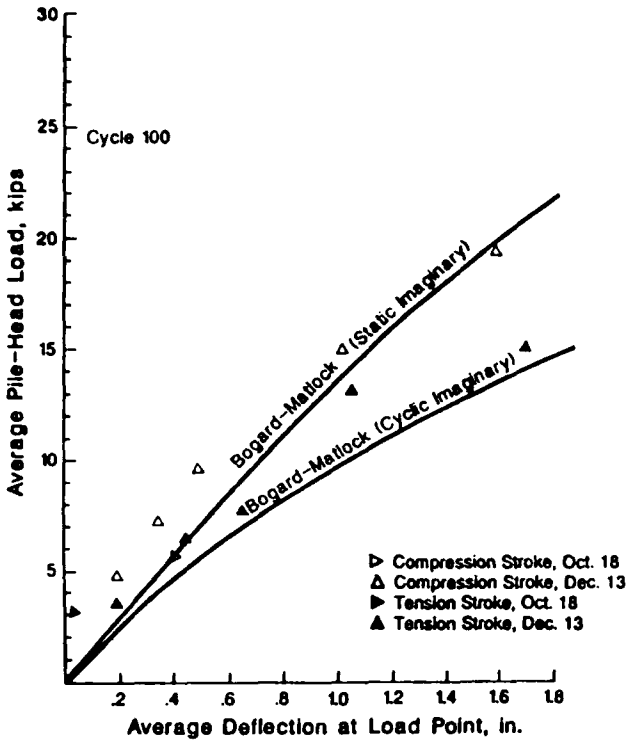

a. Comparison of measured deflections with cyclic deflections computed by the Bogard-Matlock method

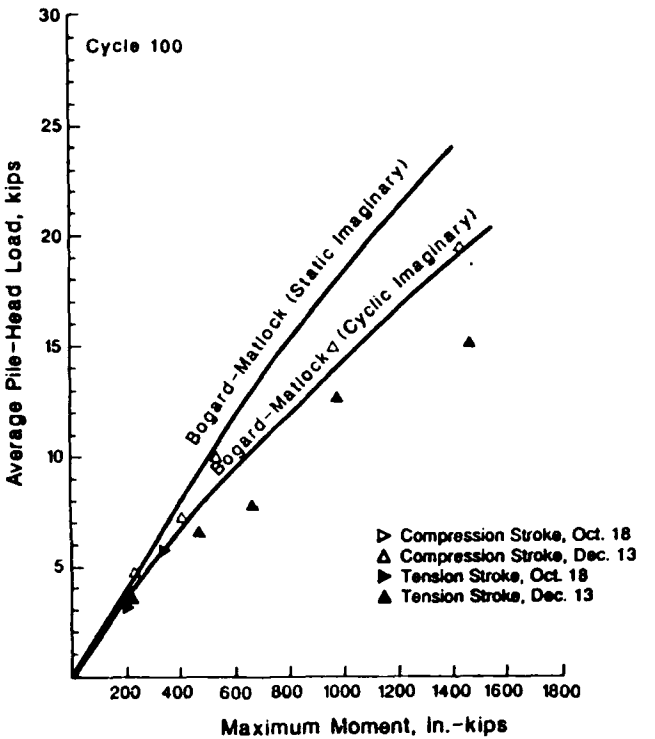

b. Comparison of measured maximum moments with cyclic maximum moments computed by the Bogard-Matlock method

Fig. 4.36 Bogard-Matlock predictions of group response for cyclic loading

Although the Bogard-Matlock procedure predicts nonlinearity in the response of the group due to reduced ultimate soil resistance, the relative differences between soil resistance between rows in the group cannot be predicted. The differences in load between rows in the group in sand was observed to be much greater than the differences in clay, so the relative differences in load between the piles in the group and an overall average are greater for the case in sand.

The deflection of the group for cyclic loading, relative to that for static loading, is seen in Fig. 4.36 to be greater than actually observed. This overprediction of the effects of cyclic loading is due in part to the p-y criteria used with the method; similar overpredictions were observed for the isolated pile. For the Bogard-Matlock procedure, the effects of cyclic loading on a large imaginary pile are quite important in estimating the effect of cyclic loading on the group. Although the mechanisms governing cyclic-load behavior in groups of piles in sand are not well understood, the concepts used in the Bogard-Matlock approach appear to greatly oversimplify the problem.

Experimental Interaction Factors

When a pile is subjected to a lateral load, the flexibility of each pile in the group is influenced by the

presence of neighboring piles. The load induces reaction in the soil and, consequently, causes deformations in the soil mass surrounding the other piles. These deformations in turn reduce the load required to produce a given deformation in the pile being affected. Such an influence is quantified in terms of pile-head behavior by the use of an α factor. This section summarizes α factors from an experimental study made by Ochoa and O'Neill(1986) for groups of free-head piles in a nonlinear sand mass.

Interaction Factors

Poulos and Randolph computed interaction factors from elastic solutions for a pair of identical, equally-loaded piles embedded in an elastic half space. The use of interaction factors for the analysis of pile groups under lateral load provides a simplified method for engineering practice. However, the response of soil to lateral load is highly nonlinear and the use of interaction factors derived from elastic theory may be inadvisable. Ochoa and O'Neill developed interaction factors experimentally for groups of laterally loaded piles embedded in sand under free-head conditions. The interaction factors from experimental results can take into account the nonlinearity of soil response and the shadowing effect. The interaction factors were derived as a function of the departure angle, the pile

spacing, the magnitude of lateral load, and the number of cycles of applied loads.

Figure 4.37 describes how interaction factors (α_{ij}) can be used to form flexibility matrices for solving for the distribution of deflection and load in simple free-head pile groups (O'Neill, 1983). The interaction factor computed from experimental results are presented in Figs. 4.38 to 4.42. The symbol $Sp_{5\%}$ shown in those figures is defined as a load on the single pile that causes a displacement at the pile head corresponding to 5% of the pile diameter. P_j is the averaged lateral load on each pile in a group; therefore, $P_j/Sp_{5\%}$ represents a level for the magnitude of applied loads. The departure angle ξ is defined in Fig. 4.43.

For conditions similar to the test conditions and for free- or pinned-head pile groups, α-factors for "Cycle 1" from Figs. 4.38 to 4.42 can be used for predictions for monotonic loading and α-factors for "Cycle 100" can be used for cyclic loading. Several features are evident in Figs. 4.38 to 4.42. First, the α-factor is lower for $\xi = 0°$ (effect of trailing pile on leading pile) than for $\xi = 180°$ (effect of leading pile on trailing pile). Second, the α-factor increases with increasing magnitude of load and, generally, decreases with increasing numbers of cycles of applied load for in-line piles. For side-by-side piles, load

$$
\begin{bmatrix}
1 & \alpha_{12} & \alpha_{13} & \alpha_{14} & \alpha_{15} & \alpha_{16} & \alpha_{17} & \alpha_{18} & \alpha_{19} & -1 \\
\alpha_{21} & 1 & \alpha_{23} & \alpha_{24} & \alpha_{25} & \alpha_{26} & \alpha_{27} & \alpha_{28} & \alpha_{29} & -1 \\
\alpha_{31} & \alpha_{32} & 1 & \alpha_{34} & \alpha_{35} & \alpha_{36} & \alpha_{37} & \alpha_{38} & \alpha_{39} & -1 \\
\alpha_{41} & \alpha_{42} & \alpha_{43} & 1 & \alpha_{45} & \alpha_{46} & \alpha_{47} & \alpha_{48} & \alpha_{49} & -1 \\
\alpha_{51} & \alpha_{52} & \alpha_{53} & \alpha_{54} & 1 & \alpha_{56} & \alpha_{57} & \alpha_{58} & \alpha_{59} & -1 \\
\alpha_{61} & \alpha_{62} & \alpha_{63} & \alpha_{64} & \alpha_{65} & 1 & \alpha_{67} & \alpha_{68} & \alpha_{69} & -1 \\
\alpha_{71} & \alpha_{72} & \alpha_{73} & \alpha_{74} & \alpha_{75} & \alpha_{76} & 1 & \alpha_{78} & \alpha_{79} & -1 \\
\alpha_{81} & \alpha_{82} & \alpha_{83} & \alpha_{84} & \alpha_{85} & \alpha_{86} & \alpha_{87} & 1 & \alpha_{89} & -1 \\
\alpha_{91} & \alpha_{92} & \alpha_{93} & \alpha_{94} & \alpha_{95} & \alpha_{96} & \alpha_{97} & \alpha_{98} & 1 & -1 \\
1 & 1 & 1 & 1 & 1 & 1 & 1 & 1 & 1 & 0
\end{bmatrix}
\begin{bmatrix} P_1 \\ P_2 \\ P_3 \\ P_4 \\ P_5 \\ P_6 \\ P_7 \\ P_8 \\ P_9 \\ \delta^g / f_H^1 \end{bmatrix}
=
\begin{bmatrix} 0 \\ 0 \\ 0 \\ 0 \\ 0 \\ 0 \\ 0 \\ 0 \\ 0 \\ P^g \end{bmatrix}
$$

$\alpha_{12}, \alpha_{13}, \ldots, \alpha_{98}$ = INTERACTION FACTOR BETWEEN SUBSCRIPTED PILES (FREE-HEADED)

$P_1, P_2, \ldots, P_9$ = PILE LOAD

P^g = GROUP LOAD

δ^g = GROUP DEFLECTION

f_H^1 = HORIZONTAL DEFLECTION OF SINGLE PILE UNDER UNIT LOAD (SINGLE PILE FLEXIBILITY)

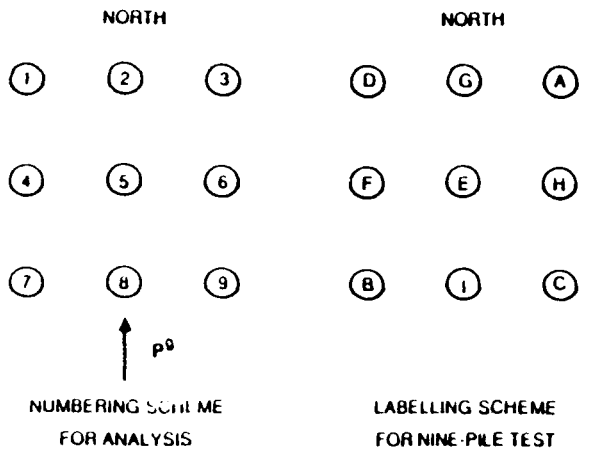

Fig. 4.37 Flexibility matrix for a nine-pile group with free-head connections (after O'Neill, 1983)

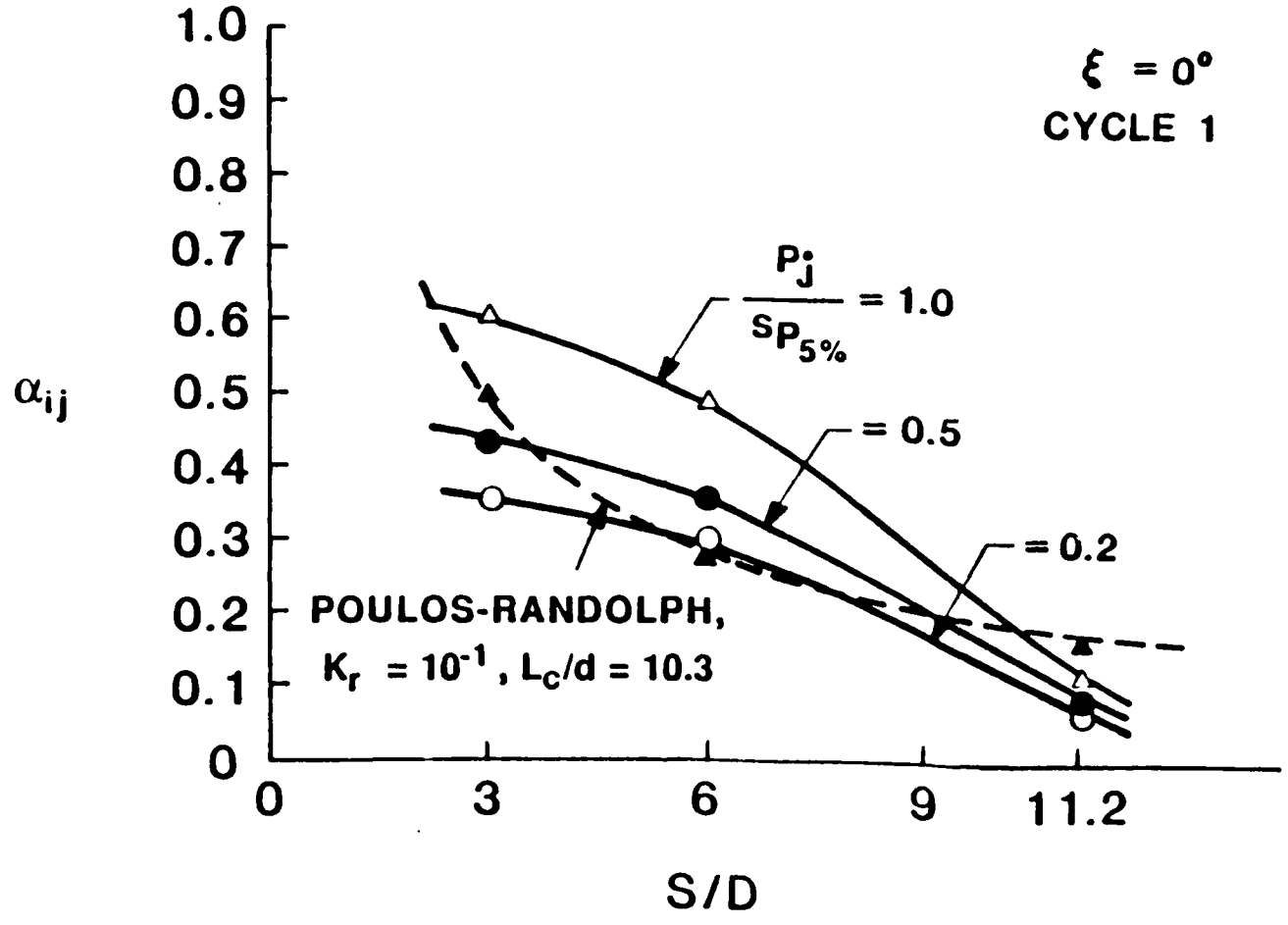

Fig. 4.38 Design chart: α_{ij} vs S/D for $\xi = 0^{o}$, Cycle 1

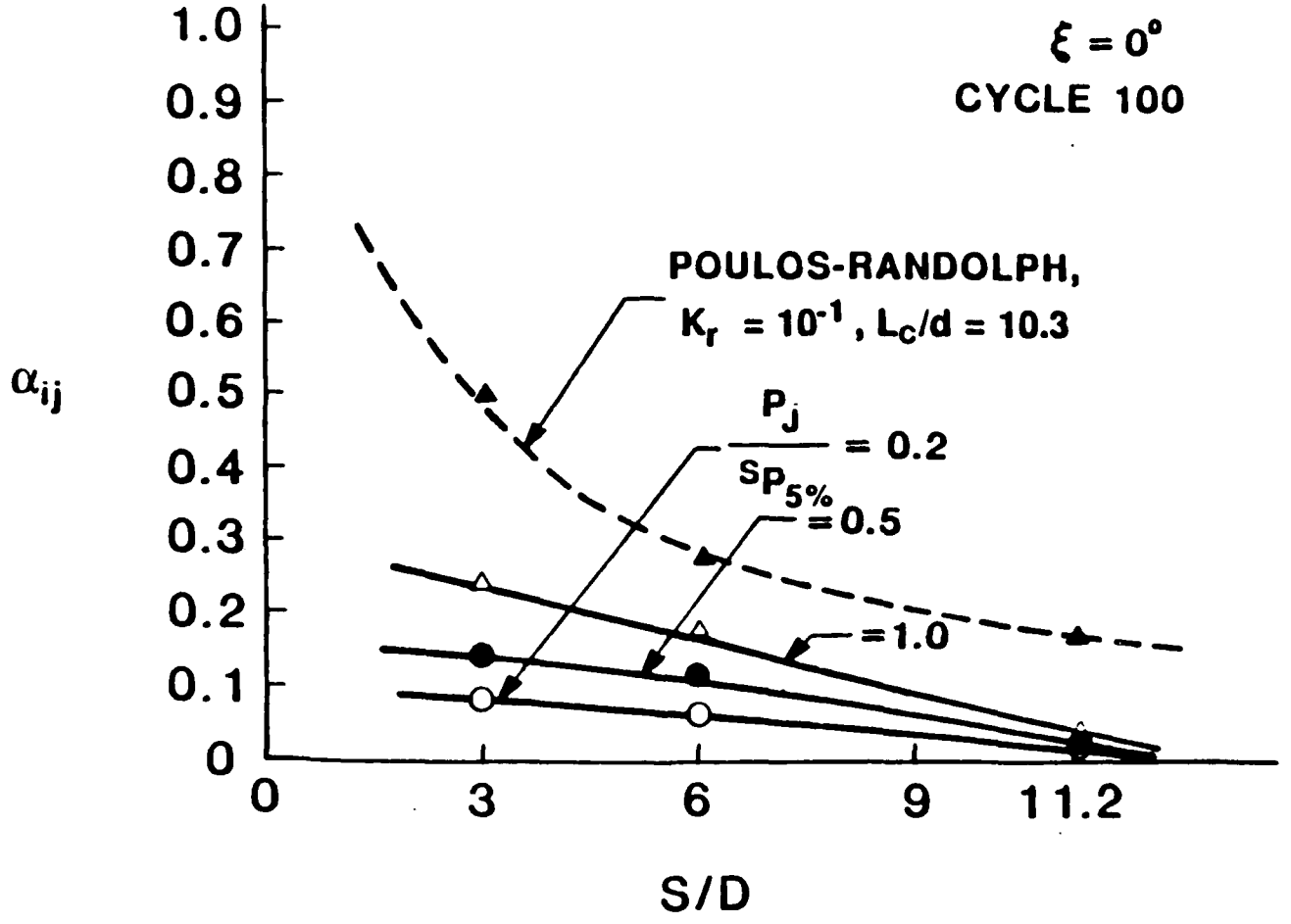

Fig. 4.39 Design chart: a_{ij} vs S/D for $\xi = 0^{o}$, Cycle 100

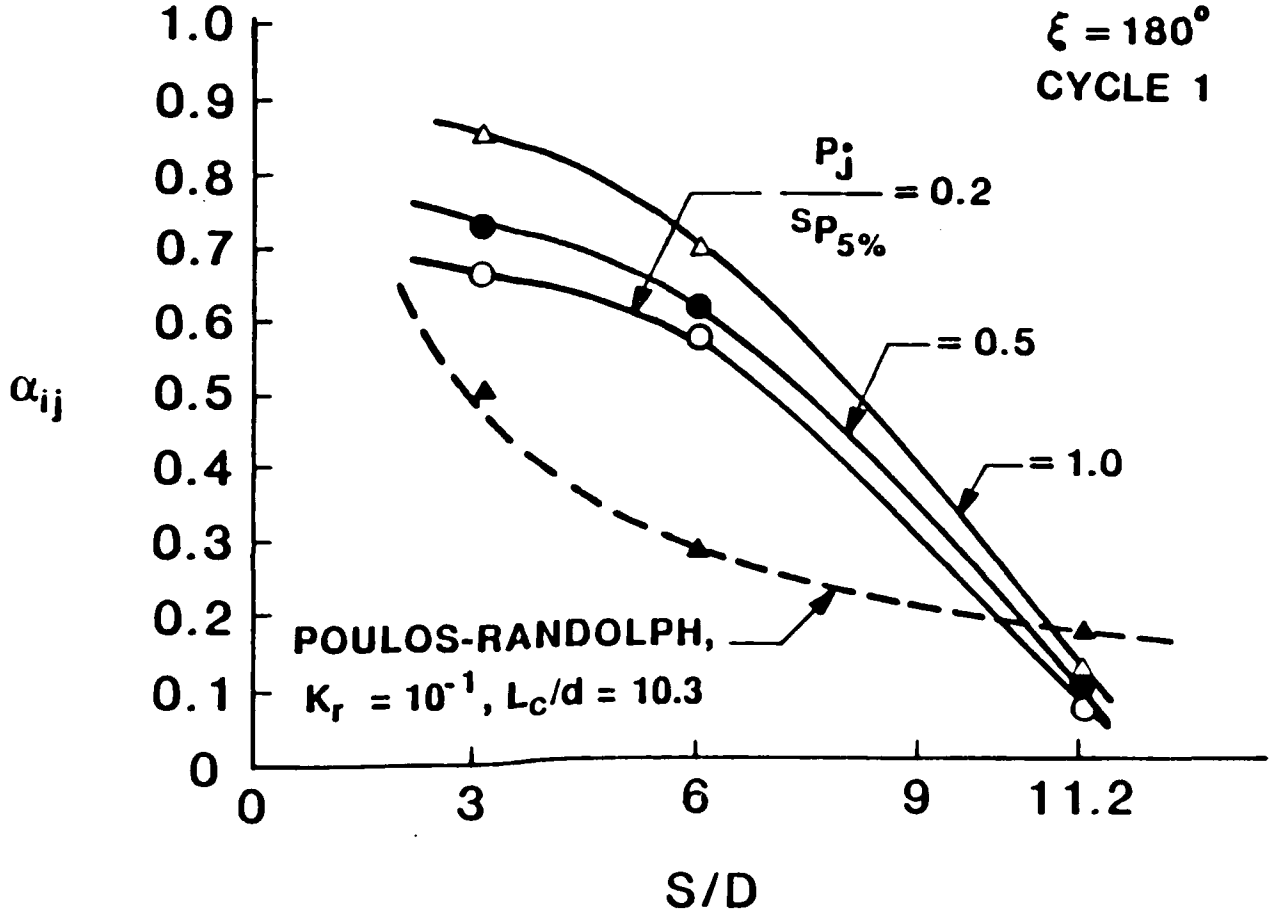

Fig. 4.40 Design chart: a_{ij} vs S/D for $\xi = 180^{o}$, Cycle 1

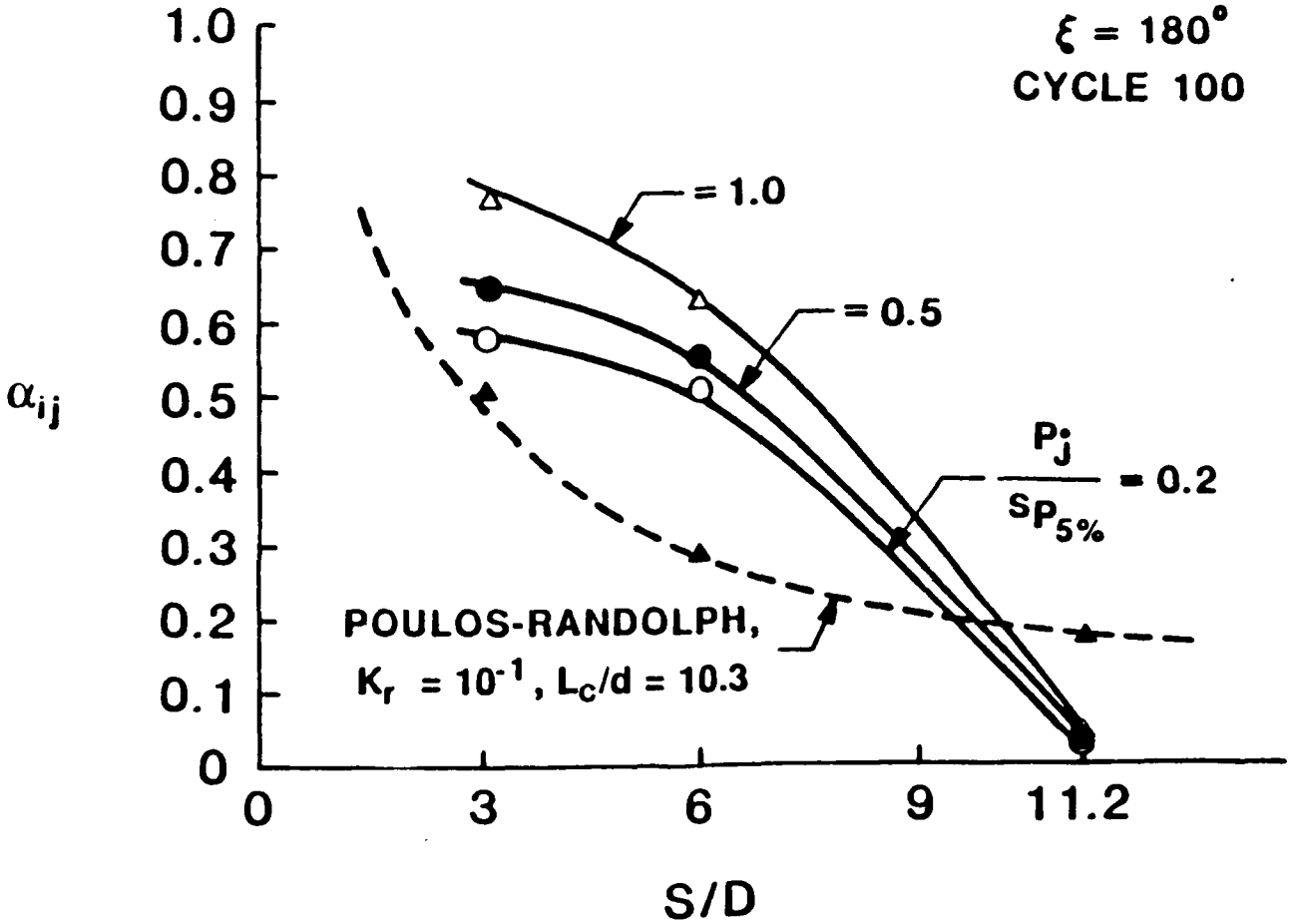

Fig. 4.41 Design chart: α_{ij} vs S/D for $\xi = 180^{\circ}$, Cycle 100

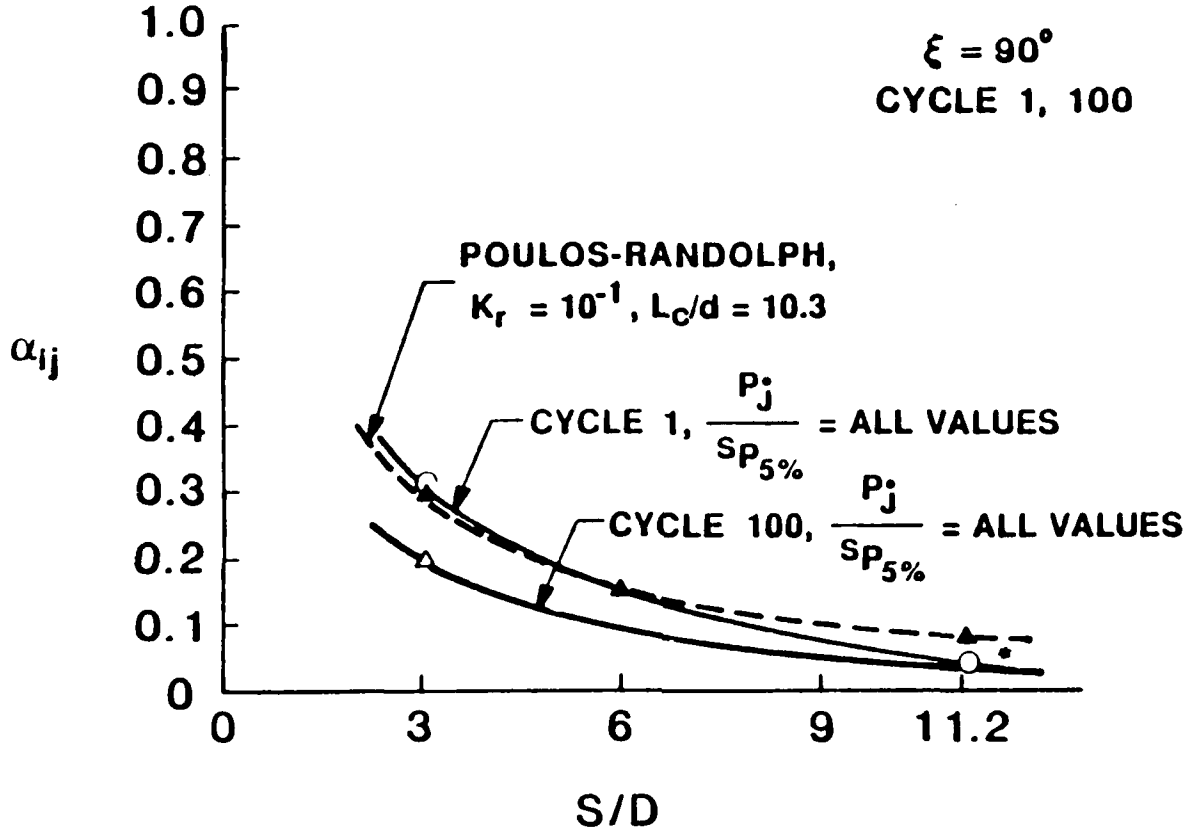

Fig. 4.42 Design chart: a_{ij} vs S/D for $\xi = 90^{o}$, Cycles 1 and 100

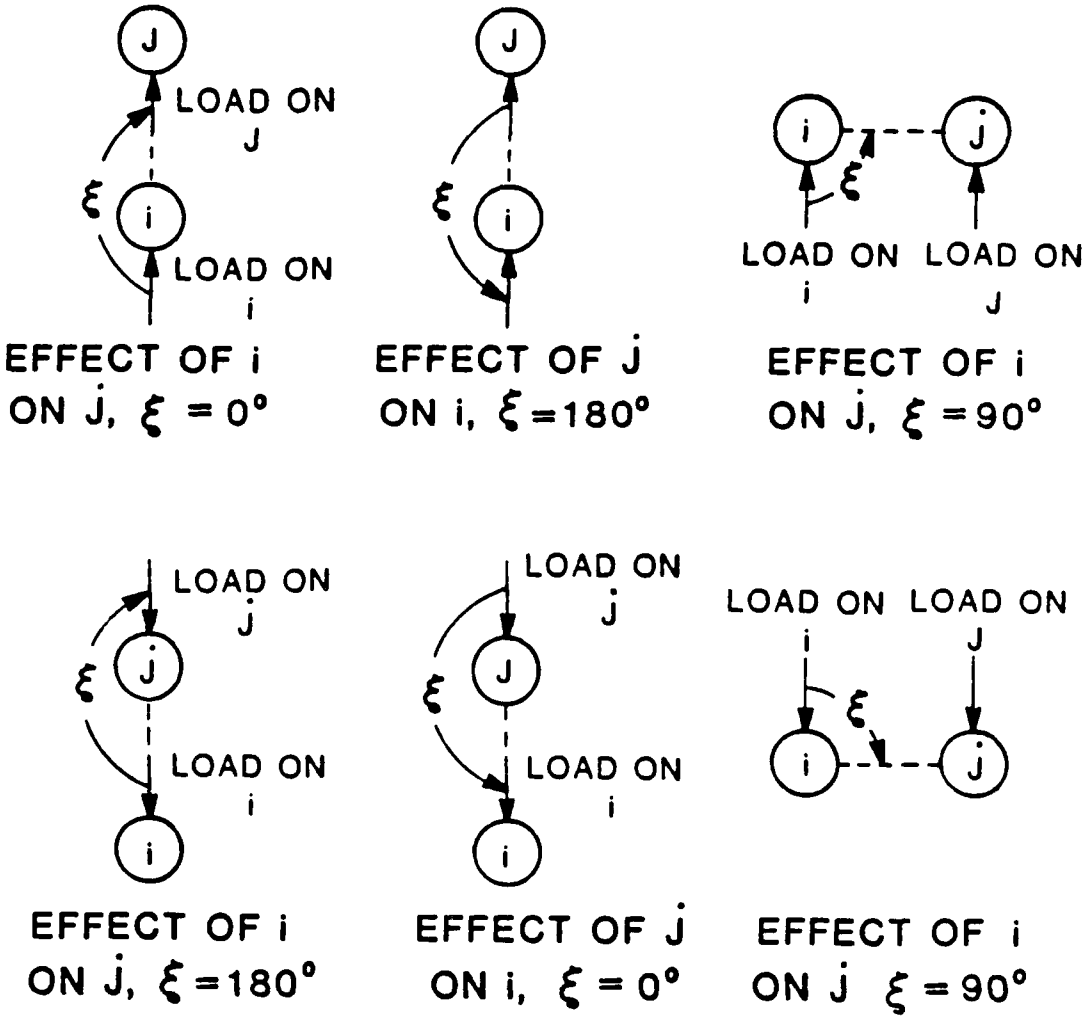

Fig. 4.43 Definition of ξ

magnitude had a minimal effect on α , and it decreased with increasing numbers of load cycles. Finally, the α-factors obtained from experimental results in sand were generally larger than those predicted by elastic theory for spacing ratio (S/D) less than 9.

Design Procedure

This section provides a step-by step design procedure for the evaluation of the behavior of a free-head pile group embedded in medium to dense sand, using the experimental interaction factors from Figs. 4.38 to 4.42.

1. Compute the average load per pile, P_j, in a group.

2. Compute the single-pile flexibility, f_{H1} (secant to single-pile load-deflection curve for the average load per pile obtained in Step 1.). The load-distribution curve is obtained from a load test or from some method of analysis.

3. Normalize the average load per pile, ($P_j/Sp_{5\%}$), by using a load for the single pile that corresponds to a displacement of 5% of the diameter of the single pile.

4. Formulate the flexibility-matrix equation (free-head) for the pile group, based on Fig. 4.37.

5. Evaluate every element (α_{ij}) in the matrix for a particular direction of load, number of cycles, load level, spacing, and departure angle between subscripted piles.

6. Compute load distribution ($P_1, \ldots\ldots, P_n$) and group deflection, δ^g, by solving the flexibility-matrix equation.

Comparison of Experimental and Predicted Behavior of Pile Group

The analysis for the nine-pile group embedded in sand, conducted by Morrison and Reese (1986), was studied using the interaction factors as described above. The distribution of load among piles in the group and group deflection are compared with the measured values. Figures 4.44 to 4.47 summarize the results obtained after solving the flexibility-matrix equation using the recommended interaction factors.

The distribution of load among the piles in the group from Figs. 4.44 to 4.47 shows that the shadowing effect can be evaluated reasonably accurately using the experimental interaction factors. Leading (front) piles developed loads larger than the loads developed by the row of trailing (rear) piles. Better agreement for distribution of load among the piles in the group and deflection of the group was obtained when the group was loaded to the south rather than to the north. In general, this method underestimated loads on the leading and second row and overestimated loads on the piles in the rear row. The deflection of the pile group predicted by the interaction-factor method has good agreement with the measured deflection as shown in Table 4.1. The experimental

CYCLE : 1
LOADING : NORTH
GROUP LOAD : 66.08K

AVERAGE LOAD PER PILE : 7.34K

$$\frac{P_j^*}{sP_{5\%}} = 0.35$$

NORTH

(1)	(2)	(3)
14.07K	10.33K	14.07K → EXPERIMENTAL α's
8.53K	9.16K	9.24K → MORRISON'S TEST
10.71K	7.82K	10.71K → POULOS-RANDOLPH α's
(4)	(5)	(6)
5.62K	3.00K	5.62K
8.05K	8.86K	6.12K
3.59K	0.38K	3.59K
(7)	(8)	(9)
5.33K	2.67K	5.33K
7.40K	3.90K	4.82K
10.71K	7.82K	10.71K

AVERAGE LOAD PER ROW

(1 2 3)
12.82K
8.97K
9.74K

(4 5 6)
4.74K
7.67K
2.52K

(7 8 9)
4.44K
5.37K
9.74K

GROUP DEFLECTION

EXPERIMENTAL α's : 0.50 in.

MORRISON'S TEST : 0.35 in.

POULOS-RANDOLPH α's : 0.46 in.

Fig. 4.44 Distribution of load and deflection of group for Cycle 1, loading north, group load = 66.08 k

CYCLE : 1
LOADING : SOUTH
GROUP LOAD : 63.47K

AVERAGE LOAD PER PILE : 7.05K

$$\frac{P_j^*}{{}^sP_{5\%}} = 0.32$$

NORTH

①	②	③
5.35K	2.74K	5.35K → EXPERIMENTAL α's
5.26K	4.56K	5.69K → MORRISON'S TEST
10.29K	7.51K	10.29K → POULOS-RANDOLPH α's
④	⑤	⑥
5.54K	3.03K	5.54K
6.25K	4.70K	5.99K
3.45K	0.36K	3.45K
⑦	⑧	⑨
13.15K	9.58K	13.15K
9.24K	10.82K	10.97K
10.29K	7.51K	10.29K

AVERAGE LOAD PER ROW

(1 2 3)
4.48K
5.17K
9.36K

(4 5 6)
4.70K
5.64K
2.42K

(7 8 9)
11.96K
10.34K
9.36K

GROUP DEFLECTION

EXPERIMENTAL α's : 0.50 in.

MORRISON'S TEST : 0.45 in.

POULOS-RANDOLPH α's : 0.46 in.

Fig. 4.45 Distribution of load and deflection of group for Cycle 1, loading south, group load = 63.47 k

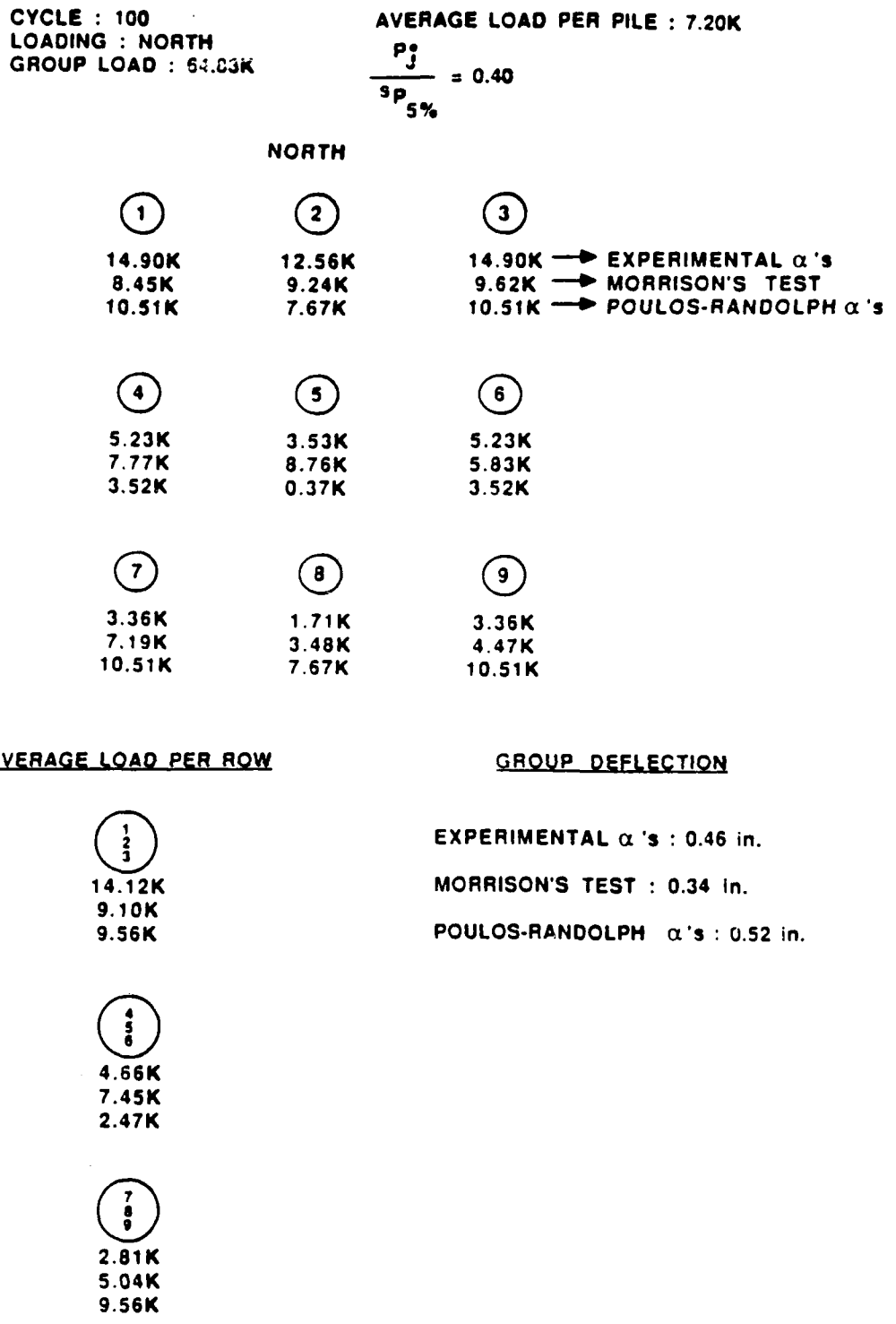

Fig. 4.46 Distribution of load and deflection of group for Cycle 100, loading north, group load = 64.83 k

CYCLE : 100
LOADING : SOUTH
GROUP LOAD : 58.48K

AVERAGE LOAD PER PILE : 6.49K

$$\frac{P_j^*}{{}^sP_{5\%}} = 0.37$$

NORTH

①	②	③
3.12K	1.63K	3.12K → EXPERIMENTAL α's
4.55K	4.22K	5.81K → MORRISON'S TEST
9.48K	6.92K	9.48K → POULOS-RANDOLPH α's
④	⑤	⑥
4.87K	3.34K	4.87K
5.29K	4.20K	5.85K
3.18K	0.33K	3.18K
⑦	⑧	⑨
13.19K	11.10K	13.89K
7.96K	10.02K	10.57K
9.48K	6.92K	9.48K

AVERAGE LOAD PER ROW

(1 2 3)
2.62K
4.86K
8.63K

(4 5 6)
4.36K
5.11K
2.23K

(7 8 9)
12.73K
9.51K
8.63K

GROUP DEFLECTION

EXPERIMENTAL α's : 0.37 in.

MORRISON'S TEST : 0.44 in.

POULOS-RANDOLPH α's : 0.42 in.

Fig. 4.47 Distribution of load and deflection of group for Cycle 100, loading south, group load = 58.48 k

Table 4.1

Load by row, as per cent of total, and deflection for nine-pile group, loading south

Row	Experimental α's	Morrison's Load Test	Poulos-Randolph α's
		CYCLE 1	
Front	56 % (0.50)	48 % (0.45)	44 % (0.46)
Second	22 % (0.50)	26 % (0.45)	11 % (0.46)
Third	21 % (0.50)	24 % (0.45)	44 % (0.46)
		CYCLE 100	
Front	65 % (0.37)	48 % (0.44)	44 % (0.42)
Second	22 % (0.37)	26 % (0.44)	11 % (0.42)
Third	13 % (0.37)	24 % (0.44)	44 % (0.42)

Note: Deflections shown in parentheses in inches

α-factors provided a better prediction of the pattern of distribution of load than did the elasticity-based factors.

Summary

The design procedures available to analyze pile groups for lateral loading are categorized into two types: the elasticity-based models and the modified load-transfer methods. Both types were seen to reproduce gross overall group behavior with only moderate errors when carefully calibrated by use of results from the testing of an instrumented single pile. However, none of the methods properly predicts the distribution of load to the piles. No conceptual models are available which can represent shadowing and load bias in terms of leading vs trailing rows. Elasticity-based models predict the distribution of the load but the prediction is greatly in error. Modified load-transfer methods have no provisions at all for predicting the distribution of load to the various piles in the group. Also, these empirical procedures were developed for soft clays and were not intended for use with sands.

All of the methods which have provisions for calculating bending stresses were not conservative in this regard, probably due in large part to the problems of distribution of load. The methods also indicated incorrect depth to maximum

moment due to reduced soil resistance near the ground surface.

The errors in prediction of response to static loading tended to be magnified somewhat for cyclic loading. Although cyclic loading was less of a concern for groups in sand than for groups in clay, the conceptual models used in these procedures do not inspire confidence for design. The elasticity-based Focht-Koch procedure presumes cyclic soil response for piles in a group to be the same as that for individual piles, while the modified load-transfer methods limit soil response to that of a large imaginary pile encompassing the group. Neither approach predicts very well the behavior that was observed.

The method using experimental interaction factors seems to be promising. However, further studies covering a variety of variables such as pile spacing, soil density, and pile-head connection are needed before this method can be confidently used in design.

CHAPTER 5
USE OF PRESSUREMETERS AT THE TEST SITE FOR PREDICTING THE BEHAVIOR OF SINGLE PILES

INTRODUCTION

The pressuremeter has been recognized as a versatile in-situ instrument for subsurface measurement and can be employed in virtually any type of soils. The instrument is showing promise as a means of obtaining p-y curves from the results of field tests. A series of pressuremeter tests were conducted by Dr. J. L. Briaud, Texas A & M University, and his research team during 1985 to 1986 at the test site at the University of Houston with the view of making predictions of pile response that could be compared with observed response (O'Neill and Dunnavant, 1984; Morrison and Reese, 1986). The soil-resistance curves were derived from pressuremeter measurements and the pile behavior was predicted with these derived p-y curves.

Two types of pressuremeters were used in this study; one is the preboring pressure (PBPMT) (Fig. 5.1), and the other one is known as the cone pressuremeter (CPMT) (Fig. 5.2). Both pressuremeters are composed of a portable control unit and a probe with a single inflatable cell. The primary difference between these two is the insertion method. For the preboring pressuremeter, a borehole is drilled and the

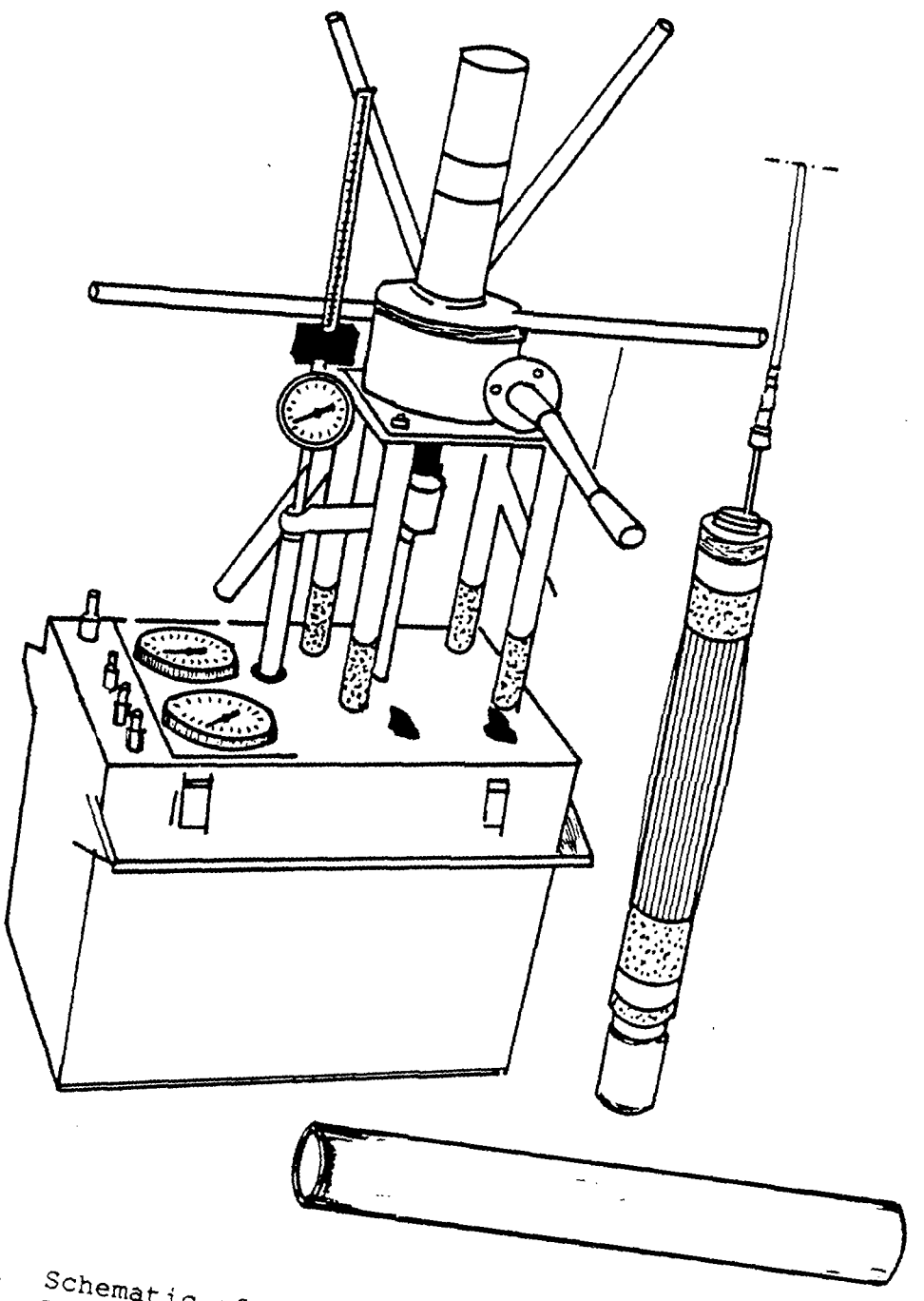

Fig. 5.1 Schematic of the preboring pressuremeter model TEXAM (PBPMT)

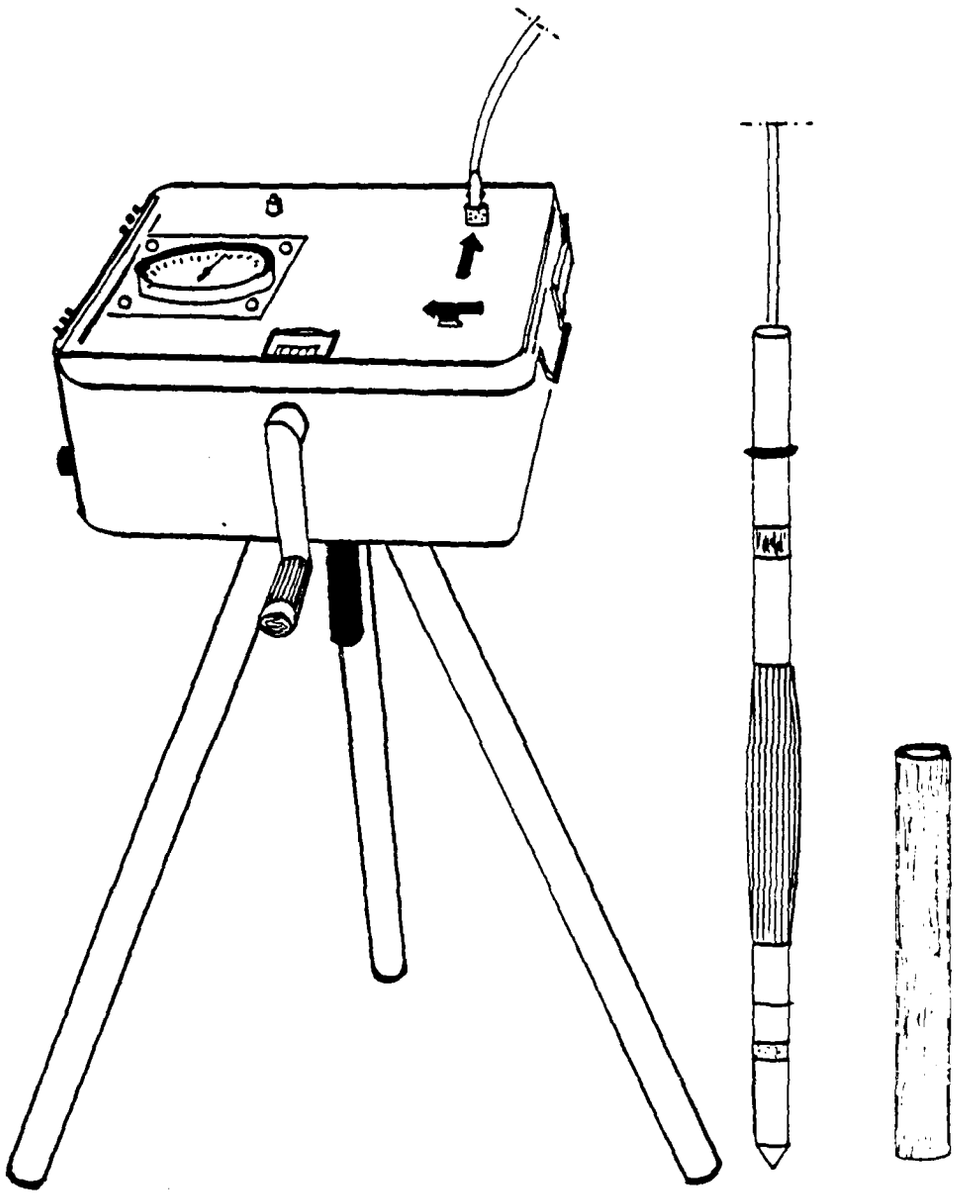

Fig. 5.2 Schematic of the cone pressuremeter model PENCEL (CPMT)

pressuremeter probe is inserted down to the test depth. For the cone pressuremeter, the probe is either pushed into the soil at a constant rate or driven with a hammer.

This chapter will summarize the methods of development of p-y curves directly from pressuremeter data, the procedures for in-situ testing, the measured soil response, and the comparison between the predicted and the measured pile behavior.

BASIC THEORY FOR SOIL-RESISTANCE CURVES

Sketches of a single pile subjected to a lateral force, Q, a vertical force, P, and a moment, M, are shown in Fig. 5.3 and can be used to solve for the static equilibrium of the pile. The stress components on an element abcd are the radial stress σ_{rr}, the shear stresses $\tau_{r\theta}$, $\tau_{z\theta}$, and τ_{rz}, the normal stress, σ_{zz} and the tangential stress $\sigma_{\theta\theta}$. For long piles with a length-to-diameter ratio larger than 3, the soil resistance is due mainly to the radial stress σ_{rr} and the shear stress $\tau_{r\theta}$.

The frontal resistance Q and the surface friction resistance F (Fig. 5.4) per unit length of a pile with a radius of r_o can be computed by integrating the radial stress σ_{rr} and the shear stress $\tau_{r\theta}$ along the pile surface. The unit frontal resistance, Q, due to σ_{rr} is

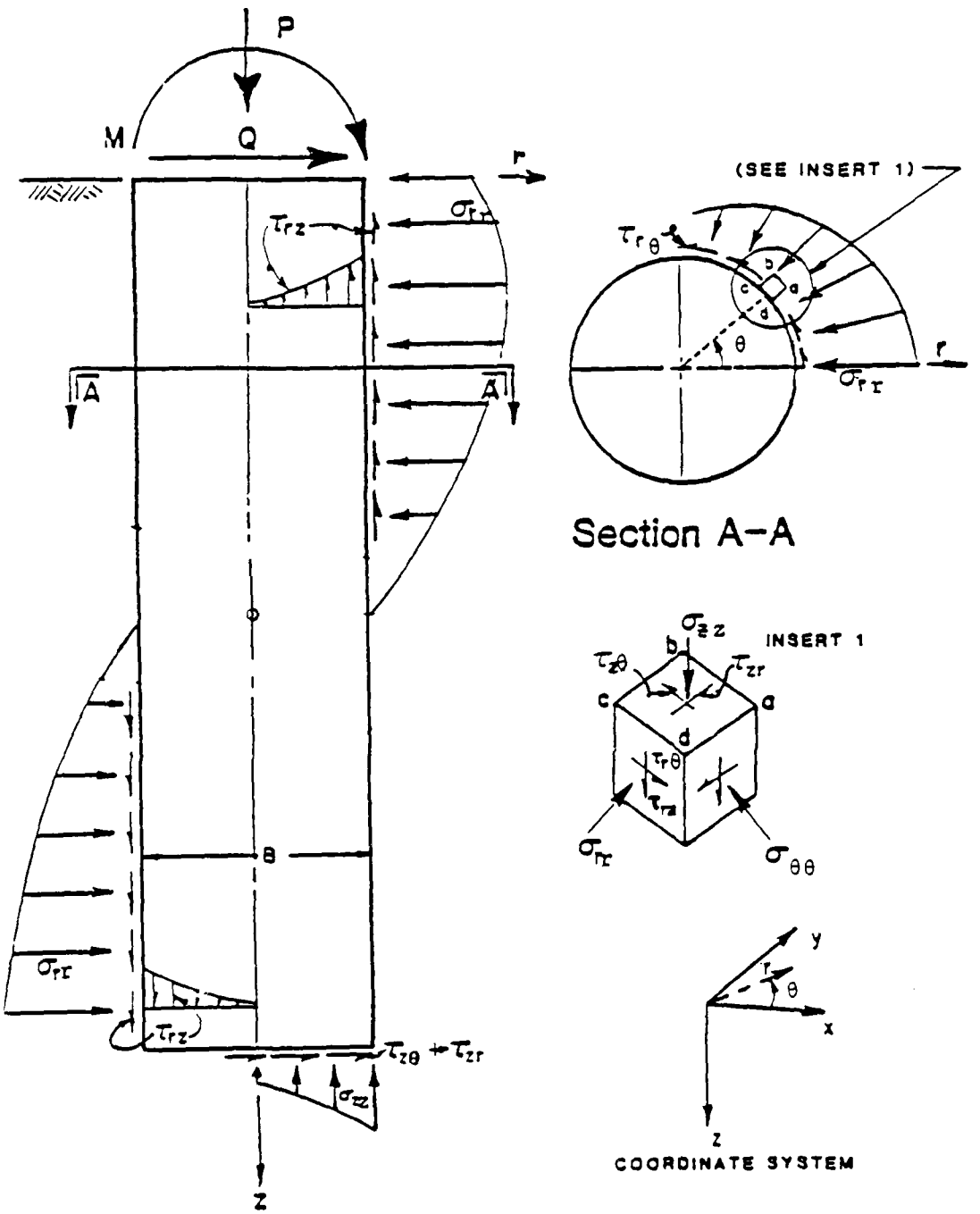

Fig. 5.3 Static equilibrium of stresses on a pile (after Digioa, et al., 1981)

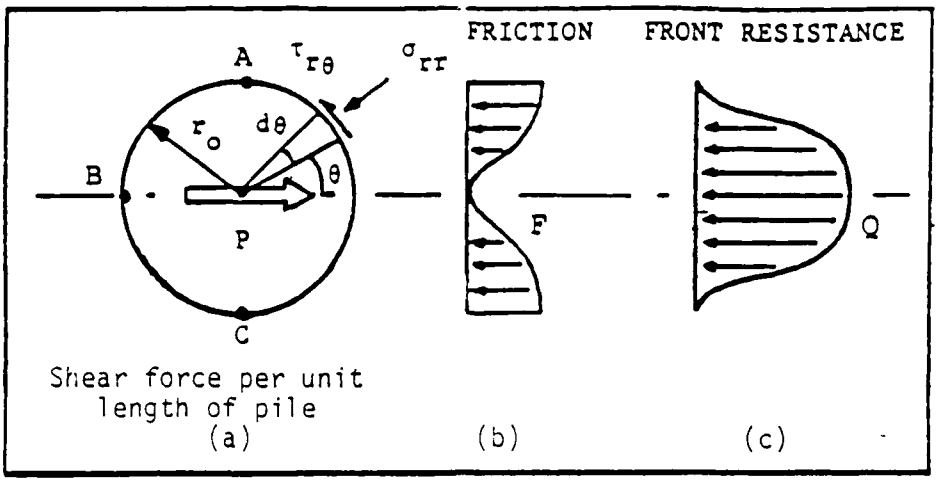

Fig. 5.4 Distribution of friction resistance and front resistance (after Briaud, et al., 1983b)

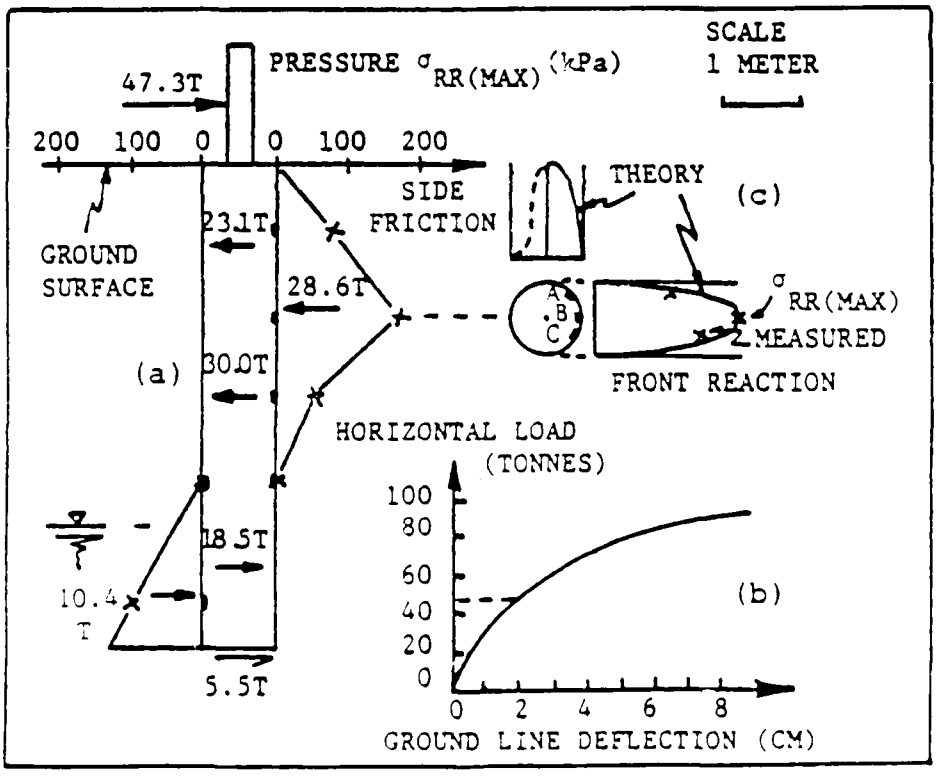

Fig. 5.5 Texas A&M University bored pile load test (after Kasch, et al., 1977)

$$Q \int_{-\frac{\pi}{2}}^{\frac{\pi}{2}} \sigma_{rr} r_o \cos\theta \, d\theta \qquad 5.1$$

Similarly, the unit friction resistance, F, due to $\tau_{r\theta}$ is

$$F = \int_{-\frac{\pi}{2}}^{\frac{\pi}{2}} \tau_{r\theta} r_o \sin\theta \, d\theta \qquad 5.2$$

For a linear elastic soil, Baguelin et al (1978) gave expressions for σ_{rr} and $\tau_{r\theta}$ as follows.

$$\sigma_{rr} = \sigma_{rr,max} \cos\theta, \qquad \sigma_{rr,max} = \frac{P}{2\pi r_o} \qquad 5.3$$

$$\tau_{r\theta} = \tau_{r\theta,max} \sin\theta, \qquad \tau_{r\theta,max} = \frac{P}{2\pi r_o} \qquad 5.4$$

The substitution of expressions for σ_{rr} and $\tau_{r\theta}$ into Eqs. 5.1 and 5.2 leads to the following expressions:

$$Q = \sigma_{rr,max} \bullet 2r_o \bullet \frac{\pi}{4} \qquad 5.5$$

and

$$F = \tau_{r\theta,max} \bullet 2r_o \bullet \frac{\pi}{4} \qquad 5.6$$

The total soil resistance p in force per unit length of pile for a horizontal movement of the pile element is found from the addition of the front resistance Q and the friction resistance F.

The Q-y Curve and the Pressuremeter Curve

A test was performed with an instrumented pile (see Fig. 5.5) in order to verify the derivation shown above. Figure 5.5a shows the pile with the resisting forces, and Fig. 5.5b shows the load-deflection curve. Figure 5.5c shows a cross-section of the pile and the location of three pressure cells (A, B, and C). The theoretical distribution of the elementary forces dQ as shown in Fig. 5.5c was found to match the measurements recorded on the three pressure cells. This validated the use of Eq. 5.5, provided $\sigma_{rr(max)}$ could be obtained. Pressuremeter tests were performed in a prebored hole and the pressuremeter curve that was obtained is shown in Fig. 5.6a. The front reaction curve was computed using Eq. 5.7 and the curve is compared with the response from the

pressure cells which measured $\sigma_{rr(max)}$ on the shaft and Fig. 5.6b shows the comparison. From the pressuremeter, p is the cell pressure ($\sigma_{rr(max)}$) and y/R is the lateral movement of the cell y divided by the pile radius R. Figure 5.6b shows very good agreement between pressure cells and pressuremeter response (Smith, 1983). This tends to prove that the curve obtained from a pressuremeter test, performed in a prebored hole, simulates well the reaction of the front pressure cell for a bored pile. In the proposed method the front resistance will be obtained as follows:

$$Q(front) = p(pmt) \bullet b(pile) \bullet S(Q) \qquad 5.7$$

where

Q(front) = the soil resistance due to front reaction (in force/unit length of pile),

p(pmt) = the net pressuremeter pressure,

b(pile) = the pile width or diameter, and

S(Q) = the shape factor = 1.0 for square piles
= $\pi/4$ for round piles.

The lateral deflection of the pile can be obtained as follows:

$$y(pile) = y(pmt) \bullet \frac{R\ (pile)}{R\ (pmt)} \qquad 5.8$$

where

y(pile) = the lateral deflection of the pile,

R(pile) = pile radius,

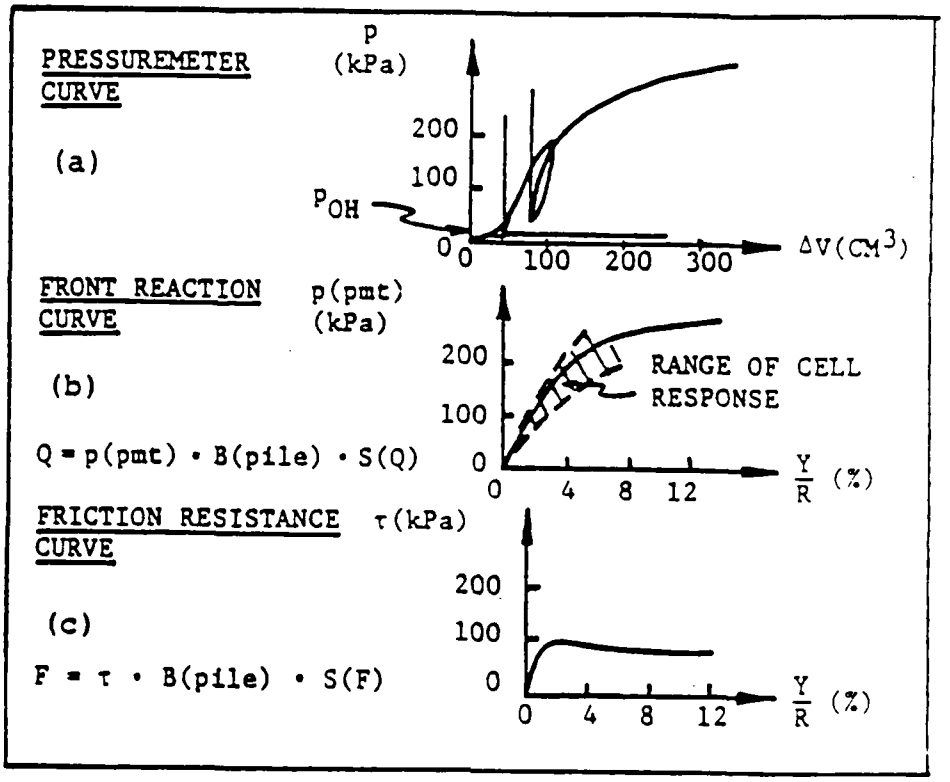

Fig. 5.6 Obtaining the Q-y and F-y curves from the pressuremeter curve (from Braiud, et al., 1983b)

y(pmt) = increase in radius of the soil cavity in the pressuremeter test, and

R(pmt) = initial radius of the soil cavity in the pressuremeter test.

If a pile is driven and fully displaces the soil, one would expect that the resulting Q-y curve would be different from the one for a bored pile in the same soil. In the case of a bored pile, preboring the hole for the pressuremeter seems to be appropriate; in the case a closed-end pile that is driven, it may be more appropriate to drive the pressuremeter in place. Alternatively, the hole can be bored, the pressuremeter expanded a first time to simulate the driving of the pile, and then expanded a second time. The Q-y curve for the driven pile is derived from the reload portion of the pressuremeter curve. This procedure has not been confirmed directly but has been proven reasonable by the good performance of the method in predicting the behavior of driven piles.

The curve that is shown in Fig. 5.6c will be discussed in the next section.

The f-y Curve and the Pressuremeter Curve

Based on the previous theoretical and experimental considerations, the friction on the sides of the pile according to the proposed method is:

$$F(side) = \tau(soil) \bullet b(pile) \bullet S(F) \qquad 5.9$$

where

F(side) = the soil resistance due to friction resistance,

τ(soil) = the soil shear stress at the soil-pile interface and at point A in Fig. 5.4a for a given pile displacement y,

b(pile) = the pile width or diameter, and

S(F) = the shape factor = 1 for square piles
= 2 for round piles.

The displacement y is obtained from Eq. 5.8. The shear stress τ(soil) increases as y increases and the F-y curve derived from the pressuremeter will exhibit the usual strain-softening or strain-hardening behavior of the soil; indeed this behavior is directly measured by the pressuremeter as discussed in the following paragraph.

It has been shown that a curve showing shear stress-strain can be obtained from the selfboring-pressuremeter curve by a theoretical method called the subtangent method (Baguelin et al., 1978). Applying the subtangent method to the curve from a pressuremeter test performed in a prebored hole (preboring pressuremeter test) leads to shear moduli which are too low and peak shear strength which is too high, compared to those obtained from selfboring pressuremeter tests. However, applying the subtangent method

to the reload curve from a preboring pressuremeter test (Fig. 5.6a) leads to shear moduli comparable to selfboring shear moduli. As a result, in the proposed approach, the reload portion of the preboring pressuremeter curve is used to obtain the τ(soil) versus y(pmt)/R(pmt) curve as shown in Fig. 5.6c.

Critical Depth

The ultimate soil resistance against a pile that is loaded laterally is dependent on the depth below the ground surface, with the minimum value occuring at the ground surface. The analytical expressions that have been derived for the ultimate soil resistance reflect, thus, two different modes of behavior: an upward and outward movement of the soil near the ground surface, and a flow-around movement at a considerable depth below the ground surface. The depth at which the analytical expressions yield the same ultimate soil resistance is called the "critical depth." The results from the pressuremeter test must be adjusted to reflect the depth at which the test was performed.

A study was made that led to a correlation between the critical depth and the relative rigidity of the pile-soil system. The relative rigidity RR is defined as follows (Briaud, et al 1983a).

$$RR = \frac{1}{b}\sqrt[4]{\frac{EI}{P_L^*}} \qquad 5.10$$

where

b = pile diameter,

E = modulus of pile material,

I = moment of inertia, and

P_L = limit pressure.

Figure 5.7 shows the results of a study (Briaud, et al., 1983b) that gives a correlation between the critical depth D_C and the relative rigidity RR. A further study by Briaud, et al. (1983b) led to the development of Fig. 5.8 which shows the value of the reduction factor α as a function of the relative depth z/D_C. With a value of α, the F-y curve can be reduced if the pressuremeter test were performed in a zone above the critical depth.

In addition to the p-y curves being affected by the depth below the ground surface, Baguelin et al (1978) noted that the results from the pressuremeter are also affected if the test were performed in about the top one meter of the soil. A study by Briaud, et al (1983b) led to the development of Fig. 5.9 which shows the reduction factor β as a function of the critical depth for the pressuremeter. The critical depth for the pressuremeter z_C is taken as 30 pressuremeter radii for clay and 60 pressuremeter radii for

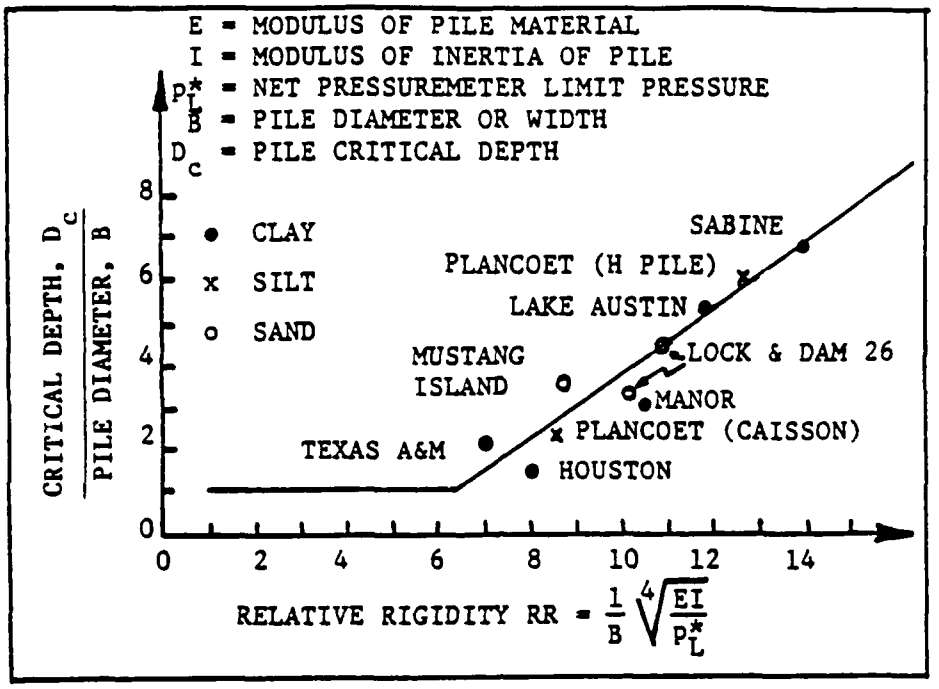

Fig. 5.7 Pile critical depth versus soil-pile relative rigidity (from Briaud, et al., 1983b)

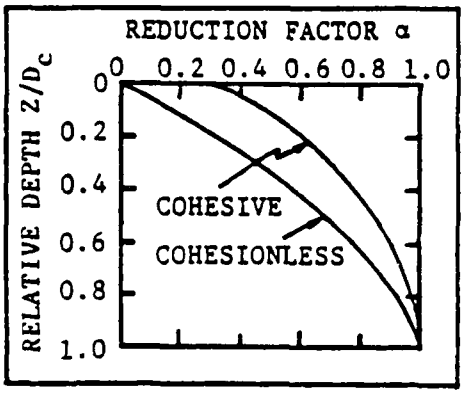

Fig. 5.8 Pile reduction factor (from Briaud, et al., 1983b)

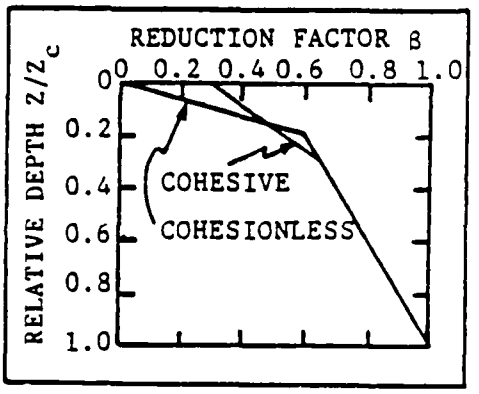

Fig. 5.9 Pressuremeter reduction factor (from Briaud, et al., 1983b)

sand. If the pressuremeter test were performed above the critical depth, the factor β should be used to correct the pressuremeter curve.

PROCEDURES EMPLOYED AT THE TEST SITE

Tests with the preboring pressuremeter were conducted at close spacings near the ground surface and down to a depth of approximately 20-pile diameters. For the cone-pressuremeter tests, the cone was pushed at a constant rate of penetration of 0.1 in. per second. If the cone could not be pushed into a stiff layer, it was penetrated with a 27.9 lb hammer dropping from 4 ft above the top of the cone until the specified depth was reached.

The cycling of the pressure applied to the pressuremeters was performed either between preset values of volume to be injected (volume-control tests) or preset values of pressure (pressure-control tests). Cycling between preset volumes was chosen when modeling the response of piles where the displacement was controlled, as were the Houston tests. (Cycling between preset pressure values would have been used had the load been controlled).

When the probe was in place and the control unit was ready for reading data, the pressure was then injected to the probe. The probe was first inflated to about 25% of the

limit pressure. The limit pressure P_L is the pressure reached when the volume of the cavity equals two times the initial volume. At that injected volume V_{cp} and pressure Pcp, the volume was held constant for a period of 15 seconds. Then, the probe was deflated to a slightly positive pressure P_r, equivalent to approximately half of the pressure P_{cp}. The injected volume V_r, corresponding to the new pressure P_r, was maintained for another period of 15 seconds. The probe was then reinflated to the same injected volume V_{cp} in order to complete a cycle (Fig. 5.10). A total of one hundred cycles were performed between V_{cp} and V_r. The period of all cycles was 30 seconds. After the first series of test was finished, a second series of 100 unload-reload cycles was performed with the pressure being increased to approximately 50% of the limit pressure. A third series of 100 unload-reload cycles was performed after increasing the pressure to approximately 75% of the limit pressure.

More detailed and background on test procedures for this method can be found in Briaud, Smith, and Meyer (1983b).

PROCEDURES FOR CONSTRUCTING p-y CURVES

Static Loading

The data correction for directly measured pressuremeter curves is important for obtaining reliable soil-resistance curves. The initial pressure reading, P_i which was taken

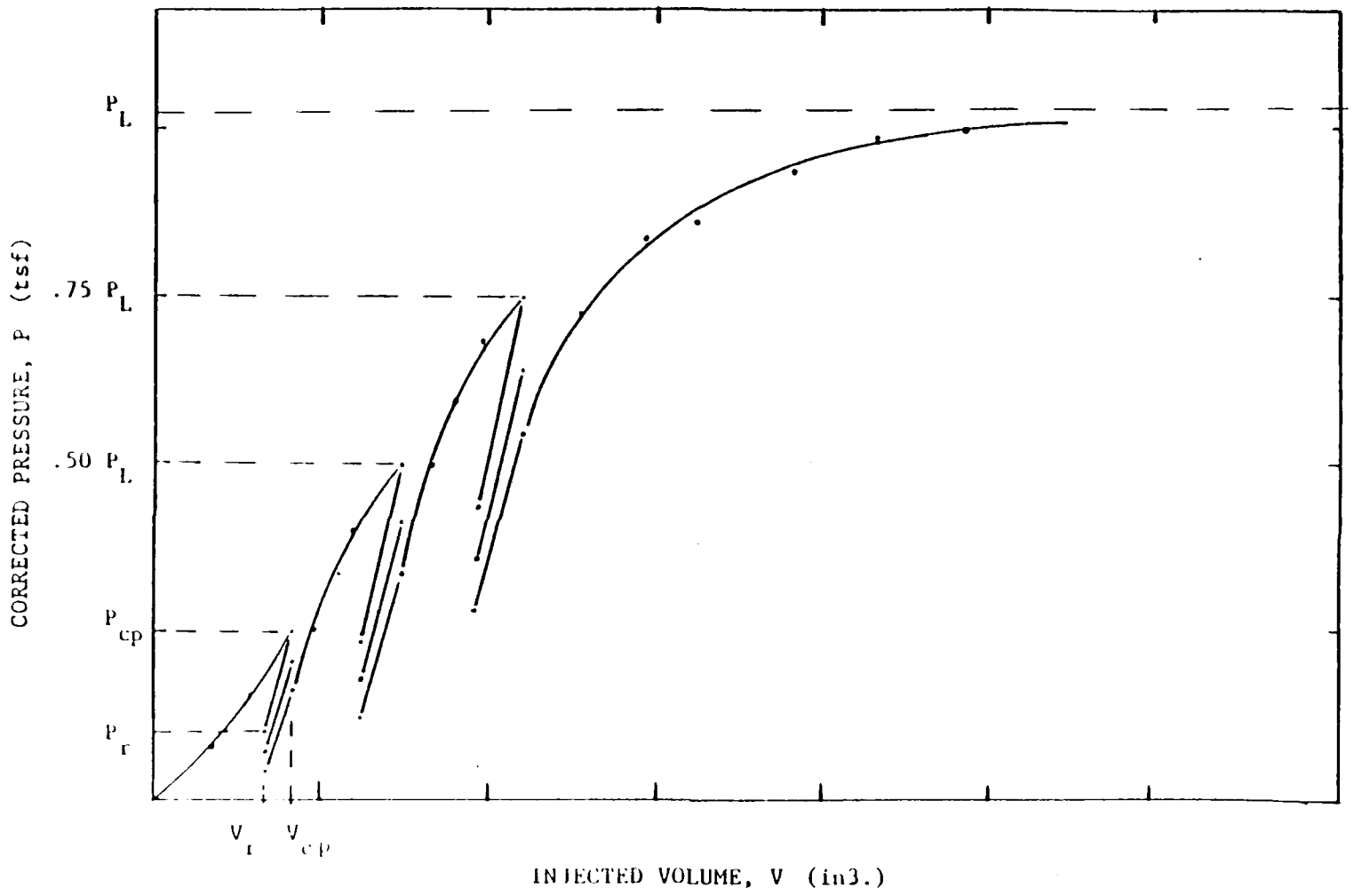

Fig. 5.10 Probe inflation in cyclic pressuremeter test with displacement control

with the probe simply supported in the air, may not equal to zero due to temperature variation or other system errors. The hydrostatic pressure, which is equal to the unit weight of the system fluid multiplied by the difference in elevation between the gauge and the pressure cell, is not included in the pressure-gauge reading, and must be added to each value recorded during the test. Because the control system is not entirely incompressible, a volume calibration was necessary. The membrane-resistance calibration was also important to determine the pressure actually required to inflate the probe in the air to any given volume. The detailed correction for raw data is described in original reports. The procedures to derive p-y curves by use of the pressuremeter method are summarized in the following.

1. Correct the pressuremeter curves for membrane resistance, system compressibility, and effects of the pressuremeter critical depth.
2. Obtain the front reaction curves (Q-y) by using Eq. 5.7 and 5.8. and together with the pressuremeter curves (Fig. 5.10) obtained from Step 2. It is noted by Briaud et al that the reload pressuremeter curves should be used for driven piles.
3. For any test within the pile critical depth apply the proper reduction factor to obtain the true Q-y curves.

AD-A196 799 EXPERIMENTAL RESEARCH INTO THE BEHAVIOR OF PILES AND PILE GROUPS SUBJECTE.. (U) ARMY ENGINEER WATERWAYS EXPERIMENT STATION VICKSBURG MS GEOEE..

3/3

UNCLASSIFIED L C REESE ET AL. JUN 88 WES/MP/GL-88-10 F/G 13/13 NL

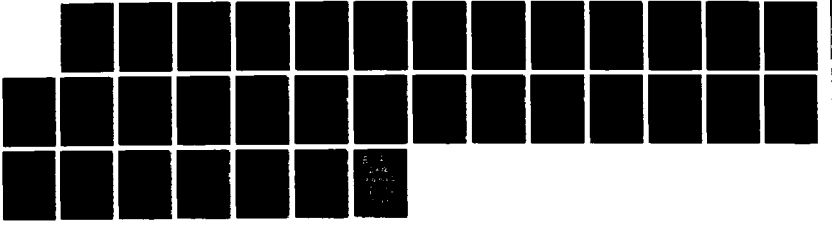

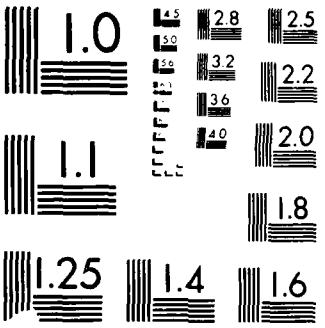

UTION TEST CHART

4. Obtain the friction resistance curve (F-y) by applying the subtangent method to the reload pressuremeter curves and then using Eq.5.8 and 5.9.
5. Obtain the p-y curves by adding at each depth the Q-y curve to the F-y curve.

Cyclic Loading

The method for cyclic p-y curves is an extension of the method used for static loading (monotonic loading). The difference is that in the case of cyclic loading the resistance of the soil decreases as the number of cycles increases. Soil degradation models are introduced into the static p-y curves, derived from the above procedure, to account for the degradation effect.

A degradation model, originally presented by Idriss et al (1978), was used to study the degradation effects where the number of cycles was less than 2000. Soil degradation is determined by

$$\frac{G_s(N)}{G_s(1)} = N^{-a} \qquad 5.11$$

where $G_S(1)$ and $G_S(N)$ are the secant shear modulus to the pressuremeter curve for cycle 1 and N respectively (Fig. 5.11). The larger the value of a, the larger the degradation of the soil stiffness with increasing number of cycles.

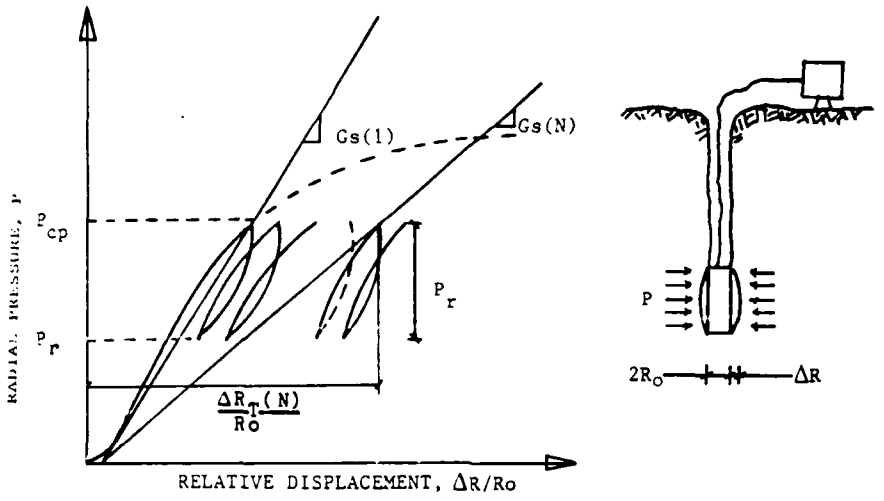

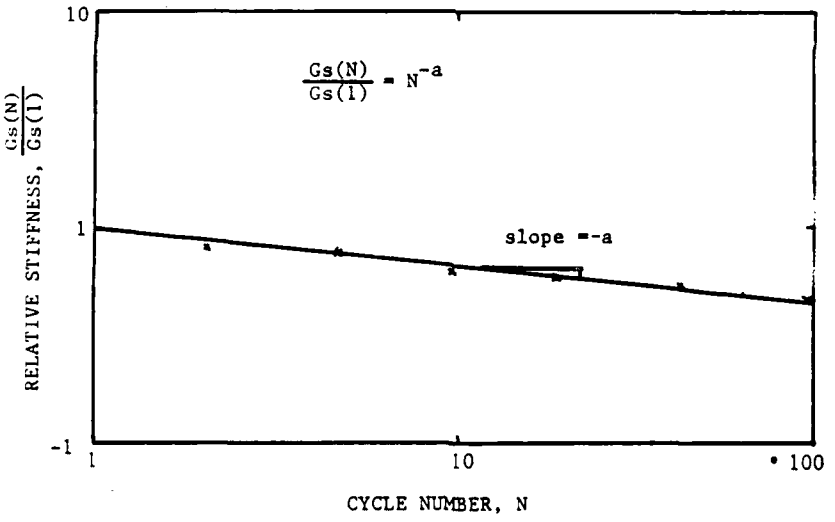

Fig. 5.11 Cyclic degradation parameters definition

A complex model (Makarim and Briaud, 1986) was proposed where the number of loading cycles is greater than 2000. The complex model is not shown here. The tests in Houston were for less than 2000 cycles and only a few loads of relatively large magnitude occur during an offshore storm.

The following simplified procedures are used to derive p-y curves under cyclic loading.

1. Develop static p-y curves by following the procedures described earlier.
2. Find the average in-situ soil degradation parameter, a, from the corrected pressuremeter curves by using Eq. 5.11 if the number of cycles is less than 2000.
3. Calculate the cyclic p-y curves from the static p-y curves by multiplying the static soil resistance P_{static} by the factor N^{-a}.

PREDICTED RESULTS FROM PRESSUREMETER TESTS IN CLAY

The pressuremeter tests for piles in clay at the University of Houston were conducted by investigators under the direction of Professor J. L. Briaud in 1983, 1984, and 1985. Twelve cyclic tests were performed with the preboring pressuremeter and 5 tests were performed with the driven or pushed pressuremeter. The results of the tests were analyzed

according to the procedures described briefly in the previous sections.

The results from the pressuremeter tests were employed for the development of p-y curves which were then used for the prediction of behavior of the single piles under lateral loading. A summary of the results of these studies for static loading and for cyclic loading is presented in the following sections.

Static Loading

Predictions of the static p-y curves of the 10.75-in. and 48-in.-diameter piles were done by using the procedures outlined earlier. The curves were predicted from the results of the preboring pressuremeter (PBPMT), from the pushed-cone pressuremeter (PCPMT)), and from driven-cone pressuremeter (DCPMT)).

An example for one of the six sets of p-y curves that were derived is shown in Fig. 5.12. The general shapes of the other sets of curves are similar to those in Fig. 5.12 but there is some significant difference in the numerical values.

The relationships between pile-head load and deflection, as predicted by the pressuremeter method, are shown in Figs 5.13 and 5.14. As it may be seen, in general, the results

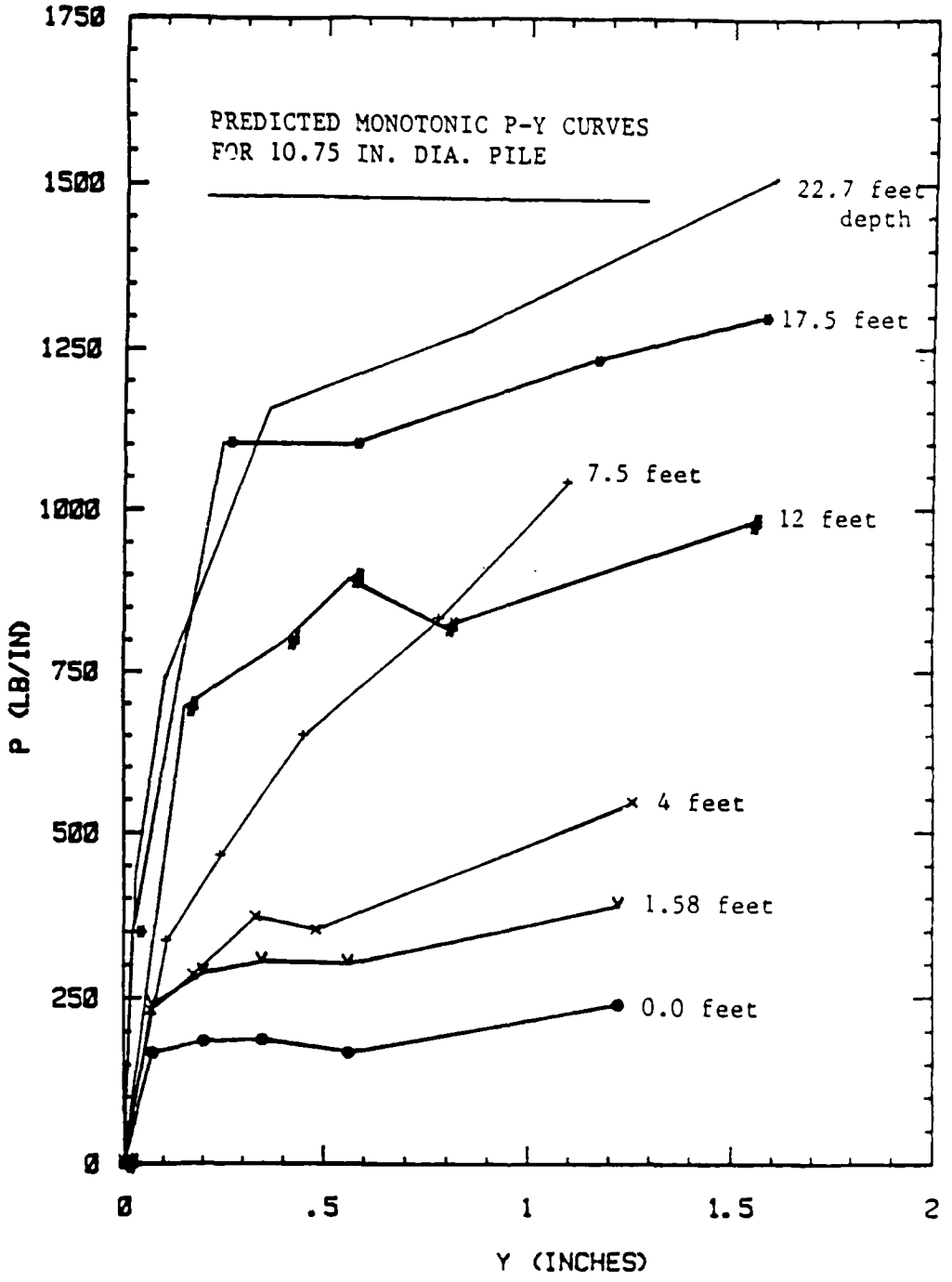

Fig. 5.12 PBPMT: predicted monotonic p-y curve for 10.75 in. diameter pile (preboring pressuremeter test)

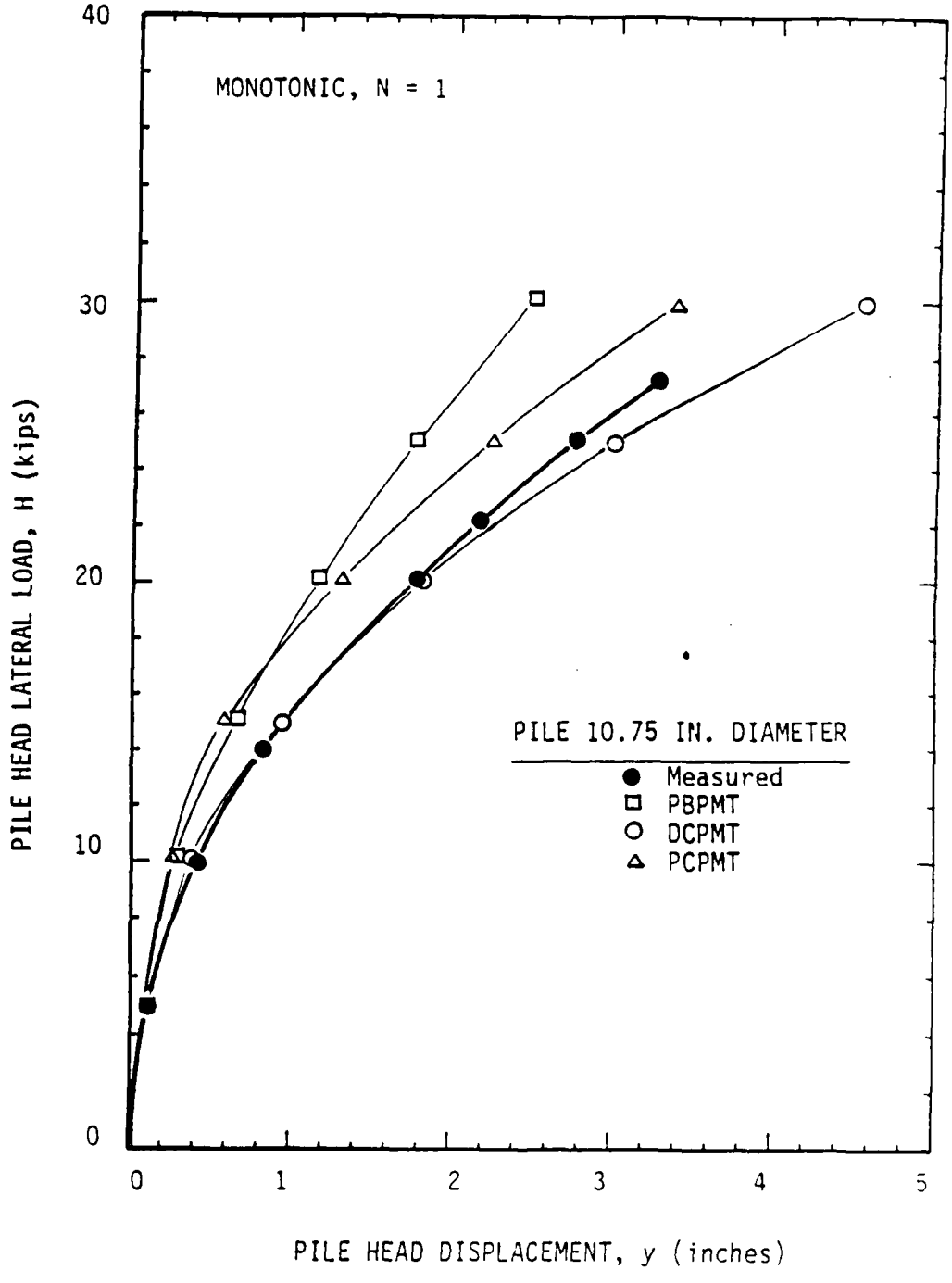

Fig. 5.13 Measured and predicted displacement of 10.75 in. diameter pile

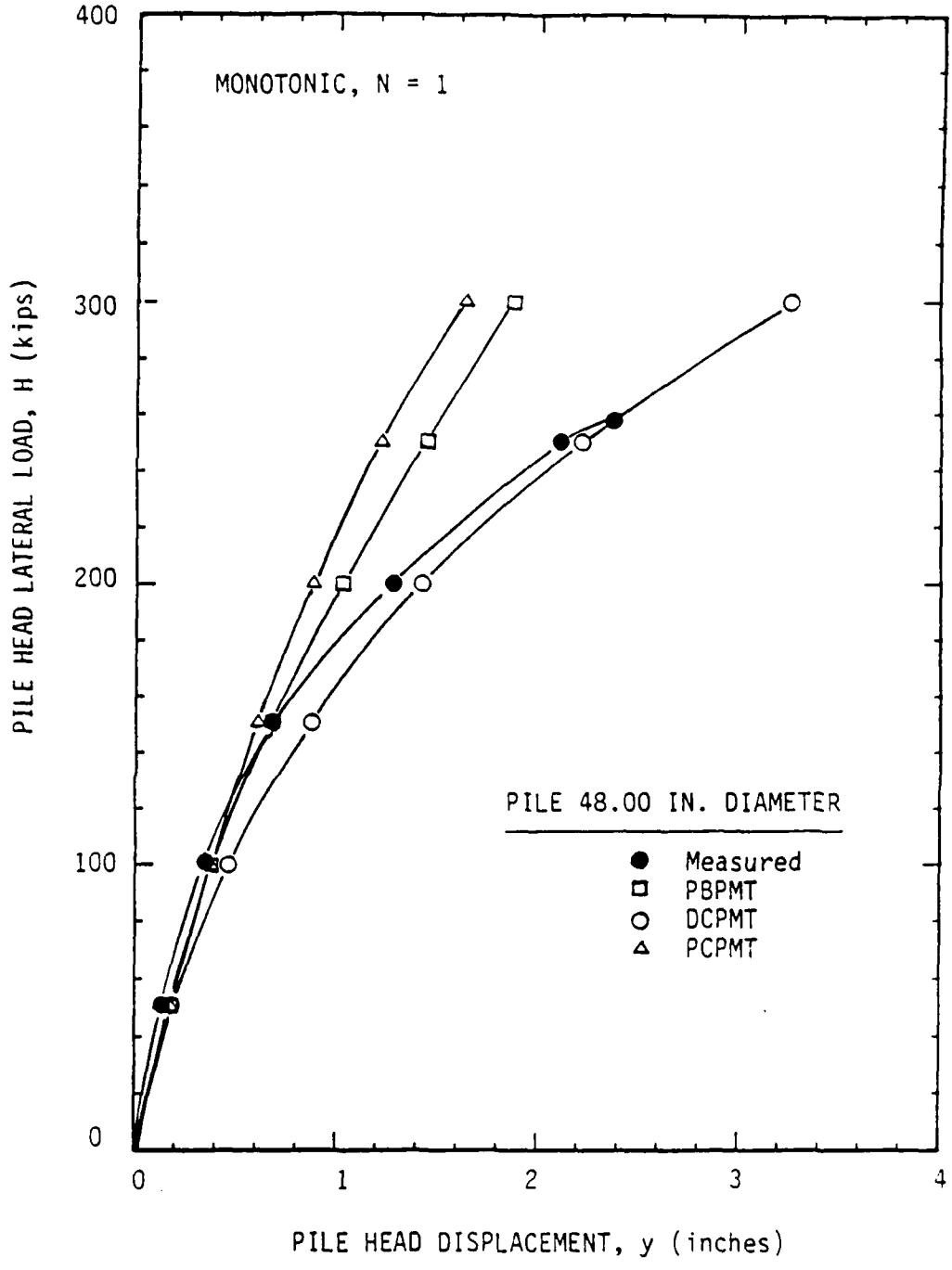

Fig. 5.14 Measured and predicted displacement of 48.00 in. diameter pile

based on the pressuremeter tests have good agreement with the measured data. The DCPMT gives better predictions for both piles, perhaps because of the similarity of the methods of installation of the pile and tne pressuremeter into the soil.

Cyclic Loading

The cyclic p-y curves were calculated from the monotonic p-y curves by multiplying the soil resistance by a factor of N^{-a} where N is the number of cycles and a is the soil degradation parameter obtained from the cyclic tests. An example of p-y curves from the PBPMT tests at a depth of 17.5 ft for the 10.75-in.-diameter pile is shown in Fig. 5.15.

Using the cyclic p-y curves derived from preboring pressuremeter tests, the load-deflection curve for 100 cycles for the 10.75-in-diameter pile is shown in Fig. 5.16 and compared with the experimental curve. Similar information for the 48-in-diameter pile is shown in Fig. 5.17. As may be seen, the agreement between the curves for the 10.75-in-diameter pile is not very good with the pressuremeter under-predicting deflection by a significant amount. For the 48-in-diameter pile, the loading of the experiment was stopped at about 125 kips. In that range of loading, the agreement between analysis and experiment is good.

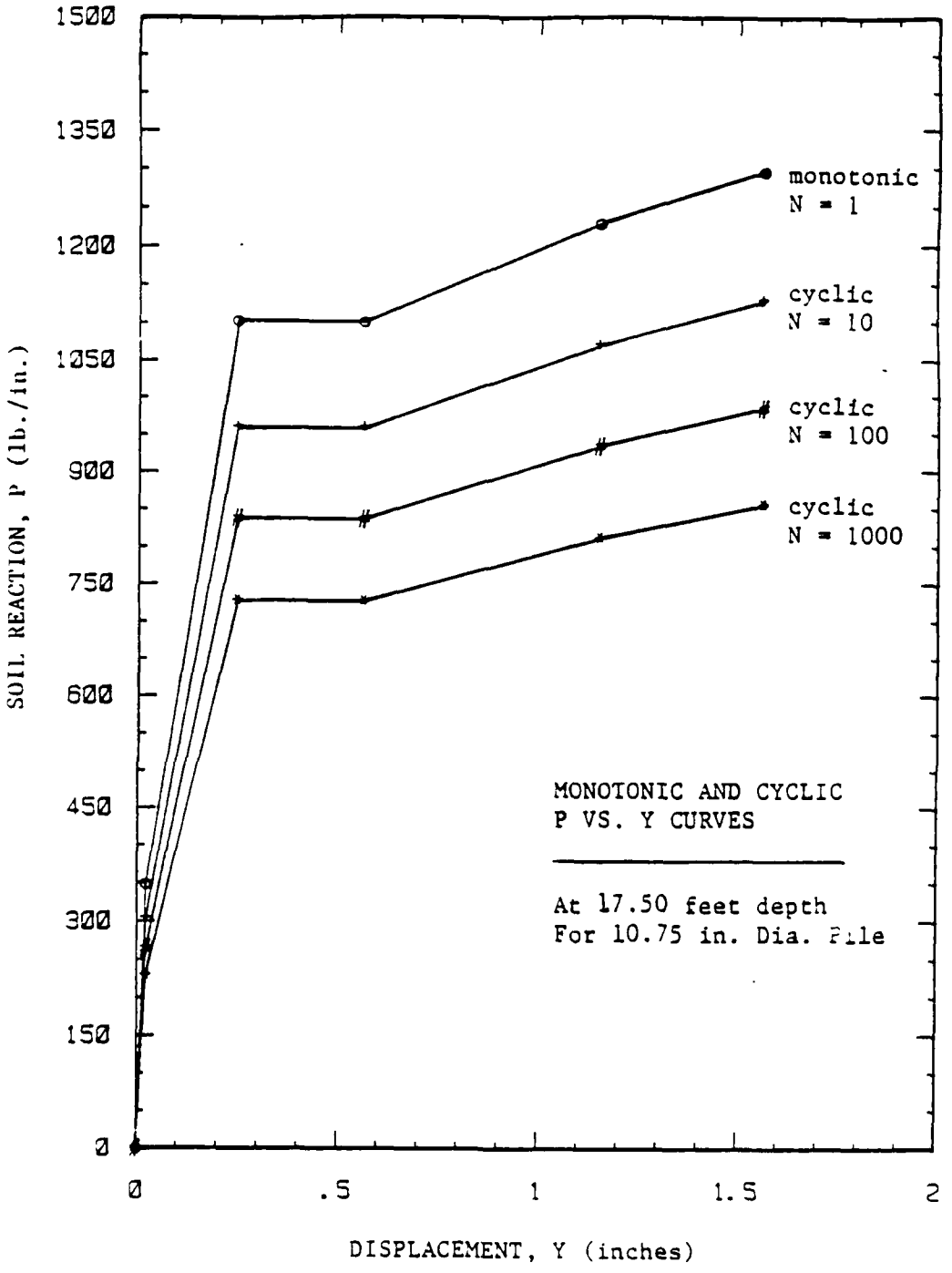

Fig. 5.15 PBPMT monotonic and cyclic p-y curves for 10.75 in. diameter pile at 17.00 ft. depth (degradation parameter a = 0.06)

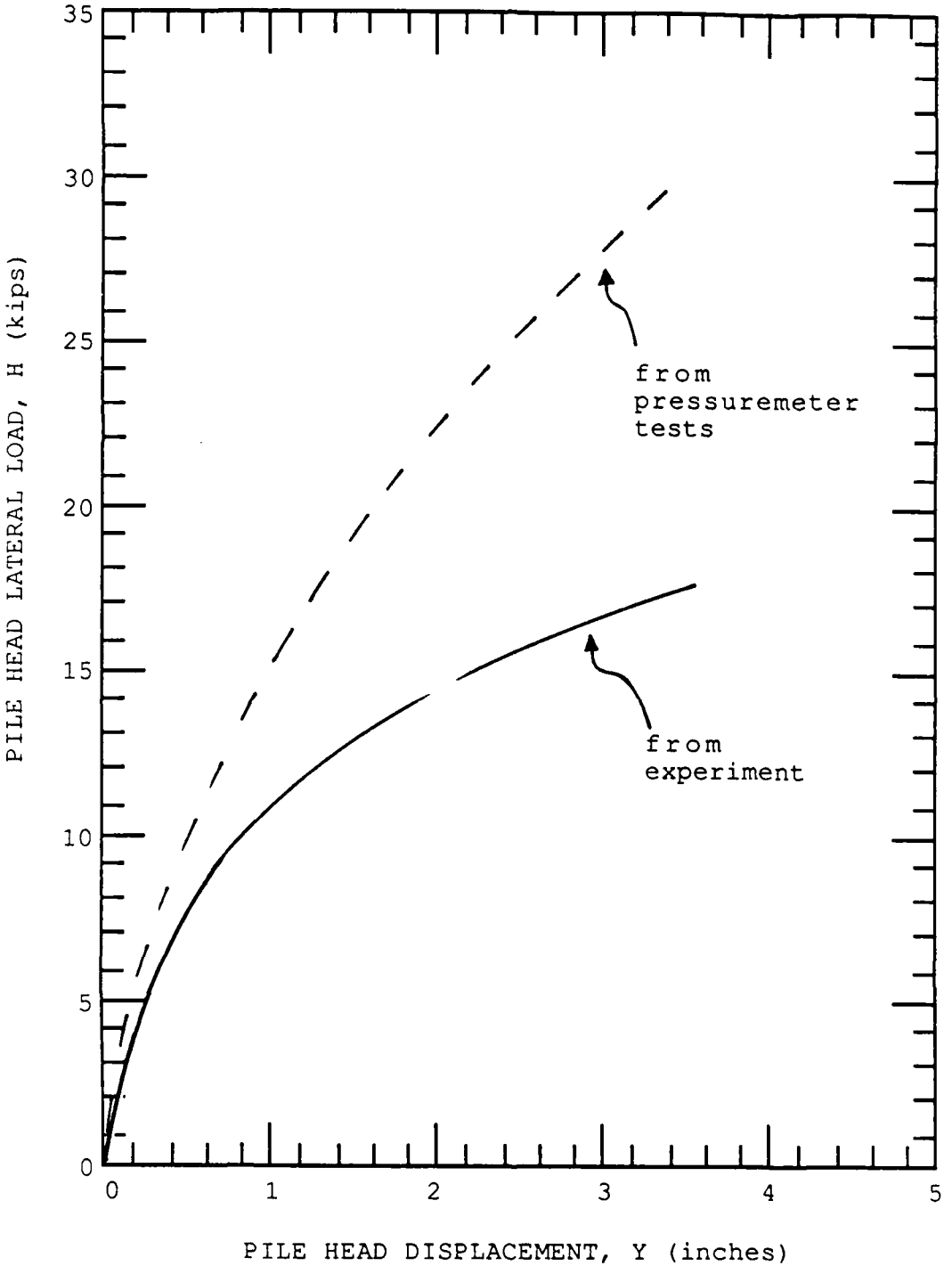

Fig. 5.16 Comparison of predicted and experimental load-deflection curves for 100 cycles for the 10.75-in.-diameter pile

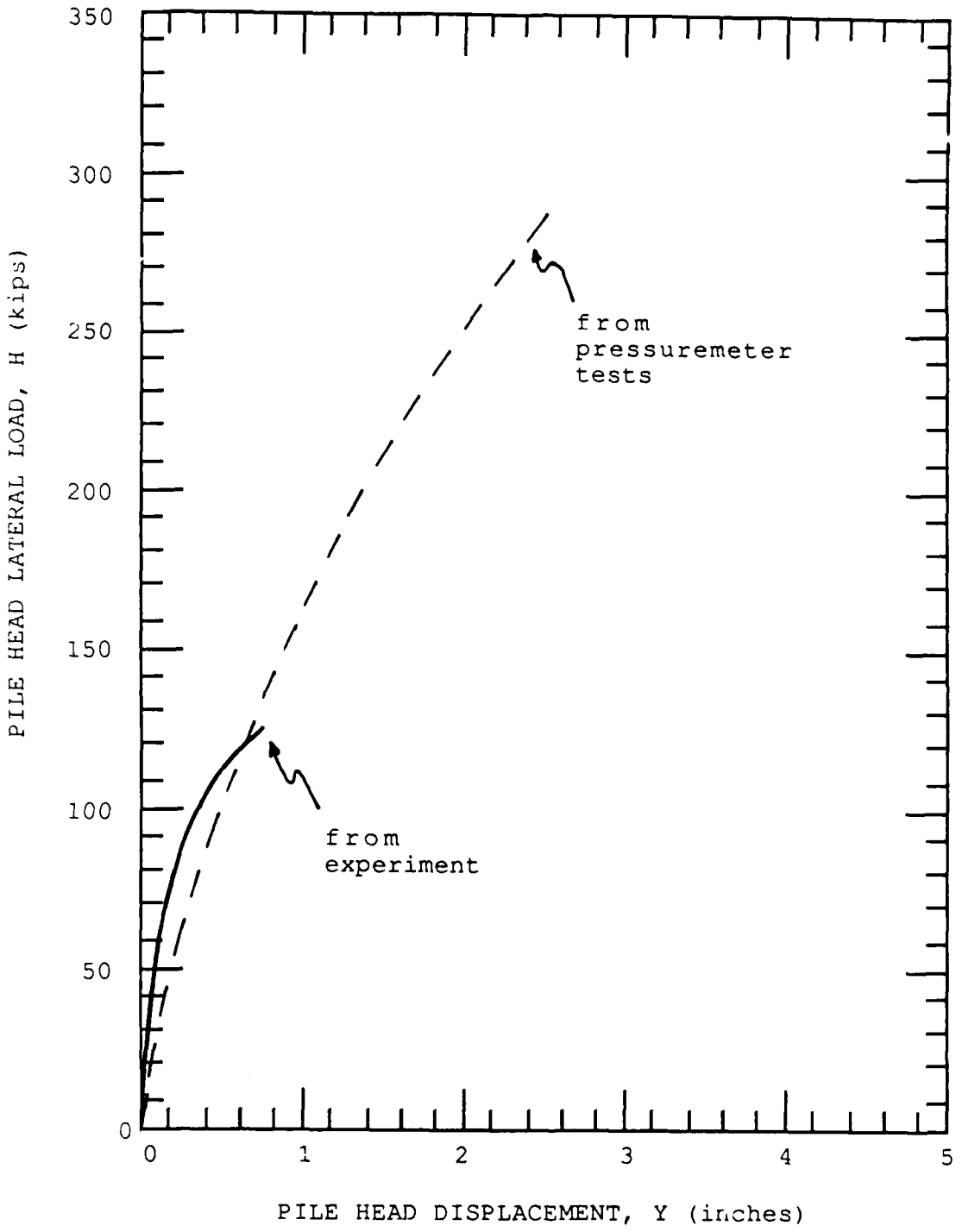

Fig. 5.17 Comparison of predicted and experimental load-deflection curves for 100 cycles for the 48-in.-diameter pile

PREDICTED RESULTS FROM PRESSUREMETER TESTS IN SAND

In the spring of 1985, eleven pressuremeter tests were conducted in sand at the University of Houston. As described in the pile-loading test for single piles in sand, the top 9.5 ft of the original clay was replaced by fine sand. Three different pressuremeter-insertion techniques were used as listed in Table 5.1.

Static Loading

Development of the static p-y curves of the 10.75-in.-diameter pile was performed by using the same procedures as for clay. Three sets of p-y curves were developed for static loading, one for each of the insertion techniques. An example of one of the sets of p-y curves that were derived is shown in Fig. 5.18. There is a considerable disagreement between the sets of p-y curves, probably because of the difference in the degree of disturbance of the sand from each of the insertion techniques.

The predicted load-deflection curves based on the pressuremeter method and the measured load-deflection curve for static loads are shown in Fig. 5.19 to Fig. 5.21. For the pushed and driven pressuremeter tests, the p-y curves were obtained by using the first-load pressuremeter-test curve. The large discrepancy between these predictions and the measured response (Fig. 5.17 and 5.18) indicates the

Table 5.1

Pressuremeter test performed at the University of Houston Foundation Test Facility Sand Site

Borehole Number	Insertion Method	Pressuremeter Type	Date
T3	Pre-bored	PBPMT / TEXAM PMT	4 / 85
T4	Pre-bored	PBPMT / TEXAM PMT	4 / 85
P2	Pushed-in	PCPMT / Cone PMT	5 / 85
D1	Driven-in	DCPMT / Cone PMT	5 / 85
D3	Driven-in	DCPMT / Cone PMT	5 / 85

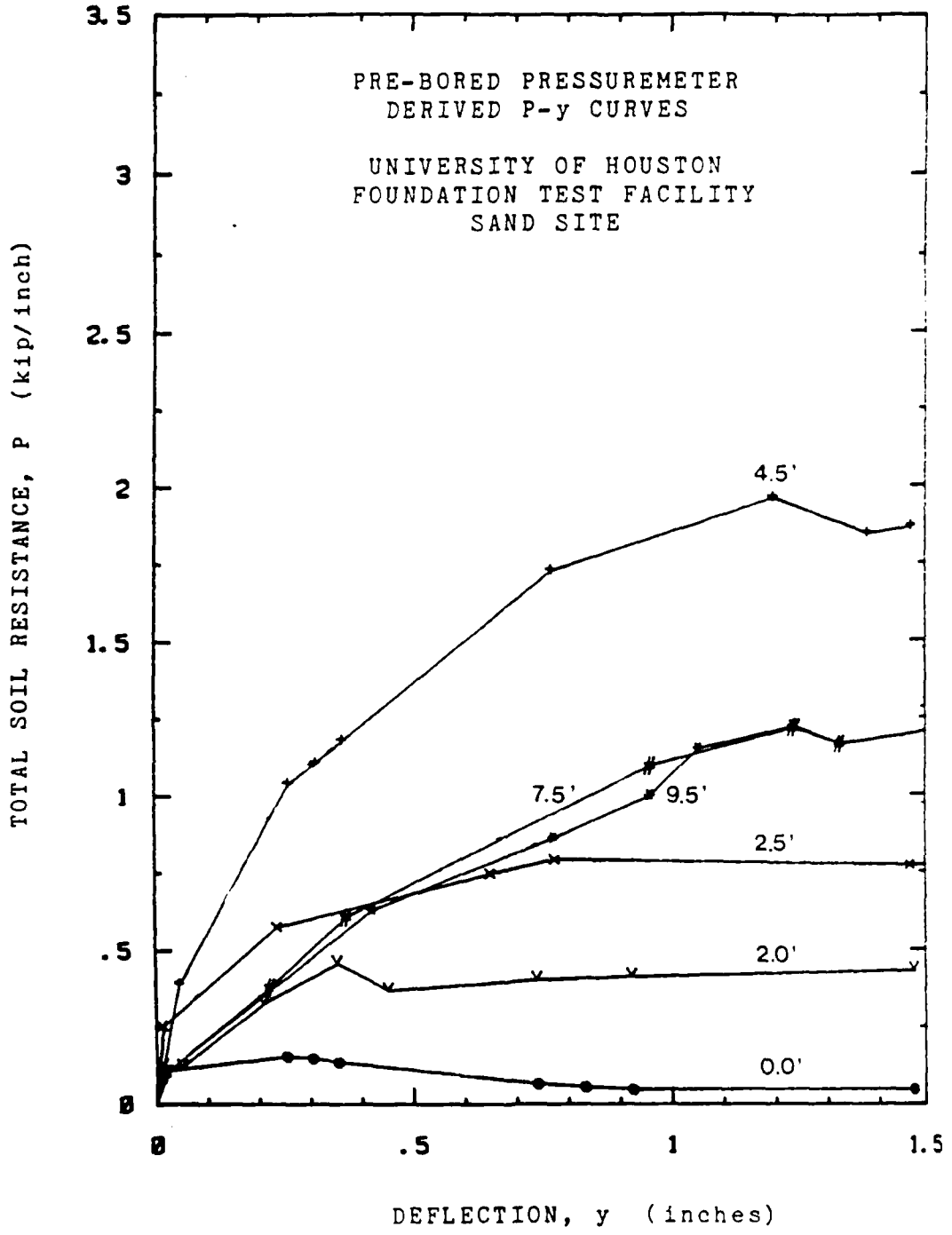

Fig. 5.18 p-y curves derived from pre-bored TEXAM pressuremeter tests at the University of Houston Sand Site

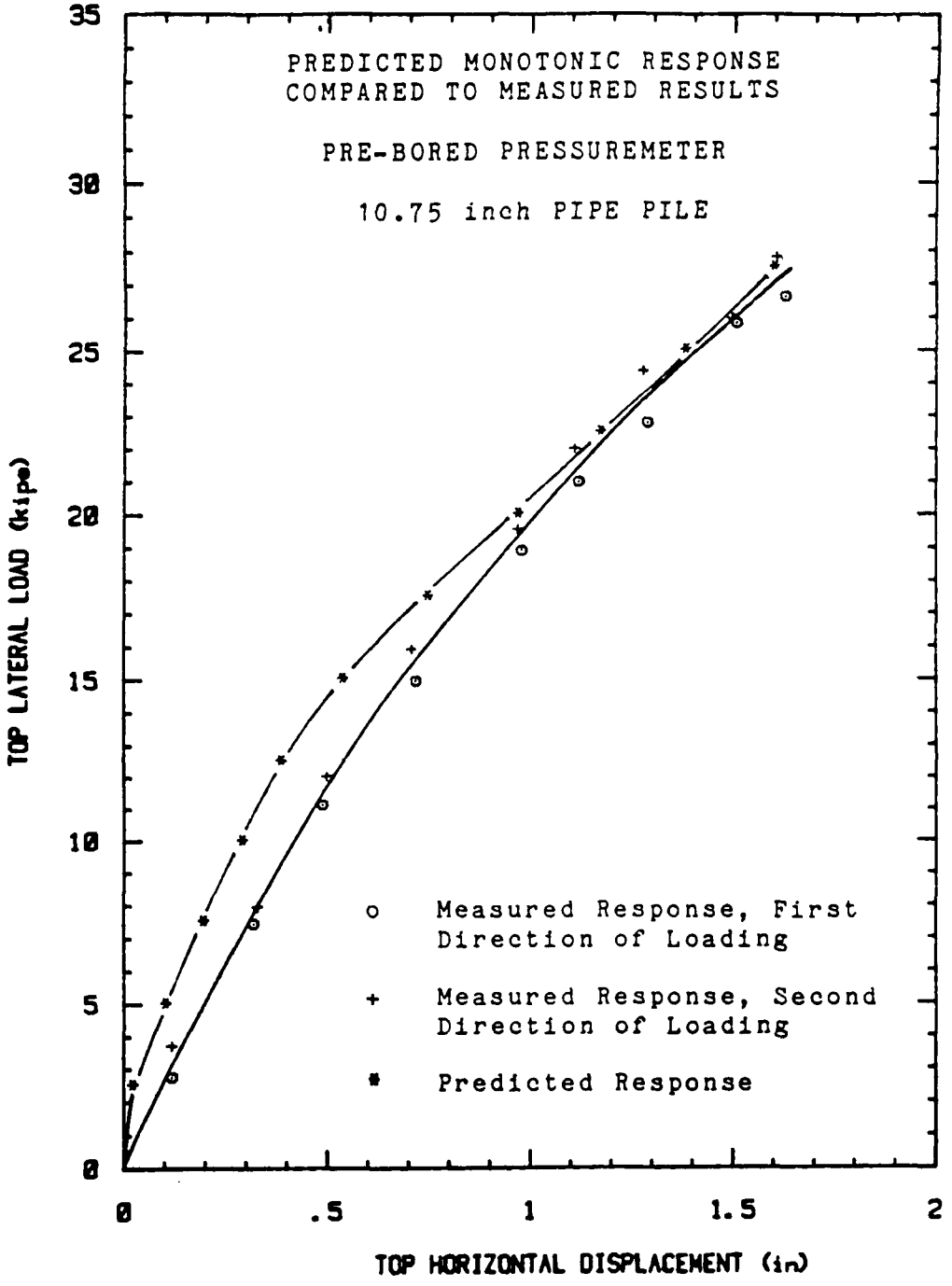

Fig. 5.19 PBPMT: Predicted monotonic response of the single pile compared to the measured response

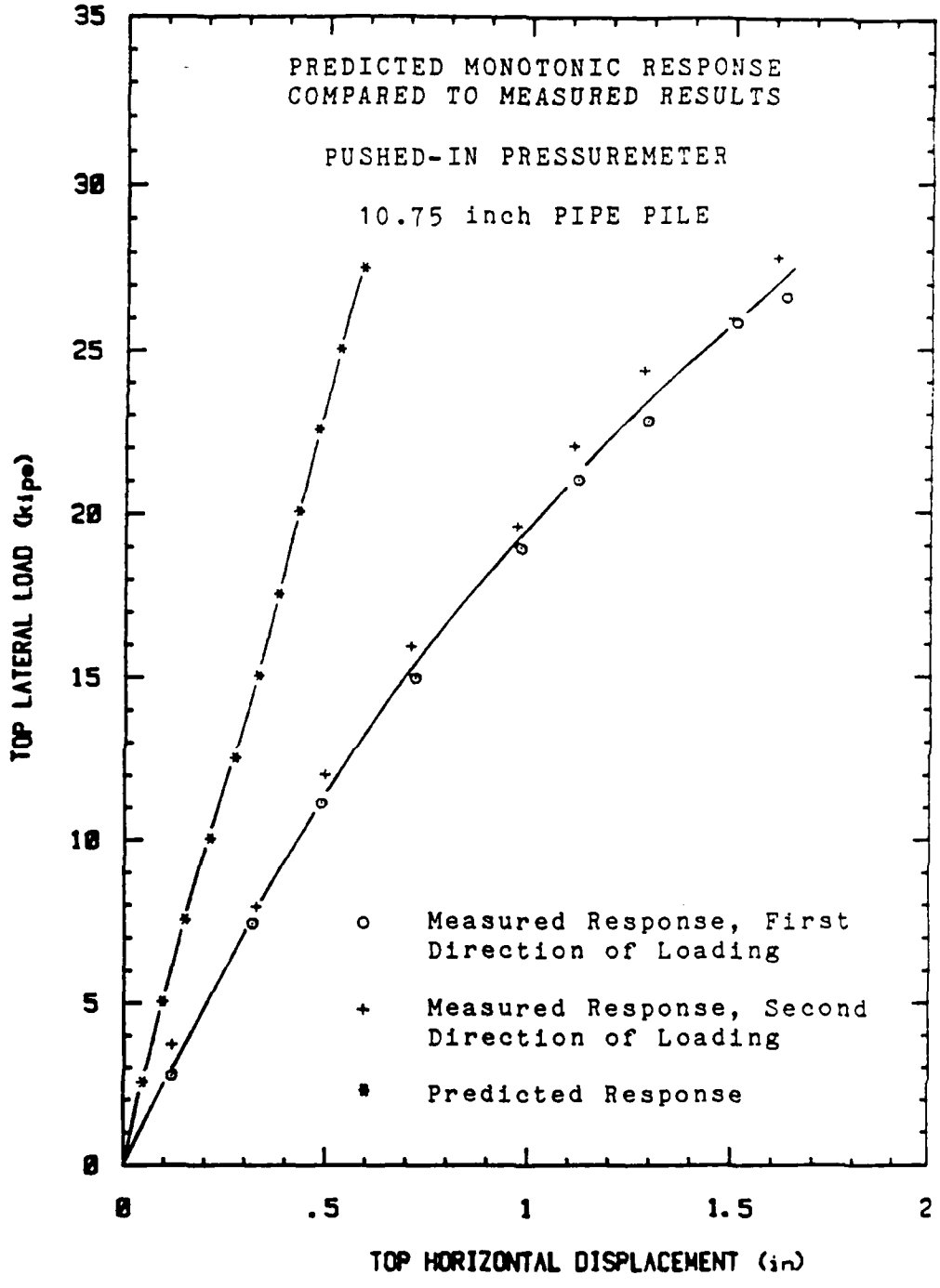

Fig. 5.20 PCPMT: Predicted monotonic response of the single pile compared to the measured response

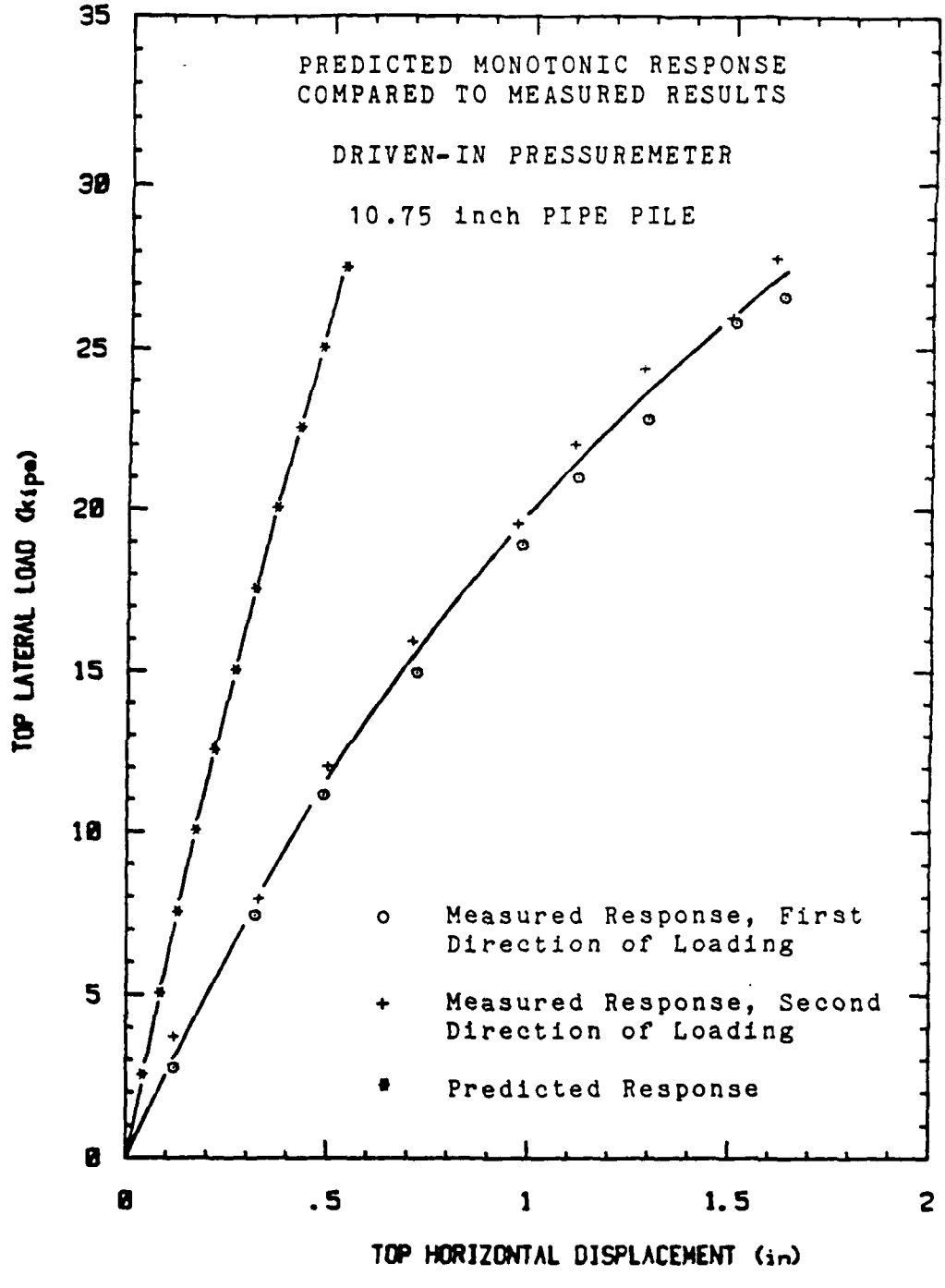

Fig. 5.21 DCPMT: Predicted monotonic response of the single pile compared to the measured response

compaction of sand around the pile did not simulate the real conditions around a driven or a pushed pile. However, the closeness between the predicted response by preboring pressuremeter test and measured response implies the compaction of the sand around the pile simulated more closely the conditions around a bored pile.

It appears that, in general, the predicted curve has a stiffer initial response. It should be noted that the pressuremeter tests were conducted after the loading tests had been completed; therefore, the densification in sand due to previous loading tests could provide a high initial modulus.

Cyclic Loading

The degradation parameter, a, based on the degradation model-1 is 0.26 for the preboring pressuremeter test, 0.23 for the pushed-cone-pressuremeter test, and 0.15 for the driven-cone-pressuremeter test. These parameters were applied to the static p-y curves to develop sets of cyclic p-y curves in sand. The newly developed cyclic p-y curves for the top sand layer and the p-y curves measured by strain-gauge method for the lower clay layer were then used to study the pile behavior as shown in Fig. 5.22 through 5.24.

As may be seen from an examination of the figures, there is a considerable difference in the results obtained from the

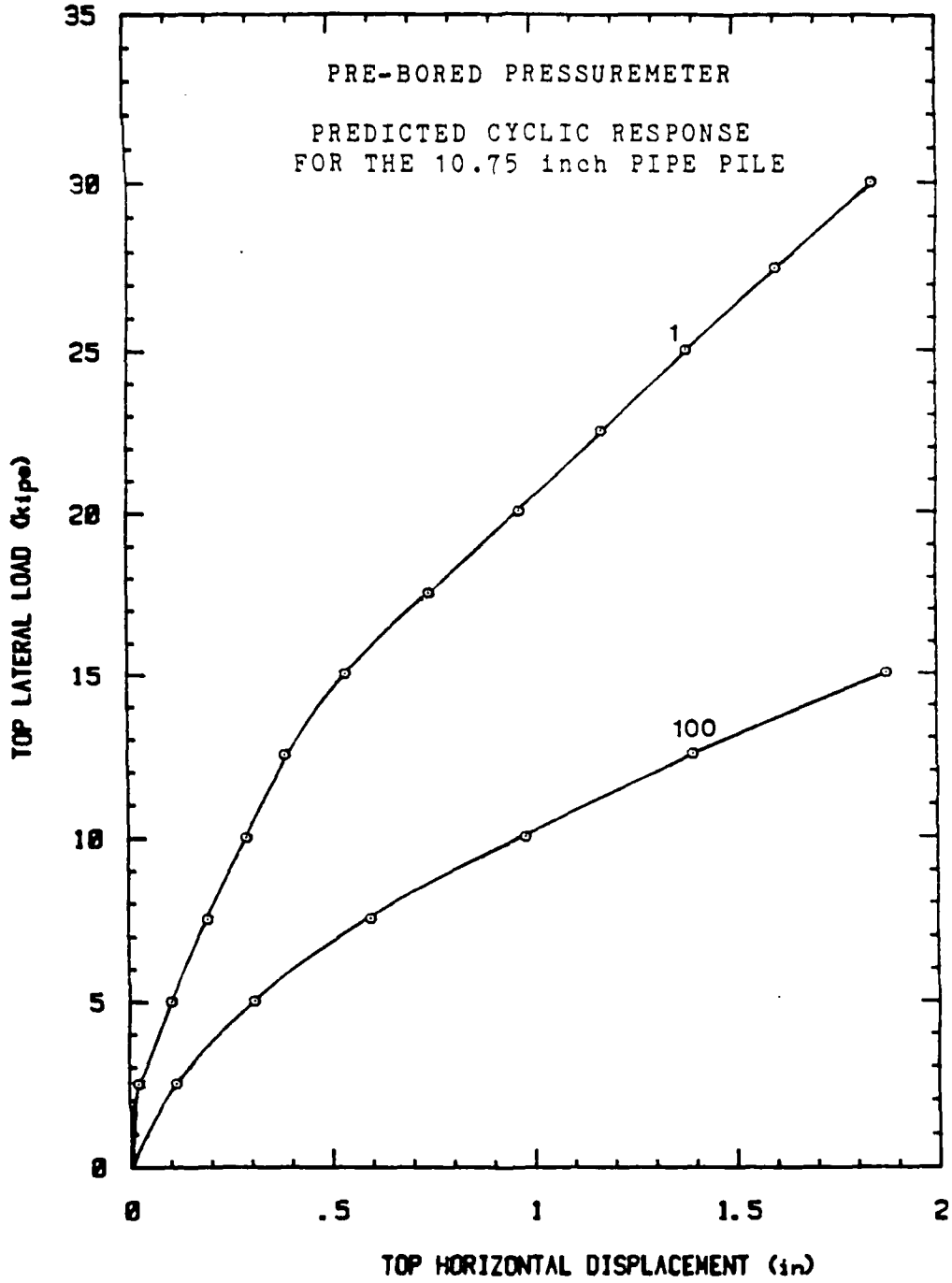

Fig. 5.22 PBPMT: Predicted cyclic response of the single pile

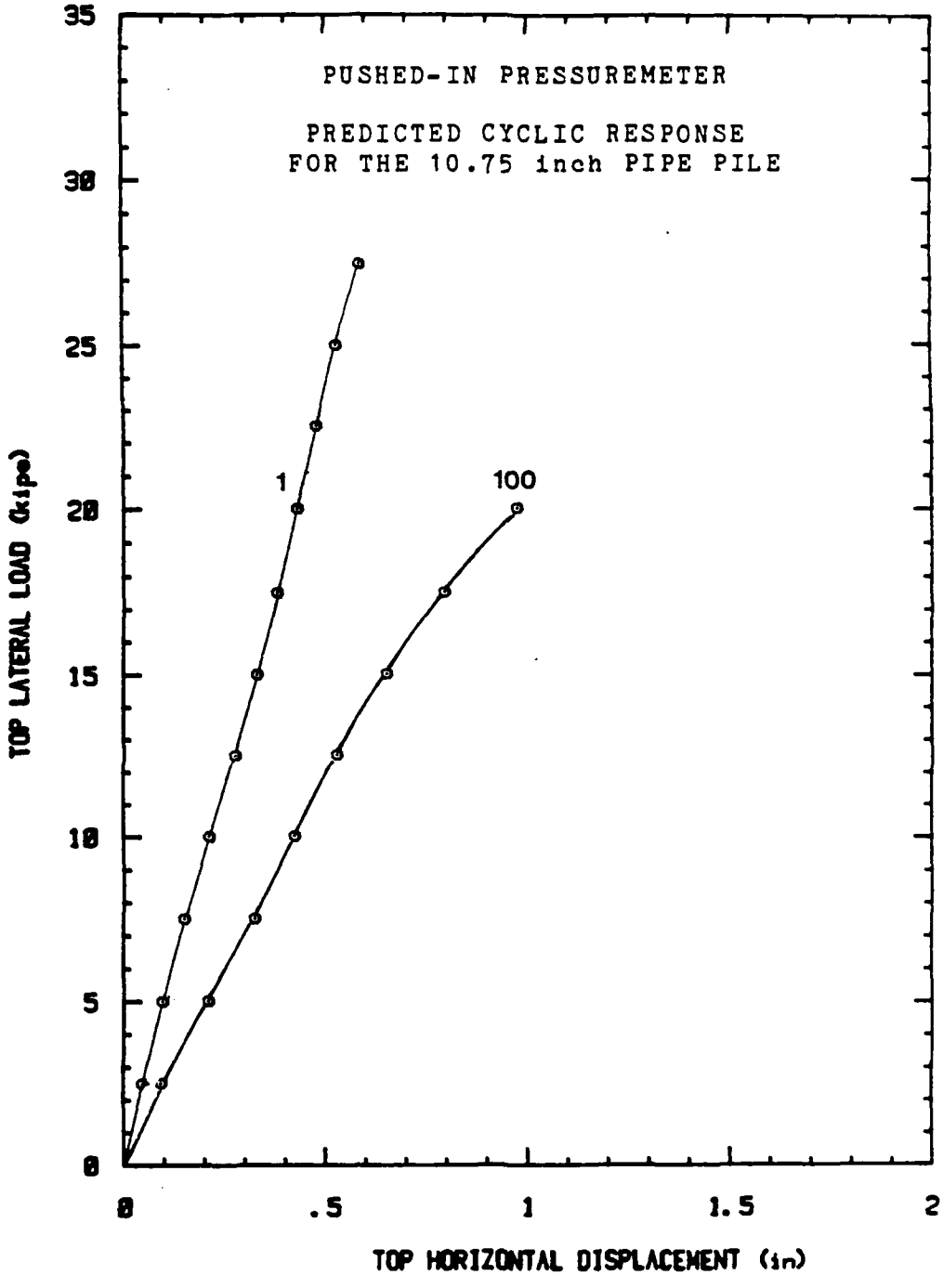

Fig. 5.23 PCPMT: Predicted cyclic response of the single pile

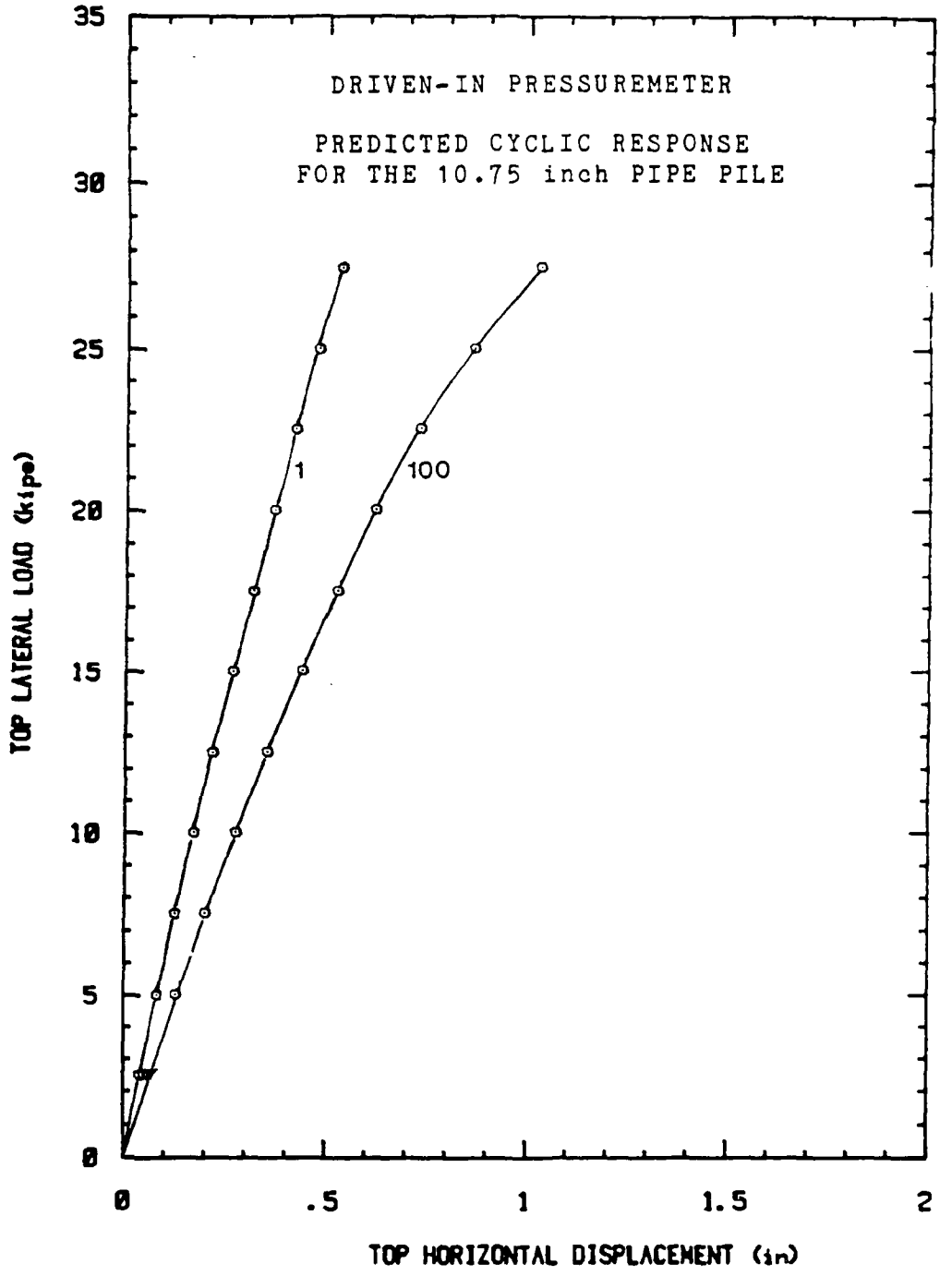

Fig. 5.24 DCPMT: Predicted cyclic response of the single pile

three different types of pressuremeters. Also, for a given lateral load, the increased deflection due to cycling is significant. For 100 cycles of loading, the predicted deflection for a given load is in the order of twice as much as that for the static case. The results for cyclic loading of the pile as predicted by the pressuremeter method are in sharp contrast to the results from the experiment, not repeated here, where the increased deflection due to cyclic loading was relatively small.

CONCLUDING COMMENTS

The results of pressuremeter tests for piles embedded in clay and in sand conducted by Dr. Briaud and his research team have been summarized briefly in this chapter. Based on the results presented, the following conclusion can be drawn.

1. The pressuremeter method in general gave a good prediction of pile behavior in clay or in sand for static (monotonic) loading when soil conditions around the pile and the pressuremeter were judged to be the same. Thus, the method of inserting the pressuremeter is important and should be such to affect the natural soil conditions in the same manner as the installation of the pile.

2. For cyclic loading in clay, the pressuremeter method yielded a pile response that was reasonably in agreement with the results from experiment. The pile behavior predicted

from the driven pressuremeter tests was in best agreement with the measured results.

3. In regard to the behavior of the 10.75-in.-diameter pile in sand under cyclic loading, the pressuremeter method was unable to make a good prediction. Good agreement was found between analysis and experiment for the testing of a 1.4-in.-diameter pile in the laboratories at Texas A & M University, not reported here, where the soil conditions around the pile and around the pressuremeter were carefully controlled. However, results in the field and in the laboratory show that a pile in sand under cyclic lateral loading will behave quite differently if the load is applied in one direction only or is applied with the load being reversed in direction. There is no manner in which the pressuremeter can be operated to predict directly this difference in cyclic behavior as a function of loading direction.

CHAPTER 6
SUMMARY OF RESULTS AND RECOMMENDATIONS FOR FURTHER STUDY

SUMMARY OF RESULTS

This report has summarized the results of experimental studies concerning the behavior of piles and pile groups subjected to lateral loading. The tests were conducted from 1984 to 1987 at the Pile Test Facility of the University of Houston. A total of six research studies were completed as described in the Introduction and the six studies have been combined in preparation of this summary report. Among those previous studies, four of them were directly related to full-scale tests for single piles and pile groups under lateral loading; the other two studies were concerned with the use of the pressuremeter in predicting the behavior of single piles. Significant results of all the experimental studies and findings in improving the understanding of the behavior of single piles and pile groups can be summarized as follows.

Single Pile Tests

1. The response of single piles to static loading was stiffer than that to cyclic loading.

2. In testing of the single pile (and the group of piles) in the submerged stiff clay, significant gapping

between the piles and the surrounding soil was observed during cyclic loading and the gapping was intensified by hydraulic erosion.

3. The appreciable cyclic degradation in clay did not begin until the pile-head displacement had reached about one percent of the diameter of the individual piles, but, once started, did not appear to stabilize even after 200 cycles.

4. Cyclic loading of the test pile in sand did not create gapping between the pile and the surrounding soil, but resulted in densification of the sand around the pile.

5. The reduction of soil resistance due to cyclic loading was much more pronounced for clay than for sand.

6. The ultimate soil resistance determined experimentally, varied significantly from than that recommended by the current p-y criteria. Modified procedures for the prediction of p-y curves were described and were used to evaluate the pile behavior.

7. The maximum bending moment in a pile during cyclic loads was greater than that for static loading under the same deflection at the pile top, due to softened soil resistance.

Pile-Group Tests

1. The response of the single pile to lateral load was stiffer than the response of the average pile in a group.

2. The response of the piles to static loading was stiffer that the response to cyclic loading.

3. The distribution of load to the piles in the group was not uniform. The leading row took a larger portion of the load than the middle row, which in turn took a larger portion than the trailing row.

4. The ultimate soil resistance for the leading row of piles was larger than the ultimate soil resistance for the middle row, which in turn was larger than that for the trailing row.

5. The reduced efficiency of the group for lateral loading was largely due to the effect of "shadowing" in which the trailing row of piles can mobilize only a limited soil resistance.

6. The relatively smaller amount of loss of soil resistance due to cyclic loading in sand than was observed for clay may be due to the significant amount of densification of the sand that occurred during two-way cyclic loading.

7. Although several of the analytical methods were able to predict with reasonable accuracy either deflections or maximum bending moment, no method was able to predict both correctly. The key element needed to correctly predict group effects is an understanding of the mechanisms producing the loss of soil resistance in the piles within the trailing rows.

8. The analytical method based on the experimental interaction factors is promising because the nonlinear soil reaction and the "shadowing" effect in the trailing row can be included in the analysis.

Pressuremeter Method for Predicting the Behavior of a Single Pile

1. The pressuremeter method in general gave a good prediction of pile behavior in clay or in sand for static (monotonic) loading when soil conditions around the pile and the pressuremeter were judged to be the same.

2. For cyclic loading in clay, the pressuremeter method yielded a pile response that was reasonably in agreement with results from experiment.

3. The comparisons between the predicted and measured cyclic responses of the single 10.75-in.-diameter pile showed

poor agreement probably because the soil conditions around the pile and the pressuremeter were different.

RECOMMENDATIONS FOR FURTHER STUDY

1. The results from recent tests, similar to those described in this report, should be obtained and analyzed. It is understood that tests have been performed in Europe and that programs of testing of single piles and groups of piles may be continuing in Europe and elsewhere.

2. On the basis of the findings reported herein, on findings of other investigators, and on the analyses of data that can be obtained on lateral loading, a report or reports should be prepared for the guidance of designers of single piles and pile groups under lateral loading. The reports may be preliminary but the results that have been obtained at the Houston site should be implemented in a timely manner.

3. The basic procedure that was employed for the instrumentation of the single piles and the pile groups for obtaining the response to lateral loading was successful and advantage should be taken of the experience that was gained.

4. The critical need is for additional data and a testing program or programs should be implemented in other kinds of soil.

5. A study should be implemented in order to take advantage of the findings reported herein in the design of superstructures that are pile-supported.

REFERENCES

API Recommended Practice for Planning, Designing, and Constructing Fixed Offshore Platforms, American Petroleum Institute, Washington, D.C., Tenth Edition, March, 1979.

Baguelin, F., Jezequel, J.F. and Shields, D.H., The Pressuremeter and Foundation Engineering, Transtech Publications, Rockport, Massachusetts, 1978.

Bogard, D. and Matlock, H., "Procedures for Analysis of Laterally Loaded Pile Groups in Soft Clay," Proceedings, Specialty Conference on Geotechnical Engineering in Offshore Practice, American Society of Civil Engineers, Austin, Texas, April, 1983.

Briaud, J.L., Lytton, R.L. and Hung, J.T., "Obtaining Moduli from Cyclic Pressuremeter Tests," Journal of the Geotechnical Engineering Division, ASCE, Vol. 109, No. 5, 1983a.

Briaud, J.L., Smith, T. D. and Meyer, B.J., "Pressuremeter Gives Elementary Model for Laterally Loaded Piles," International Symposium on In-Situ Testing of Soil and Rock, Paris, 1983b.

Brown, D. and Reese, L.C., "Behavior of a Large-Scale Pile Group Subjected to Cyclic Lateral Loading, "Geotechnical Engineering Report GR85-12, Geotechnical Engineering Center, The University of Texas at Austin, Austin, Texas, May, 1985.

Digioa, A., Davidson, H.L. and Donovan, T.D., "Laterally Loaded Drilled Piers· A Design Model," Drilled Piers and Caissons, ASCE Convention, St. Louis, 1981.

Focht, J.A., Jr., and Koch, K.J., "Rational Analysis of the Lateral Performance of Offshore Pile Groups," Preprints, Fifth Offshore Technology Conference, Houston, Texas, Vol. 2, 1973, pp. 701-708.

Ha, H.B., and O'Neill, M.W., "Field Study of Pile Group Action: Appendix A; PILGP1 Users' Guide," Report No. FHWA/RD-81/003, Federal Highway Administration, March, 1981.

Kasch, V.R, Coyle, H.M., Bartoskewitz, R.E. and Sarver, W.G., "Lateral Load Tests of a Drilled Shaft in Clay," Research Report 211-1, Texas Transportation Institute, Texas A&M University, 1977.

Little, R.L. and Briaud, J.L., "A Pressure Method for Single Piles Subjected to Cyclic Lateral Loads in Sand," Research Report No. 5357, Department of Civil Engineering, Texas A&M University, April, 1987.

Mahar, L.J. and O'Neill, M.W., "Geotechnical Characterization of Desiccated Clay," Journal of Geotechnical Engineering, ASCE, Volume 109, No. GTI, Jan., 1983, pp. 56-71.

Makarim, C.A. and Briaud, J.L., "Pressuremeter Method for Single Piles Subjected to Cyclic Lateral Loads in Overconsolidated Clay," Research Report No. 5112, Civil Engineering Department, Texas A&M University, College Station, Texas, 1986.

Matlock, H., "Correlations for Design of Laterally Loaded Piles in Soft Clay," Paper No. OTC 1204, Proceedings, Second Annual Offshore Technology Conference, Houston, Texas, Vol. 1, 1970, pp. 577-594.

Matlock, H., Ingram, W.B., Kelly, A.E., and Bogard, D., "Field Tests of the Lateral Load Behavior of Pile Groups in Soft Clay," Proceedings, Twelfth Annual Offshore Technology Conference, OTC 38871, Houston, Texas, May, 1980.

Matlock, H. and Ripperger, E.A., "Procedures and Instrumentation for Tests on a Laterally Loaded Pile," Proceedings, Eighth Texas Conference on Soil Mechanics and Foundation Engineering, Austin, Texas, 1956.

McClelland, B., "Design of Deep Penetration Piles for Ocean Structures," Journal of the Geotechnical Engineering Division, ASCE, Vol. 100, No. GT7, July 1974, pp. 709-747.

Morrison, C. and Reese, L.C., "A Lateral Load Test of a Full-Scale Pile Group in Sand," Geotechnical Engineering Report GR 86-1, Geotechnical Engineering Center, The University of Texas at Austin, Austin, Texas, August, 1986.

Poulos, H.G., "Behavior of Laterally Loaded Piles: II - Pile Groups," Journal of the Soil Mechanics and Foundations Division, ASCE, Vol. 97, No. SM5, 1971.

Ochoa, M. and O'Neill, M.W., "Lateral Pile-Group Interaction Factors for Free-Headed Pile Groups in Sand from Full-Scale Experiments," Report No. UHCE 86-12, Department of Civil Engineering, University of Houston - University Park, Houston, Texas, October, 1986.

O'Neill, M.W., "Group Action in Offshore Piles," Proceedings, Specialty Conference on Geotechnical Engineering in Offshore Practice, American Society of Civil Engineering, Austin, Texas, April, 1983.

O'Neill, M.W., and Dunnavant, T.W., "A Study of the Effects of Scale, Velocity, and Cyclic Degradability on Laterally Loaded Single Piles in Overconsolidated Clay," Report No. CE 84-7, Dept. of Civil Engineering, University of Houston University Park, Oct., 1984.

O'Neill, M.W., Hawkins, R.A., and Mahar, L.J., "Field Study of Pile Group Action," Report No. FHWA-RD-81-002, U.S. Department of Transportation, Federal Highway Administration, Offices of Research and Development, Washington, D.C., March, 1981.

O'Neill, M.W., Hawkins, R.A. and Audibert, J.M.E., "Installation of Pile Group in Overconsolidated Clay," Journal of the Geotechnical Engineering Division, ASCE, Vol. 108, NO. GT11, 1982.

Reese, L.C., Cox, W.R., and Koop, R.D., "Analysis of Laterally Loaded Piles in Sand," Proceedings, Sixth Annual Offshore Technology Conference, Vol. 2, paper no. OTC 2080, Houston, Texas, 1974, pp.473-483.

Smith, T.D., "Pressuremeter Design Method for Single Piles Subjected to Static Lateral Load," Ph.D. Dissertation, Civil Engineering, Texas A&M University, 1983.